ҚАЗАҚСТАН РЕСПУБЛИКАСЫ
ҒЫЛЫМ ЖӘНЕ ЖОҒАРЫ БІЛІМ МИНИСТРЛІГІ
SATBAYEV UNIVERSITY
МЕТАЛЛУРГИЯ ЖӘНЕ КЕН БАЙЫТУ ИНСТИТУТЫ

ISSN 2616-6445 (Online)
ISSN 2224-5243 (Print)
DOI 10.31643/2018/166445

Минералдық **ш**икізаттарды **к**ешенді **п**айдалану

4(335)

Комплексное **И**спользование **М**инерального **С**ырья

Complex **U**se of **M**ineral **R**esources

ҚАЗАН-ЖЕЛТОҚСАН 2025
OCTOBER-DECEMBER 2025
ОКТЯБРЬ-ДЕКАБРЬ 2025

ЖЫЛЫНА 4 РЕТ ШЫҒАДЫ
QUARTERLY JOURNAL
ВЫХОДИТ 4 РАЗА В ГОД

ЖУРНАЛ 1978 ЖЫЛДАН БАСТАП ШЫҒАДЫ
JOURNAL HAS BEEN PUBLISHING SINCE 1978
ЖУРНАЛ ИЗДАЕТСЯ С 1978 ГОДА

АЛМАТЫ - 2025

Бас редактор техника ғылымдарының докторы, профессор **Багдаулет КЕНЖАЛИЕВ**

Редакция алқасы:

Тех. ғыл. канд. **Ринат Абдулвалиев**, Металлургия және кен байыту институты, Алматы, Қазақстан;
Ph.D., проф. **Akçil Ata**, Сулейман Демирел университеті, Испарта, Түркия;
Ph.D., доцент **Rouholah Ashiri**, Исфахан технологиялық университеті, Исфахан, Иран;
Др. **Khaldun Mohammad Al Azzam,** Әл-Ахлия Амман университеті, Иордания;
Ph.D., **Muhammad Noorazlan Abd Azis**, Сұлтан Идрис атындағы білім беру университеті, Перак, Малайзия;
Проф., др. **Craig E. Banks**, Манчестер Метрополитен университеті, Ұлыбритания;
Проф. **Mishra Brajendra**, Вустер Политехникалық институты, Вустер, АҚШ;
Тех. ғыл. др., проф., академик **Марат Битимбаев,** Қазақстан Республикасы Ұлттық инженерлік академиясы, Алматы;
Тех. және физ.-мат. ғыл. др. **Валерий Володин,** Металлургия және кен байыту институты, Алматы, Қазақстан;
Тех. ғыл. др., проф. **Ұзақ Жапбасбаев,** Сәтбаев университеті, Алматы, Қазақстан;
Ph.D., профессор, **Yangge Zhu**, Пайдалы қазбаларды өңдеудің мемлекеттік негізгі зертханасы, Бейжің, Қытай;
Проф.,доктор **Shigeyuki Haruyama**, Ямагучи университеті, Жапония;
Тех. ғыл. др. **Сергей Квятковский,** Металлургия және кен байыту институты, Алматы, Қазақстан;
Тех.ғыл.кан., проф., академик **Ержан И. Кульдеев,** Сәтбаев университеті, Алматы, Қазақстан;
Жетекші ғылыми қызметкер, др. **Dilip Makhija,** JSW Cement Ltd, Мумбай, Үндістан;
Тех. ғыл. др. **Гүлнәз Молдабаева,** Сәтбаев университеті, Алматы, Қазақстан;
Проф., т.ғ.д. **El-Sayed Negim**, Ұлттық зерттеу орталығы, Каир, Египет;
Ph.D., проф. **Didik Nurhadiyanto**, Джокьякарта мемлекеттік университеті, Индонезия;
Доктор, қауымдастырылған проф. **Mrutyunjay Panigrahi**, Веллор Технологиялық Институты, Үндістан;
Др. **Kyoung Tae Park,** Корея сирек металдар институты (KIRAM), Корея Республикасы;
Ph.D., проф. **Dimitar Peshev**, Химиялық технология және металлургия университеті, София, Болгария;
Др. **Małgorzata Rutkowska-Gorczyca,** Вроцлав технологиялық университеті, Вроцлав, Польша;
Проф., др. **Heri Retnawati,** Джокьякарта мемлекеттік университеті, Индонезия;
Тех.ғыл.кан., проф. **Қанай Рысбеков**, Сәтбаев университеті, Алматы, Қазақстан;
Др. **Jae Hong Shin,** Корея өнеркәсіптік технологиялар институты, Корея Республикасы;
Тех. ғыл. др., проф. **Arman Shah**, Сұлтан Идрис білім беру университеті, Малайзия;
Др., проф. **Abdul Hafidz Yusoff,** Университет Малайзии Келантан, Малайзия.

Жауапты хатшы

Ph.D. **Гулжайна Касымова**

Редакция мекен жайы:
Металлургия және кен байыту институты
050010, Қазақстан Республикасы, Алматы қ., Шевченко к-сі, Уәлиханов к-нің қиылысы, 29/133,
Fax. +7 (727) 298-45-03, Tel. +7-(727) 298-45-02, +7 (727) 298-45-19
E mail: journal@kims-imio.kz, product-service@kims-imio.kz
http://kims-imio.com/index.php/main

«Минералдық шикізаттарды кешенді пайдалану» журналы ғылыми жұмыстардың негізгі нәтижелерін жариялау үшін Қазақстан Республикасы Білім және ғылым министірлігінің Білім және ғылым сапасын қамтамасыз ету комитеті ұсынған ғылыми басылымдар тізіміне енгізілген.
Меншік иесі: «Металлургия және кен байыту институты» АҚ

Журнал Қазақстан Республикасының Ақпарат және коммуникация министрлігінің Байланыс, ақпараттандыру және бұқаралық ақпарат құралдары саласындағы мемлекеттік бақылау комитетінде қайта тіркелген

2016 ж. 18 қазандағы № 16180-Ж Куәлігі

© «Металлургия және кен байыту институты» АҚ, 2025

Editor–in-chief Dr. Sci. Tech., professor **Bagdaulet KENZHALIYEV**

Editorial board:

Cand. of Tech. Sci. **Rinat Abdulvaliyev**, Institute of Metallurgy and Ore Beneficiation, Kazakhstan;
Ph.D., Prof. **Akçil Ata**, Süleyman Demirel Üniversitesi, Isparta, Turkey;
Ph.D. **Rouholah Ashiri**, associate prof. of Isfahan University of Technology, Isfahan, Iran;
Dr. **Khaldun Mohammad Al Azzam,** Department of Pharmaceutical Sciences, Pharmacological and Diagnostic Research Center, Faculty of Pharmacy, Al-Ahliyya Amman University, Jordan;
Ph.D. **Muhammad Noorazlan Abd Azis**, associate prof. of Sultan Idris Education University, Perak, Malaysia;
Prof., Dr. **Craig E. Banks,** Manchester Metropolitan University, United Kingdom;
Prof. **Mishra Brajendra**, Worcester Polytechnic Institute, Worcester, United States;
Dr.Sci.Tech., Prof. academician **Marat Bitimbayev,** National Engineering Academy of the Republic of Kazakhstan, Almaty;
Dr. Tech., Phys-math. Sci., prof. **Valeryi Volodin**, Institute of Metallurgy and Ore Beneficiation, Almaty, Kazakhstan;
Dr.Sci.Tech., Prof. **Uzak K. Zhapbasbayev,** Satbayev University, Almaty, Kazakhstan;
Ph.D., Professor, **Yangge Zhu**, State Key Laboratory of Mineral Processing, Beijing, China;
Prof. Dr. **Shigeyuki Haruyama**, Yamaguchi University, Japan;
Dr.Sci.Tech. **Sergey A. Kvyatkovskiy**, Institute of Metallurgy and Ore Beneficiation, Kazakhstan;
Prof., Dr. Sci. Tech., academician **Yerzhan I. Kuldeyev,** Satbayev University, Almaty, Kazakhstan;
Lead Scientist, Dr. **Dilip Makhija,** JSW Cement Ltd, Mumbai, India;
Dr.Sci.Tech. **Gulnaz Moldabayeva,** Satbayev University, Almaty, Kazakhstan;
Prof., Dr. Sci. Tech. **El-Sayed Negim**, Professor of National Research Centre, Cairo, Egypt;
Prof., Ph.D., **Didik Nurhadiyanto**, Yogyakarta State University, Yogyakarta, Indonesia;
Dr., Assoc. Prof., **Mrutyunjay Panigrahi**, Vellore Institute of Technology, India;
Dr. **Kyoung Tae Park,** Korea Institute for Rare Metals (KIRAM), Republic of Korea;
Professor, Ph.D. **Dimitar Peshev**, University of Chemical Technology and Metallurgy, Sofia, Bulgaria;
Dr.Sc. **Małgorzata Rutkowska-Gorczyca,** Wroclaw University of Science and Technology, Wroclaw, Poland;
Prof., Dr. **Heri Retnawati,** Yogyakarta State University (Universitas Negeri Yogyakarta), Indonesia;
Prof., Dr. Sci. Tech. **Kanay Rysbekov**, Satbayev University, Almaty, Kazakhstan;
Dr. **Jae Hong Shin,** Korea Institute of Industrial Technology, Republic of Korea;
Prof., Dr. Sci. Tech. **Arman Shah**, Universiti Pendidikan Sultan Idris, Tanjong Malim, Malaysia;
Associate Prof., Dr **Abdul Hafidz Yusoff,** Universiti Malaysia Kelantan, Malaysia.

Executive secretary

Ph.D. **Gulzhaina Kassymova**

Address:
Institute of Metallurgy and Ore Beneficiation
29/133 Shevchenko Street, corner of Ch. Valikhanov Street, Almaty, 050010, Kazakhstan
Fax. +7 (727) 298-45-03, Tel. +7-(727) 298-45-02, +7 (727) 298-45-19
E mail: journal@kims-imio.kz, product-service@kims-imio.kz
http://kims-imio.com/index.php/main

The Journal “Complex Use of Mineral Resources” is included in the List of publications recommended by the Committee for Control in the Sphere of Education and Science of the Ministry of Education and Science of the Republic of Kazakhstan for the publication of the main results of scientific activities.
Owner: “Institute of Metallurgy and Ore Beneficiation” JSC

The Journal was re-registered by the Committee for State Control in the Sphere of Communication, Information and Mass Media of the Ministry of Information and Communication of the Republic of Kazakhstan.

Certificate № 16180-Ж since October 18, 2016

© “Institute of Metallurgy and Ore Beneficiation” JSC, 2025

Главный редактор доктор технических наук, профессор **Багдаулет КЕНЖАЛИЕВ**

Редакционная коллегия:

Кан. хим. н. **Ринат Абдулвалиев**, Институт Металлургии и Обогащения, Алматы, Казахстан;
Ph.D., проф. **Akçil Ata**, Университет Сулеймана Демиреля, Испарта, Турция;
Ph.D., доцент **Rouholah Ashiri**, Исфаханский технологический университет, Исфахан, Иран;
Др. **Khaldun Mohammad Al Azzam,** Аль-Ахлия Амманский университет, Иордания;
Ph.D., доцент **Muhammad Noorazlan Abd Azis**, Образовательный университет Султана Идриса, Перак, Малайзия;
Др. тех. н., проф. **Craig E. Banks**, Манчестерский столичный университет, Соединенное Королевство;
Ph.D., проф. **Mishra Brajendra**, Вустерский политехнический институт, Вустер, США;
Др. тех. н., проф., академик **Марат Битимбаев,** Национальная инженерная академия Республики Казахстан, Алматы;
Др. тех. н. и физ.-мат. н. **Валерий Володин**, Институт Металлургии и Обогащения, Казахстан;
Др. тех. н., проф. Узак **Жапбасбаев**, КазНИТУ имени К. И. Сатпаева, Алматы, Казахстан;
Ph.D., проф. **Yangge Zhu**, Государственная ключевая лаборатория переработки полезных ископаемых, Пекин, Китай;
Проф., доктор **Shigeyuki Haruyama**, Университет Ямагути, Япония;
Др. тех. н. **Сергей Квятковский,** Институт Металлургии и Обогащения, Алматы, Казахстан;
К.т.н., проф., академик **Ержан И. Кульдеев,** КазНИТУ имени К. И. Сатпаева, Алматы, Казахстан;
Ведущий научный сотрудник, др. **Dilip Makhija,** JSW Cement Ltd, Мумбаи, Индия;
Др. тех. н. **Гульназ Молдабаева,** КазНИТУ имени К.И. Сатпаева, Алматы, Казахстан**;**
Др. тех. н., проф. **El-Sayed Negim**, Национальный исследовательский центр, Каир, Египет;
Др. тех. н., доцент **Didik Nurhadiyanto**, Джокьякартский государственный университет, Индонезия;
Доктор, Ассоц.проф. **Mrutyunjay Panigrahi,** Веллорский технологический институт, Индия;
Др. **Kyoung Tae Park,** Корейский институт редких металлов (KIRAM), Республика Корея;
Ph.D., проф. **Dimitar Peshev**, Университет химической технологии и металлургии, София, Болгария;
Др. **Małgorzata Rutkowska-Gorczyca,** Вроцлавский политехнический университет, Вроцлав, Польша;
Проф., др. **Heri Retnawati,** Джокьякартский государственный университет, Индонезия;
К.т.н., проф. **Канай Рысбеков**, КазНИТУ имени К. И. Сатпаева, Алматы, Казахстан;
Др. **Jae Hong Shin,** Корейский институт промышленных технологий, Республика Корея;
Кан. хим. н., проф. **Arman Shah**, Педагогический университет Султана Идриса, Танджунг Малим, Малайзия;
Др. проф. **Abdul Hafidz Yusoff,** Университет Малайзии, Малайзия.

Ответственный секретарь

Ph.D. **Гулжайна Касымова**

Адрес редакции:
Институт Металлургии и Обогащения
050010, Республика Казахстан, г. Алматы, ул. Шевченко, уг. ул. Валиханова, 29/133,
Fax. +7 (727) 298-45-03, Tel. +7 (727) 298-45-02, +7 (727) 298-45-19
E mail: journal@kims-imio.kz, product-service@kims-imio.kz
http://kims-imio.com/index.php/main

Журнал «Комплексное использование минерального сырья» включен в Перечень изданий, рекомендуемых Комитетом по контролю в сфере образования и науки Министерства образования и науки Республики Казахстан для публикации основных результатов научной деятельности.
Собственник: АО «Институт металлургии и обогащения»

Журнал перерегистрирован в Комитете государственного контроля в области связи, информатизации и средств массовой информации
Министерства информации и коммуникации Республики Казахстан
Свидетельство № 16180-Ж от 18 октября 2016 г.

© АО «Институт металлургии и обогащения», 2025

DOI: 10.31643/2025/6445.34
Engineering and Technology

Effect of substituting ZnO to ZnF_2 on Optical Properties of Nd^{3+}/Tm^{3+} Doped Tungsten-Bismuth-Tellurite Glass

**[1]Farah Asyiqa A.Z.N., [1]Yusof N.N., [1]Iskandar S.M., [2]Hisam R., [3]Azlan M.N.,
[4]Zaid M.H.M., [5]Abdul Hafidz Yusoff, [6*]Nurulhuda M.Y.**

[1] Universiti Sains Malaysia, 11800 USM, Penang, Malaysia
[2] Universiti Teknologi MARA, 40450, Shah Alam, Selangor, Malaysia
[3] Sultan Idris Education University, 35900 Tajung Malim, Perak, Malaysia
[4] Universiti Putra Malaysia, 43400, UPM, Serdang, Selangor, Malaysia
[5] Universiti Malaysia Kelantan, Jeli Campus, 17600 Jeli, Kelantan, Malaysia
[6]Universiti Sultan Zainal Abidin, Gong Badak Campus, 21300 Kuala Nerus, Terengganu, Malaysia

** Corresponding author email: nurulhudamy@unisza.edu.my*

Received: *May 10, 2024*
Peer-reviewed: *July 4, 2024*
Accepted: *August 29, 2024*

ABSTRACT
Present research explores the impact of varying ZnO and ZnF_2 concentrations in Nd^{3+}/Tm^{3+} doped Tungsten-Bismuth-Tellurite glass for fiber optic and solid-state application. Glasses with formula $60.97TeO_2–6.7WO_3–3.3\,Bi_2O_3–0.03Nd_2O_3–1TmO–(28\text{-}x)ZnO–xZnF_2$ where x = 0, 7, 14, 21, 28 mol% is prepared using melt-quenching technique. The absorption and photoluminescene of the glass is measured using a UV-Vis-NIR absorption and Photoluminescence spectrometer. About eight absorption bands are evidenced, centred around 467, 525, 581, 687, 726, 793, 870, 1211, and 1691 nm, corresponding to respective REIs (Nd^{3+} and Tm^{3+} ions) transitioning from the ground to their excited state. The absorbance of Tm^{3+} centred around 1691 nm improved with higher ZnF_2 contents (28% mol). Physical parameters such as density, molar volume, molar refractivity, and electronic polarizability are calculated. Seven prominent luminescence peaks of Nd^{3+} and Tm^{3+} have been identified centred around 509, 586, 611, 626, 648, 795, 800, and 890 nm. Highest luminescence enhancement is evident at 800 nm which corresponds to glass contained ratio of ZnO/ZnF_2 at 3:1. These findings highlight the role of ZnF_2 in altering the luminescence properties of the glass for fiber optics and solid-state laser applications.

Keywords: Zinc fluoride, tellurite glass, neodymium, thulium, rare-earth

	Information about authors:
Nur Farah Asyiqa Abu Zaibidin	*Master's student at School of Physics, Universiti Sains Malaysia, 11800 USM, Penang, Malaysia. Email: farahasyiqa@student.usm.my; ORCID ID: https://orcid.org/0009-0008-5121-9308*
Nur Nabihah Yusof	*Dr., School of Physics, Universiti Sains Malaysia, 11800 USM, Penang, Malaysia. Email: nurnabihah7@usm.my; ORCID ID: https://orcid.org/0000-0002-6303-4908*
Iskandar Shahrim Mustafa	*Dr., School of Physics, Universiti Sains Malaysia, 11800 USM, Penang, Malaysia. ORCID ID: https://orcid.org/0000-0003-3875-4943*
Hisam R.	*Dr., Faculty of Applied Science, Universiti Teknologi MARA, 40450, Shah Alam, Selangor, Malaysia. ORCID ID: https://orcid.org/0000-0002-9183-4988*
Muhammad Noorazlan	*Dr., Physics Department, Faculty of Science and Mathematics, Universiti Pendidikan Sultan Idris, Tanjung Malim, Perak, 35900, Malaysia. Email: azlanmn@fsmt.upsi.edu.my; ORCID ID: https://orcid.org/0000-0002-2792-4145*
Zaid M.H.M.	*Dr. Physics Department, Faculty of Science, Universiti Putra Malaysia, 43400, UPM, Serdang, Selangor, Malaysia. ORCID ID: https://orcid.org/0000-0001-6734-800X*
Abdul Hafidz Yusoff	*Dr.,Universiti Malaysia Kelantan, 17600 Jeli; Dr., Gold, Rare Earth & Material Technopreneurship Centre (GREAT) Faculty of Bioengineering and Technology Universiti Malaysia Kelantan. Jeli Campus, 17600 Jeli, Kelantan, Malaysia. ORCID ID: https://orcid.org/0000-0003-0229-886X*
Nurulhuda Mohammad Yusoff	*UniSZA Science and Medicine Foundation Centre, Universiti Sultan Zainal Abidin, Gong Badak Campus, 21300 Kuala Nerus, Terengganu, Malaysia. Email: nurulhudamy@unisza.edu.my; ORCID ID: https://orcid.org/0000-0001-8219-2920*

Introduction

The wavelength-division-multiplexing (WDM) system, employing glass that is drawn into optical fiber is experiencing exponential growth to meet demands of fast data transmission [1]. To avoid signal attenuation, new gain media with high emission cross-section, operated at NIR range could be advantages [2]. Rare earth ions (REIs) doped glass is prospective as fiber optic amplifier with possible of broad emission bands at NIR region [[3], [4]]. Specifically, neodymium (Nd^{3+}) ion and thulium (Tm^{3+}) ion-doped glass are excellent as co-doped ion where their luminescence functionalized in NIR region (800- 2000 nm) [[2], [5], [6], [7]]. Other than REIs ions, selection of glass hosts is equally important to selected REIs in developing efficient optical fiber amplifiers [[8], [9]]. Among glass, tellurite glasses are attractive since they have lower phonon energy (~750 cm $^{-1}$) compared to silica glasses (~1100 cm^{-1}), and borate glasses (1300 cm^{-1}) [10]. Tellurite glasses also exhibit wide transmission region, high refractive index, high solubility of rare earth ions, good chemical and mechanical durability; making them excellent choice as replacement of new fiber optics host [[11], [12], [13], [14]].

Tellurite glass properties can be further improved by appropriate amount of glass modifier. Tungsten oxide (WO_3) and bismuth oxide (Bi_2O_3) are selected as modifiers in the glass system. WO_3 and Bi_2O_3 are favourable in this work due to their ability to improve the glass transition temperature, density and refractive index, chemical durability, and moisture resistance, also, reduce the non-radiative loses [[15], [16], [17], [18]]. Less common glass modifier such as ZnF_2 able to reduce the phonon energy, improve the transparency, reduce hydroxide-adverse effect, decrease hygroscopic nature, possess strong transmission, and able to lower transition temperature as incorporated into tellurite glass [[14], [19], [20], [21]]. The inclusions of ZnF_2 resulting in absorbance and luminescence enhancement due to non-bridging oxygens (NBOs) generation with high polarizability that facilitate REIs transitions [22]. ZnF_2 role could be depending on its concentration within the composition [23]. For example, oxyfluorotellurite glasses increase molar volume along ZnF_2 contents. Two ligand atoms of ZnF_2, as opposed to only one oxygen in ZnO, creates more spaces and volume. This also impact the density and refractive index of the glass in general [21]. Neethish et al., claim that the replacement of ZnF_2 from BaO resulted in the destruction of the glass network and a subsequent decrease the optical band gap [24]. A few glass systems containing fluoride-based modifier also reported elsewhere such as TeO_2-ZnO-ZnF_2 [19], TeO_2-ZnO-ZnF_2 [25], TeO_2-ZnF_2 [26] B_2O_3-ZnF_2 [[20], [27]], AlF_3-ZnF_2 [28], TeO_2-BaO-BaF_2 [29], TeO_2-ZnO-BaF_2 [30], and ZnO-B_2O_3-SiO_2-ZnF_2 [31]. These findings suggest it is possible to alter optical properties of the glass by varied ZnF_2 contents during preparation process. Here ZnF_2 can lowers water absorption and reduces the multiphoton relaxation, result in improved luminescence.

The current work examines the effect of modifying the ZnO/ZnF_2 ratio in REIs doped glass. The glass formula $60.97TeO_2–6.7WO_3–3.3Bi_2O_3–0.03Nd_2O_3–1Tm_2O_3–(28\text{-}x)ZnO–xZnF_2$ is prepared using the melt-quenching technique, where x = 0, 7, 14, 21, 28 mol%. The physical parameter such as density, refractive index, molar volume, field strength, molar refractivity, electronic polarizability, and inter-nuclear properties is calculated. The optical band gap energy of the sample glasses was determined. The unusual photoluminescence curve, featuring Nd^{3+} and Tm^{3+} ion is presented. This research purposely examines the potential of ZnF_2 as a glass modifier for any possible advancement of rare earth ions (REIs) doped glass as fiber optic amplifiers.

Experimental part

Glasses with formula $60.97TeO_2–6.7WO_3–3.3Bi_2O_3–0.03Nd_2O_3–1Tm_2O_3–(28\text{-}x)ZnO–xZnF_2$ where x = 0, 7, 14, 21, 28 mol% was prepared using melt-quenching technique. The samples were labelled as TBNdTmZnF0, TBNdTmZnF7, TBNdTmZnF14, TBNdTmZnF21, and TBNdTmZnF28. The compositions were weighed 6 g per batch by a precision electronic balance according to chemical composition as in Table 1. The raw constituent was combined in alumina crucible by using a spatula to obtain a homogenous mixture. The mixtures were then placed in a high temperature furnace at 900 ˚C for 45 minutes under dry environment while the stainless-steel mold was preheated to remove residual moisture. Afterwards, the molten was quickly poured into stainless-steel mold to lessen thermal stress, enhance mechanical strength and it was kept in the annealing furnace at 300 ˚C for 6 hours before the furnace was switched off to cool down to room temperature. The Archimedes' principle method was performed to measure the density of the prepared glasses with water as immersed solution. The refractive index for each glass was obtained by using the formula given by Dimitriv & Sakka. The absorbance was recorded by UV-Vis-NIR spectrophotometer of Shimadzu UV-3600 Plus in the range of 400-2000 nm. The fluorescence spectrum in the visible to near-infrared range was recorded by FlouroMax-4 spectrofluorometer of Horiba Instruments. The data obtained from the spectrophotometer is analysed in the OriginLab software to identify the absorbance and luminescence bands, as well as to evaluate the optical band gap energy using Tauc's plot.

Table 1 - Chemical composition of the $60.97TeO_2$–$6.7WO_3$–$3.3 Bi_2O_3$–$0.03Nd_2O_3$–$1Tm_2O_3$–$(28\text{-}x)ZnO$–$xZnF_2$ (where x = 0, 7, 14, 21, 28 mol%)

Constituent/Glass	TBNdTmZnF0	TBNdTmZnF7	TBNdTmZnF14	TBNdTmZnF21	TBNdTmZnF28
TeO_2	60.97	60.97	60.97	60.97	60.97
ZnO	28.00	21.00	14.00	7.00	0.00
WO_3	6.70	6.70	6.70	6.70	6.70
Bi_2O_3	3.30	3.30	3.30	3.30	3.30
ZnF_2	0.00	7.00	14.00	21.00	28.00
Nd_2O_3	0.03	0.03	0.03	0.03	0.03
Tm_2O_3	1.00	1.00	1.00	1.00	1.00
TeO_2	60.97	60.97	60.97	60.97	60.97

Results and Discussion

Physical properties

Figure 1 shows photograph of the prepared tungsten-bismuth-tellurite glasses. The glass samples are coded as TBNdTmZnF0, TBNdTmZnF7, TBNdTmZnF14, TBNdTmZnF21, and TBNdTmZnF28, respectively according to to ZnF_2 concentration. The colour of prepared glass shows no significant colour changes as the ZnO/ZnF_2 concentration ratio varied [[32], [33]]. Alshamari et al., also mention a use of TeO_2 instead of B_2O_3 cause the glass samples colour change to more transparent light yellow instead of colourless transparent glass [34]. This could be due to impurities or defect in the glass network, where it should be transparent in high TeO_2 purity [[34], [35]].

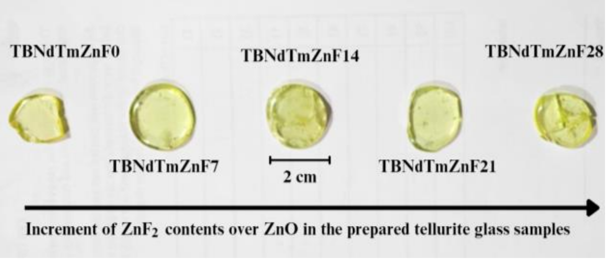

Figure 1 - As prepared Nd^{3+}/Tm^{3+} doped tungsten-bismuth-tellurite glasses with different ZnO/ZnF_2 ratio. The ZnF_2 contents (0.0-28.0 mol%) from left to right

The physical properties of Nd^{3+}/Tm^{3+} doped tellurite glasses are tabulated in Table 2 which the parameters are density, molar volume, refractive index, and polarizability is listed.

Figure **2** shows the (a) variation of density and molar volume also (b) refractive index and electronic polarizability of proposed glass. Archimedes' principle is utilized to compute the density, ρ, of the prepared glass [36].

$$\rho = \rho_w \frac{W_a}{W_a - W_w} \tag{2}$$

Where ρ_w, W_a, and W_w are density of distilled water (± 0.997 g.cm^3) weight of the sample in the air, and weight of the sample in the distilled water respectively.

The density of the glass samples shows the fluctuated trend which varies from 5.718 to 5.8156 g/cm^3 but abruptly increases in TBNdTmZnF28 glass as compared to the other glass with ZnF_2 contents. There is distinct decrease in density between 7 and 21 mol% contributed two fluoride single bonds from ZnF_2 compared to ZnO with single double bond oxygen, leading to a network that is more voluminous and loosely-packed [31]. Smaller ionic radii of F^- (133 pm) compared to O^{2-} (140 pm) also could contribute to the decrement of the density in the glass, leaving more void in the system [37]. Nevertheless, the sudden increase of density from 21 to 28% elucidates a critical concentration where structure rearrangement could occur. At in this point, addition of ZnF_2 improves the compactness and make the network tightly packed. Here, the greater molecular weight of ZnF2 (103.39 g/mol) over ZnO (81.38 g/mol) intervenes, breaking the expected trend of density's reduction [[38], [39], [40], [41]]. The equation of molar volume of the glasses is calculated as following [36].

$$M_v = \frac{M}{\rho} \tag{2}$$

Where M_V represents the molar volume, M is the molecular weight, and ρ is the density of the samples. Molar volume, M_V, typically has contrary trend with density, ρ [[33], [42]]. Molar volume, M_V, shows the linear trend with addition of ZnF_2 that lies between 26.69 to 27.91 g/cm^3 from 0 to 21 mol%. According to Azuraida et al., the increase of the space in glass network increases the molar volume [[43], [44]]. In other words, ZnF_2 creates more void as it expands the inter-atom glass system [33]. However, the decrease trend is observed at glass contained 28 mol% of ZnF_2 (27.7225 g/cm^3). This might be caused structural rearrangement as the role converted from glass modifier to network as it exceeds 20 mol%, a common concentration limit for modifier in tellurite glass system. This in turn, tightens the glass network and makes it compact [44].

Table 2 - Density, molar volume, refractive index, and polarizability of the Nd^{3+}/Tm^{3+} doped tellurite glass

Glass	**TBNdTmZnF0**	**TBNdTmZnF7**	**TBNdTmZnF14**	**TBNdTmZnF21**	**TBNdTmZnF28**
Density (g/cm^3)	5.81	5.82	5.77	5.72	5.81
Molar Volume (g/mol)	26.69	26.91	27.39	27.91	27.72
Refractive Index	1.924	1.926	1.929	1.925	1.960
Optical Band Gap Energy (eV)	3.20	3.18	3.16	3.19	2.94
Molar Refractivity (cm^3/mol)	12.64	12.77	13.03	13.23	13.48
Polarizability (×10^{-24} cm^3)	5.81	5.82	5.77	5.72	5.81
Density (g/cm^3)	26.69	26.91	27.39	27.91	27.72

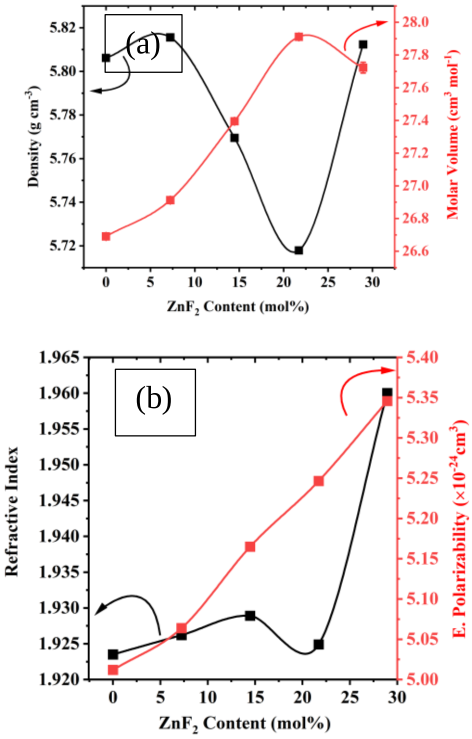

Figure 2 - Variation of (a) density and molar volume (b) refractive index and electronic polarizability with respect to the concentration of ZnF$_2$ in Nd^{3+}/Tm^{3+} doped tellurite glasses

The values of ionic concentration, N, inter-nuclear distance, r_i, polaron radius, r_p^2 , and field strength, F of ZnF$_2$ for glass samples are listed in Table 3. The polaron radius, r_p, decreases from 0.75 to 0.48 Å as ZnF$_2$ increases into the glass, leads to the high field strength, F_S, from 5.37 to 13.26 × 10^{17} cm^{-2} around Zn^{2+} ions thus, contributes to the decrease in Zn-F$_2$ bond length and increase in Zn-F$_2$ bond strength [33]. Meanwhile, internuclear distance, r_i, decrease from 1.86 to 1.18 as ZnF$_2$ [45]. This parameter explains the reduction of molar volume, M_V, as well as the increment of density, ρ, as ZnF$_2$ reaches 28 mol% in the network. The similar pattern of the mentioned parameters is recorded in the previous studies as well [[46], [47], [48]]. The concentration of an ion, N, inter-nuclear distance, r_i, polaron radius, r_p^2 , and field strength, F, are be obtained by the following equations [[46], [49]].

$$N = \text{mol\% of particular element} \times \frac{(N_A)(\rho)}{\text{glass average molecular mass}} \tag{3}$$

$$r_i = \left(\frac{1}{N}\right)^{\frac{1}{3}} \tag{4}$$

$$r_p = \frac{1}{2}\left(\frac{\pi}{6N}\right)^{\frac{1}{3}} \tag{5}$$

$$F = \frac{Z}{r_p^2} \tag{6}$$

where N_A is Avogadro's number, ρ is the density of the glass, and Z is the mass of the particular ion.

Table 3 - Ionic concentration, N, inter-nuclear distance, r_i, polaron radius, r_p^2 , and field strength, F of ZnF$_2$ for each glass sample

Glass sample	**Ionic concentration (× 10^{23} ions/cm^3)**	**Inter-nuclear distance (Å)**	**Polaron radius (Å)**	**Field strength (×10^{17} cm^{-2})**
TBNdTmZnF0	-	-	-	-
TBNdTmZnF7	1.57	1.86	0.75	5.37
TBNdTmZnF14	3.08	1.48	0.60	8.42
TBNdTmZnF21	4.53	1.30	0.52	10.9
TBNdTmZnF28	6.08	1.18	0.48	13.26

Meanwhile, the refractive index increases from 1.936 to 1.984 along ZnF_2 contents. The refractive index is calculated by utilizing optical band gap energy, E_{opt} value through Dimitrov-Sakka equation [50].

$$\frac{n^2-1}{n^2+2}=1-\sqrt{\frac{E_{opt}}{20}} \qquad (7)$$

where n is refractive index. E_{opt} is the optical band gap energy of the glass sample obtained by extrapolating linear part of the graph using Tauc's method. The absorption coefficient of the sample glasses is necessary to compute Tauc's plot. The following equations are absorption coefficient, α, from the absorption spectral data measured and also Tauc's relation [51].

$$\alpha=\frac{2.303A}{t} \qquad (8)$$

$$\alpha=\frac{B\left(\hbar\upsilon-E_{opt}\right)^r}{\hbar\upsilon} \qquad (9)$$

$$\alpha=B\exp\left(\frac{\hbar\upsilon}{E_{Urbach}}\right) \qquad (10)$$

where A, t, B, and $\hbar\upsilon$ are absorbance, thickness of glass sample, independent constant which known as band tailing parameter, photon energy respectively. The index r =1/2, 3/2, 2, 3 represents direct allowed, direct forbidden, indirect allowed, and indirect forbidden transitions respectively [52]. Both allowed transition for direct and indirect of $(\alpha\hbar\upsilon)^r$ are plotted against $\hbar\upsilon$ to attain their respective optical band gap energy, E_{opt}, by extrapolating the slope on x-axis [42]. Whereas the Urbach energy, ΔE, is obtained by using the empirical relation in eq. (10), by calculating the reciprocal of the linear slope of In(α) against energy plot [18]. The direct, indirect optical band gap energy and Urbach energy decreases with increasing ZnF_2 from 3.11 to 2.78 eV, 3.20 to 2.94 eV, and from 0.35 to 0.33 cm^{-1}, respectively, as depicted in Table 3.

Figure **3** discloses Tauc's plot for sample coded TBNdTmZnF28, revealing extrapolated direct, indirect band gap and Urbach energy. The increase in Urbach energy indicates an increase in disorderliness with ZnF_2 inclusion within the glass.

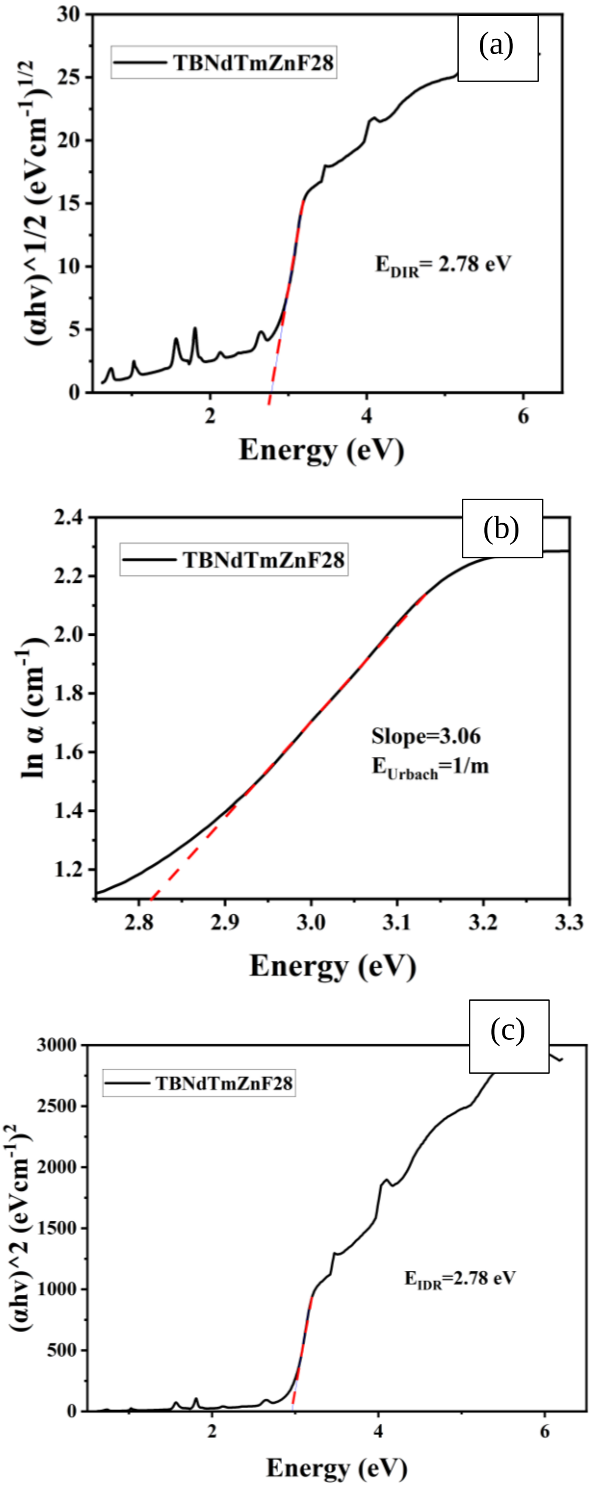

Figure 3 - (a) Direct energy band gap, (b) Indirect energy band gap, (c) Urbach energy of TBNdTmZnF28 glass

The refractive index possesses a direct relationship with the density, electric polarizability and the molecular electronic polarizability value is said to be consistent with the refractive index [41]. The electronic polarizability is one of the most important materials and it is closely related to their applicability in the field of optics and electronics

[38]. The trends refractive index and polarizability is portrayed in Table 2 and Figure 2. The polarizability of oxide and fluoride ions are computed the relation presented by Lorentz-Lorenz [53].

Table 4 - Direct energy band gap, indirect energy band gap, and Urbach energy of the Nd^{3+}/Tm^{3+} doped tellurite glasses

Constituent/Glass	**TBNdTmZnF0**	**TBNdTmZnF7**	**TBNdTmZnF14**	**TBNdTmZnF21**	**TBNdTmZnF28**
Direct Band Gap Energy (eV)	3.11	3.1	3.07	3.08	2.78
Indirect Band Gap Energy (eV)	3.20	3.18	3.16	3.19	2.94
Urbach Energy (cm^{-1})	0.35	0.28	0.20	0.18	0.33

$$a_e = \left(\frac{3}{4\pi}\right)\left(\frac{R_m}{N_a}\right) \qquad (11)$$

Where a_e is the electronic polarizability and R_m is the molar refractivity [42].

$$_M = \left(\frac{n^2-1}{n^2+2}\right)M_V \qquad (12)$$

Furthermore, the loose packing of glass network from the high molar volume, M_V, happens to increase both molar refraction, R_m, and electronic polarizability, a_e, thus, explaining the increase of the refractive index, n [39]. The prior increase in molar refractivity, R_M, from 12.64 to 13.49 cm^3/mol may lead to the increase of the electronic polarizability with value of 5.01 to 5.35 $\times 10^{-24}$ cm^3. This might attribute to more polarizable non-bridging oxygens (NBOs) compared to the less polarizable bridging oxygens (BOs) [54]. According to Komal Poojha *et al.* higher polarizability is also attributed by anion with larger ionic radii which means fluorine (3.98) that is larger compared to oxygen (3.44) [[37], [55]]. It is worth mentioning that the linear relationship between n and ρ as mentioned in Gladstone-Dale equation is invalid for present work [56].

Absorption properties

Figure 4 shows the UV-vis-NIR absorption spectra of the range of 400-2000 nm of Nd^{3+}/Tm^{3+} doped tellurite glass samples. Eight absorption band is observed at 469, 527, 584, 697, 794, 868, 1212, and 1697 nm which originated from 4f-4f electronic transitions from the ground state $^4I_{9/2}$ of Nd^{3+} and $^3H_6$ of Tm^{3+} to their respective excited levels. To be specific, the wavelength peaks at 469, 527, 584, 697, 794, and 868 are belong to Nd^{3+} which the transitions from the ground state to $^4I_{9/2}$ to $^2K_{15/2}+^4G_{11/2}$, $^4G_{7/2}$, $^4G_{5/2}$, $^4F_{9/2}$, $^4F_{5/2}$, and $^4F_{3/2}$ excited levels. Whereas the wavelength peaks of Tm^{3+} at 469, 697, 794, 1212, and 1697 are assigned to the transitions from the ground state $^3H_6$ to $^1G_4$, $^3F_{2,3}$, $^3H_4$, $^3H_5$, and $^3F_4$ excited levels. The similar absorption bands have been reported in the previous studies with the doping of Nd^{3+}/Tm^{3+} ions into tellurite glass [[1], [57]]. However, there are a few of wavelength bands overlapped at the same wavelength which are at 469, 697, and 868 nm. The transitions in the UV-Visible region appear to be less intense compared to those transitions in NIR region due to the occurrence from the ground state of Nd^{3+}, $^4I_{9/2}$ to higher levels (^4G and ^4F) and from the ground state of Tm^{3+}, $^3H_6$ to higher levels (^3F) that are spin permissible, $(\Delta S = 0)$, except $^3H_6 \rightarrow {}^1G_4$ in Tm^{3+}, where $\Delta S = 2$ thus, it explains the weak absorption of the transition at wavelength 469 nm since the spin is forbidden. Moreover, major parts of these electronic transitions has been raised on account of induced electronic dipole transitions, complying with the selection rule, $|\Delta J| \leq 6$. Moreover, the transitions for Nd^{3+} from $^4I_{9/2}$ to $^2K_{15/2}+^4G_{11/2}$, $^4G_{7/2}$, and $^4F_{9/2}$ also for Tm^{3+}, $^3H_6$ to $^3H_5$ are marked as the allowed magnetic dipole transitions owing to $\Delta J = 0, \pm 1$. Furthermore, the $^3H_6 \rightarrow {}^3F_4$, $^3H_6 \rightarrow {}^3H_5$, and $^3H_6 \rightarrow {}^3H_4$ transitions of Tm^{3+} and $^4I_{9/2} \rightarrow {}^4F_{5/2}$ transition of Nd^{3+} are called named as hypersensitive transitions as they are very sensitive to the vicinity of the host and among the most intense than other transitions [[6], [58], [59]]. These transitions obey the selection rule, $|\Delta S| = 0$, $|\Delta L| \leq 2$, and $|\Delta J| \leq 2$.

However, the absorption peak assigned by - $^4I_{9/2} \rightarrow {}^4F_{9/2}$ exhibits the most intense, but forbidden by selection rules. The intensity of the individual absorption bands largely increases with the addition of ZnF_2 concentrations.

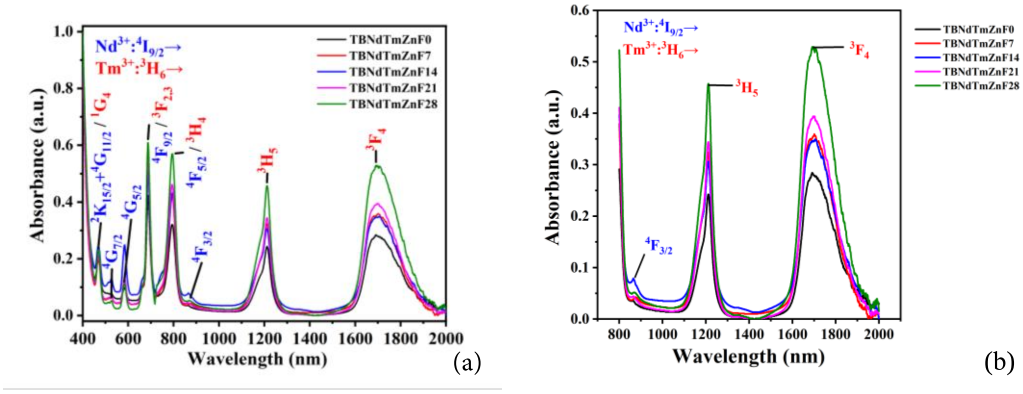

Figure 4 - Absorption spectra of (a) 400-2000 nm and (b) 800-2000 nm Nd^{3+}/Tm^{3+} doped tellurite glasses

Table 5 and Table 6 display the Nd^{3+} and Tm^{3+} ions doped tellurite glasses transition energies in wavelength number, λ (cm^{-1}), with the aquo-ion values. Major outcome of change in the characteristics of bonding between the Nd^{3+}/Tm^{3+} ions and neighbouring ligand ions (O^{2-}/F^{-}) in the host is attributed by the nephelauxetic effect [[49], [60]]. When the glass compositions in embedded with different modifiers in which also possess different charges, the band position will be varied since the ligands receive the charges from the central metal ion [55]. The nephelauxetic ratio is calculated as below [59].

$$\beta = \frac{\upsilon_B}{\upsilon_C} \qquad (13)$$

Where υ_B and υ_C are the wave number (cm^{-1}) of the corresponding transitions in the glass matric and aqua ion.

Nonetheless, bonding parameter values determine the nature of the bond between rare earth ions and their ligands (O^{2-}/F^{-}) are covalent or ionic depending on positive on the magnitude values. The formula for bonding parameter is as following [59].

$$\delta \left(\frac{1-\bar{\beta}}{\bar{\beta}}\right)\times 100 \qquad (14)$$

Where $\bar{\beta}$ is the average nephelauxetic ratio. The computed nephelauxetic ratio are 1.0917, 1.0911, 1.0912, 1.0926, and 1.0909 while the bonding parameters are -0.0840, -0.0835, -0.0836, -0.0848, and -0.0833 for glass samples TBNdTmZnF0, TBNdTmZnF7, TBNdTmZnF14, TBNdTmZnF21, and TBNdTmZnF28 respectively. The overall increase in nephelauxetic ratio also explains the shift to higher energy in absorption bands in Figure 4. As the nature of bonding between Nd^{3+}/Tm^{3+} ions and their ligands are ionic and consistent with the studied glasses [[49], [59], [60], [61]].

Table 5 - Calculated band positions (cm^{-1}), average nephelauxetic ratio ($\bar{\beta}$), bonding parameters (δ) of Nd^{3+} in aqua ion values in tellurite glasses

Energy level	TBNdTmZnF0	TBNdTmZnF7	TBNdTmZnF14	TBNdTmZnF21	TBNdTmZnF28	Aqua ion
$^4I_{9/2}\rightarrow{}^2K_{15/2} + {}^4G_{11/2}$	21322	21322	21277	21322	21277	11527
$^4I_{9/2}\rightarrow{}^4G_{7/2}$	18939	18975	18939	18975	18975	12573
$^4I_{9/2}\rightarrow{}^4G_{5/2}$	17094	17094	17123	17123	17123	14854
$^4I_{9/2}\rightarrow{}^4F_{9/2}$	14556	14556	14556	14556	14556	17167
$^4I_{9/2}\rightarrow{}^4F_{5/2}$	12594	12594	12579	12610	12579	19103
$^4I_{9/2}\rightarrow{}^4F_{3/2}$	11561	11416	11561	11561	11455	21563
$\bar{\beta}$	1.0917	1.0911	1.0912	1.0926	1.0909	-
δ	-0.0840	-0.0835	-0.0836	-0.0848	-0.0833	-

Table 6 - Calculated band positions (cm^{-1}), average nephelauxetic ratio ($\bar{\beta}$), bonding parameters (δ) of Tm^{3+} in aqua ion values in tellurite glasses

Energy level	TBNdTmZnF0	TBNdTmZnF7	TBNdTmZnF14	TBNdTmZnF21	TBNdTmZnF28	Aqua ion
$^3H_6 \rightarrow {^1G_4}$	21322	21322	21277	21322	21277	5811.0000
$^3H_6 \rightarrow {^3F_{2,3}}$	14556	14556	14556	14556	14556	8390.0000
$^3H_6 \rightarrow {^3H_4}$	12594	12594	12579	12610	12579	12720.0000
$^3H_6 \rightarrow {^3H_5}$	8251	8258	8258	8251	8251	14510.0000
$^3H_6 \rightarrow {^3F_4}$	5914	5879	5865	5900	5914	21374.0000
$\bar{\beta}$	1.4479	1.4477	1.4458	1.4480	1.4461	-
δ	-0.3094	-0.3092	-0.3083	-0.3094	-0.3085	-

Photoluminescence Properties

The spectra in

Figure **5** shows the normalised ZnF_2 dependent PL emission spectra of all glass samples in the visible and partially near infrared range (500-900 nm) under the excitation wavelength of 467 nm at room temperature. Seven prominent luminescence peaks of Nd^{3+} and Tm^{3+} are identified centred around 509, 586, 611, 626, 648, 795, 800 and 890 nm which the transitions from excited states to ground states which are at $^4G_{9/2} \rightarrow {^4I_{9/2}}$, $^4G_{5/2} \rightarrow {^4I_{9/2}}$, $^2H_{11/2} \rightarrow {^4I_{9/2}}$, $^3F_3 \rightarrow {^3H_6}$, $^3H_4 \rightarrow {^3H_6}$, $^4F_{5/2} \rightarrow {^4I_{9/2}}$, and $^4F_{3/2} \rightarrow {^4I_{9/2}}$, respectively. The intensity and bandwidth of each spectrum are observed to be sensitive to ZnF_2 contents as they are varied. At wavelength 509 nm, the intensity of $^4G_{9/2} \rightarrow {^4I_{9/2}}$ transition increases up to 21 mol% ZnF_2. Nonetheless, it is noticed that the intensity of the transitions, $^4G_{5/2} \rightarrow {^4I_{9/2}}$, $^2H_{11/2} \rightarrow {^4I_{9/2}}$, and $^4F_{3/2} \rightarrow {^4I_{9/2}}$ at 586, 626, and 890 nm have been significantly decreasing with the presence of ZnF_2 concentration. Meanwhile, at the transitions of $^3F_3 \rightarrow {^3H_6}$, $^3H_4 \rightarrow {^3H_6}$, and $^4F_{5/2} \rightarrow {^4I_{9/2}}$ at wavelength 648, 795, and 800 nm, the luminescence intensity enhanced along with the addition of ZnF_2 content up to 7 mol% and later on the intensity decreases with further addition of ZnF_2 (≥ 14 mol%) contents, due to the phenomenon of concentration quenching [62]. The strongest luminescence intensity observed at 7 mol% of ZnF_2 which is the optimum concentration of ZnF_2 obtained in the present study. However, there are two emission bands of Nd^{3+} and Tm^{3+} partially overlapped and produced a wide luminescence spectrum at wavelength 795 and 800 nm.

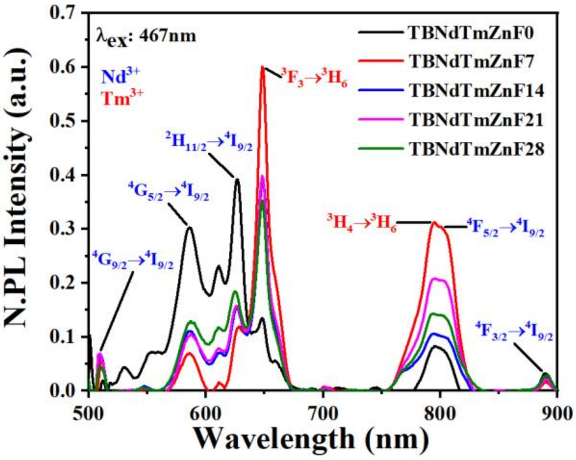

Figure 5 - Normalized PL spectra for all glass samples with the wavelength range of 500-900 nm

Figure 6 displays the partial energy diagram for the Nd^{3+}/Tm^{3+} ions, where non-radiative (NR) and radiative transitions are stipulated. In the presence of 467 nm excitation, the Nd^{3+} ions are promoted to the $^2D_{3/2}$, $^2P_{3/2}$ state while the Tm^{3+} ions are promoted to the $^1G_4$ state. Afterwards, the Nd^{3+}/Tm^{3+} ions went through multi-phonon relaxations processes and the lower states, particularly for Nd^{3+}, $^4G_{9/2}$, $^4G_{5/2}$, $^2H_{11/2}$, $^4F_{5/2}$, and $^4F^{3/2}$ while for Tm^{3+}, $^3F_3$ and $^3H_4$ are occupied. Green, orange, and red emissions are identified in Nd^{3+} ions while orange and red are detected in Tm^{3+}ions. The non-radiation transitions are attributed to the strong interaction among the respective Nd^{3+}/Tm^{3+} ions, as the distance between the ions decreases [39].

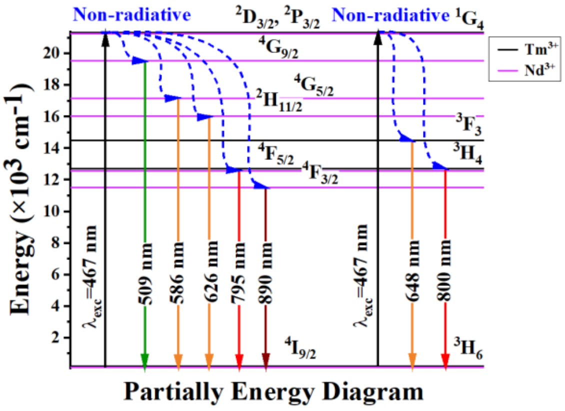

Figure 6 - Partially energy level diagram of Nd^{3+}/Tm^{3+} ions in TBNdTmZnF glasses

Conclusions

Varying the ZnO/ZnF_2 contents in Nd^{3+}/Tm^{3+} doped Tungsten-Bismuth-Tellurite glass demonstrate its substantial impact in physical and optical properties of prepared glass. The absorbance centred around 1691 nm, corresponding to Tm^{3+} ions improved with ZnF_2 contents. Physical parameters such as density, molar volume, molar refractivity, and electronic polarizability fluctuated at different ZnF_2 concentration. The changes in refractive index attributable to the polarizability differences between fluoride and oxygen anions. The prominent luminescence band is evidenced at 800 nm which highlighting the capable of ZnF_2 in tuning the luminescence properties which it shifts the wavelength towards NIR region. This work suggested that ZnF_2 can alter the optical properties of REIs doped glass, that is useful in develop better fiber optics and solid-state lasers materials operated at NIR region.

Conflicts of interest. On behalf of all authors, the corresponding author states that there is no conflict of interest.

CRediT author statement

A.Z.N. Farah Asyiqa: Conceptualization, Writing - Original Draft, Methodology, Formal analysis. **N.N.Yusof:** Conceptualization, Writing - Original Draft, Writing - Review & Editing, Funding acquisition, Supervision, Methodology**.** **S.M. Iskandar:** Writing - Review & Editing, Supervision, Methodology. **R. Hisam:** Writing - Review & Editing. **M.N. Azlan:** Writing - Review & Editing**.** **Zaid M.H.M.:** Writing - Review & Editing. **Abdul Hafidz Yusoff:** Writing - Review & Editing. **M.Y. Nurulhuda:** Writing - Review & Editing

Acknowledgements. The research was supported financially by Universiti Sains Malaysia through USM Short-Term Grant with Project No: 304/PFIZIK/6315739. We also appreciated financial support from International Kurita Grant with no: R504-LR-GAL008-0000000139-K120. The research work also was supported by UniSZA/2021/DPU1.0/21/R0325.

Cite this article as: Farah Asyiqa AZN, Yusof NN, Iskandar SM, Hisam R, Azlan MN, Zaid MHM, Abdul Hafidz Yusoff, Nurulhuda M.Y. Effect of substituting ZnO to ZnF_2 on Optical Properties of Nd^{3+}/Tm^{3+} Doped Tungsten-Bismuth-Tellurite Glass. Kompleksnoe Ispolzovanie Mineralnogo Syra = Complex Use of Mineral Resources. 2025; 335(4):5-17. https://doi.org/10.31643/2025/6445.34

ZnO-ны ZnF_2-ге ауыстырудың Nd^{3+}/Tm^{3+} легирленген Вольфрам-Висмут-Теллуритті әйнектің оптикалық қасиеттеріне әсері

[1]Farah Asyiqa A.Z.N., [1]Yusof N.N., [1]Iskandar S.M., [2]Hisam R., [3]Azlan M.N.,
[4]Zaid M.H.M., [5]Abdul Hafidz Yusoff, [6*]Nurulhuda M.Y.

[1] Сайнс Малайзия Университеті, 11800 USM, Пенанг, Малайзия
[2]MARA технологиялық университеті, 40450, Шах Алам, Селангор, Малайзия
[3] Сұлтан Ыдырыс білім университеті, 35900 Таджунг Малим, Перак, Малайзия
[4] Малайзия Путра университеті, 43400, UPM, Сердаң, Селангор, Малайзия
[5] Келантан Малайзия университеті, 17600 Джели, Келантан
[6]Сұлтан Зайнал Абидин университеті, Гонг Бадак кампусы, 21300 Куала Нерус, Теренггану, Малайзия

ТҮЙІНДЕМЕ

Зерттеу Nd^{3+}/Tm^{3+} легірленген вольфрам-висмут-теллуритті шыныдағы әртүрлі ZnO және ZnF_2 концентрацияларының оптикалық-талшықты және қатты күйде қолдану үшін әсерін зерттейді. Формуласы $60{,}97TeO_2–6{,}7WO_3–3{,}3\ Bi_2O_3–0{,}03Nd_2O_3–1TmO–(28-x)ZnO–xZnF_2$ болатын шынылар (мұнда x = 0, 7, 14, 21, 28 моль%) балқыту әдісімен дайындалады. Шынының жұтылуы және фотолюминесценциясы UV-Vis-NIR жұтылу және фотолюминесценция спектрометрінің көмегімен өлшенеді. 467, 525, 581, 687, 726, 793, 870, 1211 және 1691 нм орталықтарында сегізге жуық жұтылу жолақтары анықталған, бұл REI (Nd^{3+} және Tm^{3+} иондарының) негізгі күйден қозған күйге ауысқан күйлеріне сәйкес келеді. Орталығы 1691 нм болатын Tm^{3+} жұту қабілеті ZnF_2 мөлшері жоғары (28% моль) болғанда жақсарды. Тығыздық, молярлық көлем, молярлық сыну қабілеті және электронды поляризациялану сияқты физикалық параметрлер есептеледі. Nd^{3+} және Tm^{3+} жеті люминесценция шыңдарының 509, 586, 611, 626, 648, 795, 800 және 890 нм айналасында орналасқан. Люминесценцияның ең жоғары күшейуі 800 нм-де байқалады, бұл шыныдағы ZnO/ZnF_2 3:1 қатынасына сәйкес келеді. Бұл нәтижелер оптикалық талшықтар мен қатты күйдегі лазерлер үшін қолданылатын шынының люминесценттік қасиеттерін өзгертудегі ZnF_2 рөлін көрсетеді.

Мақала келді: *10 мамыр 2024*
Сараптамадан өтті: *4 шілде 2024*
Қабылданды: *29 тамыз 2024*

Түйінді сөздер: мырыш фториді, теллуритті шыны, неодим, тулий, сирек жер элементтері.

	Авторлар туралы ақпарат:
Nur Farah Asyiqa Abu Zaibidin	*Магистрант, Физика мектебі, Сайнс Малайзия Университеті, 11800 USM, Пенанг, Малайзия. Email: Farahasyiqa@student.usm.my; ORCID ID: https://orcid.org/0009-0008-5121-9308*
Nur Nabihah Yusof	*PhD, Физика мектебі, Сайнс Малайзия Университеті, 11800 USM, Пенанг, Малайзия. Email: nurnabihah7@usm.my; ORCID ID: https://orcid.org/0000-0002-6303-4908*
Iskandar Shahrim Mustafa	*PhD, Физика мектебі, Сайнс Малайзия Университеті, 11800 USM, Пенанг, Малайзия. ORCID ID: https://orcid.org/0000-0003-3875-4943*
Hisam R.	*Доктор, қолданбалы ғылымдар факультеті, MARA технологиялық университеті, 40450, Шах Алам, Селангор, Малайзия. ORCID ID: https://orcid.org/0000-0002-9183-4988*
Muhammad Noorazlan	*Сұлтан Ыдырыс атындағы білім университетінің жаратылыстану-математика факультеті физика кафедрасының докторы, Танджунг Малим, Перак, 35900, Малайзия. Email: azlanmn@fsmt.upsi.edu.my; ORCID ID: https://orcid.org/0000-0002-2792-4145*
Zaid M.H.M.	*Доктор, Физика кафедрасы, ғылым факультеті, Малайзия Путра университеті, 43400, UPM, Serdang, Селангор, Малайзия. ORCID ID: https://orcid.org/0000-0001-6734-800X*
Abdul Hafidz Yusoff	*PhD, Малайзия университеті Келантан, 17600 Джели; PhD, сирек жер және материалдар технологиясы кәсіпкерлік орталығы (GREAT), биоинженерия және технологиялар бөлімі, Малайзия университеті, Келантан. Джели кампусы, 17600 Джели, Келантан, Малайзия. ORCID ID: https://orcid.org/0000-0003-0229-886X*
Nurulhuda M.Y	*Сұлтан Зайнал Абидин университеті, Гонг Бадак кампусы, 21300 Куала Нерус, Теренгану, Малайзия. ORCID ID: https://orcid.org/0000-0001-8219-2920*

Влияние замены ZnO на ZnF_2 на оптические свойства Вольфрам-Висмут-Теллуритового стекла, легированного Nd^{3+}/Tm^{3+}

[1]Farah Asyiqa A.Z.N., [1]Yusof N.N., [1]Iskandar S.M., [2]Hisam R., [3]Azlan M.N.,
[4]Zaid M.H.M., [5]Abdul Hafidz Yusoff, [6*]Nurulhuda M.Y.

[1] Университет Сайнс Малайзия, 11800 USM, Пенанг, Малайзия
[2] Технологический университет MARA, 40450, Шах-Алам, Селангор, Малайзия
[3] Университет образования Султана Идриса, 35900 Таджунг Малим, Перак, Малайзия
[4] Университет Путра Малайзия, 43400, UPM, Серданг, Селангор, Малайзия
[5] Университет Малайзии Келантан, Кампус Джели, 17600 Джели, Келантан, Малайзия
[6]Университет Султана Зайнала Абидина, кампус Гонг Бадак, 21300 Куала Нерус, Теренггану, Малайзия

Поступила: *10 мая 2024*
Рецензирование: *4 июля 2024*
Принята в печать: *29 августа 2024*

АННОТАЦИЯ

Настоящее исследование изучает влияние различных концентраций ZnO и ZnF_2 в вольфрам-висмут-теллуритном стекле, легированном Nd^{3+}/Tm^{3+}, для применения в оптоволокне и полупроводниках. Стекла формулы $60{,}97TeO_2–6{,}7WO_3–3{,}3\ Bi_2O_3–0{,}03Nd_2O_3–1TmO–(28-x)ZnO–xZnF_2$, где x = 0, 7, 14, 21, 28 мол.%, получают методом закалки из расплава. Поглощение и фотолюминесценцию стекла измеряют с помощью спектрометра поглощения и фотолюминесценции UV-Vis-NIR. Выявлено около восьми полос поглощения с центрами около 467, 525, 581, 687, 726, 793, 870, 1211 и 1691 нм, соответствующих соответствующим РЗИ (ионам Nd^{3+} и Tm^{3+}), переходящим из основного в возбужденное состояние. Поглощение Tm^{3+} с центром около 1691 нм улучшалось при более высоком содержании ZnF_2 (28% мол.). Рассчитываются физические параметры, такие как плотность, молярный объем, молярная преломляющая способность и электронная поляризуемость. Были идентифицированы семь заметных пиков люминесценции Nd^{3+} и Tm^{3+}, сосредоточенных около 509, 586, 611, 626, 648, 795, 800 и 890 нм. Наибольшее усиление люминесценции наблюдается при длине волны 800 нм, что соответствует соотношению ZnO/ZnF_2 в стекле 3:1. Эти результаты подчеркивают роль ZnF_2 в изменении люминесцентных свойств стекла для волоконной оптики и твердотельных лазеров.

	Ключевые слова: фторид цинка, теллуритное стекло, неодим, тулий, редкоземельные элементы.
Nur Farah Asyiqa Abu Zaibidin	***Информация об авторах:*** *Магистрант, Школа физики, Университет Сайнс Малайзия, 11800 USM, Пенанг, Малайзия. Email: Farahasyiqa@student.usm.my; ORCID ID: https://orcid.org/0009-0008-5121-9308*
Nur Nabihah Yusof	*Доктор философии, Школа физики, Университет Сайнс Малайзия, 11800 USM, Пенанг, Малайзия. Email: nurnabihah7@usm.my; ORCID ID: https://orcid.org/0000-0002-6303-4908*
Iskandar Shahrim Mustafa	*Доктор философии, Школа физики, Университет Сайнс Малайзия, 11800 USM, Пенанг, Малайзия. ORCID ID: https://orcid.org/0000-0003-3875-4943*
Hisam R.	*Доктор, факультет прикладных наук, Технологический университет MARA, 40450, Шах Алам, Селангор, Малайзия. ORCID ID: https://orcid.org/0000-0002-9183-4988*
Muhammad Noorazlan	*Доктор кафедры физики факультета естественных наук и математики Образовательного университета Султана Идриса, Танджунг Малим, Перак, 35900, Малайзия. Email: azlanmn@fsmt.upsi.edu.my; ORCID ID: https://orcid.org/0000-0002-2792-4145*
Zaid M.H.M.	*Доктор, кафедра физики, факультет естественных наук, Университет Путра Малайзия, 43400, UPM, Серданг, Селангор, Малайзия. ORCID ID: https://orcid.org/0000-0001-6734-800X*
Abdul Hafidz Yusoff	*Доктор наук, Центр технологического предпринимательства редкоземельных металлов и материалов (GREAT), факультет биоинженерии и технологий Университета Малайзии, Кампус Джели, 17600 Джели, Келантан, Малайзия. ORCID ID: https://orcid.org/0000-0003-0229-886X*
Nurulhuda M.Y	*Университет Султана Зайнала Абидина, кампус Гонг Бадак, 21300 Куала Нерус, Тренггану, Малайзия. ORCID ID: https://orcid.org/0000-0001-8219-2920*

References

[1] Xia L, Zhang Y, Ding J, Li C, Shen X, Zhou Y. $Er^{3+}/Tm^{3+}/Nd^{3+}$ tri-doping tellurite glass with ultra-wide NIR emission. Journal of Alloys and Compounds. 2021; 863:158626. https://doi.org/10.1016/j.jallcom.2021.158626

[2] Hou G, Cao L, Zhang C, et al. Improvement of ultra-broadband near-infrared emission in Nd^{3+}-Er^{3+}-Pr^{3+} tri-doped tellurite glasses. Optical Materials. 2021; 111:110547. https://doi.org/10.1016/j.optmat.2020.110547

[3] Kaniyarakkal S, Rajasekharaudayar KC, Dagupati R, et al. Down-/Up-conversion luminescence behaviors and energy transfer analysis in Tm^{3+} and Tm^{3+}/Yb^{3+} co-doped tellurite glasses. Inorganic Chemistry Communications. 2023; 158(P1):111395. https://doi.org/10.1016/j.inoche.2023.111395

[4] Elkhoshkhany N, Marzouk S, El–Sherbiny M, et al. Enhanced thermal stability and optical and structural properties of Tm^{+3} ions in doped tellurite glasses for photonic use. Results in Physics. 2021; 24:104202. https://doi.org/10.1016/j.rinp.2021.104202

[5] Song X, Han K, Zhou D, Xu P, Xue X, Zhang P. ~2 µm emission properties and energy transfer processes in Tm^{3+} doped Bi_2O_3-GeO_2-Na_2O glass laser material. Journal of Luminescence. 2020; 224:117314. https://doi.org/10.1016/j.jlumin.2020.117314

[6] Cao J, Xu P, Song C, et al. Realization of broadband ∼1.8 µm luminescence by level population inversion in Tm^{3+} doped tellurite glass for laser applications. Journal of Non-Crystalline Solids. 2023; 617:122445. https://doi.org/10.1016/j.jnoncrysol.2023.122445

[7] Lakshminarayana G, Meza-Rocha AN, Soriano-Romero O, et al. Survey of optical and fluorescence traits of Tm^{3+}-doped alkali/mixed alkali oxides constituting B_2O_3-BaO-ZnO-LiF glasses for 0.45 µm laser and 1.46 µm fiber amplifier. Results in Physics. 2021; 26:104343. https://doi.org/10.1016/j.rinp.2021.104343

[8] Zhao D, Zhu L, Li C, Ding J, Li J, Zhou Y. Broadband near-infrared luminescence property in Nd^{3+}/Tm^{3+} co-doped tellurite glass. Journal of Alloys and Compounds. 2023; 937:168384. https://doi.org/10.1016/j.jallcom.2022.168384

[9] Djamal M, Yuliantini L, Hidayat R, et al. Spectroscopic study of Nd3+ ion-doped Zn-Al-Ba borate glasses for NIR emitting device applications. Optical Materials. 2020; 107:110018. https://doi.org/10.1016/j.optmat.2020.110018

[10] Kumar A, Anu, Sahu MK, et al. Spectral characteristics of Tb^{3+} doped ZnF_2–K_2O–Al_2O_3–B_2O_3 glasses for epoxy free tricolor w-LEDs and visible green laser applications. Journal of Luminescence. 2022; 244:118676. https://doi.org/10.1016/j.jlumin.2021.118676

[11] Siva Rama Krishna Reddy K, Swapna K, Mahamuda S, Venkateswarulu M, Rao AS. Structural, optical and photoluminescence properties of alkaline-earth boro tellurite glasses doped with trivalent Neodymium for 1.06 µm optoelectronic devices. Optical Materials. 2021; 111:110615. https://doi.org/10.1016/j.optmat.2020.110615

[12] Feng S, Zhu J, Liu C, et al. The deactivation effects of Nd^{3+} ion for 2.85 µm laser in Ho^{3+}/Nd^{3+} co-doped fluorotellurite glass. Journal of Luminescence. 2024; 266:120308. https://doi.org/10.1016/j.jlumin.2023.120308

[13] Zhu L, Zhao D, Li C, Ding J, Li J, Zhou Y. Effect of Nb_2O_5 on the ∼2.0 µm band luminescence of $Ho^{3+}/Tm^{3+}/Ce^{3+}$ tri-doped tellurite glass. Ceramics International. 2023; 49(18):30490-30500. https://doi.org/10.1016/j.ceramint.2023.06.313

[14] Zhang C, Han K, Wu T, et al. TeO_2-GeO_2-BaF_2-Tm_2O_3 glass for ∼2 µm laser materials: Analysis of luminescence features and energy transfer behavior. Ceramics International. 2022; 48(20):30546-30554. https://doi.org/10.1016/j.ceramint.2022.06.335

[15] Li C, Zhang X, Onah VC, et al. Physical and optical properties of TeO_2-WO_3-GdF_3 tellurite glass system. Ceramics International. 2022; 48(9):12497-12505. https://doi.org/10.1016/j.ceramint.2022.01.116

[16] Biswas J, Jana S. Photoluminescence of Tb^{3+}/Sm^{3+} ions co-activated in SrO - Na_2O - WO_3 - tellurite glasses for multicolor laser applications. Ceramics International. 2023; 49(15):24718-24729. https://doi.org/10.1016/j.ceramint.2023.04.215

[17] Sayyed MI, D'Souza AN, Prabhu NS, Kamath SD. Comparing basic radiation attenuation factors of tellurite glasses containing $PbCl_2$ and Bi_2O_3 with some other potential glass systems. Optik. 2022; 249:168247. https://doi.org/10.1016/j.ijleo.2021.168247

[18] Prasad RNA, Venkata Siva B, Neeraja K, Krishna Mohan N, Rojas JI. Influence of modifier oxides on spectroscopic features of Nd_2O_3 doped PbO-Ro_2O_3–WO_3–B_2O_3 glasses (with Ro_2O_3 = Sb_2O_3, Al_2O_3, and Bi_2O_3). Journal of Luminescence. 2020; 223:117171. https://doi.org/10.1016/j.jlumin.2020.117171

[19] Gunha JV, Muniz RF, Somer A, et al. The effect of fluorine replacement on the physical properties of oxyfluorotellurite glasses TeO_2-Li_2O-ZnO-ZnF_2. Journal of Non-Crystalline Solids. 2023; 603:122083. https://doi.org/10.1016/j.jnoncrysol.2022.122083

[20] Rajesham S, Sekhar KC, Shareefuddin M, Kumar JS. Impact of MoO_3 on physical and spectroscopic (optical, FTIR, Raman and EPR) studies of B_2O_3-CdO-Al_2O_3-ZnF_2 glasses for optical and shielding applications. Optik. 2023; 272:170241. https://doi.org/10.1016/j.ijleo.2022.170241

[21] Sanju, Ravina, Anu, et al. Physical, structural and optical characterization of Dy^{3+} doped ZnF_2-WO_2-B_2O_3-TeO_2 glasses for opto-communication applications. Optical Materials. 2021; 114:110937. https://doi.org/10.1016/j.optmat.2021.110937

[22] Kilic G, Issever UG, Ilik E. Synthesis, characterization and crystalline phase studies of TeO_2–Ta_2O_5–ZnO/ZnF_2 oxyfluoride semiconducting glasses. Journal of Non-Crystalline Solids. 2020; 527:119747. https://doi.org/10.1016/j.jnoncrysol.2019.119747

[23] Ravina, Naveen, Sheetal, et al. Judd-Ofelt itemization and influence of energy transfer on Sm^{3+} ions activated B_2O_3–ZnF_2–SrO–SiO_2 glasses for orange-red emitting devices. Journal of Luminescence. 2021; 229:117651. https://doi.org/10.1016/j.jlumin.2020.117651

[24] Neethish MM, Acharyya JN, Prakash GV, Ravi Kanth Kumar V V. Effect of Zinc Fluoride addition on structure of barium Borate glasses for nonlinear optical applications. Optical Materials. 2021; 121:111626. https://doi.org/10.1016/j.optmat.2021.111626

[25] Gunha JV, Muniz RF, Somer A, et al. The effect of fluorine replacement on the physical properties of oxyfluorotellurite glasses TeO2-Li2O-ZnO-ZnF2. Journal of Non-Crystalline Solids. 2023; 603:122083. https://doi.org/10.1016/j.jnoncrysol.2022.122083

[26] Abd El-Moneim A. Effect of ZnF2 and WO3 on elastic properties of oxyfluoride tellurite ZnF_2–WO_3–TeO_2glasses: Theoretical analysis. Chinese Journal of Physics. 2020; 65:412-423. https://doi.org/10.1016/j.cjph.2020.02.013

[27] Nagaraju R, Sekhar KC, Shareefuddin M, Haritha L, Lalitha G, Kumar KV. Influence of ZnF_2/PbF_2 on physical and structural characteristics of bismuth borate glasses reinforced with chromium ions. Optik. 2021; 247:168028. https://doi.org/10.1016/j.ijleo.2021.168028

[28] Zhang C, Zhang C, Yun C, Lai S. 3.1 μm mid-infrared luminescence in Er^{3+} doped ZnF_2 modified aluminum fluoride glass. Journal of Rare Earths. 2023; 41(7):997-1003. https://doi.org/10.1016/j.jre.2022.09.021

[29] Yuan J, Wang W, Ye Y, et al. Effect of BaF_2 Variation on Spectroscopic Properties of Tm^{3+} Doped Gallium Tellurite Glasses for Efficient 2.0 μm Laser. Frontiers in Chemistry. 2021; 8:1-6. https://doi.org/10.3389/fchem.2020.628273

[30] Aishwarya K, Vinitha G, Varma GS, Asokan S, Manikandan N. Synthesis and characterization of barium fluoride substituted zinc tellurite glasses. Physica B: Condensed Matter. 2017; 526:84-88. https://doi.org/10.1016/j.physb.2017.09.039

[31] Kullberg ATG, Lopes AAS, Monteiro RCC. Effect of ZnF_2 addition on the crystallization behaviour of a zinc borosilicate glass. Journal of Non-Crystalline Solids. 2017; 468(May):100-104. https://doi.org/10.1016/j.jnoncrysol.2017.04.030

[32] Vahedigharehchopogh N, Kıbrıslı O, Ersundu AE, Çelikbilek Ersundu M. Color tunability and white light generation through up-conversion energy transfer in Yb^{3+} sensitized Ho^{3+}/Tm^{3+} doped tellurite glasses. Journal of Non-Crystalline Solids. 2019; 525:119679. https://doi.org/10.1016/j.jnoncrysol.2019.119679

[33] Ahmed AA, Mawlud SQ. Physical and optical properties of ternary lead-bismuth tellurite glass. Heliyon. 2023; 9(6):e16730. https://doi.org/10.1016/j.heliyon.2023.e16730

[34] Alshamari A, Mhareb MHA, Alonizan N, et al. Gamma-ray-induced changes in the radiation shielding, structural, mechanical, and optical properties of borate, tellurite, and borotellurite glass systems modified with barium and bismuth oxide. Optik. 2023; 281:170829. https://doi.org/10.1016/j.ijleo.2023.170829

[35] Baynton PL. Colour of tellurite glasses. Nature. 1955; 176(4484):691-692. https://doi.org/10.1038/176691b0

[36] Yuliantini L, Djamal M, Hidayat R, Boonin K, Kaewkhao J, Yasaka P. Luminescence and Judd-Ofelt analysis of Nd^{3+}ion doped oxyfluoride boro-tellurite glass for near-infrared laser application. Materials Today: Proceedings. 2018; 43:2655-2662. https://doi.org/10.1016/j.matpr.2020.04.631

[37] Shannon RD. Revised effective ionic radii and systematic studies of interatomic distances in halides and chalcogenides. Acta Crystallographica. 1976; 32(5):751-767. https://doi.org/10.1023/A:1018927109487

[38] Shoaib M, Khan I, Iskakova K, et al. Investigation of luminescence properties of Ho^{3+} doped barium, zinc and gadolinium based phosphate glasses. Optik. 2022; 260:169046. https://doi.org/10.1016/j.ijleo.2022.169046

[39] Kıbrıslı O, Ersundu AE, Ersundu MÇ. Dy $^{3+}$ doped tellurite glasses for solid-state lighting: An investigation through physical, thermal, structural and optical spectroscopy studies. Journal of Non-Crystalline Solids. 2019; 513:125-136. https://doi.org/10.1016/j.jnoncrysol.2019.03.020

[40] Anigrahawati P, Sahar MR, Sazali ES. Physical, structural and spectroscopic analysis of tellurite glass containing natural magnetite Fe_3O_4 nanoparticles. Materials Chemistry and Physics. 2022; 286:126183. https://doi.org/10.1016/j.matchemphys.2022.126183

[41] Shoaib M, Khan I, Chanthima N, et al. Photoluminescence analysis of Er^{3+}-ions Doped P_2O_5-Gd_2O_3/GdF_3-BaO-ZnO glass systems. Journal of Alloys and Compounds. 2022; 902:163766. https://doi.org/10.1016/j.jallcom.2022.163766

[42] Lenkennavar SK, Eraiah B, Kokila MK. Rare earths doped oxy-fluoride glasses as candidates for generating tunable visible light. Materials Today: Proceedings. 2020; 33:2550-2554. https://doi.org/10.1016/j.matpr.2019.12.066

[43] Azuraida A, Halimah MK, Sidek AA, et al. Comparative studies of bismuth and barium boro-tellurite glass system: Structural and optical properties. Chalcogenide Letters. 2015; 12(10):497-503.

[44] Adamu SB, Halimah MK, Chan KT, Muhammad FD, Nazrin SN, Tafida RA. Eu^{3+} ions doped zinc borotellurite glass system for white light laser application: Structural, physical, optical properties, and Judd-Ofelt theory. Journal of Luminescence. 2022; 250:119099. https://doi.org/10.1016/j.jlumin.2022.119099

[45] Kaur M, Singh A, Thakur V, Singh L. Thermal, optical and structural properties of Dy^{3+} doped sodium aluminophosphate glasses. Optical Materials. 2016; 53:181-189. https://doi.org/10.1016/j.optmat.2016.01.051

[46] Ali AA, Shaaban MH. Optical and Electrical Properties of Nd^{3+} Doped TeBiY Borate Glasses. Silicon. 2018; 10(4):1503-1511. https://doi.org/10.1007/s12633-017-9633-y

[47] Krishna VM, Mahamuda S, Rani PR, Swapna K, Venkateswarlu M, Rao AS. Effect of samarium ions concentration on physical,

optical and photoluminescence properties of Oxy-Fluoro Boro Tellurite glasses. Optical Materials. 2020; 109:110368. https://doi.org/10.1016/j.optmat.2020.110368

[48] Kaur R, Bhatia V, Kumar D, Rao SMD, Pal Singh S, Kumar A. Physical, structural, optical and thermoluminescence behavior of Dy2O3 doped sodium magnesium borosilicate glasses. Results in Physics. 2019; 12:827-839. https://doi.org/10.1016/j.rinp.2018.12.005

[49] Lakshminarayana G, Vighnesh KR, Prabhu NS, et al. Dy^{3+}: B_2O_3–Al_2O_3–ZnF_2–NaF/LiF oxyfluoride glasses for cool white or day white light-emitting applications. Optical Materials. 2020; 108:110186. https://doi.org/10.1016/j.optmat.2020.110186

[50] Narasimha Rao N, Naresh P, Raghava Rao P, Swamy BJRSN, Chitti Babu A. Physical and spectroscopic properties of PbO – ZnF2 – B2O3 glasses doped with CuO. Materials Today: Proceedings. 2023; 92:817-822. https://doi.org/10.1016/j.matpr.2023.04.382

[51] Santiago de la Rosa A, Cortés-Hernández DA, Escorcia-García J, López-Herrera HU. White-light luminescence from Tm^{3+}-doped borosilicate glass-ceramics synthesized by the sol-gel route. Ceramics International. 2023; 49(14):23985-23995. https://doi.org/10.1016/j.ceramint.2023.05.002

[52] Sailaja P, Mahamuda S, Swapna K, Venkateswarlu M, Rao AS. Near-infrared photoluminescence studies of neodymium ions doped SrO-Al_2O_3-$BaCl_2$-B_2O_3-TeO2 glasses for laser and fiber amplifier applications. Optics and Laser Technology. 2022; 156:108569. https://doi.org/10.1016/j.optlastec.2022.108569

[53] Ren F, Song C, Cong Y, Wu Y, Bai Y, Zhou D. Near-infrared luminescence enhancement in Yb^{3+}/Ho^{3+} co-doped bismuth-tellurite glass by tailoring glass network. Ceramics International. 2023; 49(20):32850-32859. https://doi.org/10.1016/j.ceramint.2023.07.257

[54] Sharma A, Nazrin SN, Humaira SA, Boukhris I, Kebaili I. Impact of neodymium oxide on optical properties and X-ray shielding competence of Nd_2O_3–TeO_2–ZnO glasses. Radiation Physics and Chemistry. 2022; 195:110047. https://doi.org/10.1016/j.radphyschem.2022.110047

[55] Komal Poojha MK, Naseer KA, Matheswaran P, Marimuthu K, El Shiekh E. Effect of alkali/alkaline modifiers on Pr^{3+} ions doped lead boro-tellurite glasses for lasing material applications. Optical Materials. 2023; 143:114289. https://doi.org/10.1016/j.optmat.2023.114289

[56] Singh J. Optical Properties of Condensed Matter and Applications - Wiley Series in Materials for Electronic - amp - Optoelectronic Applications. 2006.

[57] Ding J, Li C, Xia L, Zhang Y, Li J, Zhou Y. A new Nd^{3+}/Tm^{3+}/Ho^{3+} tri-doped tellurite glass for multifunctional applications. Materials Research Bulletin. 2022; 150:111777. https://doi.org/10.1016/j.materresbull.2022.111777

[58] Shoaib M, Rooh G, Rajaramakrishna R, et al. Comparative study of Sm3+ ions doped phosphate based oxide and oxy-fluoride glasses for solid state lighting applications. Journal of Rare Earths. 2019; 37(4):374-382. https://doi.org/10.1016/j.jre.2018.09.008

[59] Monisha M, D'Souza AN, Hegde V, et al. Dy^{3+} doped SiO_2–B_2O_3–Al_2O_3–NaF–ZnF_2 glasses: An exploration of optical and gamma radiation shielding features. Current Applied Physics. 2020; 20(11):1207-1216. https://doi.org/10.1016/j.cap.2020.08.004

[60] Sasirekha C, Vijayakumar M, Yousef ES, Marimuthu K. Luminescence performance of Dy^{3+} ions incorporated modifier reliant boro-tellurite glasses for white light applications. Optik. 2023; 289:171268. https://doi.org/10.1016/j.ijleo.2023.171268

[61] Ahmadi F, Hussin R, Ghoshal SK. Judd-Ofelt intensity parameters of samarium-doped magnesium zinc sulfophosphate glass. Journal of Non-Crystalline Solids. 2016; 448:43-51. https://doi.org/10.1016/j.jnoncrysol.2016.06.040

[62] Basavapoornima C, Maheswari T, Deviprasad CJ, Kesavulu CR, Tröster T, Jayasankar CK. Thermal, structural, mechanical and 1.8 µm luminescence properties of the thulium doped Pb-K-Al-Na glasses for optical fiber amplifiers. Journal of Non-Crystalline Solids. 2020; 530:119773. https://doi.org/10.1016/j.jnoncrysol.2019.119773

Complex Use of Mineral Resources. 2025; 335(4):18-25 ISSN-L 2616-6445, ISSN 2224-5243

DOI: 10.31643/2025/6445.35
Engineering and Technology

A Comprehensive Study on Polymermodifiedbitumen Blends with PP H030 Mixing Parameters and Homogeneity

[1*]Kosparmakova S.A., [1]Seitenova G.Zh., [1]Nurakhmetova Zh.A.,[2]Dyusova R.M., [1]Jexembayeva A.E.

[1] L.N.Gumilyov Eurasian National University, Astana, Kazakhstan
[2] NAO Toraigyrov University, Pavlodar, Kazakhstan

[*] Corresponding author email: smartsam0509@gmail.com

Received: *April 22, 2024*
Peer-reviewed: *June 17, 2024*
Accepted: *September 4, 2024*

ABSTRACT

The effective inclusion of polypropylene (PPH030) into bitumen during road building is essential for improving the qualities of the material. This research examined the impact of mixing factors on the homogeneity and effectiveness of PP-bitumen blends. The experiment conducted by using granules with a size of 4.3 mm. The mixing process took place at temperatures between 158 and 160°C for a duration of 1.5 hours. Nevertheless, this procedure proved inadequate in achieving enough blending and uniformity, resulting in the existence of unabsorbed particulate matter in the mixing nozzle and vessel walls. Further tests were carried out to enhance the mixing process. The temperature was adjusted to a range of 168-175 °C, and the mixing period was prolonged to 2 hours. Additionally, the PP content was increased to 4 percent. The findings showed a significant improvement in consistency, with no visible undissolved particles. In addition, examination of the mixed samples indicated a rise in the softening point from 53.4 to 61.2 °C when the PP content was increased, accompanied by a loss in penetration and elongation capabilities. The comparison with prior findings demonstrated that the adjusted circumstances resulted in a reasonable degree of mixing, as seen by the constant softening point and decreased penetration and elongation values.

Keywords: bitumen, polymermodifiedbitumen, mixing temperature, mixing time, asphaltconcrete.

	Information about authors:
Kosparmakova Samal Akhmetalievna	*PhD of the Research and Production Center "ENU-Lab", L.N.Gumilyov Eurasian National University, Astana, 2 Satpayev str., Republic of Kazakhstan. Email: smartsam0509@gmail.com; ORCID ID: https://orcid.org/0000-0003-4700-364X*
Seitenova Gaini Zhumagalievna	*Candidate of Chemical Sciences, Associate Professor of the Department of Chemistry, L. Gumilev Eurasian National University, Astana, 2 Satpayev str., Republic of Kazakhstan. E-mail: gainiseitenova@gmail.com*
Nurakhmetova Zhanara Anuarbekovna	*PhD of the Department of Chemistry, L. Gumilev Eurasian National University, Astana, 2 Satpayev str., Republic of Kazakhstan. Email: zhanaranurakhmet@gmail.com; ORCID ID: https://orcid.org/0000-0003-2558-8579*
Dyusova Rizagul Muslimovna	*Candidate of Technical Sciences, post-doctoral student of Mechanics and Oil and Gas Business Department, NAO "Toraigyrov University", Pavlodar, 64 Lomova str., Republic of Kazakhstan. E-mail: rizagul.dyussova@gmail.com*
Jexembayeva Asel Ermekovna	*Director of the Innovation Development Department, L. Gumilev Eurasian National University, Astana, 2 Satpayev str., Republic of Kazakhstan. E-mail: dzhexembayeva_aye@enu.kz*

Introduction

Asphalt has been extensively used in road construction during the last several decades because of its excellent adhesion, temperature sensitivity, friction characteristics, resistance to ageing, and long-lasting nature. Nevertheless, the ongoing increase in traffic volume and the adverse effects of climate change, including global warming, need enhanced performance standards for bituminous pavement [1].

Out of all the efforts made to modify bitumen, adding polymer to bitumen has been one of the most widely used methods. Polyethylene (PE) and polypropylene (PP), as well as thermo-plastic elastomers like styrene-butadiene-styrene (SBS) and styrene-isoprene-styrene (SIS), have been identified as very effective modifiers for bitumen [2]. These polymers may enhance the qualities of bitumen, including increased stiffness at high temperatures, improved resistance to cracking at low temperatures, and extended fatigue life. PE and PP, being the most prevalent polyolefins, are extensively used in the manufacturing of plastics for various applications [3]. Plastic items are essential in today's lifestyle since they are lightweight, waterproof, versatile, and inexpensive to produce. Nevertheless, the escalating utilization of plastics has produced a substantial quantity of plastic trash, leading to a significant environmental issue owing to their inability to decompose naturally [4].

Consequently, there is now great interest in altering bitumen or asphalt to create polymer-modified bitumen. However, no one technique or technology can be universally applied to all types of polymers. The size of the polymers, their characteristics, and the exceptionally large surface area all contribute to enhancing the physical properties of bitumen. These improvements include increased tensile strength and modulus, reduced gas permeability, lower coefficient of thermal expansion, and maintaining the optical homogeneity of the bituminous material [5]. Various techniques may be used to integrate polymer into bitumen, including increasing the temperature, adjusting the mixing speed, and controlling the duration of mixing [6].

Through the process of high-temperature and high-shear mixing, the polymer is able to combine with the asphalt molecules, creating a cohesive network that encompasses the whole binder. This leads to a substantial enhancement of the viscoelastic characteristics when compared to the unmodified binder. This process faces challenges due to the low solubility of polymers, which restricts the number of macromolecules capable of both creating and preserving such a structure under high-temperature storage in stationary conditions, which may be required prior to applying the binder [7]. Consequently, there have been many research works focused on comprehending and enhancing the structure and storage stability of polymer-modified asphalts [8].

The uniqueness of this study is to ascertain the optimal temperature and rotation speed required to generate a homogeneous polymer-bitumen product while considering the specific properties of the polymer and bitumen produced in Kazakhstan.

Experimental part

The selected base bitumen with penetration mark BND 100/130 used in this study was supplied from the Pavlodar refinery with physical qualities in Table 1 and polymer material is polypropylene PPH030, also produced in Kazakhstan with specific characteristics including a melt flow rate of -3.3 g/10min, a yield indicator scatter within the batch of 4.6%, a bending modulus of elasticity of 1187 MPa, a mass fraction of volatile substances of 0.04%, tensile yield strength of 33.0 MPa, an elongation at the yield point of 11%, a granule size of 4.3 mm, and a smell intensity of 1 point.

Table 1 - Physical characteristics of bitumen B

Properties	Results
Penetration (25ºC, 100 gr, 5sec) 0.1 mm	118.4
Softening point, ºC	46.0
Flashpoint, ºC	>220
Specific gravity (25 ºC), gr/cm^3	1.017

The sample preparation. The polymer-modified bitumen was created by combining base bitumen with different amounts of polymers as mentioned earlier [9]. The specific percentages of polymers were selected based on the findings of review articles and research conducted by professors worldwide, which showed favourable outcomes when using 2.5-4% of the total weight of bitumen. To achieve this objective, a laboratory high-shear mixer equipped with an electronically controlled stirrer model, capable of operating at stirrer speeds ranging from 30 to 2000 rpm, was used to carry out the mixing process in Figure 1. The polymers were incrementally introduced to the bitumen by weight during the first 15 minutes of mixing, after 90 minutes of heating at a temperature of 165° C [[10], [11]]. After a two-hour interval, the mixing operation recommenced. The mixing temperature was adjusted to a range of 170-175°C, and the temperature was periodically measured using a thermometer every 30 minutes.

Figure 1 - A laboratory high-shear mixer

The test methods. Penetration testing is a widely used laboratory technique for assessing the elastic characteristics of bituminous materials, including both unblended and polymer-modified bitumen (PMB). It offers a method for assessing the rheological characteristics of bitumen at a certain temperature, namely its level of hardness or softness [12]. The penetration test entails the insertion of a standardized needle into a bitumen sample, following the parameters specified in ST RK 1226-2003. Experiments are often carried out at various temperatures, such as 25°C and 0°C. The sample is subjected to the designated testing temperature. The needle's vertical location on the surface of the specimen is guaranteed. A designated force is exerted on the needle for a certain duration of time (5 seconds). The needle's penetration into the bitumen in Figure 2, is measured in increments of tenths of a millimeter or hundredths of an inch [[13], [14]].

Figure 2 - The needle's penetration

The softening point test assesses the thermal properties of bituminous materials, specifically the viscosity of bitumen at elevated temperatures. To get precise and consistent results, it is essential to adhere to recognized guidelines such as AASHTO T 53 or ST RK 1227-2003, and ensure that the equipment is appropriately calibrated, as is customary for any other examination. A "ring-ball" gadget typically comprises of two metal rings that are concentric and a steel ball. The specimen is located inside the central cavity of the ring, while the ball is positioned directly above it. The sample is positioned inside the metal ring, with the steel ball positioned on top of it, and then exposed to regulated heating at a consistent rate of 5°C per minute [[15], [16]]. The softening point is the temperature at which the bituminous material becomes soft enough to contact the base of the ring, causing the ball to pass through the specimen in Figure 3. This change may be seen visually.

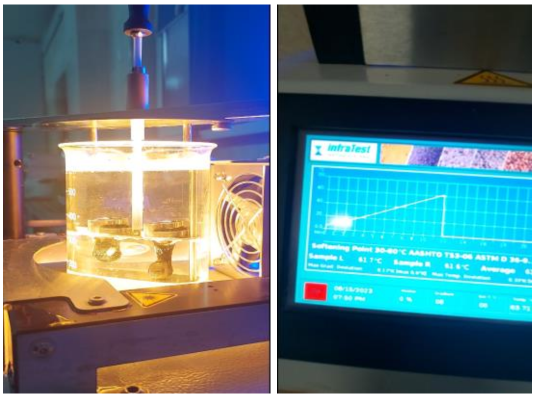

Figure 3 - The softening point test

A ductility test machine generally comprises a water bath, a collection of brass or metal molds, and a mechanism designed to apply pressure to an asphalt briquette until it reaches its breaking point [17]. The well-recognized benchmarks for evaluating the malleability of bitumen are ST RK 1374-2005 and AASHTO T 51. The procedure involves placing a representative sample of polymer-modified bitumen (PMB) in a mold and using a shaping process to create dense briquettes in Figure 4. The briquette is shaped with a predetermined cross-sectional area. A vertically aligned plasticizer is used to accommodate the cooled briquette. The briquette is regularly exposed to a consistent tensile stress, at a pace of 50 mm per minute. The bituminous material undergoes continual length measurements until it reaches the point of fracture [[18], [19]]. Ductility measures are determined by calculating the extent to which bitumen can stretch before it breaks, often measured in millimeters [[20], [21]].

Figure 4 - A ductility test briquette

Results and Discussion

The study was conducted on both unmodified and polymer-modified polymer bituminous binders to ascertain the appropriate technological temperature, mixing time, and speed. This was achieved by analyzing the correlation between penetration, softening point, and ductility tests. The optimal dosage suggested by global researchers initially began at 3%. To implement this technology, we established the ideal blending temperature and duration as 160-175 °C and 1.5 hours, respectively.

Despite using a granule size of 4.3 mm and subjecting polypropylene PPH030 to processing duration of 1.5 hours at a temperature range of 158-160 degrees Celsius, the intended level of mixing and homogeneity was not attained. An analysis of the mixing procedure revealed the existence of unabsorbed particulate matter in both the mixing nozzle and the surfaces of the mixing container. This discovery highlights a notable difficulty in attaining complete scattering and merging of the polypropylene particles within the given circumstances.

Moreover, a thorough examination of the data revealed disparities in the actual levels of penetration, softening point, and elongation features in comparison to the forecasts produced by well-established international scientific approaches and theoretical frameworks. The discrepancies are visibly shown in Figure 5 emphasizing the need for further examination and improvement of processing parameters to enhance the polymer blending process.

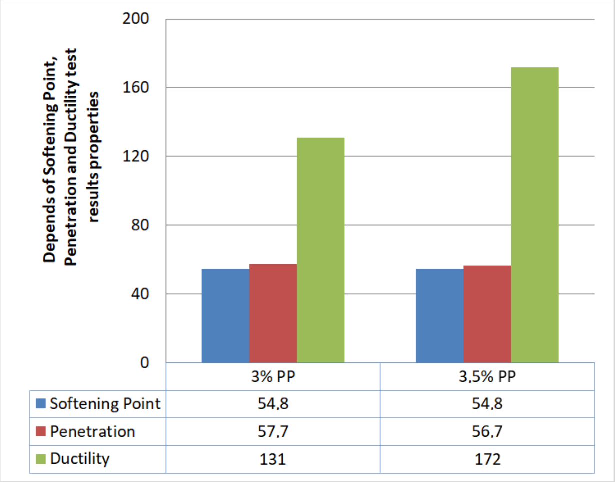

Figure 5 - A relationship between 3% and 3.5% of PP H030

Figure 5 illustrates a relationship between the quantity of polypropylene H030 and several key properties. According to theoretical expectations, an increase in the polypropylene content should correspond to an increase in consumption point while leading to a decrease in tensile properties and penetration. However, the observed elongation increase at 3.5 per cent suggests inadequacies in the mixing conditions, specifically regarding temperature and duration. This suboptimal process results in a polymer bitumen blend that lacks homogeneity, with a significant portion of polypropylene remaining undissolved.

To enhance the dissolution of polypropylene H030 and achieve homogeneity, we made the following adjustments: we increased the temperature to a range of 168-175 degrees Celsius, lengthened the mixing duration to 2 hours, and raised the polypropylene content to 4 per cent. The results of these modifications are shown in Figure 6 below.

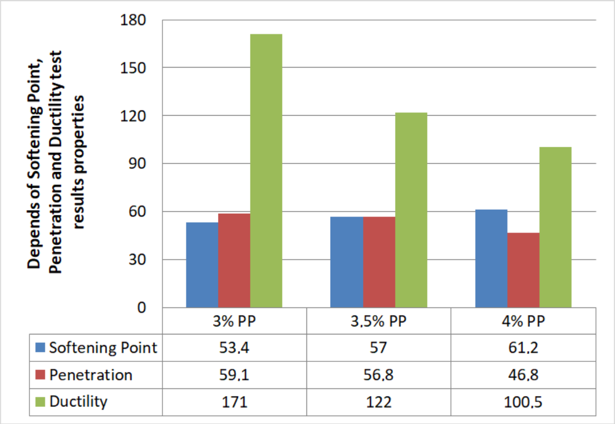

Figure 6 - A relationship between 3% and 4% of PP H030 at the new condition of mixing temperature

Figure 6 analysis reveals a homogeneous dispersion of polymer bitumens with no remaining particles. When comparing the findings obtained at temperatures below 160°C to those obtained between 168-175 °C, it was seen that the polymer bitumen mixture treated at the higher temperatures had little oxidation impact on the 3% polypropylene content. This effect was attributed to the longer processing period. The softening point exhibited a substantial rise, rising from 53.4 degrees to 61.2 degrees Celsius, as a result of a 4% increase in polypropylene content. Additionally, the data shows that the penetration decreased from 59.1 mm to 46.8 mm and the elongation decreased from 171 mm to 100.5 mm as the polypropylene content increased.

In addition, when comparing the findings at a polypropylene H030 concentration of 3.5% with the prior data, there was a rise in the softening point from 54.8 °C to 57 °C. Furthermore, the penetration and elongation values changed from 56.7 mm and 172 mm to 56.8 mm and 122 mm, respectively. The data indicate a reasonable degree of blending in the polymer bitumen mixture.

Conclusions

In conclusion, our extensive collection of over 30 experimental studies demonstrates that the homogeneity of our polymer-bitumen investigations can be significantly enhanced by employing a mixing temperature ranging from 168°C to 175°C, along with a two-hour mixing duration. Specifically, using 4.3 mm granules of polypropylene H030 ensures that the mixture achieves the desired consistency. The addition of polypropylene at a concentration equal to or exceeding 4% meets the regional technical standards for polymer bitumen. However, as polypropylene exhibits high tensile strength, chemical resistance, and a melting point of around 160°C it tends to increase the hardness of bitumen, it is essential the inclusion of plasticizers or other modifiers such as oil components or other types of polymers, to achieve the required softness and flexibility and balance the mechanical properties of the polymer-modified bitumen to incorporate additional additives. By carefully adjusting these parameters, it is ensured that the polymer bitumen meets the standards outlined in the local technical documentation while providing improved performance for road construction applications. This optimization process highlights the importance of precise control over mixing conditions and additive selection to achieve the desired material properties.

Conflicts of interest. On behalf of all authors, the corresponding author states that there is no conflict of interest.

CRediT author statement: **S. Kosparmakova**: Conceptualized the research and designed the experimental methodology. **Zh. Nurakhmetova**: Reviewed international literature and gathered information on the chemical properties changes of bitumen and polymer. **G. Seitenova**: Conducted negotiations with factory members to procure materials for the experiment. **R. Dyusova**: Provided assistance with the experimental work. **A. Jexembayeva**: Secured funding for the publication.

Acknowledgments. This research is funded by the Committee of Science of the Ministry of Science and Higher Education of the Republic of Kazakhstan (Grant No. BR21882278 Establishment of a construction and technical engineering centre to provide a full cycle of accredited services to the construction, road-building sector of the Republic of Kazakhstan).

Cite this article as: Kosparmakova SA, Seitenova GZh, Nurakhmetova ZhA, Dyusova RM. A Comprehensive Study on Polymermodifiedbitumen Blends with PP H030 Mixing Parameters and Homogeneity. Kompleksnoe Ispolzovanie Mineralnogo Syra = Complex Use of Mineral Resources. 2025; 335(4):18-25. https://doi.org/10.31643/2025/6445.35

PP H030 маркалы полимерлі битум қоспаларының араластыру параметрлерін және біртекті алынуын кешенді зерттеу

[1] Коспармакова С.А., [1] Сейтенова Г.Ж., [1] Нурахметова Ж.А., [2]Дюсова Р.М., [1]Джексембаева А.Е.

[1] Л.Н.Гумилев атындағы Еуразия ұлттық университеті, Астана, Қазақстан
[2] Торайғыров университеті КЕАҚ, Павлодар, Қазақстан

Мақала келді: *22 сәуір 2024*
Сараптамадан өтті: *17 маусым 2024*
Қабылданды: *4 қыркүйек 2024*

ТҮЙІНДЕМЕ

Жол құрылысында битумға полипропиленді (PPH030) тиімді қосу материалдың сапасын жақсарту үшін қажет. Бұл зерттеуде араластыру факторларының PP-битум қоспаларының біркелкілігі мен тиімділігіне әсері зерттелді. Экспериментте 4,3 мм түйіршіктер қолданылды. Араластыру процесі 158-160°C температурада 1,5 сағат бойы жүрді. Дегенмен, бұл процедура жеткілікті араластыру мен біркелкілікке қол жеткізу үшін жеткіліксіз болды, бұл араластырғыш саптамада және контейнер қабырғаларында сіңірілмеген қатты заттардың болуына әкелді. Араластыру процесін жақсарту үшін қосымша сынақтар жүргізілді. Температура 168-175 °C диапазонына дейін көтерілді және араластыру кезеңі 2 сағатқа дейін ұзартылды. Сонымен қатар, полипропиленнің мөлшері 4%-ға дейін өсірілді. Нәтижелер консистенцияның айтарлықтай жақсарғанын көрсетті, көрінетін ерімеген бөлшектер болмады. Сонымен қатар, аралас үлгілерді зерттеу PP мөлшерінің жоғарылауымен жұмсарту температурасының 53,4-тен 61,2 ° C-қа дейін артатынын көрсетті, бұл ену және ұзару қабілетінің төмендеуімен бірге жүрді. Алдыңғы нәтижелермен салыстыру шарттарды реттеу арқылы араластырудың қолайлы дәрежесіне қол жеткізілгенін көрсетті, бұл тұрақты жұмсарту нүктесінен және ену мен ұзартудың төмендеуінен көрінеді. Алдыңғы нәтижелермен салыстыру шарттарды түзету нәтижесінде қолайлы араластыру дәрежесіне қол жеткізілгенін көрсетті, бұл жұмсарту температурасынан және ену (пенетрация) және ұзару көрсеткіштерінің төмендеуінен көрінеді.

Түйін сөздер: битум, полимерленген битум, араластыру температурасы, араластыру уақыты, асфальтбетон.

	Авторлар туралы ақпарат:
Коспармакова Самал Ахметалыевна	*Магистр, ENU-Lab ғылыми-өндірістік орталығы директорының сапа және логистика жөніндегі орынбасары, Л.Н.Гумилев атындағы Еуразия ұлттық университеті, Сәтбаев көш., 2, Астана, Қазақстан. Email: smartsam0509@gmail.com; ORCID ID: https://orcid.org/0000-0003-4700-364X*
Сейтенова Гайни Жумагалиевна	*Химия ғылымдарының кандидаты, Химия кафедрасының қауымдастырылған профессоры, Л.Н.Гумилев атындағы Еуразия ұлттық университеті, Сәтбаев көш., 2, Астана, Қазақстан. E-mail: gainiseitenova@gmail.com*
Нурахметова Жанара Ануарбековна	*PhD, Л.Н.Гумилев атындағы Еуразия ұлттық университеті, Сәтбаев көш., 2, Астана, Қазақстан. Email: zhanaranurakhmet@gmail.com; ORCID ID: https://orcid.org/0000-0003-2558-8579*
Дюсова Ризагуль Муслимовна	*Техника ғылымдарының кандидаты, Механика және мұнай-газ ісі кафедрасының постдокторанты, Торайғыров университеті КЕАҚ, Ломов көш., 64, Павлодар, Қазақстан. E-mail: rizagul.dyussova@gmail.com*
Джексембаева Асель Ермековна	*Инновацияларды дамыту департаментінің директоры, Л.Н.Гумилев атындағы Еуразия ұлттық университеті, Сәтбаев көш., 2, Астана, Қазақстан. E-mail: dzhexembayeva_aye@enu.kz*

Комплексное исследование параметров смешивания и получения однородности полимербитумных смесей с PP H030

[1] Коспармакова С.А., [1] Сейтенова Г.Ж., [1] Нурахметова Ж.А., [2]Дюсова Р.М., [1]Джексембаева А.Е.

[1] *Евразийский Национальный Университет им. Л. Гумилева, Астана, Казахстан*
[2] *НАО Торайгыров университет, Павлодар, Казахстан*

Поступила: *22 апреля 2024*
Рецензирование: *17 июня 2024*
Принята в печать: *4 сентября 2024*

АННОТАЦИЯ

Эффективное добавление полипропилена (PPH030) в битум при строительстве дорог необходимо для улучшения качества материала. В данном исследовании изучалось влияние факторов смешивания на однородность и эффективность ПП-битумных смесей. В эксперименте использовались гранулы размером 4,3 мм. Процесс смешивания проходил при температуре 158-160°C в течение 1,5 часов. Тем не менее, эта процедура оказалась недостаточной для достижения достаточного смешивания и однородности, что привело к наличию неабсорбированных твердых частиц в смесительной насадке и на стенках емкости. Были проведены дополнительные испытания для улучшения процесса смешивания. Температура была отрегулирована до диапазона 168-175 °C, а период смешивания был продлен до 2 часов. Кроме того, содержание полипропилена было увеличено до 4 %. Результаты показали значительное улучшение консистенции, без видимых нерастворенных частиц. Кроме того, исследование смешанных образцов показало повышение температуры размягчения с 53,4 до 61,2 °C при увеличении содержания ПП, что сопровождалось снижением проникающей способности и способности к удлинению. Сравнение с предыдущими результатами показало, что в результате корректировки условий была достигнута приемлемая степень смешивания, что видно по неизменной температуре размягчения и снижению показателей пенетрации и удлинения.

Ключевые слова: битум, полимермодифицированный битум, температура смешивания, время смешивания, асфальтобетон.

	Информация об авторах:
Коспармакова Самал Ахметалыевна	*Магистр, заместитель директора по качеству и логистике научно–производственного центра ENU-Lab, Евразийский Национальный Университет им. Л. Гумилева, Астана, ул. Сатпаева 2, Казахстан. Email: smartsam0509@gmail.com; ORCID ID: https://orcid.org/0000-0003-4700-364X*
Сейтенова Гайни Жумагалиевна	*Кандидат химических наук, ассоциированный профессор кафедры Химия, Евразийский Национальный Университет им. Л. Гумилева, Астана, ул. Сатпаева 2, Казахстан. E-mail: gainiseitenova@gmail.com*
Нурахметова Жанара Ануарбековна	*PhD кафедры «Химия», Евразийский Национальный Университет им. Л. Гумилева, Астана, ул. Сатпаева 2, Казахстан. Email: zhanaranurakhmet@gmail.com; ORCID ID: https://orcid.org/0000-0003-2558-8579*
Дюсова Ризагуль Муслимовна	*Кандидат технических наук, постдокторант кафедры Механика и нефтегазовое дело, НАО Торайгыров университет, Павлодар, ул. Ломова 64, Казахстан. E-mail: rizagul.dyussova@gmail.com*
Джексембаева Асель Ермековна	*Директор Департамента развития инноваций, Евразийский Национальный Университет им. Л. Гумилева, Астана, ул. Сатпаева 2, Казахстан. E-mail: dzhexembayeva_aye@enu.kz.*

References

[1] Kosparmakova SA, Shashpan ZA, Guler M. An advanced method for the development of highly reliable asphalt concrete mixture. Kompleksnoe Ispolzovanie Mineralnogo Syra = Complex Use of Mineral Resources. 2023; 326(3):41-49. https://doi.org/10.31643/2023/6445.27

[2] Kalantar Z, Karim M, Abdelaziz M. A review of using waste and virgin polymer in pavement. Constr. Build. Mater. 2012; 33:55-62. https://doi.org/10.1016/j.conbuildmat.2012.01.009

[3] Zhang M, et al. Asphalt binder micro-characterization and testing approaches: A review. Measurement. 2020; 151:107255. https://doi.org/10.1016/j.measurement.2019.107255

[4] Kim S-S, et al. A simple test procedure for evaluating low temperature crack resistance of asphalt concrete. FHWA. OH. 2009. https://rosap.ntl.bts.gov/view/dot/17206

[5] Brief Review of the Chemistry of Polyphosphoric Acid (PPA) and Bitumen. Energy & Fuels. 2008; 22(4). https://pubs.acs.org/doi/abs/10.1021/ef800120x

[6] Sultana S, Bhasin A. Effect of chemical composition on rheology and mechanical properties of asphalt binder. Constr. Build. Mater. 2014; 72:293-300. https://doi.org/10.1016/j.conbuildmat.2014.09.022

[7] Gupta A, et al. Critical assessment of new polymer-modified bitumen for porous asphalt mixtures. Constr. Build. Mater. 2021; 307:124957. https://doi.org/10.1016/j.conbuildmat.2021.124957

[8] Samal K, et al. The polymer effects on bitumen performance properties in Kazakhstan. Geomate Journal. https://geomatejournal.com/geomate/article/view/3646. https ://doi.o rg/10.21660/2022.100.3646

[9] Feng Z-G, et al. Effect of ultraviolet aging on rheology, chemistry and morphology of ultraviolet absorber modified bitumen. Mater. Struct. 2013; 46(7):1123-1132. https://link.springer.com/article/10.1617/s11527-012-9958-3

[10] Ongel A, Hugener M. Impact of rejuvenators on aging properties of bitumen. Constr. Build. Mater. 2015; 94:467-474. https://doi.org/10.1016/j.conbuildmat.2015.07.030

[11] Kosparmakova S, Shashpan Z, Bazarbayev D. Investigating the Superpave Mixture Design Approach for Hot-Mix Asphalt in Kazakhstan. L.N. Gumilyov Eurasian National University. 2023; 2:62-71. https://doi.org/10.32523/2616-7263-2023-143-2-62-71

[12] Bulatović VO, Rek V, Marković KJ. Influence of polymer types on bitumen engineering properties. Mater. Res. Innov. 2013; 17(3):189-194. https://doi.org/10.1179/1433075X12Y.0000000059

[13] Kosparmakova S, Shashpan ZA, Guler M. Effect of Aggregate Gradation on Asphalt Concrete Properties. Kompleksnoe Ispolzovanie Mineralnogo Syra = Complex Use of Mineral Resources. 2024; 328(1):33-41. https://doi.org/10.31643/2024/6445.04

[14] Wang H, et al. Effect of laboratory aging on chemistry and rheology of crumb rubber modified bitumen. Mater. Struct. 2020; 53(2):26. https://link.springer.com/article/10.1617/s11527-020-1451-9

[15] Belyaev PS, et al. Modifikatsiya neftyanykh dorozhnykh bitumov polimernymi materialami dlya polucheniya asfal'tobetonnykh pokrytiy s uluchshennymi ekspluatatsionnymi kharakteristikami [Modification of petroleum road bitumen with polymeric materials to produce asphalt concrete pavements with enhanced performance characteristics]. Vestnik Tambovskogo gosudarstvennogo tekhnicheskogo universiteta [Vestnik of Tambov State Technical University]. 2016; 22(2):264-271. (In Russ.). https://doi.org/10.17277/vestnik.2016.02

[16] Sengoz B, Isikyakar G. Evaluation of the properties and microstructure of SBS and EVA polymer modified bitumen. Constr. Build. Mater. 2008; 22(9):1897-1905. https://doi.org/10.1016/j.conbuildmat.2007.07.013

[17] Imanbayev Y, et al. Modification of Bitumen with Recycled PET Plastics from Waste Materials. Polymers. Multidisciplinary Digital Publishing Institute. 2022; 14(21):4719. https://doi.org/10.3390/polym14214719

[18] Solomentsev AB, Revyakin SL, Onopriychuk DA. Reologicheskaya chuvstvitel'nost' dorozhnykh bitumov k polimernym dobavkam i dopustimyye tekhnologicheskiye temperatury asfal'tobetonnykh smesey [Road bitume rheological sensitivity to polymer additives and allowable technological temperatures of asphalt-concrete mixtures]. Stroitel'stvo i rekonstruktsiya [Building and Reconstruction]. 2017;(6):128-140. (In Russ.)

[19] García-Morales M, et al. Effect of waste polymer addition on the rheology of modified bitumen. Fuel. 2006; 85(7):936-943. https://doi.org/10.1016/j.fuel.2005.09.015

[20] Iwański M, Cholewińska M, Mazurek G. Viscoelastic Properties of Polymer Modified Bitumen in Warm Mix Asphalt Technology in Terms of Ageing. Procedia Eng. 2017; 172:401-408. https://doi.org/10.1016/j.proeng.2017.02.007

[21] Ahmedzade P. The investigation and comparison effects of SBS and SBS with new reactive terpolymer on the rheological properties of bitumen. Constr. Build. Mater. 2013; 38:285-291. https://doi.org/10.1016/j.conbuildmat.2012.07.090

DOI: 10.31643/2025/6445.36
Engineering and Technology

Influence of granule structure mineral fertilizers for their physical and chemical properties

[1*]Smailov B.M., [1]Beisenbayev O.K., [1]Anarbayev A.A., [2]Zakirov B.S., [3]Aravind U.K.

[1]M.Auezov South Kazakhstan Research University, Shymkent, Kazakhstan
[2] Institute of General and Inorganic Chemistry, Tashkent, Uzbekistan
[3]Cochin University of Science and Technology, Kerala, India

** Corresponding author email: baha_uppr@mail.ru*

Received: *May 28, 2024*
Peer-reviewed: *June 28, 2024*
Accepted: *September 5, 2024*

ABSTRACT
In this article, maintaining the quality and commercial properties of mineral fertilizers during repeated transshipment and long-term transportation is an important issue. The purpose of the research work is to study the structure of granules in complex mixed fertilizers and to develop methods to improve it at the production stage, thereby improving the physical and mechanical properties of the finished product. In order to improve the granular structure of the mineral fertilizer, the static strength of the granules, the mass fraction of moisture, the chemical composition, and the structural shape of the granules were determined using an electron microscope. To improve the structure and increase the strength of mineral fertilizers, a method of encapsulation was used using 0.5% aqueous solutions of organic polymers of modified polyacrylamide, followed by granulation and drying at a temperature of 75 °C and a tralchet granulator. A comparative analysis was conducted to study the structure of mineral fertilizers, diammonium phosphate, and encapsulated superphosphate using modern instrumental methods. The structure of encapsulated superphosphate was studied, and its strength was increased using 0.5% aqueous solutions of modified polyacrylamide at a temperature of 750 °C, with an increase from 40 to 2000 times. Spectral studies of superphosphate treated with polymer solutions were carried out, and structural features corresponding to the functional groups of organic compounds were identified. The research results showed that aqueous solutions of modified polyacrylamide allow structure formation, creating a polymer shell and increasing the strength of mineral fertilizer granules.

Keywords: mineral fertilizer, strength, structure, grain, research.

Information about authors:

Smailov Bakyt Matkarimovich	*PhD, Department of Scientific Research, M.Auezov South Kazakhstan University, Shymkent, Kazakhstan. E-mail: Baha_uppr@mail.ru; ORCID ID: https://orcid.org/0000-0001-7976-9776*
Beisenbayev Oral Kurganbekovich	*Doctor of technical sciences, Professor, Department of technology of inorganic and petrochemical productions, M. Auezov South Kazakhstan University, Shymkent, Kazakhstan. E-mail: oral-kb@mail.ru; ORCID ID: https://orcid.org/0000-0001-9442-213X*
Anarbayev Abibulla Abildaevich	*Doctor of chemical sciences, professor, Department of technology of inorganic and petrochemical productions, M.Auezov South Kazakhstan University, Shymkent, Kazakhstan. E-mail: abib_28@mail.ru; ORCID ID: https://orcid.org/0000-0002-0019-4381*
Zakirov Bakhtiyar Sabirjanovich	*Doctor of chemical sciences, professor, Institute of General and Inorganic Chemistry, Tashkent, Uzbekistan. E-mail: b_zakirov@bk.ru; ORCID ID: https://orcid.org/0000-0001-6664-8019*
Aravind Usha Kulangara	*PhD, professor, Cochin University of Science and Technology, Kerala, India. E-mail: uka@cusat.ac.in; ORCID ID: https://orcid.org/0000-0002-1535-5467*

Introduction

The manufacture of mineral fertilizers is an important area of the Kazakh agro complex, occupying a leading position in non-hydrocarbon, non-resource exports.

The country is experiencing an increase in the production of complex mixed mineral fertilizers for export.

The range of mineral fertilizers produced in the Republic of Kazakhstan today is changing in favor of mineral fertilizers, which meet modern consumer preferences. Complex mixed fertilizers, as a rule, are more concentrated and require lower costs for transportation, storage, and application compared to single-component fertilizers.

Improved quality of exported mineral fertilizers is a prerequisite for increasing export potential and an important factor in maintaining the competitiveness of Kazakhstani producers. Thus, the problem of preserving the quality of mineral fertilizers during numerous transshipments and long-term transportation is one of the key ones for the industry as a whole. In addition, improving the physicochemical properties of mineral fertilizers can significantly increase the efficiency of their use and avoid losses at the application stage [[1],[2]].

The consumer properties of granular mineral fertilizers - static strength of granules, caking, dustiness - are interrelated and depend on the substance constituents and building of the granules, which is largely determined by the technological parameters of the production process [[3], [4]].

Currently, modern non-destructive methods for studying the structure of solids, such as scanning electron microscopy (SEM), have appeared and become available. The use of these methods allows us to study in detail the structure and distribution of chemical elements in granules of complex mineral fertilizers, as well as their relationship with physical and chemical properties [[5],[6]].

The importance of scientific work is to study the structure of granules of complex mixed fertilizers, as well as to search and develop methods for improving them at the production stage to improve the physical and mechanical features of the eventual product.

Experimental part

Object of research. To study the properties of granular mineral fertilizers, the most popular brands of mineral fertilizers produced by Kazphosphate LLP were selected. Sample preparation and sampling for experimental work were carried out in accordance with the established procedure [7].

Research methods. *Determination of the static strength of sample granules.* The static strength of sample granules was measured according to GOST 21560.2-82. The static strength of the granules was studied using an automatic dual Rockwell hardness tester HRS150/45T-Z. The strength measurement range is from 3.0 to 20 MPa, with a relative error ±1%.

Determination of mass fraction of water. The mass fraction of hygroscopic and total water was determined by drying in an oven in accordance with [8].

Study of the structure and chemical composition of granules using scanning electron microscopy. The microstructure and a cut of a sample of the mineral fertilizers was an instrumental method determined using scanning microscopy SEM (JSM-6490lV, Jeol, Tokyo, Japan). The scale of this microstructure is x50-2000 times the increase from the actual state (600 micron, spectral 0 - 20 keV).

Study the structural features of the studied sample. An IR Fourier spectrometer (Zhimadzu IR Prestige-21 with an attenuated total internal reflection attachment, Miracle Pike Technologies (Tokyo, Japan)) was used to study the structural features of the studied sample.

To improve the structure and increase the strength of mineral fertilizers, a method of encapsulation was used using 0.5% aqueous solutions of organic polymers of modified polyacrylamide, followed by granulation and drying at a temperature of 75 °C and a tralchet granulator.

The discussion of the results

The structure of granules of complex fertilizers is determined, first of all, by the technology of their production: the method of granulation, as well as the modes of the method of introducing raw materials. In turn, the structure of granules affects the physico-chemical and physico-mechanical characteristics of granular fertilizers - static strength [[9], [10]].

The work of the author (Kochetova I.M.) presents experimental images of the results of microphotography and the distribution of chemical elements on a chip of a DAP granule of grade 18-46, treated with I-40 oil (magnification x200).

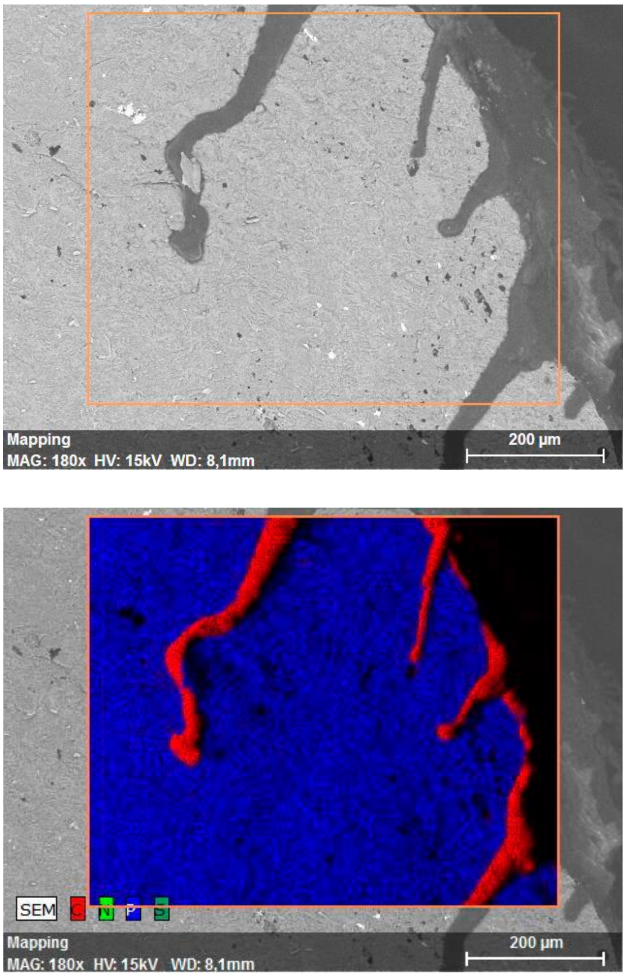

Figure 1 - Microphotograph and distribution of chemical elements on a chip of DAP granule grade 18-46 treated with I-40 oil (magnification x200)

It is noted here that the presence of surface pores largely determines the hygroscopic characteristics of the product and can also increase the consumption of conditioning additives (Figure 1).

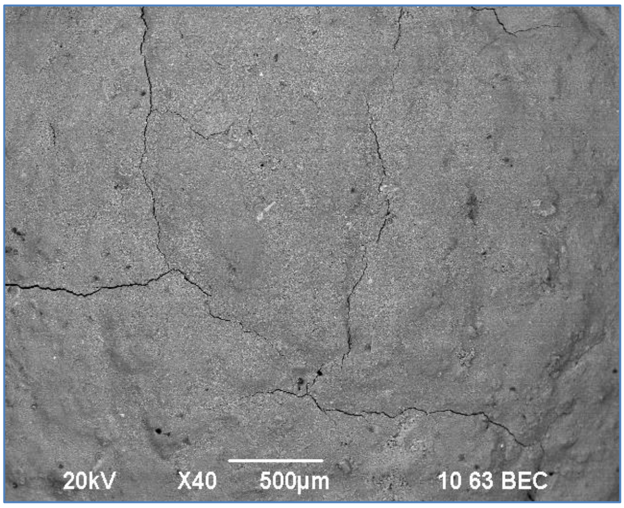

Figure 2 - The microstructure of a sample of the modified superphosphate (magnification x40)

From Figure 2, it follows that the microstructure of superphosphate granules with an X40 magnification and treated with 0.5% aqueous solutions of polycarilamide appears amorphous at a temperature of 75 ^{0}C. In the top layer of superphosphate, the formation of links occurs, leading to structuring in the form of amorphous and crystalline structures with the formation of a polymer layer on the surface of the granules. The binding of components with polymer solutions during granulation and the polymer layer on the surface of superphosphate have a positive effect on the structure and strength of the granules.

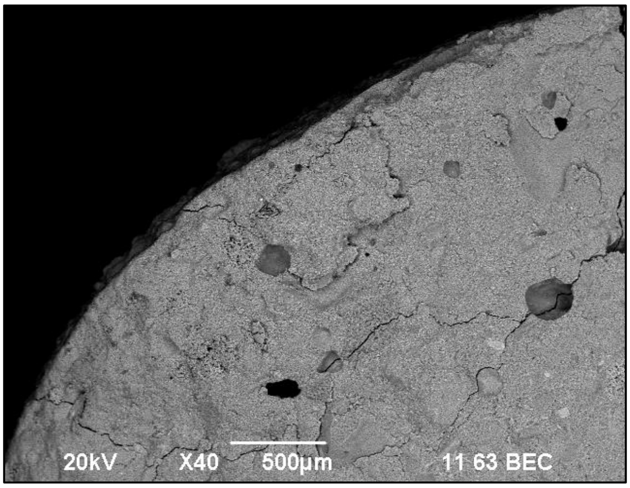

Figure 3 - The microstructure with a cut of the sample of the modified superphosphate (magnification x40)

From Figure 3, it follows that the pores of superphosphate granules are associated with cracks and are the centers for cracks, and the formation of a thin film on the surface of the granules provides an increase in strength up to 17 MPa.

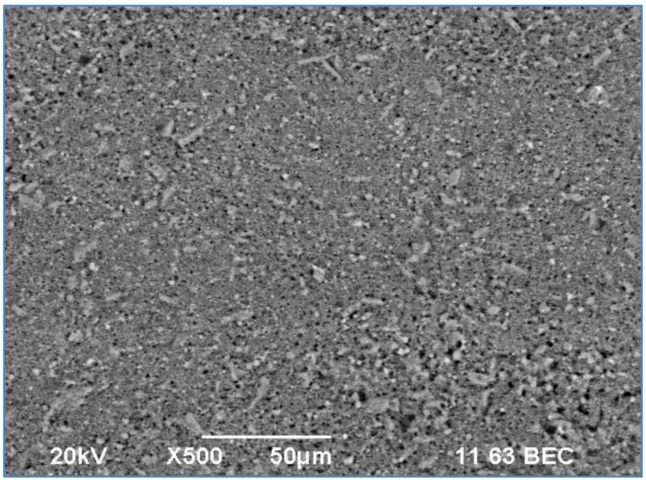

Figure 4 - The microstructure of a sample of the modified superphosphate (magnification x500)

Figure 4 shows that barrel-shaped structures with properties characteristic of phosphorus compounds were detected.

This indicates that the appearance of these fragments in the fertilizer structure is associated with the aggregation of fertilizer particles and the subsequent formation of large interconnected units due to the adsorption properties and functional groups of the polymer solutions, which influence the structural strength of the entire system (Fig.4).

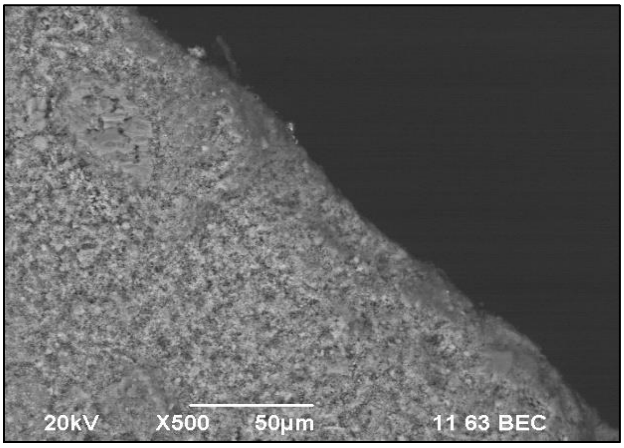

Figure 5 - The microstructure with a cut of the sample of the modified superphosphate (magnification x500)

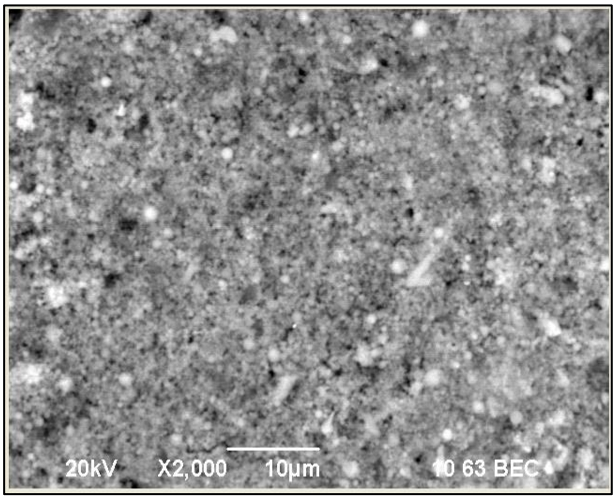

Figure 6 - The microstructure of a sample of the modified superphosphate (magnification x2000)

From Figure 6, it follows that there is a secondary adsorption layer in which the molecules are directed, and on the outside, there is a hydrophilic part that promotes coagulation binding of particles.

From Figure 7, it follows that the structure is observed on the surface of the granules, and in parallel, it is visible how a polymer layer is formed due to the interaction of the active centers of mineral fertilizers and the active functional groups of aqueous solutions of the polymer with the formation of thin films.

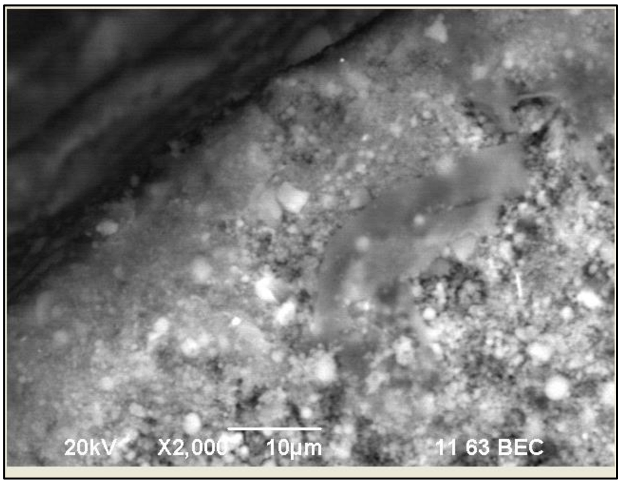

Figure 7 - The microstructure with a cut of the sample of the modified superphosphate (magnification x2000)

The improved mechanical properties of superphosphate positively impact the fertilizer's effectiveness. For example, due to its greater strength, dust formation during application is eliminated.

The obtained modified superphosphate had the following functional groups during research. The superphosphate was analyzed in an IR spectrometer (Shimadzu IR Prestige-21), and the results of the studies are shown in the table. 1 and Fig. 8.

Table 1 – Spectral data of modified superphosphate

No	Peak	Intensity	Corr. intensity
1	601.79	81.382	1.048
2	690.52	73.207	5.766
3	752.24	75.802	0.256
4	775.38	74.927	1.098
5	875.68	81.125	0.797
6	910.40	75.602	3.854
7	1002.98	68.732	3.190
8	1026.13	70.113	1.435
9	1365.60	86.484	0.112
10	1377.17	86.282	5.189
11	1558.48	86.358	0.447
12	3390.86	87.240	0.241
13	3618.46	91.620	0.855
14	3691.75	94.343	1.326

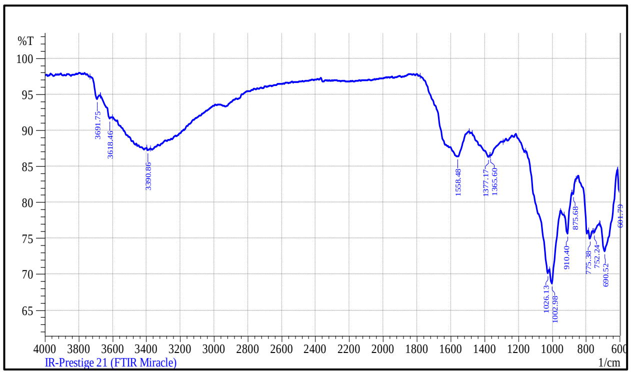

Figure 8 - IR-spectrum of modified superphosphate

As can be seen from the data in Figure 8, there are the following IR absorption spectra:

-non-intensive absorption spectra with wavelengths of 3691.75–3390.86 cm^{-1} characterize the presence of bonds (RC–COOH) carboxylic acids, bonds (RC–COH) aldehydes and ketones (R–CO–R) functional groups of superphosphate;

-non-intensive absorption spectra with wavelengths of 1558.48–1365.60 cm^{-1} characterize the presence of bonds (C–C) between carbons and (C–H) hydrocarbon groups in superphosphate;

-intensive absorption of 1026.13–910.40 cm^{-1} determines the compounds of hydroxyl, sulfur, nitrogen molecules – OH, N, S;

-Intensive absorption values of 875.68-752.24 cm^{-1} are characterize the presence of a bond between phosphorus and sulfur (P=S).

-intensive absorption values of 690.52-601.79 cm^{-1} are are characteristic of Ca^{+2} compounds in the valence state O-Ca-O.

The authors' work presents data on determining the basic physicochemical properties of fertilizer for its mechanized application to improve soils and increase crop yields [[11], [12]]. Using additions that improve the properties and increase the effectiveness of waste-based fertilizers corresponds with the modern approach to creating waste-free technologies, observed in agriculture and other branches of the economy [[13], [14]].

This work presents the results of research on the leaching of solid phosphorus-containing waste with humic acid. Such waste includes the by-products of the electrothermal processing of phosphate raw materials—phosphorus sludge and cottrel dust [[15], [16]].

Conclusions

A literature review was conducted of scientists who contributed to the study of the structure of granules and their influence on the physicochemical properties of mineral fertilizers[[17], [18], [[19], [20]].

A comparative analysis was conducted to study the structure of mineral fertilizers, diammonium phosphate, and encapsulated superphosphate using modern instrumental methods.

The structure of encapsulated superphosphate was studied and its strength was increased using 0.5% aqueous solutions of modified polyacrylamide at a temperature of 750 °C with an increase from 40 to 2000 times.

Spectral studies of superphosphate treated with polymer solutions were carried out, and structural features corresponding to the functional groups of organic compounds were identified. The research results showed that aqueous solutions of modified polyacrylamide allow structure formation, creating a polymer shell and increasing the strength of mineral fertilizer granules.

Acknowledgments. The authors express their gratitude for the work of the author Kochetova M.I. on the topic “The influence of the granule structure of complex NP, NP(S), and NPK fertilizers on their physicochemical properties,” which became the basis for studying the structure of mineral fertilizers.

CRediT author statement: **B. Smailov:** Conceptualization, formal analysis, investigation, data writing, original draft preparation, writing–review and editing. **O. Beisenbayev:** Data curation, writing draft preparation, methodology, **A. Anarbayev:** Resources, supervision. **B. Zakirov:** Investigation, visualization. **U. Aravind:** software, validation.

Conflicts of Interest. On behalf of all authors, the corresponding author declares that there is no conflict of interest.

Funding: This research was funded by the Science Committee of the Ministry of Science and Higher Education of the Republic of Kazakhstan, Grant No. BR21882181.

Cite this article as: Smailov BM, Beisenbayev OK, Anarbayev AA, Zakirov BS, Aravind UK. Influence of granule structure mineral fertilizers for their physical and chemical properties. Kompleksnoe Ispolzovanie Mineralnogo Syra = Complex Use of Mineral Resources. 2025; 335(4):26-33. https://doi.org/10.31643/2025/6445.36

Минералды тыңайтқыштар түйіршіктерінің құрылымының олардың физика-химиялық қасиеттеріне әсері

[1]Смайлов Б.М., [1]Бейсенбаев О.К., [1]Анарбаев А.А., [2]Закиров Б.С., [3]Aravind U.K.

[1]М. Әуезов атындағы Оңтүстік Қазақстан Зерттеу Университеті, Шымкент, Қазақстан
[2]Жалпы және бейорганикалық химия институты, Ташкент, Өзбекістан
[3]Кочиндік ғылым және технология университеті, Керала,Үндістан

Мақала келді: *28 мамыр 2024*
Сараптамадан өтті: *28 маусым 2024*
Қабылданды: *5 қыркүйек 2024*

ТҮЙІНДЕМЕ

Минералды тыңайтқыштарды қайта тиеу және ұзақ мерзімге тасымалдау кезінде олардың сапасы мен тауарлық қасиеттерін сақтау маңызды мәселелердің бірі болып табылады. Ғылыми-зерттеу жұмысының мақсаты – күрделі аралас тыңайтқыштардың түйіршіктерінің құрылымын зерттеу, сонымен қатар дайын өнімнің физика-механикалық қасиеттерін жақсарту мақсатында өндіріс сатысында оны жетілдіру әдістерін табу және әзірлеу. Минералды тыңайтқыштың түйіршікті құрылымын жақсарту мақсатында түйіршіктердің статикалық беріктігі, ылғалдың массалық үлесі, түйіршіктердің химиялық құрамы мен құрылымдық пішіні электронды микроскоптың көмегімен анықталды. Минералды тыңайтқыштардың құрылымын жақсарту және беріктігін арттыру үшін модификацияланған полиакриламидтің органикалық полимерлерінің 0,5% сулы ерітінділерін қолданып, кейіннен түйіршіктеу және контейнерлік гранулятордың көмегімен 75 °C температурада кептіру арқылы капсуляция әдісі қолданылды. Заманауи аспаптық әдістерді қолдана отырып, минералды тыңайтқыштардың диаммоний фосфаты мен капсулаланған суперфосфаттың құрылымына салыстырмалы талдау жасалды. Капсулаланған суперфосфаттың құрылымы мен оның беріктігі модификацияланған полиакриламидтің 0,5% сулы ерітінділерін 75 °C температурада 40-тан 2000 есеге дейін арттыру арқылы зерттелінді. Полимер ерітінділерімен өңделген суперфосфатқа спектрлік зерттеулер жүргізіліп, органикалық қосылыстардың функционалдық топтарына сәйкес келетін құрылымдық ерекшеліктері анықталды. Зерттеу нәтижелері модификацияланған полиакриламидтің сулы ерітінділері құрылымды қалыптастыруға, полимер қабықшасын жасауға және минералды тыңайтқыш түйіршіктерінің беріктігін арттыруға мүмкіндік беретінін көрсетті.

Түйін сөздер: минералды тыңайтқыш, беріктілік, құрылым, түйіршік, зерттеу.

	Авторлар туралы ақпарат:
Смайлов Бакыт Маткаримулы	*PhD доктор, ғылыми зерттеу департаменті, М. Әуезов атындағы Оңтүстік Қазақстан зерттеу университеті, Шымкент, Қазақстан. E-mail: Baha_uppr@mail.ru; ORCID ID: https://orcid.org/0000-0001-7976-9776*
Бейсенбаев Орал Қорғанбекулы	*Техника ғылымдарының докторы, профессор, мұнай хихимиясы және бейорганикалык заттар өндірісінің технологиясы факультеті, М. Әуезов атындағы Оңтүстік Қазақстан зерттеу университеті, Шымкент, Қазақстан. E-mail: oral-kb@mail.ru; ORCID ID: https://orcid.org/0000-0001-9442-213X*
Анарбаев Абибулла Абилдаұлы	*Техника ғылымдарының докторы, профессор, мұнай хихимиясы және бейорганикалык заттар өндірісінің технологиясы факультеті, М. Әуезов атындағы Оңтүстік Қазақстан зерттеу университеті, Шымкент, Қазақстан. E-mail: abib_28@mail.ru; ORCID ID: https://orcid.org/0000-0002-0019-4381*
Закиров Бахтияр Сабиржанұлы	*Химия ғылымдарының докторы, профессор, жалпы және бейорганикалық химия институты, Ташкент, Узбекстан. E-mail: b_zakirov@bk.ru; ORCID ID: https://orcid.org/0000-0001-6664-8019*
Aravind Usha Kulangara	*PhD доктор, профессор, Кочин ғылым және технология университеті, Керала, Үндістан. E-mail: uka@cusat.ac.in; ORCID ID: https://orcid.org/0000-0002-1535-5467*

Влияние структуры гранул минеральных удобрений на их физико-химические свойства

[1]Смайлов Б.М., [1]Бейсенбаев О.К., [1]Анарбаев А.А., [2]Закиров Б.С., [3]Aravind U.K.

[1]Южно-Казахстанский Исследовательский Университет имени М. Ауезова, Шымкент, Казахстан
[2]Институт общей и неорганической химии, Ташкент, Узбекистан
[3]Кочинский университет науки и технологии, Керала, Индия

Поступила: *28 мая 2024*
Рецензирование: *28 июня 2024*
Принята в печать: *5 сентября 2024*

АННОТАЦИЯ

Сохранение качественных и товарных свойств минеральных удобрений при многократной перевалке и длительной транспортировке является одним из важных вопросов. Цель научно-исследовательской работы – изучить структуру гранул комплексных смешанных удобрений, а также найти и разработать методы ее улучшения на этапе производства с целью улучшения физико-механических свойств готового продукта. С целью улучшения зернистой структуры минерального удобрения с помощью электронного микроскопа определяли статическую прочность гранул, массовую долю влаги, химический состав и структурную форму гранул. Для улучшения структуры и повышения прочности минеральных удобрений был использован метод капсуляция с применением 0,5% водных растворов органических полимеров модифицированного полиакриламида, с последующей грануляцией и сушкой при температуре 75 °С с помощью таральчетного гранулятора. Проведен сравнительный анализ структуры минеральных удобрений диаммонийфосфата и инкапсулированного суперфосфата с использованием современных инструментальных методов. Изучена структура инкапсулированного суперфосфата, и его прочность была повышена с использованием 0,5%-ных водных растворов модифицированного полиакриламида при температуре 750°С с увеличением от 40 до 2000 раз. Проведены спектральные исследования суперфосфата, обработанного полимерными растворами, и идентифицированы структурные особенности, соответствующие функциональным группам органических соединений. Результаты исследований показали, что водные растворы модифицированного полиакриламида позволяют формировать структуру, создавая полимерную оболочку и повышая прочность гранул минерального удобрения.

Ключевые слова: минеральное удобрение, прочность, структура, зерно, исследование.

	Информация об авторах:
Смайлов Бакыт Маткаримулы	*PhD доктор, департамент научных исследований, Южно-Казахстанский исследовательский университет им. М. Әуезова, Шымкент, Қазақстан. E-mail: Baha_uppr@mail.ru; ORCID ID: https://orcid.org/0000-0001-7976-9776*
Бейсенбаев Орал Қорғанбекович	*Доктор технических наук, профессор, Факультет технологии производства нефтехимических и неорганических веществ, Южно-Казахстанский исследовательский университет им. М. Әуезова, Шымкент, Қазақстан. E-mail: oral-kb@mail.ru; ORCID ID: https://orcid.org/0000-0001-9442-213X*
Анарбаев Абибулла Абилдаевич	*Доктор технических наук, профессор, Факультет технологии производства нефтехимических и неорганических веществ, Южно-Казахстанский исследовательский университет им. М. Әуезова, Шымкент, Қазақстан. E-mail: abib_28@mail.ru; ORCID ID: https://orcid.org/0000-0002-0019-4381*
Закиров Бахтияр Сабиржанович	*Доктор химических наук, профессор, Институт Общей и неорганической химии, Ташкент, Узбекстан. E-mail: b_zakirov@bk.ru; ORCID ID: https://orcid.org/0000-0001-6664-8019*
Aravind Usha Kulangara	*PhD доктор, профессор, Кочинский университет науки и технологии, Керала, Индия. E-mail: uka@cusat.ac.in; ORCID ID: https://orcid.org/0000-0002-1535-5467*

References

[1] Skovorodnikov PV, Cherepanova MV. Peculiarities of organomineral fertilizer granulation by the pelletizing method. Bulletin of the Tomsk Polytechnic University. Geo Assets Engineering. 2019; 330(9);51-59. https://doi.org/10.18799/24131830/2019/9/2255

[2] Erkinov RV, Ismoilova GI, Usmonova ZSh, Khusanova MN, Dekhkanov ZK. Physico-chemical properties of ammonium nitrate with the addition of ash. Universum: technical sciences. 2021; 4(85); https://doi.org/10.32743/UniTech.2021.85.4-4.68-70

[3] Nazarbek U, Nazarbekova S, Raiymbekov Y, Kambatyrov M, Abdurazova P. Prolonged action fertilizer encapsulated by CMC. e-Polymers. 2023; 23:20230013. https://doi.org/10.1515/epoly-2023-0013

[4] Lisowska A, Filipek-Mazur B, Komorowska M, Niemiec M, Bar-Michalczyk D, Kuboń M, Tabor S, Gródek-Szostak Z, Szeląg-Sikora A, Sikora J, et al. Environmental and Production Aspects of Using Fertilizers Based on Waste Elemental Sulfur and Organic Materials. Materials. 2022; 15:3387. https://doi.org/10.3390/ma15093387

[5] Omarov B, Zhantassov K, Zhantassov M, Kirgizbayeva K, Altybayev Z. Methods for obtaining humate-containing fertilizers from brown coal. International Journal of Coal Preparation and Utilization. 2024; 1:1–14. http://dx.doi.org/10.1080/19392699.2024.2330409

[6] Lisowska Aneta, Filipek-Mazur B, Józef Sołtys, Marcin Niemiec, Olga Gorczyca, Dominika Bar-Michalczyk, Monika Komorowska, et al. Preparation, Characterization of Granulated Sulfur Fertilizers and Their Effects on a Sandy Soils. 2022. https://doi.org/10.3390/ma15020612

[7] GOST 21560.0-82. Mineral fertilizers. Methods of sampling and preparation of samples.

[8] MVI No. 1104-00209438-130-10. Determination of the static strength of mineral fertilizer granules, 2010.

[9] Chawalit Raksarikorn, Intanon Pumisak, Intanon Ruankuan. Influence of Organic Granular Fertilizer, Chemical and Granular Organic Fertilizer with Hormone Mixed Formula (Ho), and Chemical Fertilizer to the Yield and Starch Content of Cassava. Revista de Gestão Social e Ambiental. 2024; 18(5):1-16. https://doi.org/10.24857/rgsa.v18n5-019

[10] Suzanne E Allaire, Léon Etienne Parent. Physical Properties of Granular Organic-based Fertilisers. Biosystems Engineering. 2024; 87(1):79-87. https://doi.org/10.1016/j.biosystemseng.2003.09.006

[11] Omar González-Cueto., Rafael Alejandro Salcerio-Salaberry and etc. Physical and Chemical Characterization of the Organ-Mineral Fertilizer Agromena – G. Revista Ciencias Técnicas Agropecuarias. 2023; 32(3):e08.

[12] Ramūnas Mieldažys, Eglė Jotautienė, Algirdas Jasinskas, Juozas Pekarskas, Raimonda Zinkevičienė. Investigation of physical-mechanical properties and impact on soil of granulated manure compost fertilizers. 2019; 27(3):153-162. https://doi.org/10.3846/jeelm.2019.10794

[13] Hati K, Bandyoopadhay K. Fertilizers (Mineral, Organic), Effect On Soil Physical Properties. In: Gliński J, Horabik J, Lipiec J. (eds) Encyclopedia of Agrophysics. Encyclopedia of Earth Sciences Series. Springer, Dordrecht. 2021. https://doi.org/10.1007/978-90-481-3585-1201

[14] Lisowska A, Filipek-Mazur B, Sołtys J, Niemiec M, Gorczyca O, Bar-Michalczyk D, Komorowska M, Gródek-Szostak Z, Szeląg-Sikora A, Sikora J, Kuboń M. Preparation, Characterization of Granulated Sulfur Fertilizers and Their Effects on a Sandy Soils. Materials (Basel). 2022; 15(2):612. https://doi.org/10.3390/ma15020612

[15] Schjnning P, Christensen BT, Carstensen B. Physical and chemical properties of a sandy loam receiving animal manure, mineral fertilizer. 1994; 45(3). https://doi.org/10.1111/j.1365-2389.1994.tb00508.x

[16] Ostroha R, Yukhymenko M, Lytvynenko O, Lytvynenko A. Production of encapsulated organomineral fertilizers in a fluidized bed granulator. Acta Mechanica Slov. 2020; 24(2):50-55. https://doi.org/10.21496/ams.2020.031

[17] Dormeshkin OB, Muminov NSh, Khoshimov BT. Research of changes in the salt composition of complex fertilizers at the franco-pole stage. Universum: technical sciences. 2024; 6(123). https://7universum.com/ru/tech/archive/item/17669

[18] Nazarbek U, Abdurazova P, Nazarbekova S, Raiymbekov Y, Kambatyrov M. Processing of Phosphoric SolidWaste by Humic Acid Leaching Method. Inorganics. 2023; 11:90. https://doi.org/ 10.3390/inorganics11030090

[19] Saydullayev A, Namazov Sh, Mirsalimova S, N Usanbaev N, Temirov U. Influence of the amount and fineness of grinding of ammonium sulfate on the properties of sulfate-containing urea. IOP Conference Series: Earth and Environmental Science. 2023; 1142(1). https://doi.org/10.1088/1755-1315/1142/1/012091

[20] Temirov U, Doniyarov N, Jurakulov B, et al. Obtaining complex fertilizers based on low-grade phosphorites. E3S Web of Conferences. 2021; 264:04009. https://doi.org/10.1051/e3sconf/202126404009

Complex Use of Mineral Resources. 2025; 335(4):34-41 ISSN-L 2616-6445, ISSN 2224-5243

DOI: 10.31643/2025/6445.37
Engineering and Technologies

Research and development of wood-cement composites as sustainable building materials based on secondary resources

[1,2*]Ilmaliyev Zh., [3]Zhatkanbayev Ye.Ye., [4]Kurtibay K.A.

[1] Institute of Metallurgy and Ore Beneficiation JSC, Satbayev University, Almaty, Kazakhstan
[2]Urban Group LLP, Kazakhstan
[3] Kulazhanov Kazakh University of Technology and Business Joint-Stock Company, Astana, Kazakhstan
[4]Research and Production Center for Ecological and Industrial Biotechnology LLP, Astana, Kazakhstan

** Corresponding author email: jans2009@mail.ru*

Received: *July 11, 2024*
Peer-reviewed: *August 26, 2024*
Accepted: *September 6, 2024*

ABSTRACT

Conversion of waste into innovative materials that contribute to the sustainable development of infrastructure and the construction industry is an important task in today's society. Wood-cement composites which are building materials that combine wood components and a cement matrix are studied herein. These composites have a number of such advantages as high strength, excellent thermal insulation properties, durability and environmental friendliness. The manufactured composite material is a lightweight concrete based on secondary resources, binders and mineral components. Standardized measuring equipment and methods intended to analyze the chemical composition and physical and chemical properties of wood-cement composites (arbolite) were used in laboratory experimental tests. All samples studied were 40 mm × 40 mm × 160 mm lightweight concrete. Four options to obtain a wood-cement composite in various combinations of binders, minerals and other additives were proposed in the research work. All samples were tested to determine the physical and mechanical characteristics and the optimal composition with improved properties. Secondary resources in the form of wood waste and ash from combined heat and power plants (CHPP) were obtained from industrial structures of the Republic of Kazakhstan. An X-ray diffraction analysis of the CHPP ash was performed to determine the chemical mineral composition that showed a high content of silicon. According to the test results, the CH-4 sample demonstrated high physical and mechanical characteristics. The compression strength of the wood-cement composite sample reached 37.1 MPa, and the bending strength was 7.4 MPa on the 28th day, which proves the high performance properties of this composite.

Keywords: wood waste, CHP ashes, wood-cement composites, building materials, secondary resources, arbolite.

Information about authors:

Ilmaliyev Zhanserik	*Candidate of Legal Sciences, Institute of Metallurgy and Ore Beneficiation JSC, 050010, Almaty, Shevchenko str., 29; Project Manager of Urban Group LLP, Kazakhstan. E-mail: jans2009@mail.ru; ORCID ID: https://orcid.org/0000-0002-0979-0665*
Zhatkanbayev Yerlan Yerzhanovich	*D.Sc. in Engineering, Associate Professor, Kulazhanov Kazakh University of Technology and Business Joint-Stock Company, Kazakhstan, Astana, Kayim Mukhamedkhanov str., 37 A. ORCID ID: https://orcid.org/0000-0003-0656-239X*
Kurtibay Kuanysh	*Master of Natural Sciences, Researcher of the Research and Production Center for Ecological and Industrial Biotechnology LLP, Kazakhstan, Astana, Alikhan Bokeihan str., 27, office 49. ORCID ID: https://orcid.org/0000-0001-7822-0263*

Introduction

The United Nations (UN) Sustainable Development Goals (SDGs), established on September 15, 2015, under the title "Transforming our world: The 2030 Agenda for Sustainable Development" are crucial in context. Some of these UN Sustainable Development Goals, such as building resilient infrastructure, promoting inclusive and sustainable industrialization and innovation (Goal 11), sustainable cities and human settlements (Goal 11) and ensuring sustainable consumption and production patterns (Goal 12), are closely linked in improving the preparation of composite materials with the use of industrial waste for infrastructure development and construction in cities and communities' points of the world [1].

Global environmental challenges and the need for sustainable development of infrastructure and the construction industry have prompted scientists and engineers to look for innovative solutions to create efficient materials using secondary resources in recent decades. One of the promising areas is the development of wood-cement composites (DCC) with the use of wood waste. Wood-cement composites combine the properties of organic and inorganic materials, which provides them with high mechanical characteristics, durability, environmental friendliness and resistance to adverse environmental influences. Researchers have found that it is possible to improve the characteristics of arbolite concrete composites by purposefully changing their properties and structure with the use of various additives from industrial and vegetable waste [2].

Wood waste is a significant economic and environmental problem. Recent studies found that more than fifty million cubic meters of wood waste are generated annually in the European Union [3]. Given the current technological capabilities, the potential for recycling wood waste is still relatively low. It is due to the lack of sustainable methods and technologies for the reuse and recycling of secondary resources [4]. To date, the possibility to recycle wood waste can be either production of energy in the form of a renewable energy source, or use as an additive for building materials [5]. A study demonstrated that a structural arbolite with a strength of 1.5 to 6.0 MPa and a density in the range of 600–950 kg/m³ can be produced using organic cellulose aggregates in the form of wood waste [6]. These materials not only improve the mechanical properties of arbolite but also contribute to its environmental sustainability and energy efficiency. Arbolite has strength, biostability, fire resistance, frost resistance and other characteristics due to the mineral binder in the composition that not only make it more durable but also increases its performance in various conditions [7].

Research on wood sawdust and cement composites has been conducted by many scientists. In the works of Chowdhury S. and others [8], it was found that replacing part of the cement with wood ash leads to an increase in the flexural strength of the composite. The use of wood ash can improve the material's resistance to moisture and aggressive chemicals, as well as reduce its cost and environmental impact due to waste recycling. Furtos and colleagues investigated the properties of geopolymer composites reinforced with wood fiber and found that the inclusion of wood fiber helps to reduce the density and thermal conductivity of these new materials [9]. Coatanlem P. and colleagues conducted a study of lightweight concrete to which wood chips were added and confirmed that such concrete can be produced using wood chips as an additive [10]. They also found that the adhesion between wood chips and cement matrix could be improved by pre-soaking the chips in a liquid glass solution. Xiao Song and co-workers [11] demonstrated that cement-based wood composites made by the hydrostatic method with the addition of wood chips exhibited maximum flexural strength at a wood content of 30% and a particle size of 5.0–10.0 mm, while modification of wood with NaOH and silane binder improved their performance. Kasai et al. [12] used wood particles from construction waste to produce wood chip concrete, which had a density of 0.92 to 1.25 g/cm³ and demonstrated flexural strength in the range of 4–7 MPa and compressive strength from 5 to 8 MPa; The ratio between flexural strength and compressive strength was 0.5-0.9, which was higher than that of ordinary concrete, indicating the reinforcing effect of wood particles, and the addition of synthetic lightweight aggregates reduced the density to about 0.78 g/cm³ and resulted in lower flexural and compressive strength values, which were 2.05 and 2.2 MPa, respectively. In a study by Alireza Ashori et al. [13], the feasibility of using waste wooden railway sleepers as a filler for wood cement composites was investigated and the effects of pressing temperature (25 and 60 °C) and calcium chloride content (3%, 5% and 7% by weight of cement) on the physical and mechanical properties of the boards were assessed, finding that the addition of calcium chloride improved the properties of the boards and the maximum strength properties were achieved at pressing temperature of 25 °C and calcium chloride content of 7%, making WTRS suitable for use in lightweight concrete structures such as paneling, ceilings and partitions. A. Quiroga and colleagues investigated the effects of different wood treatment methods such as water extraction, alkaline hydrolysis and inhibitor retention on the mechanical properties of wood fibre and wood-cement composites, finding that alkaline hydrolysis was the most effective method to suppress inhibitors and improve the properties of the composites, and presented empirical relationships describing the effects of treatment on the compressive modulus and compressive strength [14]. Insulation materials with outstanding thermal insulation properties can be produced using corn cob particles. Shao and colleagues investigated the addition of these particles to solutions by varying their concentration (2.25%, 4.5% and 6.75%) and size (200 µm and 500 μm) [15]. Their work showed that this approach was effective in preventing self-shrinkage cracking. At the same time, Owczarek studied the effect of 1 mm corn cob particles on the mechanical properties of materials [16], finding that the addition of these particles reduced thermal conductivity and increased flexural strength. Kun Zhang and colleagues investigated eco-concrete with corn cob granules [17], shavings and wood chips, assessing the effect of replacing corn cob particles on the physical and mechanical properties of concrete. Using NMR and MRI, they found that the addition of biomass increased the content of harmful pores, which reduced the compressive strength. However, with the addition of wood chips up to 50%, the uniaxial compressive strength increased by 18.9% to 2.565 MPa, meeting the requirements for self-supporting wall blocks.

The purpose of this study is to develop an effective technology for the production of wood-cement composites with improved performance characteristics, such as mechanical, thermophysical properties, as well as to reduce the cost of building material due to the use of secondary natural and industrial resources.

Experimental part

2.1 Materials

This study used wood waste in the form of poplar sawdust from a wood processing plant in Karaganda, the Republic of Kazakhstan. The sawdust was crushed and sieved to produce a homogeneous fraction that is about 5mm in size for use in wood-cement composite. Ash from the Ekibastuz CHPP, Ekibastuz town, the Republic of Kazakhstan, and Portland cement of the M 400 brand were also used as a binder. Talcchlorite, calcium chloride, aluminum sulfate, hydrated lime and liquid glass of grade A were used in different combinations and ratios as an additive. Some samples of wood-cement composites were reinforced with polypropylene fibers of the Polyfiber PM54 brand with a fiber length of 18 mm.

2.2 Preparation of wood-cement composites

Wood-cement composites were manufactured in various combinations and ratios of mineral binder, reinforcing substances and additives with the use of wood sawdust. The preliminary test of composites was performed for four combinations (Table 1).

The sequence of introduction of components into the mixer was as follows. 50% of the consumed water was added to the mass of wood sawdust during the preparation process. It was stirred during 5 minutes to ensure its even distribution in the cement matrix. Then mineral and other additives, a reinforcing substance and a binder in the form of Portland cement and the CHPP ash according to the formulation and the rest of the water were introduced into the mass. The mixture was stirred for 1.5-2 hours. The finished cement paste was transferred into pre-prepared molds and formwork.

The formwork was a collapsible hollow cylinder with blind ends with a steel working pipe placed inside. The blocks were formed on a vibrating table, and the mixture was laid in layers.

Table 1 – Data on the quantitative contents of the preliminary test for wood-cement composite samples.

Name		CH-1	CH-2	CH-3	CH-4
		m, kg	**m, kg**	**m, kg**	**m, kg**
Organic filler	Wood sawdust	3.65	3.65	3.50	3.50
Binder	Portland cement M400	3.17	3.17	3.00	3.00
	CHPP ash	–	–	0.12	0.05
Supplements	Hydrated lime	0.16	0.16	0.45	0.45
	Grade A liquid glass	0.43	0.43	0.45	0.45
	Aluminum sulfate	0.20	0.20	0.15	–
	Calcium chloride	–	–	–	0.15
	Talcchlorite	0.45	0.45	0.45	0.45
Reinforcement	Polyfiber PM54 Polypropylene Fiber	0.01	–	0.01	–
Moistening	Water	2.5	2.5	3.3	3.3

The formwork was a collapsible hollow cylinder with blind ends with a steel working pipe placed inside. The blocks were formed on a vibrating table, and the mixture was laid in layers. The specimens were 40 mm × 40 mm × 160 mm as specified in JTG 3420–2020 (Test Methods for Cement and Concrete for Road Construction) [18]. In 24 hours after demolding, the samples were placed in a curing chamber with a temperature of 20 ± 2 °C and a relative humidity of more than 95%. Bending and compression strength tests were performed in 5 and 28 days, respectively. These conditions provided optimal parameters for the assessment of the mechanical properties of the composite material. The finished wood-cement composites were stacked and stored for further tests (Figure 1).

Figure 1 – Ready-made wood-cement composite blocks

2.3 Methods of analysis and testing.

2.3.1 Determination of the chemical composition of the CHPP ash.

Phase identification of the fly ash sample was performed with the powder X-ray diffraction method using the Rigaku Mini Flex II Desktop X-ray diffractometer manufactured by Rigaku Corporation (Tokyo, Japan) [19].

2.3.2 Compression and bending tests

The compression and bending tests of wood-cement composites were performed under the requirements of the JTG3420-2020 (ISO) specifications. For this purpose, three samples of 40 mm × 40 mm × 160 mm were prepared and kept under standard curing conditions for 5 and 28 days. After that, the samples were subjected to bending and compression tests [20]. Bending and compression strength tests were performed on the AGS-X series universal testing machine (Shimadzu, Japan).

The bending strength was determined by the equation (1). The average of the test results of three specimens was chosen as a representative bending strength. If the difference between the mean values was greater than ±10%, the test data were considered heterogeneous and the average of the remained data was taken as the final bending test results.

$$R_f = \frac{1.5 F_f L}{b^3} \tag{1}$$

Where R_f is the ultimate bending strength; F_f is the breaking load, N; L – a span of supports (100), mm; b is the cross-section width of the specimen (40), mm.

The compression strength was determined by equation (2), and the results were rounded to the nearest maximum and minimum values obtained during the tests. The average of the remained data was then calculated and taken as the final compression strength of the specimen.

$$R_c = \frac{F_c}{A} \tag{2}$$

Where R_c is the ultimate compressive on strength; F_c is the breaking load, N; A is the compressed area of the specimen, 40 mm × 40 mm.

Discussion of the results

3.1 X-ray diffraction analysis (XRD)

X-ray diffraction analysis was performed to determine the mineral composition of the CHPP ash. An X-ray of the sample is shown in Figure 2. X-ray diffraction analysis confirmed the presence of the minerals specified in Table 2.

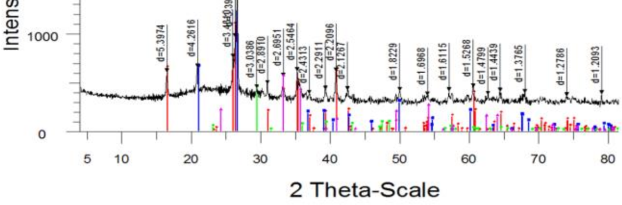

Figure 2 - X-ray diffraction pattern of the CHPP ash

Table 2 – X-ray diffraction analysis of the composition of the CHPP ash

Name	Formula	Content, %
Sillimanite	Al_2SiO_5	32.5
Mullite, syn A	$Al(Al_{0.83}Si_{1.08}O_{4.85})$	27.2
Hedenbergite	$CaFe+2Si_2O_6$	12.4
Quartz low, syn	SiO_2	8.7
Hematite, syn	Fe_2O_3	6.7

XRD analysis confirmed the presence of the minerals - Sillimanite (AI2SiO5), Mullite, syn A (Al(Al0.83 Si1.08 O4.85), Hedenbergite (CaFe+2Si2O6), Quartz low, syn (SiO2) and Hematite, syn (Fe2O3) in the CHPP ash sample. The XRD result showed that the silicon mineral content in the sample was higher than other existing minerals in the CHPP ash sample.

3.2 Compression and bending strength

Samples of the wood-cement composite were prepared in different combinations of components (Table 1) and tested for compression and bending strength on a universal testing machine AGS-X series (Shimadzu, Japan) to determine the optimal formulation. The test parameters were calculated according to equations (1) and (2). The following samples were tested: CH-1, CH-2, CH-3 and CH-4. The results obtained at the end of the tests are shown in Figure 3-4.

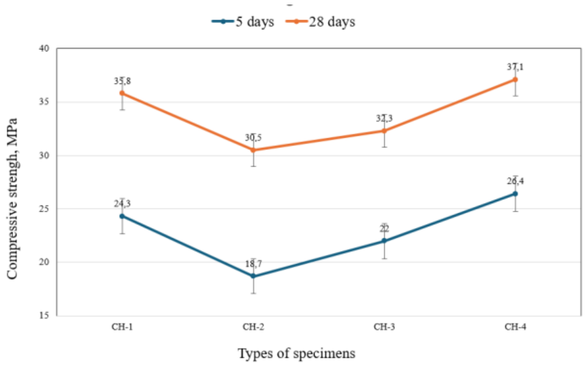

Figure 3 – Compression strength

Figure 3 shows that the wood-cement composite samples showed the same trend in compression strength on Day 5 and Day 28. The CH-4 sample had the highest compression strength, and the CH-2 sample had the least one of the prepared samples. The other two wood-cement composite samples showed relatively similar compression strength.

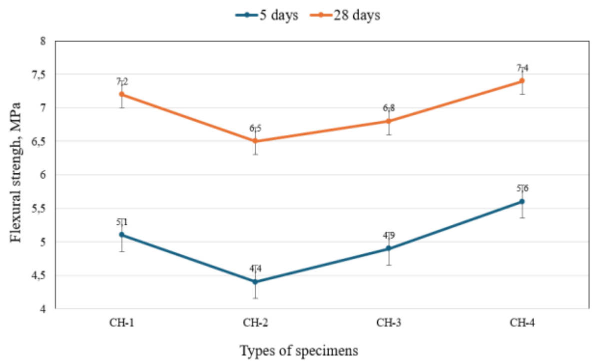

Figure 4 – Bending strength

As shown in Figure 4, the bending strength had a similar change tendency for the bending strength on Day 5 and Day 28 of the physical-mechanical measurement when it was tested with the testing machine. On the 28th day, the CH-4 sample showed the highest bending strength. Thus, the addition of CHPP ash and the use of calcium chloride as a mineral additive, as specified in Table 1, significantly improved the compression and bending strength of the CH-4 sample. So, we prove that the use of secondary resources such as CHPP ash and sawdust, in combination with mineral additives, can be an effective way to improve the performance of wood-cement composites, contributing to the creation of more sustainable and durable building materials.

Conclusions

A scientific study on the development of wood-cement composite blocks for use as building materials was carried out herein. Various mineral additives and secondary resources, such as wood sawdust and ash from the thermal power plant, were combined to achieve this goal, and several options for arbolite blocks were proposed. These components have shown high potential for the creation of wood-cement composites with improved physical and mechanical properties. Secondary resources in the form of wood waste and ash from combined heat and power plants (CHPP) were obtained from industrial structures of the Republic of Kazakhstan. An X-ray diffraction analysis of the CHPP ash was performed to determine the chemical mineral composition that showed a high content of silicon.

The CH-4 sample stood out among the proposed samples after the tests demonstrating high strength characteristics. The compression strength of the CH-4 sample reached up to 37.1 MPa, and the bending strength increased up to 7.4 MPa on Day 20. It proves the efficiency of use of secondary resources in the development and production of wood-cement composites for construction purposes. Recycling secondary resources into new materials that contribute to the sustainable development of infrastructure and the construction industry is an urgent task in the modern world.

This article can serve as an important reference and theoretical resource for the integration of wood waste into the composition of cement composites. It is planned in the future to continue research aimed at optimization of the proportion of wood chips in composites to improve their mechanical properties. Besides, future research will focus on the durability of these composites, their resistance to various external influences and operating conditions, as well as on identification of additional advantages and possible limitations on the use of wood waste in building materials.

Conflict of interest. The authors state that they have no known competing financial interests or personal relationships that could affect the work presented in this article.

CRediT author statement. Zh. Ilmaliyev: Supervision, Conceptualization, Methodology, Software. **K.Kurtibay:** Data processing, Writing - Original draft preparation, Review and editing. **Ye.Zhatkanbayev:** Visualization, Investigation, Software, Validation.

Acknowledgements. The work was supported by the Science Found ation JSC [Grant No. DP216814444].

Cite this article as: Ilmaliyev Zh, Zhatkanbayev YeYe, Kurtibay KA. Research and development of wood-cement composites as sustainable building materials based on secondary resources. Kompleksnoe Ispolzovanie Mineralnogo Syra = Complex Use of Mineral Resources. 2025; 335(4):34-41. https://doi.org/10.31643/2025/6445.37

Қайта өңделген ресурстарға негізделген тұрақты құрылыс материалдары ретінде ағаш цемент композиттік материалдарын зерттеу және дамыту

[1,2*]Ильмалиев Ж., [3]Жатканбаев Е.Е, [4]Куртибай К.А

[1] Металлургия және кен байыту институты АҚ, Сәтбаев университеті, Алматы, Қазақстан
[2]Urban Group ЖШС, Қазақстан
[3]Құлажанов атындағы Қазақ технология және бизнес университеті АҚ, Астана, Қазақстан
[4] Экологиялық және өндірістік биотехнологиялар ғылыми-өндірістік орталығы ЖШС, Астана, Қазақстан

Мақала келді: *11 шілде 2024*
Сараптамадан өтті: *26 тамыз 2024*
Қабылданды: *6 қыркүйек 2024*

ТҮЙІНДЕМЕ

Қалдықтарды инфрақұрылым мен құрылыс индустриясының тұрақты дамуына ықпал ететін инновациялық материалдарға айналдыру қазіргі қоғамдағы маңызды мәселе болып табылады. Бұл жұмыста ағаш компоненттері мен цемент матрицасын біріктіретін құрылыс материалдары болып табылатын ағаш-цемент композиттері зерттеледі. Бұл композиттердің жоғары беріктігі, тамаша жылу оқшаулағыш қасиеттері, беріктігі және қоршаған ортаға зиянсыздығы сияқты бірқатар артықшылықтары бар. Өндірілетін композиттік материал қайта өңделген ресурстарға, байланыстырғыштарға және минералды компоненттерге негізделген жеңіл бетон болып табылады. Зертханалық тәжірибелік сынақтар кезінде стандартталған өлшеу құралдары мен ағаш-цемент композиттерінің (арболит) химиялық құрамы мен физика-химиялық қасиеттерін талдау әдістері қолданылды. Барлық сыналған үлгілердің өлшемдері 40 мм × 40 мм × 160 мм болатын жеңіл бетон болды. Зерттеу жұмысында байланыстырғыштардың, минералдардың және басқа да қоспалардың әртүрлі комбинацияларында ағаш-цемент композициясын алудың төрт нұсқасы ұсынылды. Барлық үлгілер физикалық-механикалық сипаттамаларын және жақсартылған қасиеттері бар оңтайлы құрамды анықтау үшін сынақтан өтті. Ағаш қалдықтары мен жылу электр станцияларының күлі түріндегі қайталама ресурстар Қазақстан Республикасының өнеркәсіптік құрылымдарынан алынды. Химиялық минералдық құрамын анықтау үшін ЖЭС күліне рентгендік дифракциялық талдау жүргізілді, оның нәтижесінде кремнийдің жоғары мөлшері анықталды. Сынақ нәтижелері бойынша СН-4 үлгісі жоғары физикалық және механикалық сипаттамаларды көрсетті. Ағаш-цементті композициялық үлгінің қысуға беріктігі 37,1 МПа-ға жетті, ал иілу беріктігі 28-ші күні 7,4 МПа болды, бұл осы композиттің жоғары өнімділік қасиеттерін дәлелдейді.

Түйін сөздер: ағаш ағаш қалдықтары, ЖЭС күлі, ағаш-цемент композиттері, құрылыс материалдары, қайталама ресурстар, арболит (ағаш ұнтағы қосылып жасалатын жеңіл бетон түрі).

Ильмалиев Жансерик	***Авторлар туралы ақпарат:*** *Заң ғылымдарының кандидаты, Металлургия және кен байыту институты АҚ, 050010, Алматы, Шевченко к-сі, 29; Urban Group ЖШС жоба жетекшісі, Қазақстан. E-mail: jans2009@mail.ru; ORCID ID: https://orcid.org/0000-0002-0979-0665*
Жатканбаев Ерлан	*Т.ғ.д., доцент, Құлажанов атындағы Қазақ технология және бизнес университеті АҚ, Қайым Мұхамедханов көш., 37 А, Астана, Қазақстан. ORCID ID: https://orcid.org/0000-0003-0656-239X*
Куртибай Куаныш	*Ғылым магистрі, Экологиялық және өндірістік биотехнологиялар ғылыми-өндірістік орталығы ЖШС ғылыми қызметкері, Әлихан Бөкейхан көш., 27, Астана, Қазақстан. ORCID ID: https://orcid.org/0000-0001-7822-0263*

Исследование и разработка древесно-цементных композитных материалов как устойчивых строительных материалов на основе вторичных ресурсов

[1,2*]Ильмалиев Ж., [3]Жатканбаев Е.Е, [4]Куртибай К.А

[1] АО Институт металлургии и обогащения, Satbayev University, Алматы, Казахстан
[2]Urban Group LLP, Казахстан
[3]АО Казахский университет технологий и бизнеса имени Кулажанова, Астана, Казахстан
[4]ТОО Научно-производственной центр экологической и промышленной биотехнологии, Астана, Казахстан

Поступила: *11 июля 2024*
Рецензирование: *26 августа 2024*
Принята в печать: *6 сентября 2024*

АННОТАЦИЯ

Преобразование отходов в инновационные материалы, способствующие устойчивому развитию инфраструктуры и строительной отрасли, представляет собой важную задачу в современном обществе. В данной работе исследованы древесно-цементные композиты, которые представляют собой строительные материалы, объединяющие древесные компоненты и цементную матрицу. Эти композиты обладают рядом преимуществ, таких как высокая прочность, отличные теплоизоляционные свойства, долговечность и экологичность. Изготовленный композиционный материал представляет собой легкий бетон на основе вторичных ресурсов, связующих веществ и минеральных компонентов. При лабораторных экспериментальных испытаниях использовались стандартизированные измерительные оборудования и методики анализа химического состава и физико-химических свойств древесно-цементных композитов (арболита). Все исследуемые образцы были легким бетоном размером 40 мм × 40 мм × 160 мм. В исследовательской работе было предложено четыре варианта получения древесно-цементного композита в различных комбинациях связующих веществ, минеральных и других добавок. Все образцы подвергались испытаниям для определения физико-механических характеристик и оптимального состава с улучшенными свойствами. Вторичные ресурсы в виде древесных отходов и золы ТЭЦ были получены из промышленных структур Республики Казахстан. Проведен рентгеноструктурный анализ золы ТЭЦ для определения химического минерального состава, который выявил высокое содержание кремния. По результатам испытаний образец CH-4 продемонстрировал высокие физико-механические характеристики. Прочность на сжатие образца древесно-цементного композита достигла 37,1 МПа, а прочность на изгиб составила 7,4 МПа на 28-й день, что доказывает высокие эксплуатационные свойства данного композита.

Ключевые слова: древесные отходы, золы ТЭЦ, древесно-цементные композиты, строительные материалы, вторичные ресурсы, арболит.

Ильмалиев Жансерик	***Информация об авторах:*** *Кандидат юридических наук, АО Институт металлургии и обогащения, 050010, Алматы, ул. Шевченко, 29; Руководитель проектов компании Urban Group LLP, Казахстан. E-mail: jans2009@mail.ru; ORCID ID: https://orcid.org/0000-0002-0979-0665*
Жатканбаев Ерлан	*Доктор технических наук, доцент, АО Казахский университет технологий и бизнеса имени Кулажанова, ул. Кайыма Мухамедханова, 37 А, Астана, Казахстан. ORCID ID: https://orcid.org/0000-0003-0656-239X*
Куртибай Куаныш	*Магистр естествознания, научный сотрудник ТОО Научно-производственный центр экологической и промышленной биотехнологии, ул. Алихан Бокейхан 27, Астана, Казахстан. ORCID ID: https://orcid.org/0000-0001-7822-0263*

References

[1] United Nations. General Assembly Resolution A/RES/70/1. Transforming Our World: The 2030 Agenda for Sustainable Development. New York. 2015.

[2] Isakulov B, Abdullaev H, Mukasheva A, Akishev U, & Ordabayeva G. Investigation of the formation of microstructure and strength characteristics of slag-alkaline arbolite. EUREKA: Physics and Engineering. 2023; 2:209-221. https://doi.org/10.21303/2461-4262.2023.002814

[3] Bergeron FC. Energy and climate impact assessment of waste wood recovery in Switzerland. Biomass and Bioenergy. 2016; 94:245-257.

[4] Ramage M H, Burridge H, Busse-Wicher M, Fereday G, Reynolds T, Shah D U, Scherman O. The wood from the trees: The use of timber in construction. Renewable and sustainable energy reviews. 2017; 68:333-359. https://doi.org/10.1016/j.rser.2016.09.107

[5] Faraca G, Tonini, D, & Astrup T F. Dynamic accounting of greenhouse gas emissions from cascading utilisation of wood waste. Science of the Total Environment. 2019; 651:2689-2700. https://doi.org/10.1016/j.scitotenv.2018.10.136

[6] Bazhirov N S, Dauletiyarov M S, Bazhirov T S, Serikbayev B E, & Bazhirova K N. Research of waste of aluminum production as the raw components in technology of composite cementing materials. News of the national academy of sciences of the Republic of Kazakhstan. Series of geology and technical sciences. 2018; 1(427):93-98. https://doi.org/10.32014/2021.2518-1491.31

[7] Gonov M E. Mechanical properties of fiber-reinforced concrete under dynamic compression. Probl. Strength Plast. 2022; 84:130-148.

[8] Chowdhury S, Mishra M, & Suganya O M. The incorporation of wood waste ash as a partial cement replacement material for making structural grade concrete: An overview. Ain Shams Engineering Journal. 2015; 6(2):429-437. https://doi.org/10.1016/j.asej.2014.11.005

[9] Furtos G, Molnar L, Silaghi-Dumitrescu L, Pascuta P, Korniejenko K. Mechanical and thermal properties of wood fiber reinforced geopolymer composites. Journal of Natural Fibers. 2022; 19(13):6676-6691. https://doi.org/10.1080/15440478.2021.1929655

[10] Coatanlem P, Jauberthie R, & Rendell F. Lightweight wood chipping concrete durability. Construction and building Materials. 2006; 20(9):776-781.

[11] Song X, Zhou H, Liu Z, Li X, & Han C. Fabrication and mechanical properties of waste wood chips/cements composites for paving materials. Journal of Wood Chemistry and Technology. 2023; 43(3):164-175. https://doi.org/10.1080/02773813.2023.2202191

[12] Kasai Y, Kawamura M, & Zhou J D. Study on wood chip concrete with used timber. Special Publication, 1998; 179:905-928.

[13] Ashori A, Tabarsa T, & Amosi F. Evaluation of using waste timber railway sleepers in wood–cement composite materials. Construction and Building Materials. 2012; 27(1):126-129.

[14] Quiroga A, Marzocchi V, & Rintoul I. Influence of wood treatments on mechanical properties of wood–cement composites and of Populus Euroamericana wood fibers. Composites Part B: Engineering. 2016; 84:25-32. https://doi.org/10.1016/j.compositesb.2015.08.069

[15] Shao K, Du Y, & Zhou F. Effect of bio-based internal curing agent on the performance of high-performance mortar. Journal of Building Engineering. 2022; 49:104092. https://doi.org/10.1016/j.jobe.2022.104092

[16] Owczarek M. Study of the workability and mechanical properties of concrete with added ground corncobs. Materiali in tehnologije. 2022; 54(4):479-483. https://doi.org/10.17222/mit.2019.182

[17] Zhang K, Wang C, Zhao Y, Bi J, Shen M, & Deng X. Study on the effect of wood admixture on the physical and mechanical properties of corn cob ecological recycled concrete. Journal of Building Engineering. 2024; 88:109116. https://doi.org/10.1016/j.jobe.2024.109116

[18] JTG 3420-2020. Testing Methods of Cement and Concrete for Highway Engineering. Ministry of Transport of the People's Public of China: Beijing, China. 2020.

[19] McCarthy G J, Johansen D M, Steinwand S J, & Thedchanamoorthy A. X-ray diffraction analysis of fly ash. Advances in X-ray Analysis. 1987; 31:331-342. https://doi.org/10.1154/S037603080002214X

[20] Liu Z, Han C, Li Q, Li X, Zhou H, Song X, & Zu F. (2022). Study on wood chips modification and its application in wood-cement composites. Case Studies in Construction Materials. 2022; 17:e01350. https://doi.org/10.1016/j.cscm.2022.e01350

DOI: 10.31643/2025/6445.38
Metallurgy

Hydrothermal treatment of sinters containing thiosalts of non-ferrous metals

[1*] Kvyatkovskiy S.A., [1] Kozhakhmetov S.M., [1] Semenova A.S., [1] Dyussebekova M.A., [2] Shakhalov A.A.

[1] Institute of Metallurgy and Ore Beneficiation JSC, Satbayev University, Almaty, Kazakhstan
[2] Kazakhmys Corporation LLP, Balkhash, Republic of Kazakhstan

** Corresponding author email: s.kvyatkovskiy@satbayev.university*

Received: *May 30, 2024*
Peer-reviewed: *July 11, 2024*
Accepted: *September 10, 2024*

ABSTRACT
Preliminary experiments have shown that the solution to the environmental problem of recycling copper-electrolyte smelting slags is by sulfidization followed by leaching and subsequent separation of selenium, tellurium, arsenic, and antimony from the solution. The first operation of this technology, which provides high selectivity, is sintering. The results obtained indicate the formation of metal thiosalts during sintering in the presence of sodium sulfate and carbonate and a reducing agent at a temperature of 800 ^{0}C. An increase in temperature leads to the melting of individual components of the charge and a slowdown in the process of sulfidization of slag components. At lower temperatures, a decrease in the activity of the charge components is observed. The optimal addition of Na_2SO_4 was 27 % of the slag weight, and Na_2CO_3 - 8.5 % of the slag weight. Reducing agent consumption is 27 % of the slag weight, sintering time is 2 hours. The optimal parameters for leaching the resulting cakes are temperature 90 ^{0}C, L:S ratio = 3:1, leaching duration 2 hours, and sodium sulfide concentration 2 mol/l. The best results for cake melting from cake leaching are temperature 1200 ^{0}C, heating rate 10 ^{0}C/min, and holding time 30 minutes. Charge composition: cake, 30 % soda ash by weight of cake, 11 % activated carbon. During the smelting, a metallized phase was obtained, consisting mainly of lead (90-91 %), and slag was obtained with a residual content of lead and copper of no more than 0.5 %.

Keywords: slag, sintering, sintering, leaching, cake, smelting.

	Information about authors:
Kvyatkovskiy S.A.	*Doctor of Technical Sciences, Chief of the Laboratory of Pyrometallurgy Heavy Non-Ferrous Metals, Institute of Metallurgy and Ore Beneficiation JSC, Satbayev University, Shevchenko str., 29/133, 050010, Almaty, Kazakhstan. Email: s.kvyatkovskiy@satbayev.university; ORCID ID: https://orcid.org/0000-0002-9686-8642*
Kozhakhmetov S.M.	*Doctor of Technical Sciences, Professor, Chief Researcher of Laboratory of Pyrometallurgy Heavy Non-Ferrous Metals, Institute of Metallurgy and Ore Beneficiation JSC, Satbayev University, Shevchenko str., 29/133, 050010, Almaty, Kazakhstan. Email: s.kozhakhmetov@satbayev.university; ORCID ID: https://orcid.org/0000-0002-6955-4381*
Semenova A.S.	*Master, Lead Engineer of the Laboratory of Pyrometallurgy Heavy Non-Ferrous Metals, Institute of Metallurgy and Ore Beneficiation JSC, Satbayev University, Shevchenko str., 29/133, 050010, Almaty, Kazakhstan. Email: a.semenova@satbayev.university; ORCID ID: https://orcid.org/0000-0003-4054-8268*
Dyussebekova M.A.	*Doctor PhD, Junior Researcher of the Laboratory of Pyrometallurgy Heavy Non-Ferrous Metals, Institute of Metallurgy and Ore Beneficiation JSC, Satbayev University, Shevchenko str., 29/133, 050010, Almaty, Kazakhstan. Email: m.dyussebekova@satbayev.university; ORCID ID: https://orcid.org/0000-0002-4359-9784*
Shakhalov A.A.	*Engineer, Kazakhmys Corporation LLP, Balkhash, Republic of Kazakhstan. Email: a_shakhalov@inbox.ru; ORCID ID: https://orcid.org/0000-0002-6336-7534*

Introduction

The complex composition of artificial raw materials, comprising various heavy, minor, rare, and noble metals, presents substantial obstacles in devising technologies to transform them into viable products for the market. There is considerable focus on further processing copper smelting residues, including those derived from slag in copper smelting [[1], [2], [3], [4], [5], [6], [7]]. The wide possibilities for purposefully changing the properties of chemical compounds of non-ferrous metals to clarify fundamental issues of the relationship between the structure and properties of a substance, as well as to solve several applied problems, served as the basis for the development of a direction based on the metallurgy of thiosalts. One of the most promising is the improvement of functional properties, as well as the acquisition of new characteristics [[8], [9], [10]].

One of the ways to search for and develop new phases and materials using the method of directed synthesis is the study of phase equilibria. A large amount of research has been carried out in this direction. The phase diagrams of $CuInS_2$-$FeInS_2$, phase equilibria in the Cu_2S-La_2S_3-EuS system, and the polythermal section in the FeS-Sb_2S_3-Sm_2S_3 system were studied. Using DTA and X-ray diffraction methods, phase equilibria in the Cu_2S-Cu_3AsS_4-S system were studied, diagrams of the side quasi-binary systems Cu_2S-Cu_3AsS_4-S and Cu_3AsS_4-S were constructed, the fields of primary crystallization of phases, types and coordinates of non- and monovariant equilibria were determined [[11], [12], [13], [14]]. Phase equilibria in the Cu-Cu_2Se-As system have been studied [15]. The phase equilibria in the quasi-ternary system Ag_2S-SnS_2-Sb_2S_3 along the Ag_2SnS_3-$AgSbS_2$ cross section have been studied. It has been established that the Ag_2SnS_3-$AgSbS_2$ system is a quasi-binary cut of the eutectic type [16]. A phase magnetic diagram of solid solutions of the $CoCrS_4$-$Co_{0.5}Ga_{0.5}Cr_2S_4$ system has been constructed; the most common solid solutions on the diagram are those based on the ferrimagnetic semiconductor $CoCr_2S_4$, which exhibits properties in the field of magnetic ordering when measuring the temperature dependence of the dynamic susceptibility [17].

The electrical-physical properties of $(Sb_2S_3)1$-$x(PbCuSbS_3)x$ solid solutions, which are p-type semiconductors, have been studied [18]. The influence of the ratio of starting substances on the phase composition and electrical-physical properties of $Cu_{1.85}ZnSnS_4$ and $Cu_{1.5}Zn_{1.15}Sn_{0.85}S_4$ solid solutions obtained from binary sulfides and sulfur in the melt has been studied. It has been shown that $Cu_{1.5}Zn_{1.15}Sn_{0.85}S_4$ and $Cu_{1.85}ZnSnS_4$ solid solutions are p-type semiconductors [19]. The crystal structures of $SrLnCuS_3$ (Ln = Er, Yb) compounds were defined using methods of minimizing the derivative difference in the anisotropic approximation for all atoms. The structure of $SrLnCuS_3$ compounds is described by two-dimensional $[LnCuS_3]$ layers formed by distorted CuS_4 tetrahedra and LnS_6 octahedra, between which Sr^{2+} ions are located [20]. The ternary system Nd_2S_3-Ga_2S_3-EuS has been studied. A projection of the liquidus surface was constructed and the boundaries of the glass formation region were determined. It has been established that during thermolysis in an inert atmosphere at a temperature of 1010 K, glass $(Ga_2S_3)_{0.7}(Nd_2S_3)_{0.25}(EuS)_{0.05}$ softens and then crystallizes at 1110 K [21].

The results of studies of the spectral and luminescent properties of non-stereometric Ag-In-S and Cu-Zn-S nanoparticles obtained in aqueous solutions are summarized. The possibilities of size-selective deposition of nanoparticles from colloidal systems with photoluminescence quantum yields have been demonstrated [22]. The FeS-PbS system was studied using thermal, X-ray diffraction and microstructural analysis methods, and microhardness was measured. The system is a quasi-binary section and belongs to the eutectic type [23]. The Cu_2GeS_3-Ag_2GeS_3 system was studied in the temperature range 300-380 K. Current-generating reactions were determined, with the help of which standard thermodynamic functions of formation and standard entropies of Cu_2GeS_3 compounds and Cu_2-$xAgxGeS_3$ solid solutions were calculated [24].

Due to the dramatically changed composition of the mineral raw materials of copper production, the amount of impurities that must be extracted and disposed of is increasing. Such impurities are lead, zinc, arsenic, and antimony, which negatively affect the main process of copper extraction, reducing technical and economic indicators. The use of previously developed technologies does not allow for achieving high selectivity, as a result which there is a need to create a new complex technology that allows the extraction of all valuable metals into commercial products and the disposal of toxic components.

Experimental part

The object of research is the smelting slag produced by the precious metal shop of the Balkhash copper smelter. Slag is an oxidized material, the chemical composition of which includes, wt. %: 49.5 Pb, 17.3 SiO2, 1.5 Cu, 3.75 Sb, 13.3 Ba, 0.65 As, 4.5 Na, 0.2 Se, 0.24 Te, Au 0.39 g/t, Ag 7.3 g/t, 14.66 others. Experiments to identify optimal conditions for processing slags were carried out in three stages.

Stage 1 - sintering of slag with sodium sulfate and carbonate in the presence of carbon. Sintering was carried out in alundum crucibles in similar furnaces NTS 08/16 Nabertherm GmbH and SNOL 12/16. The sintering temperature is 500-800 ^{0}C, the heating rate of the furnaces to the experimental temperature is 10 ^{0}C/min. The holding time of the charge at the experimental temperature is 2 hours. The crucible was cooled with the furnace. After the experiment, the crucible was broken, the resulting cake was weighed and stored in a desiccator in an inert atmosphere to prevent the decomposition of the resulting sulfides and thiosalts. The sulfidization of non-ferrous metals, including the formation of their thiosalts, was previously established using microprobe analysis of sintered samples.

The 2-nd stage of the experiments consisted of leaching the resulting sinters. Leaching was carried out using standard laboratory equipment with a mechanical stirrer and electrical heating. The sinter was crushed in an amount of 100 g and leached at a ratio of sinter and sodium sulfide solution of 3:1, and 4:1 at temperatures of 50, 75, and 90 ^{0}C, leaching duration 1-2 hours. The content of sodium sulfide in the solution was 0-2 mol/l. The solution after filtration was analyzed for the content of antimony, arsenic, selenium and tellurium; the cake was washed with hot distilled water, dried at 50 ^{0}C and weighed. The cake and the resulting solution were analyzed for the content of major metals.

The 3rd stage consisted of melting the resulting sinter to get lead and noble metals into a separate phase. Meltings were carried out in the same furnaces as sintering at the first stage. The temperature of the melts varied between 1150-1250 ^{0}C, the heating rate to the experimental temperature was 10 ^{0}C/min. The exposure time at the experimental temperature was 30 minutes for all experiments. The sinter was melted with soda ash and activated carbon in various ratios.

At all stages of the experimental work, the problem of identifying optimal conditions for sintering, leaching and melting of leach sinters was solved.

Results and Discussion

Experiments carried out to study the process of sintering precious metal slag with sodium sulfate and carbonate in the presence of carbon indicate the possibility of obtaining a sinter containing metal sulfides and thiosalts. At temperatures of 500-600 ^{0}C, sintering of the charge components practically did not occur, therefore, sintered sinters obtained at a temperature of 800 ^{0}C were used, in which the process of formation of thiosalts took place. A temperature of 800 ^{0}C should be considered critical since at a higher temperature the components begin to melt.

The optimal addition of Na_2SO_4 was 27 % of the slag weight, and Na_2CO_3 - 8.5 % of the slag weight. The consumption of the reducing agent in the experiments was 6, 7, 8 g or 20, 23, 27 % of the weight of the slag, the sintering time was 2 hours. Each experiment was repeated 3 times, and approximately the same results were obtained for the weight of the sinter. The main technological parameters are given in Table 1.

Table 1 – Indicators of the sintering process of slag with charge components

Experiment no.	Sintering conditions	Charge composition, g				Sinter weight, g
		slag	Na_2SO_4	Na_2CO_3	coal	
1	t – 800 ^{0}C τ – 2 h	30	7.65	2.55	6	38.3-39.1
2					7	39.3-39.5
3					8	39.8-39.9

For leaching, cakes No. 1-3 were used, obtained in the corresponding experiments at a temperature of 800 ^{0}C with the addition of carbonate, sodium sulfate and a reducing agent to the mixture. The cake was filtered, dried and analyzed for lead, gold, silver and copper content. The solutions were analyzed for content

The results of leaching of three cakes obtained at 90 ^{0}C are presented in table 2 and in figures 1 and 2.

Table 2 - Compositions of sinter leaching products at optimal leaching parameters (temperature 90 ^{0}C, L:S = 3:1, leaching duration 2 hours, sodium sulfide content in solution 2 mol/l)

Sinter sample number	Solution composition, g/l				Cake composition				
	As	Sb	Te	Se	Pb, %	Cu, %	Au g/t	Ag, g/t	SiO_2, %
1	0.21	3.60	0.16	0.11	63.8	1.8	0.24	4.3	21.0
2	0.19	3.60	0.14	0.09	68.6	1.9	0.19	3.9	19.5
3	0.17	3.51	0.14	0.13	69.3	1.7	0.20	3.8	19.8

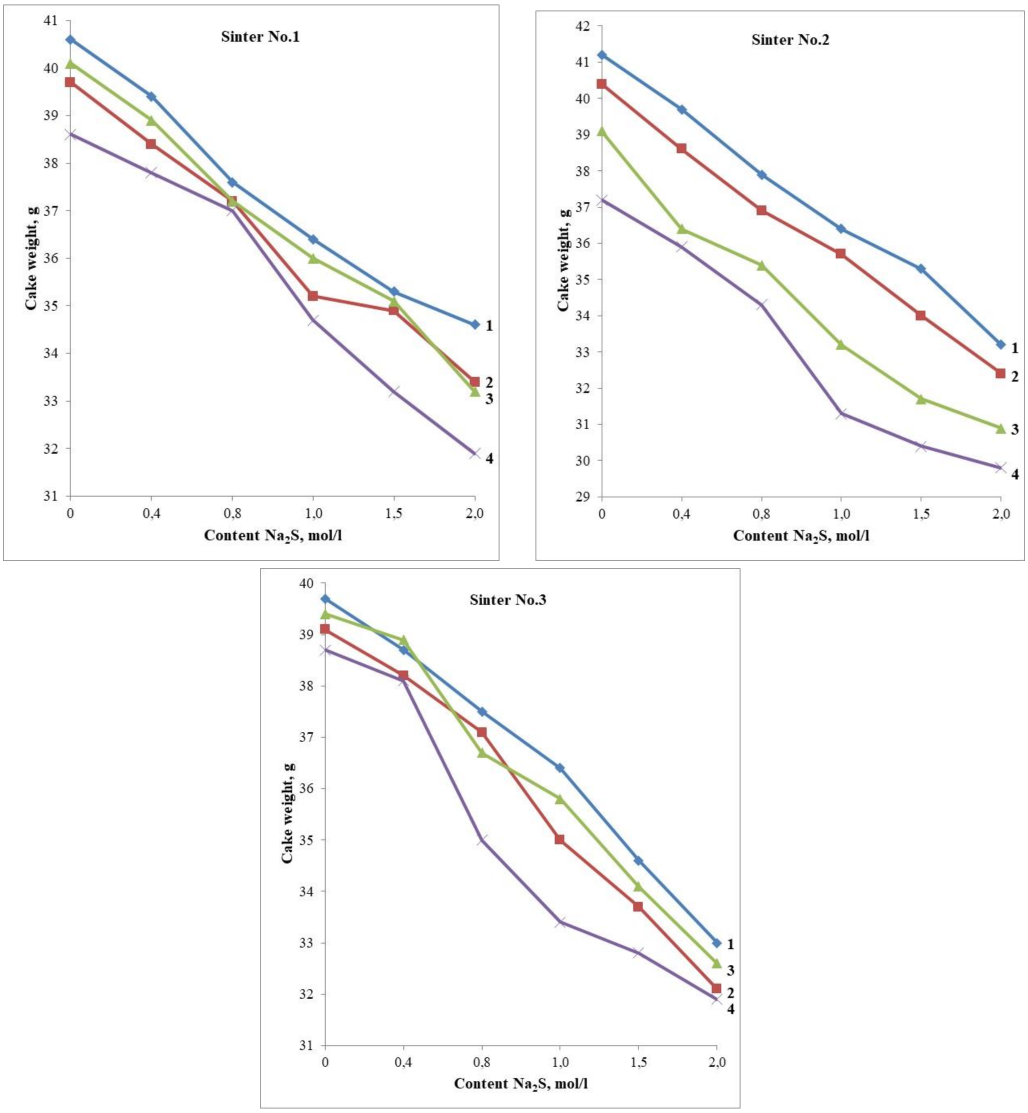

Conditions for cake leaching: 1–1 h, L:S=3:1; 2 – 2 hours, L:S=3:1; 3 – 1 hour, L:S=4:1; 4 – 2 hours, L:S=4:1.

Figure 1 – Variation in cake weight as a function of Na₂S concentration, L:S ratio, and leaching duration at 90°C

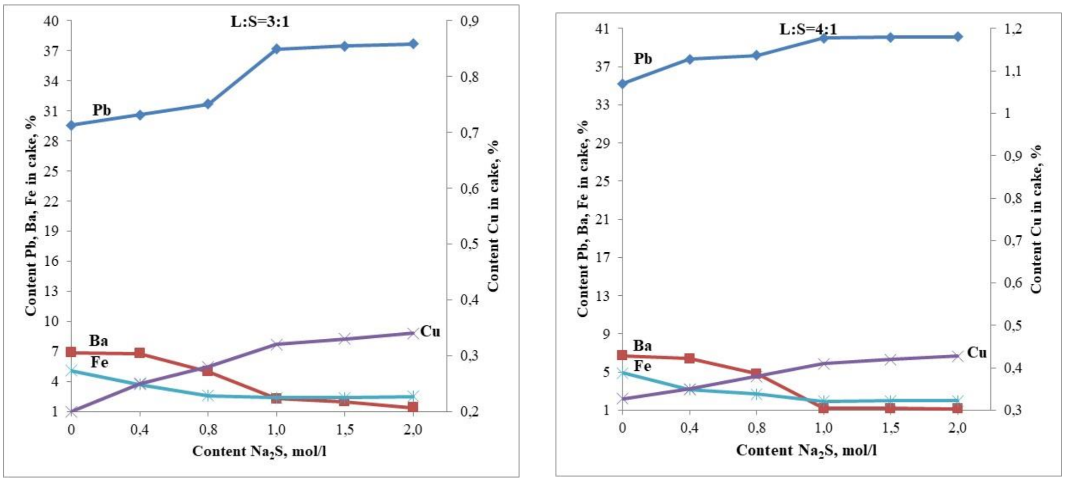

Figure 2 – Variations in metal content in leaching cake No. 2 based on sodium sulfide concentration at 90°C

The change in the weight of the cake remaining after leaching depending on the concentration of sodium sulfide in the solution and L:S is quite predictable. With an increase in the concentration of sodium sulfide in the solution, an increase in L:S and leaching time, the transition of sinter components into the solution increases. This is especially clearly visible when leaching sinter No. 2. Accordingly, during leaching in the residual cakes, the content of copper and lead increases and the content of arsenic and antimony decreases.

It has been established that the most complete leaching of the resulting cakes (slag, sulfate and sodium carbonate in the presence of a reducing agent) occurs at a temperature of 90 ^{0}C, L:S ratio = 3:1, leaching duration of 2 hours and sodium sulfide concentration in solution of 2 mol/l.

The 3rd stage of the experimental work consisted of melting the resulting cakes in order to get lead and noble metals into a separate phase. All previously obtained cakes were combined and averaged, thus, the average composition of the cakes was used for the melts. Meltings were carried out in the same furnaces as sintering at the first stage. The temperature of the melts varied between 1150-1250 ^{0}C, and the heating rate to the experimental temperature was 10 ^{0}C /min. The exposure time at the experimental temperature was 30 minutes for all experiments. The cake was melted with soda ash and activated carbon in various ratios.

Conditions for smelting:

- smelting No. 1: temperature 1150 ^{0}C, heating rate 10 ^{0}C /min, holding time 30 min; charge composition: 100 g cake, 25 g soda ash, 9 g activated carbon;
- smelting No. 2: temperature 1200 ^{0}C, heating rate 10 ^{0}C /min, holding time 30 min; charge composition: 100 g cake, 30 g soda ash, 11 g activated carbon;
- smelting No. 3: temperature 1200 ^{0}C, heating rate 10 ^{0}C /min, holding time 30 min; composition of the charge: 100 g cake, 30 g soda ash, 5 g activated carbon.

The results of the analysis of the compositions of the resulting products are shown in Table 3.

During the smelting, a metallized phase was obtained, consisting mainly of lead (90-91 %), and slag was obtained with a residual content of lead and copper of no more than 0.5 %. Thus, the optimal conditions for the processes of sintering slags with sodium sulfate and sodium carbonate in the presence of a reducing agent, leaching of cakes in a sodium sulfide solution and the process of melting leaching cakes with soda ash and activated carbon were determined.

Table 3 – Results of chemical analysis of cake leaching

Smelting no.	Content in metal			Content in slag, %		
	Pb, %	Au, g/t	Ag, g/t	Pb	Cu	Zn
1	90.81	0.8	14.4	0.2	0.3	0.02
2	91.79	0.9	14.1	0.5	0.4	0.02
3	91.85	0.85	13.8	0.3	0.3	0.01

Conclusions

The results obtained indicate the formation of metal thiosalts during sintering in the presence of sodium sulfate and carbonate and a reducing agent at a temperature of 800 ^{0}C. An increase in temperature leads to the melting of individual components of the charge and a slowdown in the process of sulfidization of slag components. At lower temperatures, a decrease in the activity of the charge components is observed. The best results were obtained with the addition of Na_2SO_4 – 27 % of the slag weight, and Na_2CO_3 – 8.5 % of the slag weight. Reducing agent consumption is 27 % of the slag weight, sintering time is 2 hours.

The optimal parameters for leaching the resulting cakes are temperature 90 ^{0}C, L:S ratio = 3:1, leaching duration 2 hours, sodium sulfide concentration 2 mol/l.

The best results for cake melting are temperature 1200 ^{0}C, heating rate 10 ^{0}C /min, and holding time 30 minutes. Charge composition: cake, 30 % soda ash by weight of cake, 11 % activated coal. During the smelting, a metallized phase was obtained, consisting mainly of lead (90-91 %), and slag was obtained with a residual content of lead and copper of no more than 0.5 %.

Conflicts of interest. On behalf of all authors, the corresponding author states that there is no conflict of interest.

CRediT author statement: **S. Kvyatkovskiy:** the idea of research; provided the support for the project and revised the draft; **S. Kozhakhmetov**: writing – review & editing; **A. Semenova**: performed the experiments and calculations; **M. Dyussebekova** and **A. Shakhalov**: data checking.

Acknowledgements. This research was funded by the Science Committee of the Ministry of Science and Higher Education of the Republic of Kazakhstan (Grant No. AP14869407, 2022-2024).

Cite this article as: Kvyatkovskiy SA, Kozhakhmetov SM, Semenova AS, Dyussebekova MA, Shakhalov AA. Hydrothermal treatment of sinters containing thiosalts of non-ferrous metals. Kompleksnoe Ispolzovanie Mineralnogo Syra = Complex Use of Mineral Resources. 2025; 335(4):42-49. https://doi.org/10.31643/2025/6445.38

Құрамында түсті металдардың тиотұздары бар күйежентекті гидротермиялық өңдеу

[1*] Квятковский С.А., [1] Кожахметов С.М., [1] Семенова А.С., [1] Дюсебекова М.А., [2] Шахалов А.А.

[1] Металлургия және кен байыту институты АҚ, Сәтбаев университеті, Алматы, Қазақстан
[2] Қазақмыс Корпорациясы ЖШС, Балқаш, Қазақстан

Мақала келді: *30 мамыр 2024*
Сараптамадан өтті: *11 шілде 2024*
Қабылданды: *10 қыркүйек 2024*

ТҮЙІНДЕМЕ

Алдын ала жүргізілген тәжірибелер мыс-электролитті балқыту қождарын қайта өңдеудің экологиялық мәселесін шешу сульфидтеу, одан кейін шаймалау және одан кейін ерітіндіден селен, теллур, мышьяк, сурьманы бөліп алу арқылы жүзеге асыруға болатындығын көрсетті. Жоғары селективтілікті қамтамасыз ететін бұл технологияның бірінші операциясы күйежентектеу болып табылады. Алынған нәтижелер 800 ^{0}С температурада натрий сульфаты мен карбонатының және тотықсыздандырғыштың қатысуымен күйежентектеу кезінде металл тиотұздарының түзілетінін көрсетеді. Температураның жоғарылауы шикіқұрамның жеке құрамдас бөліктерінің балқуына және қож компоненттерінің сульфидтену процесінің баяулауына әкеледі. Төмен температурада шикіқұрам компоненттерінің белсенділігінің төмендеуі байқалады. Na_2SO_4 оңтайлы қосындысы қож салмағының 27 %, Na_2CO_3 – қож салмағының 8,5 % құрады. Тотықсыздандырғыштың шығыны қож салмағының 27 % құрайды, күйежентектеу уақыты 2 сағат. Алынған сүзінділерді шаймалаудың оңтайлы параметрлері: температура 90 ^{0}С, L:S қатынасы = 3:1, шаймалау ұзақтығы 2 сағат, натрий сульфидінің концентрациясы 2 моль/л. Күйежентекті шаймалаудан алынған сүзінділерді балқыту үшін ең жақсы нәтижелер: температура 1200 ^{0}С, қыздыру жылдамдығы 10 ^{0}С/мин, ұстау уақыты 30 минут кезінде болады. Шикіқұрамның құрамы: сүзінді, сүзіндінің салмағы бойынша 30% кальцинденген сода, 11% белсендірілген көмір. Балқыту кезінде негізінен қорғасыннан (90-91%) тұратын металданған фаза, ал қорғасын мен мыстың қалдық мөлшері 0,5 % аспайтын қож алынды.

Түйін сөздер: қож, күйежентектеу, күйежентек, шаймалау, сүзінді, балқыту.

	Авторлар туралы ақпарат:
Квятковский Сергей Аркадьевич	*Техника ғылымдарының докторы, ауыр түсті металдар пирометаллургиясы зертханасының меңгерушісі, Металлургия және кен байыту институты АҚ, Сәтбаев университеті, Шевченко к-сі, 29/133, 050010, Алматы, Қазақстан. Email: s.kvyatkovskiy@satbayev.university; ORCID ID: https://orcid.org/0000-0002-9686-8642*
Кожахметов Султанбек Мырзахметович	*Техника ғылымдарының докторы, профессор, ауыр түсті металдар пирометаллургиясы зертханасының бас ғылыми қызметкері, Металлургия және кен байыту институты АҚ, Сәтбаев университеті, Шевченко к-сі, 29/133, 050010, Алматы, Қазақстан. Email: s.kozhakhmetov@satbayev.university; ORCID ID: https://orcid.org/0000-0002-6955-4381*
Семенова Анастасия Сергеевна	*Магистр, ауыр түсті металдар пирометаллургиясы зертханасының жетекші инженері, Металлургия және кен байыту институты АҚ, Сәтбаев университеті, Шевченко к-сі, 29/133, 050010, Алматы, Қазақстан. Email: a.semenova@satbayev.university; ORCID ID: https://orcid.org/0000-0003-4054-8268*
Дюсебекова Марал Адельбековна	*PhD, ауыр түсті металдар пирометаллургиясы зертханасының кіші ғылыми қызметкері, Металлургия және кен байыту институты АҚ, Сәтбаев университеті, Шевченко к-сі, 29/133, 050010, Алматы, Қазақстан. Email: a.semenova@satbayev.university; ORCID ID: https://orcid.org/0000-0002-4359-9784*
Шахалов Александр Александрович	*Қазақмыс корпорациясы ЖШС инженері, Балқаш, Қазақстан. Email: a_shakhalov@inbox.ru; ORCID ID: https://orcid.org/0000-0002-6336-7534*

Гидротермальная переработка спеков содержащих тиосоли цветных металлов

[1*] Квятковский С.А., [1] Кожахметов С.М., [1] Семенова А.С., [1] Дюсебекова М.А., [2] Шахалов А.А.

[1] АО Институт металлургии и обогащения, Satbayev University, Алматы, Казахстан
[2] ТОО Корпорация Казахмыс, Балхаш, Казахстан

Поступила: *30 мая 2024*
Рецензирование: *11 июля 2024*
Принята в печать: *10 сентября 2024*

АННОТАЦИЯ

Предварительными экспериментами показано, что решение экологической проблемы утилизации шлаков плавки медеэлектролитных шлаков достигается путем сульфидизации с последующим выщелачиванием и последующим выделением из раствора селена, теллура, мышьяка, сурьмы. Первой операцией этой технологии, обеспечивающей высокую селективность, является спекание. Полученные результаты свидетельствуют о прохождении процесса образования тиосолей металлов при спекании в присутствии сульфата и карбоната натрия и восстановителя при температуре 800 ^{0}C. Повышение температуры приводит к оплавлению отдельных компонентов шихты и замедлению процесса сульфидизации компонентов шлака. При более низких температурах наблюдается снижение активности компонентов шихты. Оптимальная добавка Na_2SO_4 составляла 27 % от веса шлака, Na_2CO_3 - 8,5 % от веса шлака. Расход восстановителя – 27 % от веса шлака, время спекания – 2 часа.

Оптимальные параметры выщелачивания полученных кеков - температура 90 ^{0}C, соотношении Ж:Т = 3:1, продолжительность выщелачивания 2 ч., концентрация сульфида натрия 2 моль/л. Лучшие результаты плавки кека от выщелачивания спеков – температура 1200 ^{0}C, скорость нагрева 10 ^{0}C/мин, выдержка 30 мин. Состав шихты: кек, 30 % кальцинированной соды от веса кека, 11 % активированного угля. При плавках была получена металлизированная фаза, состоящая в основном, из свинца (90-91 %) и был получен шлак с остаточным содержанием свинца и меди не более 0,5 %.

Ключевые слова: шлак, спекание, спек, выщелачивание, кек, плавка.

Информация об авторах:

Квятковский Сергей Аркадьевич	*Доктор технических наук, заведующий лабораторией пирометаллургии тяжелых цветных металлов, АО Институт металлургии и обогащения, Satbayev University, ул. Шевченко, 29/133, 050010, Алматы, Казахстан. Email: s.kvyatkovsky@satbaev.university; ORCID ID: https://orcid.org/0000-0002-9686-8642*
Кожахметов Султанбек Мырзахметович	*Доктор технических наук, профессор, главный научный сотрудник лаборатории пирометаллургии тяжелых цветных металлов, АО Институт металлургии и обогащения, Satbayev University, ул. Шевченко, 29/133, 050010, Алматы, Казахстан. Email: s.kozhakhmetov@satbaev.university; ORCID ID: https://orcid.org/0000-0002-6955-4381*
Семенова Анастасия Сергеевна	*Магистр, ведущий инженер лаборатории пирометаллургии тяжелых цветных металлов АО Институт металлургии и обогащения, Satbayev University, ул. Шевченко, 29/133, 050010, Алматы, Казахстан. Email: a.semenova@satbaev.university; ORCID ID: https://orcid.org/0000-0003-4054-8268*
Дюсебекова Марал Адельбековна	*Доктор PhD, младший научный сотрудник лаборатории пирометаллургии тяжелых цветных металлов, АО Институт металлургии и обогащения, Satbayev University, ул. Шевченко, 29/133, 050010, Алматы, Казахстан. Email: m.dyussebekova@satbayev.university; ORCID ID: https://orcid.org/0000-0002-4359-9784*
Шахалов Александр Александрович	*Инженер ТОО Корпорация Казахмыс, Балкаш, Казахстан. Email: a_shakhalov@inbox.ru; ORCID ID: https://orcid.org/0000-0002-6336-7534*

References

[1] Kenzhaliyev B, Kvyatkovskiy S, Dyussebekova M, Semenova A, Nurhadiyanto D. Analysis of Existing Technologies for Depletion of Dump Slags of Autogenous Melting. Kompleksnoe Ispolzovanie Mineralnogo Syra = Complex Use of Mineral Resources. 2022; 323(4):23-29. https://doi.org/10.31643/2022/6445.36

[2] Koizhanova A, Kenzhaliyev BK, Magomedov D, Erdenova M, Bakrayeva A, Abdyldaev N. Hydrometallurgical studies on the leaching of copper from man-made mineral formations. Kompleksnoe Ispolzovanie Mineralnogo Syra = Complex Use of Mineral Resources. 2023; 330(3):32-42. https://doi.org/10.31643/2024/6445.26

[3] Gorai B, Jana RK, Premchand. Characteristics and utilisation of copper slag - a review. Resources, Conservation and Recycling. 2003; 39:299-313. https://doi.org/10.1016/S0921-3449(02)00171-4

[4] Zhengqi Guo, Deqing Zhu, Jian Pan, Tengjiao Wu and Feng Zhang. Improving Beneficiation of Copper and Iron from Copper Slag by Modifying the Molten Copper Slag. Metals. 2016; 6:86. https://doi.ogr/10.3390/met6040086

[5] Tleugabulov S, Aitkenov N, Zhabalova G, Belichko A, UlevaG. Metallurgical processing of converter slag. Kompleksnoe Ispolzovanie Mineralnogo Syra = Complex Use of Mineral Resources. 2021; 318(3):35-42. https://doi.org/10.31643/2021/6445.26

[6] Kundu T, Senapati S, Das SK, Angadi SI, Rath SS. A comprehensive review on the recovery of copper values from copper slag. Powder Technology. 2023; 426:118693. https://doi.org/10.1016/j.powtec.2023.118693

[7] Klaffenbach E, Montenegro V, Guo M, Blanpain B. Sustainable and Comprehensive Utilization of Copper Slag: A Review and Critical Analysis. Journal of Sustainable Metallurgy. 2023; 9:468-496. https://doi.org/10.1007/s40831-023-00683-4

[8] Lampeka YD, Tsymbal LV. Preparation, structure and functional properties of MoS2 and WS2 nanocomposites with inorganic chalcogenide semiconductors: a review. Theoretical and experimental chemistry. 2017; 53(4):211-234. https://doi.org/10.1007/s11237-017-9523-9

[9] Monga D, Sharma S, Shetti N P, Basu S, Reddy K R, Aminabhavi T M. Advances in transition metal dichalcogenide-based two-dimensional nanomaterials. Materials Today Chemistry. 2021; 19:100399. https://doi.org/10.1016/j.mtchem.2020.100399

[10] Kopilov NI, Lata VA, Toguzov MZ. Vzaimodeistviya i fazovie sostoyaniya v rasplavah sulfidnih system [Interactions and phase states in melts of sulfide systems] Almaty: Gilim. 2001, 438. (in Russ.).

[11] Abdullaeva SS, Mammadov FM, Bakhtiyarly IB. Quasi-binary section CuInS2-FeIn2S4. Russian Journal of Inorganic Chemistry. 2020; 65(1):100-105. https://doi.org/10.1134/S0036023619110020

[12] Ruseikina AV, Andreev OV. Phase equilibria in the Cu2S-La2S3-EuS. Russian journal of inorganic chemistry. 2017; 62(5): 610-618. https://doi.org/10.1134/S0036023617050199

[13] Aliev OM, Asadov MM, Azhdarova DS, Mamedov SG, Ragimova VM. Polythermal section FeSb2S4-FeSm2S4 the FeS-Sb2S3-Sm2S3 system. Russian journal of inorganic chemistry. 2018; 63(6):833-836. https://doi.org/10.1134/S0036023618060037

[14] Gasanova ZT, Mashadieva LF, Babanly MB, Yusibov YA. Phasr equilibria in the Cu2S-Cu3AsS4-S system. Russian journal of inorganic chemistry. 2017; 62(5):591-597. https://doi.org/10.1134/S0036023617050126

[15] Mashadieva LF, Babanly MB, Gasanova ZT, Yusibov YA. Phase equilibria in the Cu-Cu2Se-As system. Russian journal of inorganic chemistry. 2017; 62(5):598-603. https://doi.org/10.1134/S0036023617050151

[16] Mammadov SH, Mammadov AN, Kurbanova RC. Quasi-binary section Ag2SnS-AgSbS2. Russian journal of inorganic chemistry. 2020; 65(2):217-221. https://doi.org/10.1134/S00360236001012X

[17] Aminov TG, Busheva EV, Shabunina GG, Novotortsev VM. Magnitic phase diagram of solid solution in the CoCr2S4-Cu0,5Ga0,5Cr2S4 system. Russian journal of inorganic chemistry. 2018; 63(4):519-529. https://doi.org/10.1134/S003602361804022

[18] Aliyev OM, Ajdarova DS, Maksudova TF, Mamedov SH, Agayeva RM. Phase relations along the Cu2S(Sb2S3, PbSb2S4, Pb5Sb4S11)-PbCuSbS3 joins in the pseudoternary system Cu2S-PbS-Sb2S3 and physical properties of (Sb2S3)1-x(PbCuSbS3)x solid solutions. Inorganic Materials. 2018; 54(12):1199-1204. https://doi.org/10.1134/S000168518120014

[19] Gapanovich MV, Agapkin MD, Rakitin VV, Kolesnikova AM, Novikov GF, Odin IN, Sedlovets DM. Effect of precursor mixture composition on the phase composition and electrical transport properties of Cu1,85ZnSnS4 and Cu1,5Zn1,15Sn0,85S4 kesterite solid solutions prepared in molten KI.Inorganic Materials. 2018; 54(8):760-766. https://doi.org/10.1134/S00201685180806X

[20] Ruseikina AV, Solov'ev LA, Galenko EO, Grigor'ev MV. Refined crystal structures of SrLnCcuS3 (Ln = Er, Yb). Russian Journal of Inorganic Chemistry. 2018; 63(9):1225-1231. https://doi.org/10.1134/s0036023618090140

[21] Serikbaeva AK, Aimova MZ, Mamyrbaeva KK, et al. Development of a method for reprocessing technogenic lead production raw materials to extract rhenium and arsenic. Metallurgist. 2021; 65(3-4):340-348. https://doi.org/10.1007/s11015-021-01162-5

[22] Raevskaya AE, Stroyuk OL, Kuchmy SY. Nanoparticles of Ag-In-S and Cu-In-S in aqueous media: preparation, spectral and luminescent properties. Theoretical and Experimental Chemistry. 2017; 53(5):338-348. https://doi.prg/10.1007/s11237-017-9533-7

[23] Gasanova UA, Aliev OM, Bakhtiyarly IB, Mamedov SG. The FeS-PbS system. Russian Journal of Inorganic Chemistry. 2019; 64(2):242-246. https://doi.org/10.1134/S0036023619020074

[24] Alverdiev I J, Abbasova VA, Yusibov YV, Tagiev DB, Babanly MB. Thermodynamic study of Cu2GeS3 and Cu2-xAgxGeS3 solid solutions by the emf method with a Cu4RbCl3I2 solid electrolyte. Russian Journal of Electrochemistry. 2018; 54(2):195-200. https://doi.org/10.1134/S10231935180200027

Complex Use of Mineral Resources. 2025; 335(4):50-58 ISSN-L 2616-6445, ISSN 2224-5243

DOI: 10.31643/2025/6445.39
Metallurgy

Effect of amino acids on the extraction of copper from sub-conditional raw materials

[1]Abdulvaliev R.A., [1]Surkova T.Yu., [1]Baltabekova Zh.A., [1]Yessimova D.M., [2]Stachowicz M., [1]Smailov K.M., *[1]Dossymbayeva Z.D., [1]Berkinbayeva A.N.

[1]Institute of Metallurgy and Ore Beneficiation JSC, Satbayev University, Almaty, Kazakhstan
[2] Wroclaw University of Science and Technology, Wroclaw, Poland

Corresponding author email: z.dosymbaeva@satbayev.university

Received: *May 28, 2024*
Peer-reviewed: *June 28, 2024*
Accepted: *September 13, 2024*

ABSTRACT

The decrease in the quality of mineral raw materials processed by industry, as well as the increase in requirements for environmental protection, necessitate the development of new directions in the technology of their processing. Biogeotechnology refers to one of the modern areas of scientific and technological progress in the field of processing mineral raw materials. Biologically active additives are increasingly used along with the use of microorganisms in the extraction processes for non-ferrous and precious metals, in particular amino acids which are an integral part of the culture liquid of microorganisms. The processes of sulfuric acid leaching of copper from low-grade ore in the presence of amino acids of different structures and their effect on copper electrolysis were studied. Low-grade ore from one of the Kazakhstan deposits was used as the starting raw material. The copper content in the ore is 0.39%. The diffusion nature of the restrictions was established during the study of the kinetics of the process of sulfuric acid leaching of copper, and the rate constants and value of the effective activation energy were calculated, which amounted to 1.817 kJ/mol. The effect of amino acids with different structures on the leaching process was studied. The positive effect was increased in the glycine - leucine - cysteine - histidine - asparagine series. Depending on the structure of the amino acid, the degree of copper extraction into the solution increases in the range of 1-15%. The effect of aminoacetic acid as a biologically active additive on the process of electrolysis of copper from poor solutions was studied. It was established that the process is inhibited by the reduction of monovalent copper to the metallic state in the presence of glycine.

Keywords: amino acids, copper, leaching, mineral raw materials, microorganisms.

	Information about authors:
Abdulvaliev R.A.	*Candidate of Technical Sciences, head of the laboratory of alumina and aluminum, Institute of Metallurgy and Ore Beneficiation JSC, Satbayev University, Almaty, Kazakhstan. Email: r.abdulvaliyev@satbayev.university; ORCID ID: https://orcid.org/0000-0001-6747-6984*
Surkova T.Yu.	*Candidate of technical sciences, a leading researcher of a laboratory ofspecial methods of hydrometallurgy named after B.B. Beisembayev, Institute of Metallurgy and Ore Beneficiation JSC, Satbayev University, Almaty, Kazakhstan. Email: t.surkova@satbayev.university; ORCID ID: https://orcid.org/0000-0001-8271-125X*
Baltabekova Zh.A.	*Researcher, Institute of Metallurgy and Ore Beneficiation JSC, Satbayev University, Almaty, Kazakhstan. Email: zh.baltabekova@satbayev.university; ORCID ID: https://orcid.org/0000-0003-3076-0652*
Yessimova D.M.	*Researcher, Institute of Metallurgy and Ore Beneficiation JSC, Satbayev University, Almaty, Kazakhstan. Email: d.yessimova@satbayev.university; ORCID ID: https://orcid.org/0000-0002-1582-6732*
Stachowicz M.	*Ph.D. Eng. Wroclaw University of Science and Technology | WUT · Faculty of Mechanical Engineering, Wroclaw, Poland. Email: mateusz.stachowicz@pwr.edu.pl; ORCID ID: https://orcid.org/0000-0003-2995-269X*
Smailov K.M.	*Researcher, Institute of Metallurgy and Ore Beneficiation JSC, Satbayev University, Almaty, Kazakhstan. Email: k.smailov@satbayev.university; ORCID ID: https://orcid.org/0000-0002-9277-5254*
Dossymbayeva Z.D.	*Researcher, Institute of Metallurgy and Ore Beneficiation JSC, Satbayev University, Almaty, Kazakhstan. Email: z.dosymbaeva@satbayev.university; ORCID ID: https://orcid.org/0000-0001-9144-208X*
Berkinbayeva A.N.	*Candidate of technical sciences, a head of chemical analytical laboratory, Institute of Metallurgy and Ore Beneficiation JSC, Satbayev University, Almaty, Kazakhstan. E-mail: a.berkinbayeva@satbayev.university; ORCID ID: https://orcid.org/0000-0002-2569-9087*

Introduction

Currently, SX-EW technology (leaching - liquid extraction - electrochemical reduction) is widely introduced into the world industry to process low-grade copper ores. It involves sulfuric acid leaching of the original ore [1]. The copper extraction degree into solution depends primarily on the composition of the original ore. This method is most suitable for oxidized ores. Up to 90% copper can be extracted into solution from oxidized ores during sulfuric acid leaching [2]. Biooxidation is used along with sulfuric acid leaching for ores with more complex mineralogical composition, in particular for sulfide and mixed ores. Biooxidation is an attractive alternative to traditional physical and chemical methods of ore beneficiation, due to the reduced resource intensity of the technology and less harmful effects on the environment [[3], [4]]. Biotechnology for the extraction of copper from low-grade ore was first introduced on an industrial scale in 1982 at the *Lo Aguirre copper mine of Sociedad Minera Pudahuel* (Chile). Then a similar process was introduced at 17 enterprises, including 10 mines in Chile, as well as in the USA, Peru, and Australia [5].

Such metals as copper, uranium, nickel and gold are obtained with the use of biohydrometallurgy [[6], [7], [8]]. The basis of biohydrometallurgical technologies are the microbial oxidation processes for hard-to-open minerals by acidophilic microorganisms [9]. The use of microorganisms in the processes of extraction of non-ferrous and precious metals can significantly increase the complexity of the use of raw materials and ensure effective environmental protection.

At the same time, some works dedicated to the leaching of low-grade copper-containing ores in the presence of amino acids, which are an integral part of the culture fluid during bioleaching, appeared recently.

The authors studied the leaching of chalcopyrite concentrate from the Sarcheshmeh copper mine (Kerman, Iran) in a solution of aminoacetic acid (glycine) in the presence of oxygen [[10], [11]]. The effect of such parameters as glycine concentration (0.4–2 M), temperature (30–90 °C), stirring speed (250–750 rpm), pH (9–12), oxygen consumption (0.5 –2 l/min) and pulp density (1–20%) was studied. Research was performed to extract copper from chalcopyrite concentrate. The results show that an increase in temperature from 30 to 60 ˚C increases copper recovery, while at temperatures above 60 ˚C, there is a decrease in copper recovery, probably as a result of the conversion of glycine to glycinate and a decrease in oxygen solubility. Moreover, long leaching times at higher pH levels (10.5 and 12) result in decreased copper recovery, primarily due to the chemical precipitation of copper sulfide and crystallization of copper glycinate. When pulp density increases from 1 to 20%, copper recovery decreases significantly. According to the results obtained, the authors recommend using glycine leaching under optimal conditions in the presence of oxygen for the processing of low-grade chalcopyrite concentrates and ores, as well as tailings shows the efficiency of leaching copper contained in low-grade ores in a solution of 0.1 mol/dm^3 sodium chloride, in the presence of 0.05 mol/dm^3 glycine or aspartic acid at a temperature of 80 ^{o}C for 15 hours [12]. The copper extraction degree achieved was 90%. The object of study was ore crushed to a particle size of 2–3 mm with a copper content of 1.0%. Good results were also obtained with the use of phenylalanine hydrochloride, serine hydrochloride and protein hydrolysates. Baker's yeast was used with a crude protein content of 52% and nucleic acids of 5.8% to obtain protein hydrolysates. Copper recovery was at least 92%. It was established that the ability of protein hydrolyzate to interact with copper ions is due to its amino acid composition, i.e. the high content of aspartic acid and glycine.

Thus, it follows from the above sources that bioleaching is increasingly introduced into the technological process; however, bioprocesses are quite lengthy. Besides, they require adaptation of microorganisms to environmental conditions, and therefore, copper leaching study with the use of substandard ores with sulfuric acid in the presence of amino acids, and the effect of their structure on the leaching process characteristics, is of great interest.

The final stage of SX–EW technology is copper electrolysis. The process conditions continuously change during its electrolytic separation from dilute solutions in a periodic mode: with a decrease in copper concentration, the limiting current density continuously decreases, and it increasingly exceeds the limit while maintaining a constant electrolysis current density, and the evolution of hydrogen becomes more and more intense [13]. It is especially noticeable during the extraction of copper from waste electrolytes and poor solutions. In addition to reducing process performance, there is a negative impact of released gases (sulfur dioxide and hydrogen in large quantities) on the environment. At the same time, describes new methods for the formation of electrolytes using amino acids as buffering, complexing and surfactant additives for nickel [14]. They help to reduce the negative burden on the environment without compromising the quality of the final product.

In connection with the above, the purpose of this work is to study the influence of amino acids, in particular, their structure on the degree of leaching of copper with sulfuric acid from substandard ores, as well as on its electrolytic reduction from sulfuric acid solutions.

Experimental part

Research methods. Test experiments intended to leach the original copper ore were performed to determine the optimal conditions for its leaching. A unit including a reactor with a mechanical stirrer of the PE 8399 brand from Ekros was used to leach the original ore. Optimal conditions were established. They are sulfuric acid concentration – 40 g/dm^3, room temperature, process duration – 4 hours, S:L ratio = 1:4.

The leaching process kinetics was studied by transfer of a solution of sulfuric acid in the amount of 0.1 dm^3 (acid concentration was 40 g/dm^3) and ore in a ratio S:L = 1:4, as well as the specified amount of amino acid, in 0.25 dm^3 conical flasks. The concentration of aminoacetic acid (glycine) was 0.05, 0.1 and 0.5 M/dm^3, and that of leucine, asparagine, histidine and cysteine was 0.5 M/dm^3. The flasks were hermetically sealed, and their contents were intensively mixed on an orbital shaker. The number of flasks was equal to the number of samples taken during the sorption process and corresponded to the number of points on the graph. All experiments were performed in duplicate. The result was equal to the average value.

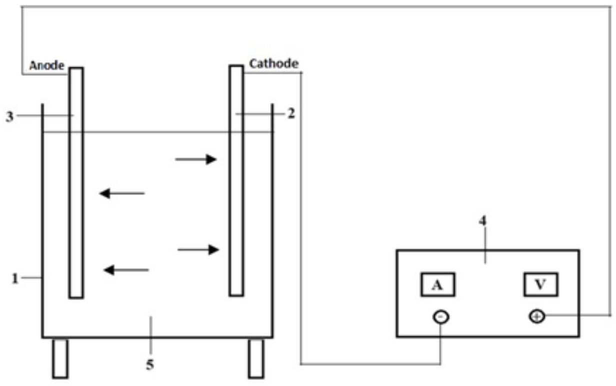

Figure 1 – Unit for copper electrolysis
1 - electrolysis bath; 2- cathode; 3 – anode;
4 – rectifier; 5 – electrolyte

Copper electrolysis was performed in a unit schematically shown in Figure 1. Stainless steel was used as the anode, and lead was used as the anode. The concentration of copper sulfate was 1 g/dm^3 and glycine - 0.05-0.5 M/dm^3.

Analysis methods

The quantitative content of copper was determined in leaching solutions of the original ore, as well as during the electrolysis process with the use of an Optima 8000DV inductively coupled plasma (ICP) atomic emission spectrometer.

X-ray diffraction data of the ore were obtained with a D8 Advance diffractometer (Bruker AXS GmbH) with a cobalt anode, a - Cu radiation, and X-ray fluorescence data - with a Venus 200 “PANalytical” wave-dispersive spectrometer. Diffraction patterns were interpreted, and interplanar distances were calculated with EVA software. The samples were interpreted, and phases were searched with the use of the “Search/match” program with the ASTM card database.

The method of scanning electron microscopy (SEM) and X-ray spectral microanalysis (XMA) was performed on a JEOL device - JXA-8230.

Substandard ore was used during the research. It was crushed to a particle size of 0.071 mm. Comprehensive studies of this ore were previously performed using X-ray fluorescence, chemical, and X-ray phase analysis, as well as scanning electron microscopy (SEM) and X-ray spectral microanalysis (XMA). The main component of the ore is quartz according to phase analysis (Table 1), i.e. the ores are dominated by silicate rocks, with smaller quantities containing clinochlore, muscovite, albite and microcline.

Table 1 - Phase composition of ore from the Bayskoye deposit

Name	Formula	Content, %
Quartz, syn	SiO2	39.4%
Albite	Na(AlSi3O8)	21.5%
Microcline, intermediate	KAlSi3O8	16.8%
Clinochlore-1MIIb, ferroan	(Mg,Fe)6(Si,Al)4O10(OH)8	11.4%
Muscovite-2M1	KAl2(AlSi3O10)(OH)2	10.8%

The elemental composition of the ore is presented in Table 2. It follows from there that the main elements are creamium, potassium, calcium, sodium, magnesium and iron.

Table 2 - Results of X-ray fluorescence analysis of the initial ore of the Bayskoye deposit

O	Na	Mg	Al	Si	P	S	Cl	K	Ca	Ti
56.142	1.413	1.385	7.077	25.813	0.078	1.142	0.027	1.837	0.753	0.614
Mn	Fe	Cu	Zn	As	Rb	Sr	Zr	Ni	Pb	
0.018	3.006	0.626	0.04	0.014	0.011	0.011	0.012	0.175	0.007	

The ore, along with copper, also contains zinc and lead according to scanning electron microscopy and X-ray microanalysis (Fig. 2), i.e. the ore is classified as polymetallic, and the host rock, along with silicates, includes chlorides and antimony compounds. The copper content in the ore sample was 0.39% according to chemical analysis.

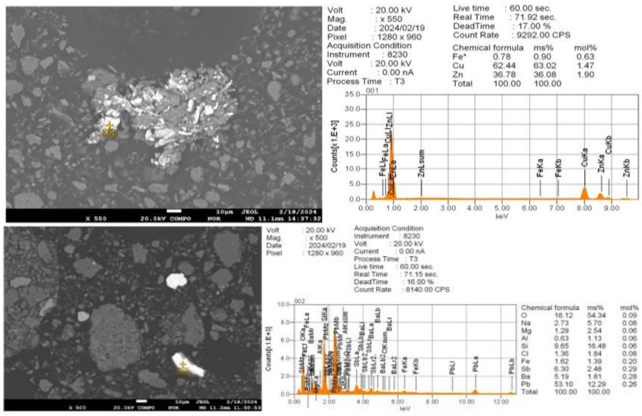
Volt : 20.00 kV
Mag. : x 550
Date : 2024/02/19
Pixel : 1280 x 960
Acquisition Condition
Instrument : 8230
Volt : 20.00 kV
Current : 0.00 nA
Process Time : T3

Live time : 60.00 sec.
Real Time : 71.92 sec.
DeadTime : 17.00 %
Count Rate : 9292.00 CPS

Chemical formula		ms%	mol%
Fe*	0.78	0.90	0.63
Cu	62.44	63.02	1.47
Zn	36.78	36.08	1.90
Total	100.00	100.00	

Volt : 20.00 kV
Mag. : x 500
Date : 2024/02/19
Pixel : 1280 x 960

Acquisition Condition
Instrument : 8230
Volt : 20.00 kV
Current : 0.00 nA
Process Time : T3
Live time : 60.00 sec.
Real Time : 71.15 sec.
DeadTime : 16.00 %
Count Rate : 8140.00 CPS

Chemical formula		ms%	mol%
O	18.12	54.34	0.09
Na	2.73	5.70	0.08
Mg	1.29	2.54	0.06
Al	0.63	1.13	0.06
Si	9.65	16.48	0.06
Cl	1.36	1.84	0.08
Fe	1.62	1.39	0.20
Sb	6.30	2.48	0.29
Ba	5.19	1.81	0.28
Pb	53.10	12.29	0.26
Total	100.00	100.00	

Figure 2 – Results of scanning electron microscopy and X-ray microanalysis

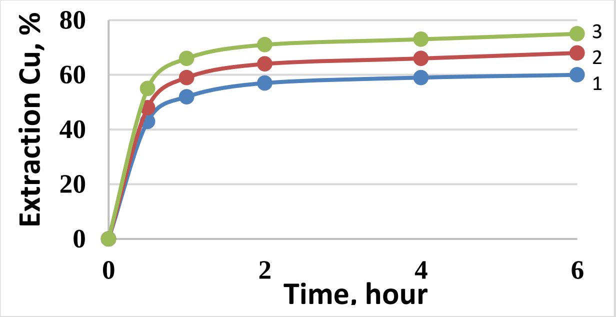

Figure 3 – Kinetic curves of copper leaching with sulfuric acid solution, temperature, °C: 1 - 20; 1 – 40; 3 – 60.

The kinetics of the copper leaching process from this raw material with sulfuric acid was studied in the process of studying the physical and chemical patterns of dissolution of non-ferrous metals. Figure 3 shows the kinetic curves of copper leaching at temperatures of 20, 40, and 60 °C.

Based on the results obtained with the use of the Arrhenius equation, the copper leaching rate constants presented in Table 3 and the effective activation energy were calculated. It was 1.817 kJ/mol.

Table 1.2.3 – Values of copper leaching rate constants at different temperatures and their logarithms

Leaching rate constant	*T*, K		
	293.0	313.0	333.0
К · 10^{-4}, sec^{-1}	4.61	5.18	5.66
lgK	-3.337	-3.285	-3.247

The calculated value of the effective activation energy (1.817 kJ/mol) indicates that the limiting stage of the leaching of copper compounds is diffusion.

In practice, there are several methods intended to remove diffusion inhibition. It is an increase in temperature, the speed of mixing the solution, and the use of surfactants.

It can be assumed that amino acids will also prove to be an additive that stimulates the process because the formation of copper complex compounds with amino acids is possible according to the literature. It can help to increase the degree of copper extraction into solution [[15], [16]].

The effect of amino acid concentration, using glycine as an example, on the kinetics of copper leaching was studied during the research. The glycine concentration was 0.05 and 0.5 M/dm^3. The results obtained are presented in Table 4. It follows from Table 4 that the main amount of copper is leached during the first two hours. The copper extraction degree increases as the concentration of amino acids increases. When the glycine concentration increases from 0.05 to 0.5 M/dm^3, the degree of copper extraction increases from 64.8 to 75.1%.

Table 4 - Dependence of the degree of copper extraction on the concentration of glycine in the solution.

Extraction rate, %				
Time of	Glycine concentration, M/dm^3			
	0	0.05	0.1	0.5
30	39.9	42.1	45.5	48.1
60	50.3	53.3	57.8	62.8
120	55.4	57.6	66.4	70.1
240	60.2	62.2	69.5	73.9
360	61.9	64.8	70.9	75.1

Studies were performed for the leaching process of this ore in the presence of the following amino acids: cysteine, histidine, asparagine and leucine, to identify the effect of the amino acid structure on the degree of copper extraction. The results obtained are presented in Figure 4, and it follows from it that the copper extraction degree during the leaching process increases in the presence of amino acids located in the line of glycine - leucine – cysteine - histidine - asparagine, i.e., the opposite relationship is observed in comparison with the gold leaching in the presence of amino acids [[17], [18], [19], [20]].

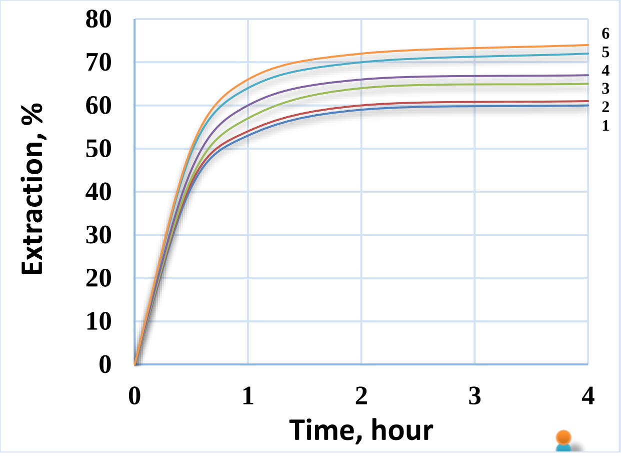

Figure 4 - Effect of amino acid structure on the degree of sulfuric acid leaching of copper.
1-blank; 2-asparagine; 3- histidine; 4-cysteine; 5- leucine; 6-glycine

It can be assumed based on the results obtained that if the effect of the amino group in the resulting complexes predominates during cyanide leaching of gold then there is the effect of the carboxyl group, on the contrary, during leaching copper with sulfuric acid, i.e. the higher the contribution of ionic bonding to the formation of copper complexes with amino acids, the higher the positive effect of the amino acid on the copper extraction degree during sulfuric acid leaching. Consequently, aliphatic amino acids have the strongest effect on copper leaching.

The effect of aminoacetic acid (glycine) on the electrolytic reduction of copper was studied with the use of model solutions as an example. We focused on the copper content in poor electrolytes. The concentration of copper and sulfuric acid was 1.0 and 100 g/dm^3, respectively. $CuSO_4 \cdot 5\ H_2O$ was used to prepare the model solution.

Electrolysis was performed on the unit shown in Figure 1. In the first stage, the optimal electrolysis time was determined. The duration of the experiments was sequentially 0.5; 1.0; 2.0; 4.0 and 6.0 hours, current density 0.2 A/m^2. The resulting kinetic curve is presented in Figure 5.

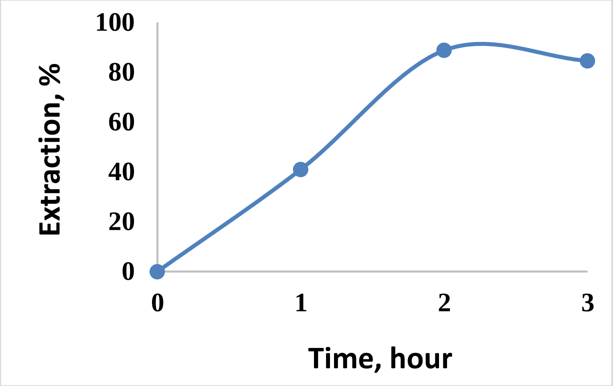

Figure 5 – Kinetic curve of copper electrolysis
It follows from the figure that the optimal duration of the process is 2 hours

Study of the sediment after 2 hours of electrolysis by the X-ray phase method showed that metallic copper was its basis. Besides, it contains a small amount of cuprous oxide and copper sulfate pentahydrate (Table 5). This composition of the sediment may indicate a staged reduction of copper.

The divalent copper ions are reduced first to the monovalent state, and then to metallic copper:

$$Cu^{+2} + e = Cu^{+}$$
$$Cu^{+} + e = Cu^{0}$$
$$Cu^{+2} + 2e = Cu^{0}$$

Partial adsorption of the original electrolyte takes place in addition.

After 4 hours, the sediment also contains lead, along with copper. This fact indicates that by this time there is a partial dissolution of the anode - lead, which forms lead sulfate and is partially deposited on the cathode (Table 6). The data obtained once again confirm the fact that the optimal duration of copper electrolysis should be considered to be 2 hours at a given current density.

Table 5 - Composition of the cathode deposit after 2 hours of electrolysis

Name	Formula	Content, %
Copper	Cu	88.9
Cuprite, syn	Cu_2O	7.4
Chalcanthite, syn	$CuSO_4 \cdot 5H_2O$	3.7

Table 6 - Composition of the cathode deposit after 4 hours of electrolysis

Name	Formula	Content, %
Cuprite, syn	Cu	72.5
Anglesite, syn	$Pb(SO_4)$	13.4
Copper	Cu_2O	11.1
Kobyashevite	$CuSO_4 \cdot 5H_2O$	3.0

Copper electrolysis was performed at the next stage under the same conditions in the presence of aminoacetic acid - glycine. The glycine concentration was 0.1 and 0.5 M. The results obtained are presented in Figure 6.

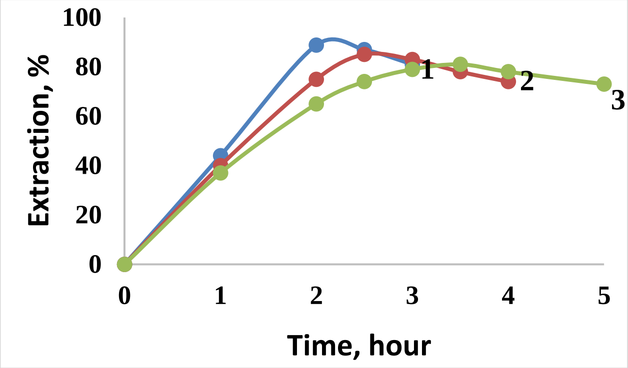

Figure 6 - Kinetic dependence of copper electrolysis in the presence of glycine
Amino acid concentration:
1- in the absence of an amino acid; 2 - 0.1M; 3 – 0.5M

As it follows from the figure, the presence of glycine in the solution increases the recovery time of copper, i.e. glycine in this case plays the role of a depressant. It is confirmed by X-ray phase analysis data (Table 7, 8), according to which the process is inhibited by the reduction of monovalent copper to the metallic state.

Table 7 - Results of X-ray phase analysis of the cathode product (glycine concentration 0.5 M)

Name	Formula	Content, %
Copper(I) oxide | Copper Oxide	Cu_2O	57.2%
Copper	Cu	33.5%
Chalcanthite, syn	$Cu_2SO_4 \cdot 5H_2O$	9.3%

Table 8 - Results of X-ray phase analysis of the cathode product (glycine concentration 0.1 M)

Name	Formula	Content, %
Copper(I) oxide | Copper Oxide	Cu_2O	31.1%
Copper	Cu	59.1%
Chalcanthite, syn	$Cu_2SO_4 \cdot 5H_2O$	8.8%

Thus, amino acids as bio-additives play a positive role in the leaching of copper from low-grade ore, and they are depressants of the copper reduction process during electrolysis. An increase in the concentration of amino acids increases the inhibition of the discharge of copper ions.

Conclusions

Biohydrometallurgical technologies are widely used for the production of non-ferrous and precious metals. The use of microorganisms can significantly increase the complexity of the use of raw materials and ensure effective environmental protection. Recently, bio-additives, in particular amino acids, which are an integral part of the culture liquid of microorganisms, are increasingly used in the production cycle, along with microorganisms.

The effect of amino acids on the leaching and subsequent electrolysis of copper from low-grade copper-containing ore, which includes quartz, albite, microcline, clinochlore, and muscovite, was studied. The copper content in the ore is 0.39%. The kinetics of the ore-leaching process with sulfuric acid was studied. The diffusion nature of the restrictions was established with the use of the Arrhenius equation, and the rate constants were calculated.

The effect of amino acids with different structures on the leaching process was studied. It was shown that the concentration of the amino acid, as well as its structure, affects the degree of copper extraction that decreases in the line of glycine - leucine - cysteine - histidine - asparagine.

The final stage of hydrometallurgical copper processing is electrolysis. It was found based on a study of the use of aminoacetic acid - glycine as an additive to the electrolyte during the electrolysis process that its presence inhibits the process of reduction of monovalent copper to the metallic state.

Thus, amino acids, predominantly of the aliphatic series, play a positive role as biological additives in the leaching of copper from low-grade ore, and they act as depressants for the copper reduction process during electrolysis, and an increase in the concentration of amino acids increases the inhibition of the discharge of copper ions.

Conflicts of interest. On behalf of all authors, the corresponding author states that there is no conflict of interest.

CRediT author statement: **R. Abdulvaliev**: Conceptualization, Methodology, Software. **T. Surkova**: Data curation, Writing draft preparation. **D.Yessimova, K. Smailov**: Visualization, Investigation. **Zh.Baltabekova, A. Berkinbayeva**: Supervision. **M. Stachowicz**: Software, Validation. **Z. Dossymbayeva**: Reviewing and Editing.

Acknowledgements. This work was supported by the Ministry of Science and Education of the Republic of Kazakhstan [BR18574018].

Cite this article as: Abdulvaliev RA, Surkova TYu, Baltabekova ZhA, Yessimova DM, Stachowicz M, Smailov KM, Dossymbayeva ZD, Berkinbayeva AN. Effect of amino acids on the extraction of copper from sub-conditional raw materials. Kompleksnoe Ispolzovanie Mineralnogo Syra = Complex Use of Mineral Resources. 2025; 335(4):50-58. https://doi.org/10.31643/2025/6445.39

Амин қышқылдарының сапасы төмен шикізаттардан мыс алуға әсері

[1]Абдулвалиев Р.А., [1]Суркова Т.Ю., [1]Балтабекова Ж.А., [1]Есимова Д.М., [2]Stachowicz M., [1]Смаилов К.М., [1]Досымбаева З.Д., [1]Беркинбаева А.Н.

[1] Металлургия және кен байыту институты АҚ, Сәтбаев университеті, Алматы, Қазақстан
[2] Вроцлав ғылым және технология университеті, Вроцлав, Польша

Мақала келді: *28 мамыр 2024*
Сараптамадан өтті: *28 маусым 2024*
Қабылданды: *13 қыркүйек 2024*

ТҮЙІНДЕМЕ
Өнеркәсіптік жолмен өңделетін минералды шикізат сапасының төмендеуі, сонымен қатар қоршаған ортаны қорғау талаптарының артуы оларды өңдеу технологиясының жаңа бағыттарын дамытуды қажет етеді. Биогеотехнология минералдық шикізатты өңдеу саласындағы ғылыми-техникалық прогрестің қазіргі заманғы бағыттарының біріне жатады. Түсті және асыл металдарды алу процестерінде микроорганизмдерді қолданумен қатар, биологиялық белсенді қоспалар, атап айтқанда микроорганизмдердің сұйықтығының құрамдас бөлігі болып табылатын аминқышқылдары көбірек қолданылады. Әртүрлі құрылымдағы амин қышқылдарының қатысында төмен сапалы кеннен мысты күкірт қышқылымен шаймалау процестері, сондай-ақ олардың мыс электролизіне әсері зерттелді. Бастапқы шикізат ретінде қазақстандық кен орындарының бірінің төмен сапалы кені пайдаланылды. Кендегі мыс мөлшері 0,39% құрайды. Шектеулердің диффузиялық сипаты мысты күкірт қышқылымен шаймалау процесінің кинетикасын зерттеу кезінде белгіленіп, жылдамдық константалары мен тиімді белсендендіру энергиясы есептелді, ол 1,817 кДж/моль болды. Құрылымы әртүрлі аминқышқылдарының шаймалау процесіне әсері зерттелді. Оң әсердің жоғарылауы глицин – лейцин – цистеин – гистедин – аспарагин қатарында көрсетілген. Амин қышқылының құрылымына байланысты ерітіндіге мыстың алыну дәрежесі 1-15% аралығында артады. Кедей ерітінділерден мысты электролиздеу процесіне биологиялық белсенді қоспа ретінде аминсірке қышқылының әсері зерттелді. Глициннің қатысуымен бір валентті мысты металдық күйге келтіру арқылы процесс тежелетіні анықталды.

Түйін сөздер: мыс, шаймалау, минералды шикізат,, амин қышқылдары, микроорганизмдер.

	Авторлар туралы ақпарат:
Абдулвалиев Р.А.	*Техника ғылымдарының кандидаты, глинозем және алюминий зертханасының меңгерушісі, Металлургия және кен байыту институты АҚ, Сәтбаев университеті, 050010, Шевченко к-сі, 29, Алматы, Қазақстан. Email: r.abdulvaliyev@satbayev.university; ORCID ID: https://orcid.org/0000-0001-6747-6984*
Суркова Т.Ю.	*Техника ғылымдарының кандидаты, Б.Б.Бейсембаев атындағы гидрометаллургияның арнайы әдістері зертханасының жетекші ғылыми қызметкері, Металлургия және кен байыту институты АҚ, Сәтбаев университеті, 050010, Шевченко к-сі, 29, Алматы, Қазақстан. Email: t.surkova@satbayev.university; ORCID ID: https://orcid.org/0000-0001-8271-125X*
Балтабекова Ж.А.	*Ғылыми қызметкер, Металлургия және кен байыту институты АҚ, Сәтбаев университеті, 050010, Шевченко к-сі, 29, Алматы, Қазақстан. Email: zh.baltabekova@satbayev.university; ORCID ID: https://orcid.org/0000-0003-3076-0652*

Есимова Д.М.	*Ғылыми қызметкер, Металлургия және кен байыту институты АҚ, Сәтбаев университеті, 050010, Шевченко к-сі, 29, Алматы, Қазақстан. Email: d.yessimova@satbayev.university; ORCID ID: https://orcid.org/0000-0002-1582-6732*
Stachowicz M.	*Ph.D. Eng., Вроцлав ғылым және технология университеті | WUT · Машина жасау факультеті, Вроцлав, Польша. Email: mateusz.stachowicz@pwr.edu.pl; ORCID ID: https://orcid.org/0000-0003-2995-269X*
Смаилов К.М.	*Ғылыми қызметкер, Металлургия және кен байыту институты АҚ, Сәтбаев университеті, 050010, Шевченко к-сі, 29, Алматы, Қазақстан. Email: k.smailov@satbayev.university; ORCID ID: https://orcid.org/0000-0002-9277-5254*
Досымбаева З.Д.	*Ғылыми қызметкер, Металлургия және кен байыту институты АҚ, Сәтбаев университеті, 050010, Шевченко к-сі, 29, Алматы, Қазақстан. Email: z.dosymbaeva@satbayev.university; ORCID ID: https://orcid.org/0000-0001-9144-208X*
Беркинбаева А.Н.	*Химия-аналитикалық зертханасының меңгерушісі, техника ғылымдарының кандидаты, Металлургия және кен байыту институты АҚ, Сәтбаев университеті, 050010, Шевченко к-сі, 29, Алматы, Қазақстан. E-mail: a.berkinbayeva@satbayev.university; ORCID ID: https://orcid.org/0000-0002-2569-9087*

Влияние аминокислот на извлечение меди из некондиционного сырья

[1]Абдулвалиев Р.А., [1]Суркова Т.Ю., [1]Балтабекова Ж.А., [1]Есимова Д.М., [2]Stachowicz M.,
[1]Смаилов К.М., [1]Досымбаева З.Д., [1]Беркинбаева А.Н.

[1] АО Институт металлургии и обогащения, Satbayev University, Алматы, Казахстан
[2] Вроцлавский университет науки и технологий, Вроцлав, Польша

Поступила: *28 мая 2024*
Рецензирование: *28 июня 2024*
Принята в печать: *13 сентября 2024*

АННОТАЦИЯ

Снижение качества перерабатываемого промышленностью минерального сырья, а также увеличение требований к охране окружающей среды обуславливают необходимость разработки новых направлений в технологии их переработки. Биогеотехнология относится к одному из современных направлений научно-технического прогресса в области переработки минерального сырья. Наряду с применением микроорганизмов в процессах извлечения цветных и благородных металлов все шире используют биологически активные добавки, в частности, аминокислоты, которые являются составной частью культуральной жидкости микроорганизмов. Нами рассмотрены процессы сернокислотного выщелачивания меди из низкосортной руды в присутствии аминокислот разной структуры, а также влияние их на электролиз меди. В качестве исходного сырья использовали низкосортную руду одного из Казахстанских месторождений. Содержание меди в руде -0,39%. Исследованием кинетики процесса сернокислотного выщелачивания меди установлен диффузионный характер ограничений, рассчитаны константы скорости и значение эффективной энергии активации, которое составило 1,817 кДж/моль. Изучено влияние аминокислот разной структуры на процесс выщелачивания. Показано увеличение положительного влияния в ряду: глицин – лейцин – цистеин - гистедин, - аспарагин. В зависимости от структуры аминокислоты степень извлечения меди в раствор увеличивается в пределах 1-15%. Изучено влияние аминоуксусной кислоты в качестве биологически активной добавки на процесс электролиза меди из бедных растворов. Установлено, что в присутствии глицина процесс тормозится восстановлением одновалентной меди до металлического состояния.

Ключевые слова: медь, выщелачивание, минеральное сырье, аминокислоты, микроорганизмы.

Информация об авторах:

Абдулвалиев Р.А.	*Кандидат технчеких наук, заведующий лабораторией глинозема и алюминия, АО Институт металлургии и обогащения, Satbayev University, 050010, ул. Шевченко, 29, Алматы, Казахстан. Email: r.abdulvaliyev@satbayev.university; ORCID ID: https://orcid.org/0000-0001-6747-6984*
Суркова Т.Ю.	*Кандидат технических наук, ведущий научный сотрудник лаборатории спецметодов гидрометаллургии им.Б.Б.Бейсембаева, АО Институт металлургии и обогащения, Satbayev University, 050010, ул. Шевченко, 29, Алматы, Казахстан. Email: t.surkova@satbayev.university; ORCID ID: https://orcid.org/0000-0001-8271-125X*
Балтабекова Ж.А.	*Научный сотрудник, АО Институт металлургии и обогащения, Satbayev University, 050010, ул. Шевченко, 29, Алматы, Казахстан. Email: zh.baltabekova@satbayev.university; ORCID ID: https://orcid.org/0000-0003-3076-0652*
Есимова Д.М.	*Научный сотрудник, АО Институт металлургии и обогащения, Satbayev University, 050010, ул. Шевченко, 29, Алматы, Казахстан. Email: d.yessimova@satbayev.university; ORCID ID: https://orcid.org/0000-0002-1582-6732*
Stachowicz M.	*Ph.D. Eng., Вроцлавский университет науки и технологий | WUT · Факультет машиностроения, Вроцлав, Польша. Email: mateusz.stachowicz@pwr.edu.pl; ORCID ID: https://orcid.org/0000-0003-2995-269X*

Смаилов К.М.	*Научный сотрудник, АО Институт металлургии и обогащения, Satbayev University, 050010, ул. Шевченко, 29, Алматы, Казахстан. Email: k.smailov@satbayev.university; ORCID ID: https://orcid.org/0000-0002-9277-5254*
Досымбаева З.Д.	*Научный сотрудник, АО Институт металлургии и обогащения, Satbayev University, 050010, ул. Шевченко, 29, Алматы, Казахстан. Email: z.dosymbaeva@satbayev.university; ORCID ID: https://orcid.org/0000-0001-9144-208X*
Беркинбаева А.Н.	*Кандидат технических наук, заведующий химико-аналитической лабораторией АО Институт металлургии и обогащения, Satbayev University, 050010, ул. Шевченко, 29, Алматы, Казахстан. E-mail: a.berkinbayeva@satbayev.university; ORCID ID: https://orcid.org/0000-0002-2569-9087*

References

[1] Telyakov N M, Darin A A, Luganov V A. Prospects for the use of biotechnologies in metallurgy and processing. Notes of the Mining Institute. 2016; 217:113-124.

[2] Muravyov M I, Fomchenko N V, Kondratyeva T F. Biohydrometallurgical technology for obtaining copper from complex copper concentrate. Applied biochemistry and microbiology. 2011; 47(6):607-614.

[3] Kenzhaliyev B, Surkova T, Berkinbayeva A, Dossymbayeva Z, Yesimova D. & Abdikerim B. On methods of modifying natural minerals. Challenges of Science. 2021; VI:128-133. https://doi.org/10.31643/2021.20

[4] Koizhanova AK, Berkinbayeva AN, Sedelnikova GV, Kenzhaliyev BK, Azlan MN, Magomedov DR, Efremova YM. Research of biochemical gold recovery method using high-arsenic raw materials. Metalurgija. 2021; 60(3-4):423-426.

[5] Sidelnikova GV, Savari EE, Kim DH. The use of biotechnology is a promising way to involve in the exploitation of deposits with refractory gold ores. Mining Journal. 2006; 10:52–57.

[6] Johnson D B. Biomining – biotechnologies for extracting and recovering metals from ores and waste materials. Current Opinion in Biotechnology. 2014; 30:24-31. https://doi.org/10.1016/j.copbio.2014.04.008

[7] Koizhanova AK, Kenzhaliyev BK, Magomedov DR, Erdenova MB, Bakrayeva AN, Abdyldaev NN. Hydrometallurgical studies on the leaching of copper from man-made mineral formations. Kompleksnoe Ispolzovanie Mineralnogo Syra = Complex Use of Mineral Resources. 2024; 330(3):32-42. https://doi.org/10.31643/2024/6445.26

[8] Kvon SS, Nesterova VI, Omarova AYe, Kulikov VY, Chsherbakova YeP. Study of the mineral composition of promising copper ores of the Republic of Kazakhstan. Kompleksnoe Ispolzovanie Mineralnogo Syra = Complex Use of Mineral Resources. 2023; 325(2):87-93. https://doi.org/10.31643/2023/6445.22

[9] Kondratieva T F, Bulaev A G, Muravyov M I. Microorganisms in biogeotechnologies for processing sulfide ores. Moscow: Nauka. 2015, 212.

[10] Maryam Khezri, Bahram Rezai, Ali Akbar Abdollahzadeh, Mehdi Molaeinasab, Benjamin P Wilson, Mari Lundström. Glycine leaching of Sarcheshmeh chalcopyrite concentrate at high pulp densities in a stirred tank reactor. Minerals Engineering. 2020; 157:106555. https://doi.org/10.1016/j.mineng.2020.106555

[11] Kenzhaliyev B, Ketegenov T, Kamunur K, Batkal A, Nadirov R. Efficient Copper Recovery from Chalcopyrite Using an «Isopropanol–Sulfuric Acid–Sodium Dodecyl Sulfate» System. Minerals. 2023; 13(10):1346. https://doi.org/10.3390/min13101346

[12] Krasnoshtanova A A. Hydrolysis of protein substances in the biomass of industrial microorganisms: abstract of thesis for Ph.D. in Chemistry. 1995, 146.

[13] Zakharyan SV. Research and development of hydrometallurgical technology for processing poor copper-sulfide raw materials of the Zhezkazgan region with the extraction of copper and related valuable components by the sorption method: abstract of the thesis for D.Sc. in Engineering. Yekaterinburg. 2019, 332.

[14] Taranina OA, Evreinova NV, Shoshina IA, Naraev VN, Tikhonov KI. Electrodeposition of nickel from sulfate solutions in the presence of aminoacetic acid. Russian Journal of Applied Chemistry. 2010; 83(1):58-61.

[15] Ogorodnikova N P. Chemical interaction of metals - copper, iron and manganese with α- and β-amino acids in aqueous and organic media: abstract of the thesis for Ph.D. in Chemistry. Rostov-on-Don. 2010, 162.

[16] Bakhytuly N, Kenzhegulov A, Nurtanto M, Aliev A, & Kuldeev E. Microstructure and tribological study of TiAlCN and TiTaCN coatings. Kompleksnoe Ispolzovanie Mineralnogo Syra = Complex Use of Mineral Resources. 2023; 327(4):99-110. https://doi.org/10.31643/2023/6445.45

[17] Kenzhaliyev B, Surkova T, Koizhanova A, Yessimova D, Amanzholova L, Dosymbayeva Z. Study of the Cyanide Leaching of Gold from Low-Grade Raw Materials in the Presence of Amino Acids. Inorganics. 2023; 11:461. https://doi.org/10.3390/inorganics11120461

[18] Eksteen J J, Oraby EA, Tanda B. A conceptual process for copper extraction from chalcopyrite in alkaline glycinate solution. Minerals Engineering. 2023; 108:53-66. https://10.1016/j.mineng.2017.02.001

[19] Nabizadeh A, Aghazadeh V. Dissolution study of chalcopyrite concentrate in oxidative ammonia/ ammonium carbonate solutions at moderate temperature and ambient pressure. Hydrometallurgy. 2015; 152:61-68. https://doi.org/10.1016/j.hydromet.2014.12.009

[20] Oraby E, Eksteen J. The selective leaching of copper from a gold–copper concentrate in glycine solutions. Hydrometallurgy. 2014; 150:14-19.

DOI: 10.31643/2025/6445.40
Metallurgy

Enlarged laboratory experiments of ferrous metallurgy dust sintering with calcium chloride

[1]Dosmukhamedov N.K., [1*]Koishina G.M., [2]Zholdasbay E.E., [2]Argyn A.A., [2]Icheva Yu.B.

[1] Satbayev University, Almaty, Kazakhstan
[2] O.A. Baikonurov Zhezkazgan University, Zhezkazgan, Kazakhstan

** Corresponding author email: gulzada.koishina@mail.ru*

Received: *June 6, 2024*
Peer-reviewed: *June 30, 2024*
Accepted: *September 16, 2024*

ABSTRACT

In this work, large-scale laboratory experiments were carried out on high-temperature sintering of clinker with $CaCl_2$. New data were obtained on extracting zinc, lead and related impurities into the targeted products of high-temperature sintering under process scaling conditions. The optimal parameters for high-temperature sintering have been established: t =900 °C, τ = 60 minutes, $CaCl_2$ consumption is 1.3 times higher than its consumption from the stoichiometric required amount (SRA). High-quality zinc sublimates were obtained. The maximum extraction of zinc into sublimates was achieved - 98.2%. New data on changes in the quantitative ratios of clinker ingredients under sintering conditions have been obtained. It has been established that zinc in the form of chloride is concentrated in sublimations. The obtained results form the basis of the final stage of the chlorination technology for processing lead-containing zinc dust from ferrous metallurgy and were used in the developing of a general technology for the selective extraction of zinc and lead into marketable products.

Keywords: dust, lead, zinc, extraction, chlorinating sintering.

	Information about authors:
Dosmukhamedov Nurlan Kalievich	*Candidate of Technical Sciences, Professor, Satbayev University, 050013, Almaty, 22 Satbayev St., Kazakhstan. E-mail: nurdos@bk.ru; ORCID ID: https://orcid.org/0000-0002-1210-4363*
Koishina Gulzada Myngyshkyzy	*PhD, Satbayev University, 050013, Almaty, 22 Satbayev St., Kazakhstan. E-mail: gulzada.koishina@mail.ru; ORCID ID: https://orcid.org/0000-0003-0592-3843*
Zoldasbay Erzhan Esenbaiuly	*PhD, O.A. Baikonurov Zhezkazgan University, 100600, Zhezkazgan, 1b Alashahan st., Kazakhstan. E-mail: zhte@mail.ru; ORCID ID: https://orcid.org/0000-0002-9925-4435*
Argyn Aidar Abdilmalikuly	*PhD, O.A. Baikonurov Zhezkazgan University, 100600, Zhezkazgan, 1b Alashahan st., Kazakhstan. E-mail: aidarargyn@gmail.com; ORCID ID: https://orcid.org/0000-0001-5001-4687*
Icheva Yulianna Borisovna	*Candidate of Technical Sciences, O.A. Baikonurov Zhezkazgan University, 100600, Zhezkazgan, 1b Alashahan st., Kazakhstan. E-mail: isheva1967@mail.ru*

Introduction

Today, accumulated dust from ferrous metallurgy occupies huge areas and requires disposal. Ferrous metallurgy specks of dust, in particular zinc-containing specks of dust, are characterized by a complex chemical and phase composition. The need for their processing lies in the fact that they contain valuable metals. On average, the zinc content in dust is estimated at 8-10%. The return of zinc-containing dust to smelting negatively affects the technological parameters and smelting modes: an increase in the zinc content in the resulting smelting products and the formation of localized deposits in the furnace. Several methods are known, but they are not applicable due to the multi-component composition of the dust obtained under different melting conditions and parameters [[1], [2], [3], [4], [5], [6], [7]]. Processing of zinc sublimates (in the form of oxides) by fuming and other processes leads to environmental degradation, an example is the processing of zinc sublimates at Kazakhmys LLP [[8], [9], [10], [11], [12], [13], [14], [15], [16], [17], [18], [19]]. The use of a pulverized coal mixture leads to a large yield of CO_2.

Based on the above, it follows that solving the problem of complex processing of ferrous and non-ferrous metallurgy dust is an urgent task and requires finding new ways to process them.

In previously completed work [20], we presented the general concept of combined chlorination technology for the complex processing of dust from Kazferrostal LLP (Almaty), obtained from processing ferrous scrap into EAF. The technology includes the selective extraction of iron, lead and zinc into targeted products through stage-by-stage processing. The results of the studies showed the fundamental possibility of developing a technology for producing commercial products from dust: an iron-containing product, high-quality lead and zinc sublimates with a high recovery of lead and zinc in them, over 98%.

At the initial stage of the technology, a magnetic fraction (~70% Fe) is separated from dust using the magnetic separation method, which is sent for agglomeration before blast furnace remelting. The non-magnetic dust fraction (46.74% Zn, 5.48% Pb) is subjected to low-temperature chlorinating sintering with NH_4Cl with selective extraction of lead into sublimates. The resulting zinc-rich clinker, in the second stage, is subjected to high-temperature sintering with $CaCl_2$ with selective extraction of zinc from it into sublimates and the production of final clinker with a high iron content, suitable for producing steel.

Lead and zinc sublimates of high quality can be used as commercial products and sent for sale, or, after processing by known methods (smelting, electrolysis), they can be processed to obtain pure lead and zinc. The minimum content of impurities in them will allow further operations to be carried out with low material costs.

The purpose of this research is to test the reproducibility and accuracy of the results of the method for extracting zinc from clinker by high-temperature sintering with calcium chloride [21] under scaling conditions with the establishment of optimal technological process parameters.

Materials and research methods

As the initial object, clinker was used, obtained after low-temperature sintering of dust with NH4Cl, composition, wt.%: 49.74 Zn; 0.23 Pb; 20.08 Fe; 7.74 SiO2; 18 O and others.

The conditions, experimental procedures and methods for studying the initial and resulting products were similar to those used in laboratory experiments [21]. Technological experiments were carried out with an initial sample of clinker of 500 g. The consumption of $CaCl_2$ in the experiments was 1.0; 1.1; 1.3 and 1.5 times higher than its stoichiometric required amount (SRA) for chlorination of zinc oxide, which was calculated based on the zinc content in clinker. Experiment temperatures were 600, 700, 800, 900 and 1000 °C. Duration – 60 minutes. Each experiment at a given temperature and $CaCl_2$ flow rate was repeated three times in order to be reproducible and obtain accurate results. The average value was taken as the final result.

The number of sublimations was determined by the difference between the initial sample and the resulting clinker, taking into account the content of lead, zinc and iron in them. The degree of extraction of zinc and lead into sublimates was determined by the formula:

$$\text{ƐMe} = \frac{(g1\times m1) - (g2\times m2)}{(g1\times m1)}, \qquad (1)$$

where: g_1 – a mass fraction of the element in the original clinker;

m_1 – mass of the initial clinker sample, 500 g;

g_2 - a mass fraction of the element in the clinker after sintering;

m_2 - a mass of clinker after sintering.

Based on the results of experiments, the material balance and extraction of zinc and lead into sintering products were calculated with a comparative analysis of the data.

Results and discussion

The established values of Δ H>0 kJ/mol for the reaction of zinc oxide with $CaCl_2$ show that the chlorination process is endothermic and the efficiency of the ongoing reactions during high-temperature sintering of clinker is closely related to temperature.

To check the effectiveness of extraction of Zn and Pb from clinker, the mixture (clinker + given $CaCl_2$ flow rate) in an amount of 500 g was subjected to sintering at a temperature of 600-1000 °C for 60 minutes at an airflow rate of 100 ml/min.

The study of the influence of temperature on the dynamics of changes in the content of Zn and Pb in the sintering products was carried out at a constant sintering time of 60 minutes and consumption of $CaCl_2$ 1.3 times higher than its stoichiometric required amount (SRA) for the reduction of zinc compounds to chloride. The choice of parameters is determined by the need to conduct a comparative assessment of the results for reproducibility and accuracy with laboratory experiments.

The effect of temperature on the content of zinc and lead in sublimates and clinker is shown in Fig. 1.

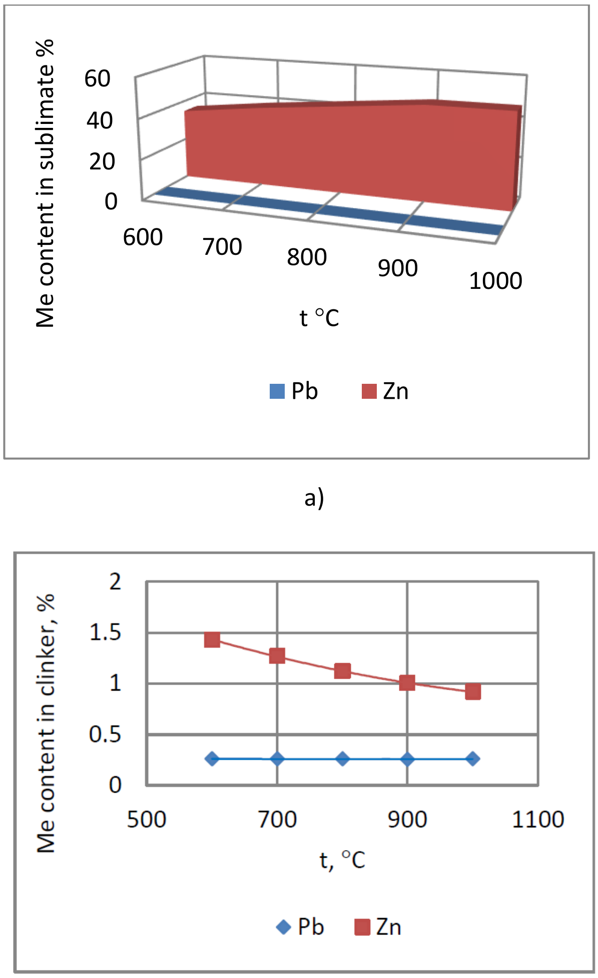

a)

b)

Fig. 1 - Dependence of Zn and Pb content in sublimates (a) and clinker (b) on temperature

As can be seen in Fig. 1 (a), under high-temperature sintering conditions, the main contribution to the formation of sublimates is made by zinc chloride. The Zn content in sublimates changes greatly with increasing temperature: an increase in temperature from 600 to 1000 °C increases the zinc content in sublimates from ~35 to ~41%. At high temperatures of 800 °C and above, the lead content in sublimates is minimal and varies slightly within low limits from 0.003 to 0.002%. The fact seems quite natural, since in the considered temperature range 600-1000 °C, the Zn content in clinker shows a sharp decrease from 1.43 to 0.92%. At the same time, as can be seen in Fig. 1 (b), the nature of the curve of the change in lead content practically does not change and shows a stable value at the level of 0.26%.

SEM images of clinkers obtained after chlorination sintering at a temperature of 700, 800, 900 and 1000 °C are presented in Fig. 2.

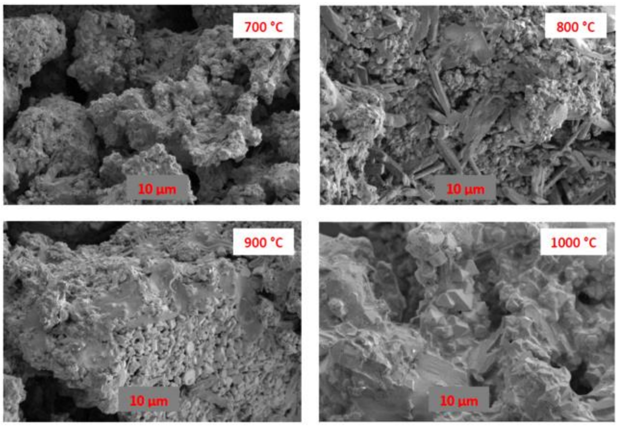

Fig.2 - SEM images of samples (clinker) chlorinated at different temperatures: 700 °C, 800 °C, 900 °C, 1000 °C

In the range of 700-900 °C, with increasing temperature, calcined clinker gradually begins to sinter and undergoes phase transitions. At elevated temperatures due to a decrease in the porosity of the material, kinetic conditions chlorination reactions are hindered: $CaCl_2$ particles are not completely in contact with zinc and lead compounds. At temperatures above 1000 °C, clinker begins to melt (Fig. 2), and at higher temperatures (above 1200 °C) it passes into the liquid phase, which seriously reduces the extraction of zinc and lead into sublimates. Consequently, an increase in the sintering temperature, although it provides high productivity, significantly increases the material costs of the process: the consumption of chlorinating agent increases ($CaCl_2$), and the quality of the resulting sublimates decreases. Based on the obtained results and taking into account the established patterns of the influence of temperature on the quality of the resulting sublimates, as well as taking into account the cost of calcium chloride and energy consumption, a temperature of 900 °C was taken as the optimal temperature for the sintering process.

In the process of high-temperature chlorinating sintering of clinker, the distribution of Zn and Pb between products is significantly affected by the consumption of $CaCl_2$ - as an active chlorinating reagent, providing effective selective chlorination of zinc with low energy consumption and minimal environmental pollution.

The physicochemical essence of the process of high-temperature sintering of clinker with $CaCl_2$ can be interpreted as a direct and indirect mechanism of metal chlorination [22].

The mechanism of direct chlorination can be represented by the reaction:

$$CaCl_2 + MeO = 2CaO + MeCl_2, \qquad (2)$$

where solid calcium chloride reacts directly with the metal oxide to form the corresponding chloride.

The indirect mechanism of metal chlorination is usually represented as a stepwise one: first, the decomposition reaction of solid $CaCl_2(s)$ occurs due to oxygen to its oxide with the formation of gaseous chlorine ($Cl_2(g)$). The chlorine then reacts with the metal oxide and reduces it to the corresponding chloride. The general mechanism is described by the occurrence of reactions:

$$2CaCl_{2(s)} + O_{2(g)} = 2CaO + 2Cl_{2(g)}, \qquad (3)$$

$$2MeO_{(s)} + 2Cl_{2\,(g)} = 2MeCl_{2(g)} + O_{2(g)}. \qquad (4)$$

The physicochemical patterns that occur during the sintering of clinker with $CaCl_2$ can be interpreted by the mechanism of direct chlorination, wherein the ZnO-Fe_2O_3-$CaCl_2$ system, at temperatures above the melting point of $CaCl_2$ (>700 °C), calcium chloride with zinc oxide reacts directly according to reaction (1) to form gaseous $ZnCl_2$.

The effect of $CaCl_2$ consumption on the zinc content in sintering products, set at an optimal temperature of 900 °C, is shown in Fig. 3.

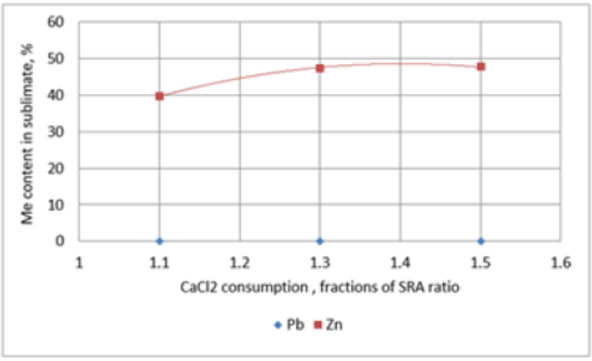

a)

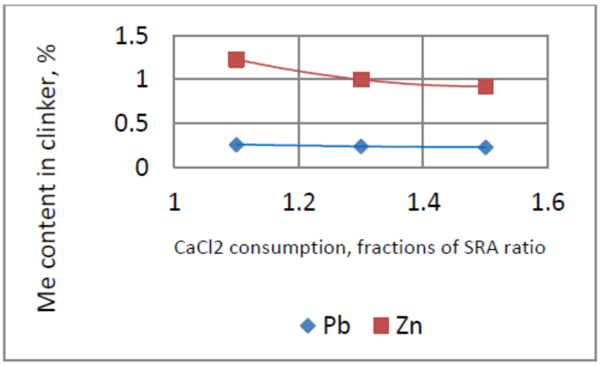

b)

Fig.3 - Dynamics of changes in the content of Zn and Pb in sublimates (a) and clinker (b) depending on the consumption of $CaCl_2$: t =900 °C, τ =60 minutes.

As can be seen in Fig. 3, the Zn content in the sintering products strongly depends on the $CaCl_2$ consumption. Interesting results were obtained in experiments conducted without the addition of $CaCl_2$. When simply heating the clinker at 900 °C for 60 minutes, the residual content of Zn and Pb in the resulting clinker, although insignificant, showed a decrease from the initial 50.46% and 0.24% to 49.78% and 0.21%, respectively. This phenomenon is explained by the fact that at high temperatures, zinc and lead compounds present in clinker in the form of solid chlorides, having high vapor pressure, partially begin to sublime.

With an increase in the consumption of $CaCl_2$ from 1.1 to 1.3 times higher than its consumption from the SRA, the zinc content in the sublimates increases from ~40 to ~50% (Fig. 3 (a)). With a maximum zinc content in sublimates, the lead content in them is minimal and amounts to ~0.002%.

An increase in the consumption of $CaCl_2$ increases its contact with the oxides of Zn and Pb and promotes the intensification of the chlorination process, accelerating the speed and completeness of the reactions. However, it has been established that with an increase in the consumption of $CaCl_2$ (above its SRA = 1.3), the zinc content in the sublimates slows down. This is explained by the fact that when the consumption of calcium chloride is equal to SRA = 1.3, the processes of formation of zinc chloride and its sublimation are almost completed. This is evidenced by the established minimum contents of Zn, and Pb in clinker, equal to 0.92% and 0.23%, respectively, at a consumption of $CaCl_2$ = 1.5 SRA (Fig. 3 (b)). It follows that the optimal conditions for high-temperature chlorinating sintering, ensuring high extraction of zinc into sublimates, are achieved at consumption of $CaCl_2$ not exceeding its stoichiometric required amount by 1.3 times for the reduction of zinc from its oxide.

The dynamics of the extraction of lead and zinc into sublimates depending on the consumption of $CaCl_2$ is shown in Fig. 4.

Figure 4 shows that with a consumption of $CaCl_2$ 1.5 times higher than its consumption from the SRA for the reduction of zinc oxide to its chloride, a high extraction of Zn into sublimates is achieved, equal to 98.4%, with a minimum extraction of lead into sublimates - 2,6%. At the same time, a large excess of $CaCl_2$ in the process increases the extraction of volatile lead chlorides and impurities into sublimates, which will significantly reduce the quality of the resulting zinc sublimates. Based on this, and also taking into account the increase in material costs, it is advisable to take the optimal consumption of calcium chloride in the work as 1.3 times higher than the consumption from the SRA required to reduce zinc oxide to volatile zinc chloride.

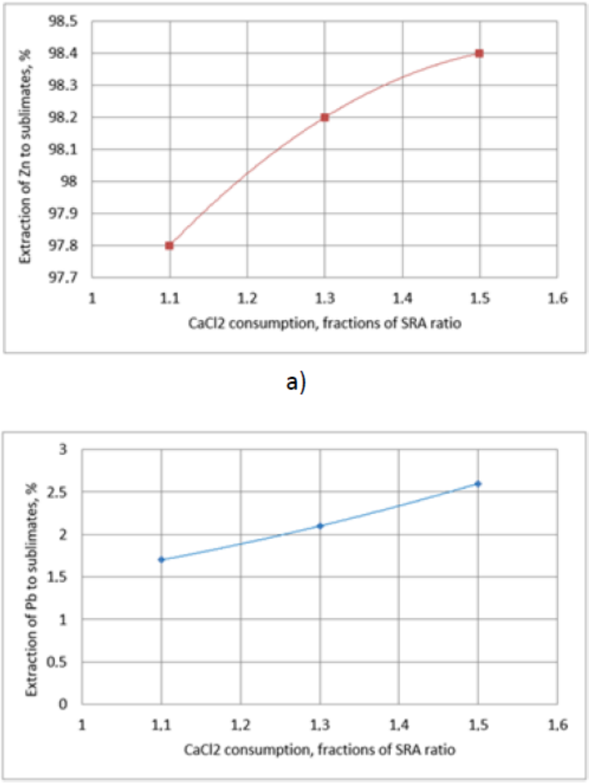

a)

b)

Fig.4 - Dependence of extraction of zinc (a) and lead (b) to sublimates from $CaCl_2$ consumption: t =900 °C, τ =60 minutes

Thus, the obtained results completely confirm the previously established patterns of behaviour of zinc and lead obtained in laboratory conditions. Optimal process parameters corresponding to t =900 °C, process time - 60 minutes and $CaCl_2$ consumption 1.3 times higher than its consumption from SRA for the recovery of zinc from its oxide provide a high recovery of zinc into sublimates of more than 98%.

The yield of products at optimal parameters after sintering was, % of the weight of the charge (clinker + $CaCl_2$): clinker - 43%; sublimates – 50%, others.

High-quality zinc sublimates were obtained, wt.%: 47.39 Zn; 0.005 Pb; 51.77 Cl, others. Composition of the final clinker, wt.%: 22.53 Fe; 4.1 Si; 44 Ca; 18.26 Cl; 7.21 O; 0.26 Pb; 1.0 Zn, others. Extraction of zinc into sublimates – 98.2%.

The obtained data are in good agreement with laboratory experiments [21], which show the high reproducibility of the process under scaling conditions and the accuracy (more than 98%) of the results obtained.

The establishment of quantitative relationships between Zn, Pb, Fe and associated impurities in the final clinker has a great practical importance. To carry out the calculations, the contents of all possible impurities were established within the lower limits of their detection in the clinker obtained after sintering. Based on the results, the clinker ingredients (kg/t) were determined and their ratios were calculated, which are presented in Fig. 5.

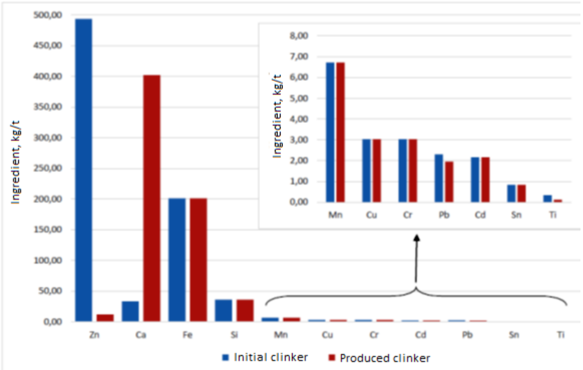

Fig.5 - Ingredients of clinker obtained after high-temperature sintering: t =900 °C, τ =60 minutes

It is easy to see that the amount of basic ingredients (Zn, Ca, Fe, Si) of clinker undergoes significant changes after sintering: the amount of Zn in clinker sharply decreases from 480 kg to ~10 kg, while the contents of Fe and Si remain almost at the same level. A significant increase in the amount of calcium in clinker from 30 kg to 400 kg is explained by the introduction of an additional amount of calcium chloride into the process as a chlorinating reagent. From the general spectrum of detected impurities, a decrease in the content of lead and titanium from their base content in the original clinker was established by 1.2 and 2.3% abs., respectively. The remaining impurities are almost completely concentrated in clinker. The obtained results show that the sublimates in the process are mainly represented by zinc chloride vapors with a minimal content of lead, titanium and tin chlorides. With further processing of the resulting zinc sublimates, their presence will not require a significant increase in costs.

Conclusions

It has been established that the minimum zinc content in clinker of 1.01% is achieved at a temperature of 900 °C. A high zinc content in sublimates of 47.42% was achieved at a consumption of $CaCl_2$ 1.3 times higher than its SRA for the reduction of zinc oxide.

The optimal parameters for high-temperature sintering have been established: $t = 900$ °C, $\tau = 60$ minutes, $CaCl_2$ consumption is 1.3 times higher than its consumption from the SRA. High-quality zinc sublimates were obtained, wt.%: 47.39 Zn; 0.005 Pb; 51.77 Cl, others. The maximum extraction of zinc into sublimates was achieved - 98.2%.

New data were obtained on changes in the quantitative ratios of clinker ingredients under sintering conditions. It has been established that the most important ingredient (Zn) of clinker, due to the high volatility of its chloride, is concentrated in sublimates during the sintering process. Minor loss of volatile impurities is characterized by lead, titanium and tin chlorides. The remaining impurities are concentrated in clinker in the form of oxides and chlorides.

The obtained results were used in the construction of a common technology for the selective extraction of zinc and lead from ferrous metallurgy dust.

Conflict of interest. On behalf of all authors, the corresponding author confirms that there is no conflict of interest.

CRediT author statement: **N.Dosmukhamedov**: Supervision, Conceptualization, Methodology. **G.Koishina:** Data curation, Writing- Original draft preparation. **A.Argyn:** Investigation. **Yu.Icheva:** Investigation, Software, Validation: **E.Zholdasbay:** Writing- Reviewing.

Acknowledgements. The research was carried out within the framework of grant funding from the Science Committee of the Ministry of Science and Higher Education of the Republic of Kazakhstan for 2023-2025 in the priority area “Rational use of water resources, flora and fauna, ecology” of the project AP19679572 “Development of a new technology for recycling zinc dust from steelmaking production with the production of marketable products".

Cite this article as: Dosmukhamedov NK, Koishina GM, Zholdasbay EE, Argyn AA, Icheva YuB. Enlarged laboratory experiments of ferrous metallurgy dust sintering with calcium chloride. Kompleksnoe Ispolzovanie Mineralnogo Syra = Complex Use of Mineral Resources. 2025; 335(4):59-66. https://doi.org/10.31643/2025/6445.40

Қара металлургия шаңын кальций хлоридімен бірге күйежентектеудің кеңейтілген зертханалық тәжірибелері

[1]Досмухамедов Н.К., [1]Қойшина Г.М., [2]Жолдасбай Е.Е., [2]Арғын А.Ә., [2]Ичева Ю.Б.

[1]Сәтбаев университеті, Алматы, Қазақстан
[2]Ө.А. Байқоңыров атындағы Жезқазған университеті, Жезқазған, Қазақстан

Мақала келді: *6 маусым 2024*
Сараптамадан өтті: *30 маусым 2024*
Қабылданды: *16 қыркүйек 2024*

ТҮЙІНДЕМЕ

Жұмыста клинкерді $CaCl_2$-мен жоғары температурада күйежентектеу бойынша іріленген-зертханалық тәжірибелер жүргізілді. Процесті масштабтау жағдайында жоғары температуралы күйежентектеудің мақсатты өнімдеріне мырыш, қорғасын және ілеспе қоспаларды бөліп алу бойынша жаңа деректер алынды. Жоғары температуралы күйежентектеудің оңтайлы параметрлері анықталды: $t=900$ °C, $\tau=60$ минут, $CaCl_2$ шығыны СҚМ-нен 1,3 есе көп. Жоғары сапалы мырыш возгондары алынды. Возгондарға мырыштың максималды бөлінуі қол жеткізілді - 98,2 %. Күйежентектеу жағдайында клинкер ингредиенттерінің сандық арақатынастары туралы жаңа мәліметтер алынды. Возгонда мырыштың хлорид түрінде болатындығы анықталды. Алынған нәтижелер қара металлургиядағы қорғасыны бар мырыш шаңын өңдеудің хлорлау технологиясының соңғы сатысының негізін құрайды және цинк пен қорғасынды тауарлық өнімге іріктеп алудың жалпы технологиясын құруда қолданылатын болады.

Түйін сөздер: шаң, қорғасын, мырыш, бөліп алу, хлорлы күйдіру.

	Авторлар туралы ақпарат:
Досмухамедов Нурлан Калиевич	*Т.ғ.к., профессор, Satbayev University, 050013, Алматы, Сәтбаев көш. 22, Қазақстан. E-mail: nurdos@bk.ru; ORCID ID: https://orcid.org/0000-0002-1210-4363*
Қойшина Гүлзада Мыңғышқызы	*PhD, Satbayev University, 050013, Алматы, Сәтбаев көш. 22, Қазақстан. E-mail: gulzada.koishina@mail.ru; ORCID ID: https://orcid.org/0000-0003-0592-3843*
Жолдасбай Ержан Есенбайұлы	*PhD, Ө.А. Байқоңыров атындағы Жезқазған университеті, 100600, Жезқазған, Алашахан көш. 1б, Қазақстан. E-mail: zhte@mail.ru; ORCID ID: https://orcid.org/0000-0002-9925-4435*

Арғын Айдар Әбділмәлікұлы	*PhD, Ө.А. Байқоңыров атындағы Жезқазған университеті, 100600, Жезқазған, Алашахан көш. 1б, Қазақстан. E-mail: aidarargyn@gmail.com; ORCID ID: https://orcid.org/0000-0001-5001-4687*
Ичева Юлианна Борисовна	*Т.ғ.к., Ө.А. Байқоңыров атындағы Жезқазған университеті, 100600, Жезқазған, Алашахан көш. 1б, Қазақстан. E-mail: isheva1967@mail.ru*

Укрупненно-лабораторные опыты спекания пыли черной металлургии совместно с хлоридом кальция

[1]Досмухамедов Н.К., [1]Койшина Г.М., [2]Жолдасбай Е.Е., [2]Аргын А.А., [2]Ичева Ю.Б.

[1] Satbayev University, Алматы, Казахстан
[2]Жезказганский университет имени О.А. Байконурова, Жезказган, Казақстан

Поступила: *6 июня 2024*
Рецензирование: *30 июня 2024*
Принята в печать: *16 сентября 2024*

АННОТАЦИЯ

В работе проведены укрупненно-лабораторные опыты по высокотемпературному спеканию клинкера с $CaCl_2$. Получены новые данные по извлечению цинка, свинца и сопутствующих примесей в целевые продукты высокотемпературного спекания в условиях масштабирования процесса. Установлены оптимальные параметры высокотемпературного спекания: t=900 °C, τ=60 минут, расход $CaCl_2$ в 1,3 раза превышающий его расход от СНК. Получены цинковые возгоны высокого качества. Достигнуто максимальное извлечение цинка в возгоны – 98,2 %. Установлены количественные соотношения ингредиентов клинкера в условиях спекания. Установлено, что цинк в виде хлорида в возгонах. Полученные результаты составляют основу заключительной стадии хлорирующей технологии переработки свинецсодержащей цинковой пыли черной металлургии и будут использованы при построении общей технологии для селективного извлечения цинка и свинца в товарные продукты.

Ключевые слова: пыль, цинк, свинец, извлечение, хлорирующее спекание.

	Информация об авторах:
Досмухамедов Нурлан Калиевич	*К.т.н., профессор, Satbayev University, 050013, Алматы, ул. Сатпаева 22, Казахстан. E-mail: nurdos@bk.ru; ORCID ID: https://orcid.org/0000-0002-1210-4363*
Койшина Гулзада Мынгышкызы	*PhD, Satbayev University, 050013, Алматы, ул. Сатпаева 22, Казахстан. E-mail: gulzada.koishina@mail.ru; ORCID ID: https://orcid.org/0000-0003-0592-3843*
Жолдасбай Ержан Есенбайулы	*PhD, Жезказганский университет имени О.А. Байконурова, 100600, Жезказган, ул. Алашахана 1б, Казахстан. E-mail: zhte@mail.ru; ORCID ID: https://orcid.org/0000-0002-9925-4435*
Аргын Айдар Абдилмаликулы	*PhD, Жезказганский университет имени О.А. Байконурова, 100600, Жезказган, ул. Алашахана 1б, Казахстан. E-mail: aidarargyn@gmail.com; ORCID ID: https://orcid.org/0000-0001-5001-4687*
Ичева Юлианна Борисовна	*К.т.н., Жезказганский университет имени О.А. Байконурова, 100600, Жезказган, ул. Алашахана 1б, Казахстан. E-mail: isheva1967@mail.ru*

References

[1] Ashrit SS, Sarkar S, Singh R, Yadav S Z, Chatti RV. Characterization of blast furnace flue dust – A multi analytical techniques approach. Metall. Res. Technol. 2020; 117:606-613.

[2] Zhang J, Zhang Y, Long Y, Du P, Tian T, Ren Q. Multi-source ferrous metallurgical dust and sludge recycling: present and future prospects. Crystals. 2024; 14(3):273. https://doi.org/10.3390/cryst14030273

[3] Li Y, Feng H, Wang J, She X, Wang G, Zuo H, Xue Q. Current status of the technology for utilizing difficult-to-treat dust and sludge produced from the steel industry. J. Clean. Prod. 2022; 367:132909.

[4] Kadyrov AS, Kunaev VA, Georgiadi IV. Prospects for Processing of Ferrous Metallurgical Waste Based on Arcelormittal Temirtau Experience. Metallurgist. 2018; 62:22-28. https://doi.org/10.1007/s11015-018-0620-3

[5] Berdiyarov BT, Khojiev ShT, Rakhmataliev Sh, Karimov OM. Processing of secondary ferrous waste is a technology for processing dust generated in furnaces. Education And Science In The Xxi Century. 2023; 38(2):21.

[6] Yakornov SA, Panshin AM, Kozlov PA, Ivakin DA. Development of technology and instrumental scheme of pyrometallurgical processing of ferrous metallurgy dusts. Tsvetnye Metally. 2017; 9:56-66. https://doi.org/10.17580/tsm.2017.09.06

[7] de Araújo JA, Schalch V. Recycling of electric arc furnace (EAF) dust for use in steel making process. J. Mater. Res. Technol. 2014; 3:274-279. https://doi.org/10.1016/j.jmrt.2014.06.003

[8] Brandner U, Antrekowitsch J, Leuchtenmueller M. A review on the fundamentals of hydrogen-based reduction and recycling concepts for electric arc furnace dust extended by a novel conceptualization. International Journal of Hydrogen Energy. 2021; 46(62):31894-31902. https://doi.org/10.1016/j.ijhydene.2021.07.062

[9] Kovtun O, Levchenko M, Höntsch S, Lohmeier L, Schreiner M, Gräbner M, Volkova O. Recycling of Iron-Rich Basic Oxygen Furnace Dust using Hydrogen-based Direct Reduction. Resources, Conservation & Recycling Advances. 2024, 200225. https://doi.org/10.1016/j.rcradv.2024.200225

[10] Pei P, Wang J, Wang Y, Hu W, Wang B, Zhou J. Waste control by waste: Extraction of valuable metals from mixed metallurgical dust by boiling furnace roasting. Separation and Purification Technology. 2024; 346:127452. https://doi.org/10.1016/j.seppur.2024.127452

[11] Halli P, Agarwal V, Partinen J, Lundström M. Recovery of Pb and Zn from a citrate leach liquor of a roasted EAF dust using precipitation and solvent extraction. Separation and Purification Technology. 2020; 236:116264. https://doi.org/10.1016/j.seppur.2019.116264

[12] Frueholz R, Conde AS, Habermaier C, Spiess S, Birklbauer L, Wallner M, Haberbauer M. Zinc removal from metallurgical dusts with iron-and sulfur-oxidizing bacteria. Minerals Engineering. 2024; 206:108535. https://doi.org/10.1016/j.mineng.2023.108535

[13] Binnemans K, Jones PT, Manjón Fernández Á, Masaguer Torres V. Hydrometallurgical processes for the recovery of metals from steel industry by-products:A critical review. J.Sustain. Metal. 2020; 6(4):505-540. https://doi.org/10.1007/s40831-020-00306-2

[14] Kang MJ, Kwon YK, Yu S, Lee PK, Park HS, Song N. Assessment of Zn pollution sources and apportionment in agricultural soils impacted by a Zn smelter in South Korea. J. Hazard. Mater. 2019; 364:475-487.

[15] Dong W, Wang Y, Peng J, Li Y, Cao X, Di Y, Huang Y, Li R. Extracting zinc from ironworking dust having a high zinc content by vacuum silicothermic reduction. Process Safety and Environmental Protection. 2024; 182:1237-1249. https://doi.org/10.1016/j.psep.2023.12.036

[16] Deng X, Huang R, Lv X, Yang J, Yang J. Separation and recovery of metallic zinc and iron concentrate from blast furnace dust by vacuum carbothermal reduction. Process Safety and Environmental Protection. 2022; 162:746-751. https://doi.org/10.1016/j.psep.2022.04.050

[17] Zhu D, Wang D, Pan J, Tian H, Xue Y. A study on the zinc removal kinetics and mechanism of zinc-bearing dust pellets in direct reduction. Powder Technology. 2021; 380:273-281. https://doi.org/10.1016/j.powtec.2020.11.077

[18] She X, Wang J, Wang G, Xue Q, Zhang X. Removal Mechanism of Zn, Pb and Alkalis from Metallurgical Dusts in Direct Reduction Process. J. Iron Steel Res. Int. 2014; 21:488-495. https://doi.org/10.1016/S1006-706X(14)60076-5

[19] Nayak N. Characterization of blast furnace flue dust-an assessment for its utilization. Mater. Today Proc. 2022; 50(5):2078-2083. https://doi.org/10.1016/j.matpr.2021.09.417

[20] Dosmukhamedov NK, Koishina GM, Zholdasbay EE, Argyn AA. Extraction of lead during low-temperature sintering of dust from melting scrap metal in an electric arc furnace with ammonium chloride. CIS Iron and Steel Review. 2024; 2.

[21] Koishina GM, Dosmukhamedov N K, Kaplan VA, Zholdasbay EE, Argyn AA. Extraction of zinc from dust of electric arc furnace by high temperature chlorinating sintering. Engineering Journal of Satbayev University. 2024.

[22] Xing Z, Cheng G, Yang H, Xue X, Jiang P. Mechanism and application of the ore with chlorination treatment: A review. Minerals Engineering. 2020; 154:106404. https://doi.org/10.1016/j.mineng.2020.106404

DOI: 10.31643/2025/6445.41
Metallurgy

Pyrolysis of synthetic copper telluride in an inert atmosphere

Nitsenko A.V., *Linnik X.A., Volodin V.N., Tuleutay F.Kh., Bakhytuly N.

Institute of Metallurgy and Ore Beneficiation JSC, Satbayev University, Almaty, Kazakhstan

** Corresponding author email: xenija_linnik@mail.ru*

Received: *July 23, 2024*
Peer-reviewed: *September 16, 2024*
Accepted: *September 26, 2024*

ABSTRACT

The paper presents the study results of the thermal behavior of synthetic copper telluride in an inert atmosphere at pressures of 92 and 0.07 kPa under isothermal and non-isothermal vacuum-thermal conditions. The thermal analysis results showed that the synthesized copper telluride undergoes polymorphic transformations at 185.7, 259, 318, 350, 470, and 834.5 °C. These transformations were established by early studies and are characteristic of copper tellurides of stoichiometric and non-stoichiometric compositions. It was found that the reduction of the pressure in the system slightly increases the final value of mass loss of the synthetic sample. The X-ray phase analysis results of the residues obtained at constant and increasing temperatures at a pressure of 0.07 kPa showed the absence of the formation of new phases relative to the initial composition. A change in the quantitative ratio of the available phases was found in the direction of an increase in the amount of $Cu_{0.656}Te_{0.344}$ relative to the initial composition with an increase in the process temperature.

Keywords: pyrolysis, tellurium, copper, copper telluride, phase composition, thermal analysis

Information about authors:

Nitsenko Alina Vladimirovna	*Candidate of Technical Sciences, Head of the Vacuum Processes Laboratory of the Institute of Metallurgy and Ore Beneficiation JSC, Satbayev University, Shevchenko str., 29/133, 050010, Almaty, Kazakhstan. Email: alina.nitsenko@gmail.com; ORCID ID: https://orcid.org/0000-0001-6753-0936*
Linnik Xeniya Alexandrovna	*Master of Technical Sciences, Junior Researcher of the Vacuum Processes Laboratory of the Institute of Metallurgy and Ore Beneficiation JSC, Satbayev University, Shevchenko str., 29/133, 050010, Almaty, Kazakhstan. Email: xenija_linnik@mail.ru; ORCID ID: https://orcid.org/0000-0002-0683-1409*
Volodin Valeriy Nikolaevich	*Doctor of Technical Sciences, Professor, Chief Researcher of the Vacuum Processes Laboratory of the Institute of Metallurgy and Ore Beneficiation JSC, Satbayev University, Shevchenko str., 29/133, 050010, Almaty, Kazakhstan. Email: volodinv_n@mail.ru; ORCID ID: https://orcid.org/0000-0003-0116-1423*
Tuleutay Farkhad Khanafiyauly	*Master of Technical Sciences, Junior Researcher of the Vacuum Processes Laboratory of the Institute of Metallurgy and Ore Beneficiation JSC, Satbayev University, Shevchenko str., 29/133, 050010, Almaty, Kazakhstan. Email: farkhat_kaldybek@mail.ru; ORCID ID: https://orcid.org/0000-0003-0802-283X*
Bakhytuly Nauryzbek	*Ph.D., Head of the Laboratory of Physical Methods of Analysis of the Institute of Metallurgy and Ore Beneficiation JSC, Satbayev University, Shevchenko str., 29/133, 050010, Almaty, Kazakhstan. Email: n.bakhytuly@satbayev.university; ORCID ID: https://orcid.org/0000-0003-3087-0616*

Introduction

Due to the depletion of natural resources and, as a consequence, the involvement of poor and substandard raw materials in production, the issue of improving existing technologies for processing copper-containing raw materials remains relevant today [[1], [2], [3], [4], [5]]. At the same time, the final stage of most copper production around the world continues to be copper electrorefining.

A multicomponent product – copper electrolyte sludge containing chalcogenes in the form of their compounds with copper, silver, and gold is produced during the electrorefining of copper [[6], [7], [8]]. First of all, the sludge serves as a raw material to obtain noble metals, besides the products of its processing are selenium and tellurium. There is quite a wide range of methods of sludge processing associated with the complexity and diversity of chemical and phase compositions of sludge. Some of the proposed methods can be found in [[7], [8], [9], [10], [11], [12], [13], [14], [15], and [16]].

Schemes intended to obtain tellurium from copper-electrolyte sludge are a process combining hydro-, pyro-, and electrometallurgy methods [[13], [14], [17], [18]]. A valuable product in this scheme is copper telluride in addition to tellurium of different purity. Copper telluride contains phases of both stoichiometric (Cu_2Te) and non-stoichiometric compositions ($Cu_{2-x}Te$) and includes impurities of other elements and compounds [[19], [20], [21], [22], [23]]. Some companies prefer to accumulate or sell copper telluride at relatively low prices rather than further separate tellurium and copper. This approach is associated with the presence of technological and technical difficulties due to multistage, significant consumption of reagents, formation of large volumes of wastewater containing heavy metals, etc. Therefore, the development of an economical and environmentally safe process for the extraction of Te and Cu from copper telluride is of great importance for the metallurgical industry.

In this regard, there has been a growing interest of scientists in the issue of the creation of new and improvement of existing technologies for processing copper telluride in recent years.

Traditionally, the tellurium-containing middling product is subjected to oxidative-alkaline leaching with the addition of NaOH at the first stage [[14], [17]]. As a result, tellurium is concentrated in the solution in the form of sodium tellurite (Na_2TeO_3), and copper – in the residue. The solution is further sent for electrolysis, and the copper-containing residue is sent for copper extraction. Liang Xu et al. [22] compared the classical leaching method at atmospheric pressure with their proposed autoclave leaching. The best performance was achieved with autoclave leaching: more than 95 % of tellurium was transferred into solution. The residue contained exclusively crystalline phase Cu_2O that allows it to be returned to copper production. Neutralization of the tellurium-containing solution with sulfuric acid is proposed to precipitate tellurium in the TeO_2 form. The resulting tellurium-containing residue contains 95 % of TeO_2. When H_2O_2 was used in a two-stage oxidative-alkaline leaching process [24], the degree of tellurium recovery was 93 %. The total through the recovery of tellurium was almost 90 %, and the content of TeO_2 in the obtained residue was 96 %. The authors also suggest that the tellurium-containing residue should be sent to the electrolytic production of elemental tellurium.

The most preferable methods well combined with schemes intended to obtain the pure element, are pyrometallurgical ones. According to the dependences of tellurium vapor pressure over solid Cu_2Te specified in studies [[25] and [26]], decomposition of the compound into copper and tellurium is possible only at above 2704 °C [27]. As a consequence, pyrometallurgical methods have not found both application in practice and the development of research in this area.

An effective way to reduce process temperature is to perform the process at low pressure. Besides, the use of a vacuum contributes to the improvement of the personnel's working conditions because the process is performed in hermetically sealed and compact equipment. However, theoretically, the production of tellurium by decomposition of Cu_2Te in real conditions of the vacuum-thermal method is also not possible, due to the low dissociation pressure of liquid copper telluride at the rate of 0.7 kPa at 1780 °C. Nevertheless, we have established the fact of extraction of tellurium from industrial copper telluride in an inert atmosphere (argon) during the development of a pyrometallurgical method of tellurium extraction at low pressure in oxide form [28]. In this regard, it is of interest to study the pyrolysis of copper telluride in an inert atmosphere to determine the presence or absence of the formation of less stable phases during vacuum-thermal processing.

The state diagram of the tellurium-copper system is given in [29] and is characterized by the presence of three compounds of stoichiometric composition: Cu_2Te, Cu_4Te_3, and CuTe. Further studies of the system summarized in [30] showed that the Cu_2Te phase has several polymorphic modifications: A-Cu_2Te, B-Cu_2Te, C-Cu_2Te, D-Cu_2Te, and E-Cu_2Te; whose formation depends on the synthesis temperature of the compound. The presence of peritectoid and eutectoid reactions at below 317 °C resulted in the formation of phases stable at elevated temperatures ($Cu_{13+x}Te_7$, $Cu_{9\pm x}Te_5$, and Cu_9Te_5), as well as phases existing at room temperature as monophase or in alloy with other phases ($Cu_{13+x}Te_7$, $Cu_{9\pm x}Te_5$, Cu_7Te_4, and $Cu_{3-x}Te_2$). In this case, the compound Cu_2Te is the only congruently melting one in the system. Its melting temperature is generally accepted to be 1125 °C.

The analysis of available information has shown that the matter of structural changes in copper telluride close to the composition Cu_2Te at atmospheric pressure up to temperatures of 500-600 °C is well enough studied. At the same time, there is no data on the behavior of telluride at higher temperatures and low pressure.

This paper presents the results of our laboratory study of the thermal behavior of synthetic copper telluride in an inert atmosphere at pressures of 92 and 0.07 kPa under isothermal and non-isothermal vacuum-thermal conditions.

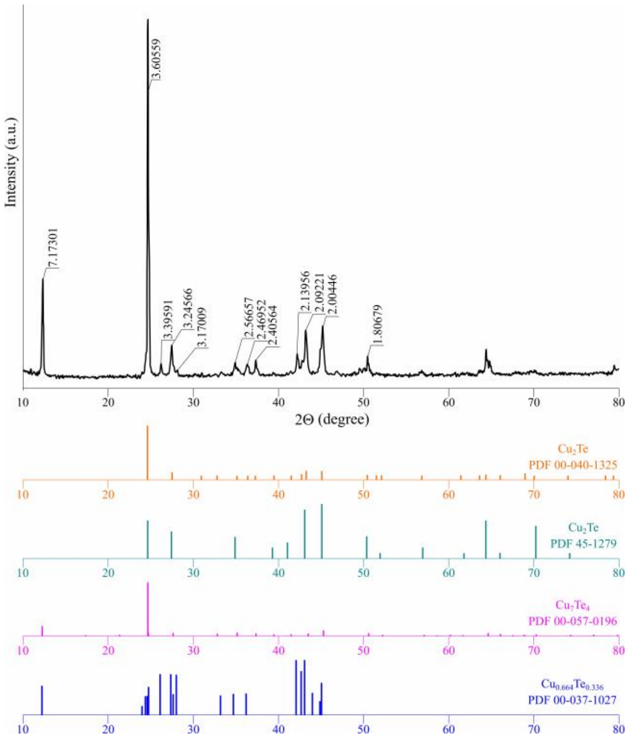

Figure 1 – Phase composition of synthetic copper telluride

Experimental part

Material Synthesis.

Synthetic copper telluride obtained by direct fusion of the initial components in an evacuated quartz ampoule was used in this paper.

Synthesis and production of copper telluride were performed in RT 50/250/ 13 tubular electric furnaces (Nabertherm, Germany) with a B-180 controller. The vacuum system consisting of a 2NVR-5DM UHL4 vacuum rotary vane pump (Vacuummash, Russia) and McLeod manometer was used for ampoules evacuation. Argon (as an inert gas) was used to wash the ampoules. The material of the ampoules was quartz glass.

The initial components for synthetic copper telluride production were electrolyte copper shavings (99.99 %) and elemental tellurium powder (99.98 %) taken in the amounts of 49.92 wt. % of Cu and 50.08 wt. % of Te which corresponds to the stoichiometric composition of the compound Cu_2Te: 66.667 at. % of Cu and 33. 333 at. % of Te. The synthesis temperature was 1200 °C. The heating rate of the suspension to the required temperature was 2 °C/min. The synthesis time was 6 hours. Slow cooling of the obtained alloys in the furnace was performed after the expiration of the specified holding time.

X-ray phase analysis with Bruker D8 Advance diffractometer with Cu-Kα radiation was used to identify the phase composition. The obtained X-ray diffractograms were analyzed using the ICDD PDF-2 (relies on 2020) and literature data [[31], [32]].

The object of the study.

The phase composition of the averaged sample of the obtained copper telluride is shown in Figure 1. The synthesized material is mainly represented by a mixture of copper tellurides with stoichiometric (Cu_2Te) and non-stoichiometric ($Cu_{2-x}Te$) compositions. The phase of Cu_7Te_4 (or $Cu_{1.75}Te$) is the base of the alloy. Besides, there is a phase $Cu_{0.664}Te_{0.336}$ (or $Cu_{1.91}Te$) in the alloy. The heterogeneity of composition can be explained by the fact that the production of homogeneous samples having reproducible stoichiometric composition is complicated since the generally accepted melting point of the compound (1125 °C) exceeds the boiling point of Te (990 °C) [33]. A slight shift and differences in the intensity and shape of the peaks are possible due to the different grain sizes of milled samples, defects in the crystal structure, and the joint presence of several polymorphic modifications of copper telluride [34].

Pyrolysis of the copper telluride.

The experimental part intended to study copper telluride pyrolysis was performed with the use of vacuum units with horizontal and vertical reactor arrangements.

The horizontal unit (Figure 2) consists of a Nabertherm electric furnace with a B-180 controller, a 2NV3-5DM UHL4 vacuum pump, and a quartz reaction vessel where a boat with a suspension of a given mass was placed. A split porcelain condenser required to collect the condensing material was placed on the boat. Chromel-alumel thermocouple (DTPK021-1.2/0.7 thermoelectric converter) with a single-channel TRM1 microprocessor meter-regulator was used to control the temperature in the reaction zone. The pressure was measured with a McLeod manometer with an accuracy of ±10 Pa and an M110 aneroid barometer with an accuracy of ±0.13 kPa.

The methodology of the experiment was as follows. An alundum boat with a copper telluride sample of a given mass was placed in the reactor. The system was sealed and flushed with argon several times. The required pressure in the system was created using a vacuum pump and controlled by a barometer and manometer. When the pressure in the reactor reached the desired value, the retort with the sample was transferred into an electric furnace heated to the required temperature so that the sample was in the isothermal zone of the furnace. The reactor was removed from the furnace and cooled under vacuum after the end of the process. The system was then disassembled. The boat with the residue was weighed. The residue was further pulverized and sent for quantitative and qualitative analyses. The extraction degree was calculated from the quantitative analysis based on the difference in tellurium content in the initial sample and the vacuuming residue. The sample was weighted before and after the experiment on PA214C analytical scales (Ohaus-Pioneer) with an accuracy of ±0.1 mg.

The material composition was studied by X-ray fluorescence analysis using an Axios "PANalytical" wave dispersive combined spectrometer.

X-ray phase analysis on a Bruker D8 Advance diffractometer with Cu-Kα emission, and ICDD PDF-2 bar graph reference database (2020) was used to identify the phase composition.

A horizontal unit (Figure 3) was used to determine the mechanism of mass loss during the heating of copper telluride under non-isothermal conditions at a pressure of 0.07 kPa. The apparatus was a retort made of two parts: the lower one was made of alloy steel, placed in the RT 50/250/13 electric furnace, and the upper one was made of heat-resistant glass. A crucible with a sample of copper telluride was mounted on a hollow suspension inside the steel retort. The junction of a platinum and platinum-rhodium thermocouple was placed inside the suspension at the level of the crucible with suspension. The suspension was supported on the scales of the mass loss measurement system placed in the upper part of the retort. The retort parts were articulated by a rubber seal placed outside the high-temperature zone. The lower and upper parts of the retort were separated by screens to reduce heat flow from the high-temperature zone. The upper part of the retort contained the pressure measurement system, channels for gas evacuation and argon filling, and thermocouple end outlets. The mass, pressure, and temperature measurement systems had signal outputs to a multi-point potentiometer that recorded measurements on a chart tape.

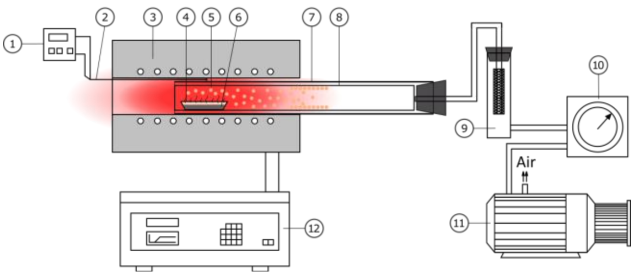

1 – temperature controller in the reaction zone; 2 – control thermocouple; 3 – electric furnace; 4 – boat; 5 – isothermal zone; 6 – suspension; 7 – reactor; 8 – split condenser; 9 – filter; 10 – barometer and manometer; 11 – vacuum pump; 12 – furnace controller

Figure 2 – Scheme of the unit intended to study the pyrolysis process of copper telluride

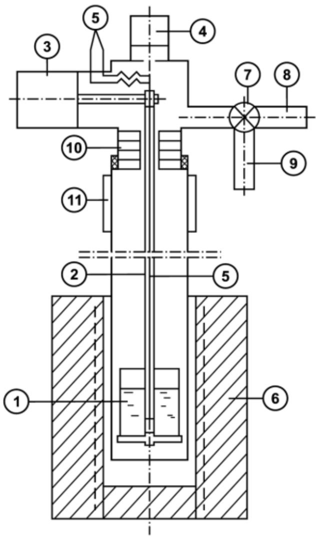

1 – crucible; 2 – suspension; 3 – weight measurement system; 4 – pressure measurement system; 5 – thermocouple; 6 – electric furnace; 7 – flow valve; 8 – gas evacuation channel; 9 – inert gas supply channel; 10 – screen; 11 – caisson

Figure 3 – Scheme of the unit intended to study the pyrolysis process of copper telluride

A sample of the alloy was placed in a quartz crucible and then mounted on a suspension with a disconnected retort outside the heating zone to experiment. Then the lower part of the retort was articulated with the upper one. Gases were evacuated from the retort by a vacuum pump and filled with argon during studies in an inert atmosphere. Then the lower part of the retort was placed in the isothermal zone of the electric furnace, and the furnace heating was switched on. The mass loss of the material sample and the change in its temperature, as well as the change in pressure in the system, were recorded during the heating process of the furnace synchronously. A leak valve was used to keep the pressure in the system constant. The retort was removed from the furnace at the end of the process. The curve of mass change over time was used to determine the degree of mass loss of the material at certain time intervals.

A thermal analysis was performed with the use of an STA 449 F3 Jupiter synchronous thermal analysis instrument to find phase and structural transformations occurring in synthetic copper telluride during heating in an inert atmosphere at a pressure of 92 kPa. The furnace space was evacuated before heating, (evacuated volume level ~ 92 %) and then purged with inert gas for 5 minutes. The heating of the sample was performed at a rate of 5 °C/min in an atmosphere of highly purified argon. The total volume of incoming argon was kept within the range of 100-110 ml/min. The results were processed with the use of NETZSCH Proteus software.

Results and Discussion

Several researchers, for example [[35], [36], [37], [38], [39], [40], [41], and [42]], studied the structural changes in copper telluride of various compositions up to temperatures of 500-600 °C. Thus Stevels [35] showed by a combination of thermal and X-ray phase analyses that the compound of Cu_2Te (or $Cu_{2-x}Te$, where $0 \le x \le 0.2$) underwent 4 polymorphic transformations at 190, 260, 310, and 475 °C. It was noted that the compound Cu_7Te_4 (or $Cu_{1.75}Te$) had the following transformation temperatures: 255, 305, and 340 °C. In the paper [36], found by thermal analysis that the compound $Cu_{2-x}Te$ (where $0 < x < 0.16$) underwent structural changes at 172, 305-320, 360, and 425-560 °C. Similar temperatures of polymorphic transformations were obtained for the compound $Cu_{2-x}Te$ (where $x < 0.05$) [37] and for the compound containing 35.2 at. % of Te [38]. At the same time, [39] states that the combination of endothermic effects with maximum development at 180, 305, 345, and 465 °C shows the presence of the compound $Cu_{2-x}Te$ with a homogeneity range of 33.3-34.2 at. % Te, which corresponds to the compound Cu_2Te.

Figure 4 shows the results of the thermal analysis of copper telluride in an argon atmosphere at a pressure of 92 kPa. As it can be seen the DTA curve showed several endothermic effects of varying intensity during heating of the synthesized material at a rate of 7 °C/min. Their extremes occurred at the following temperatures: 185.7, 259.5, 318, 350, 470, 507.8, 834.5, and 948.5 °C. An additional endothermic effect with an extremum was recorded on the dDTA curve at 459.5 °C.

For clarity, the temperatures of phase transitions from various sources, including our study, are summarized in Table 1. It should be noted that the differences in the temperatures of polymorphic transformations are related to the amount of tellurium in the compound, as well as differences in the methods used to obtain the data. The presence of transformation in the interval 255-275 °C, according to [37], indicates the presence of the rhombohedral phase of telluride in the initial compound.

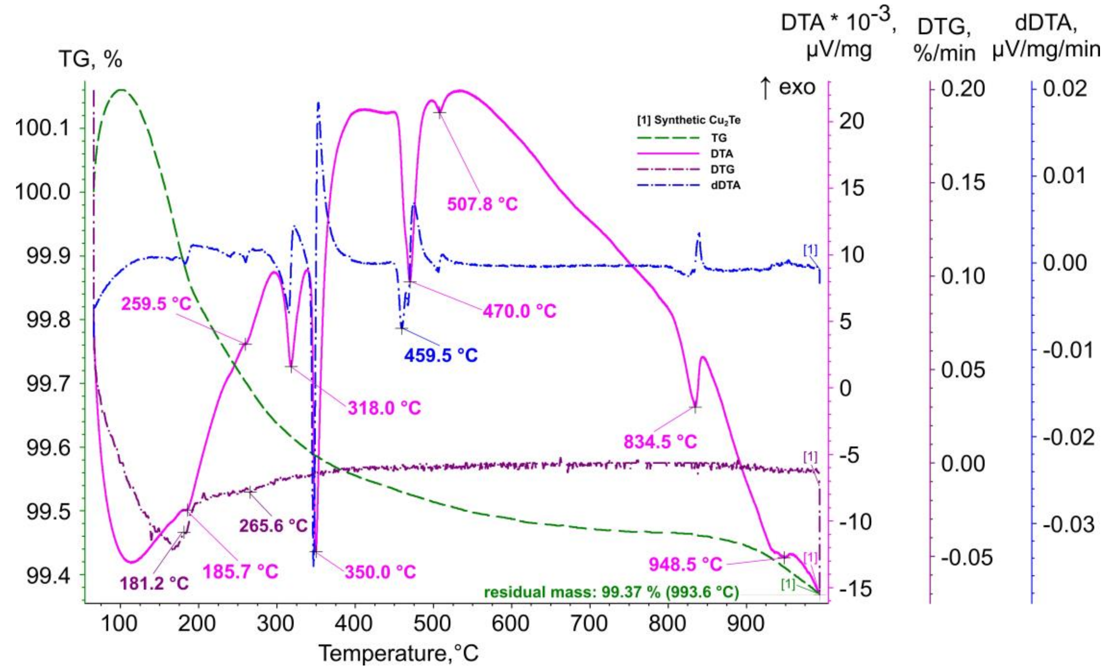

Figure 4 – Thermogram of synthetic copper telluride at atmospheric pressure

Table 1 – Temperatures of polymorphic transformations in Cu_2Te

Source	Temperatures of polymorphic transformations in Cu2Te					
[35]	190	260	310		475	
		255	305	340		
[36]	172		305-320	360	425-560	
[37]	175	275	320	365		575
[38]	190		310	360	460	550
[39]	180		305	345	465	
[42]	160	258	317	360		568
our research	185.7	259	318	350	470	

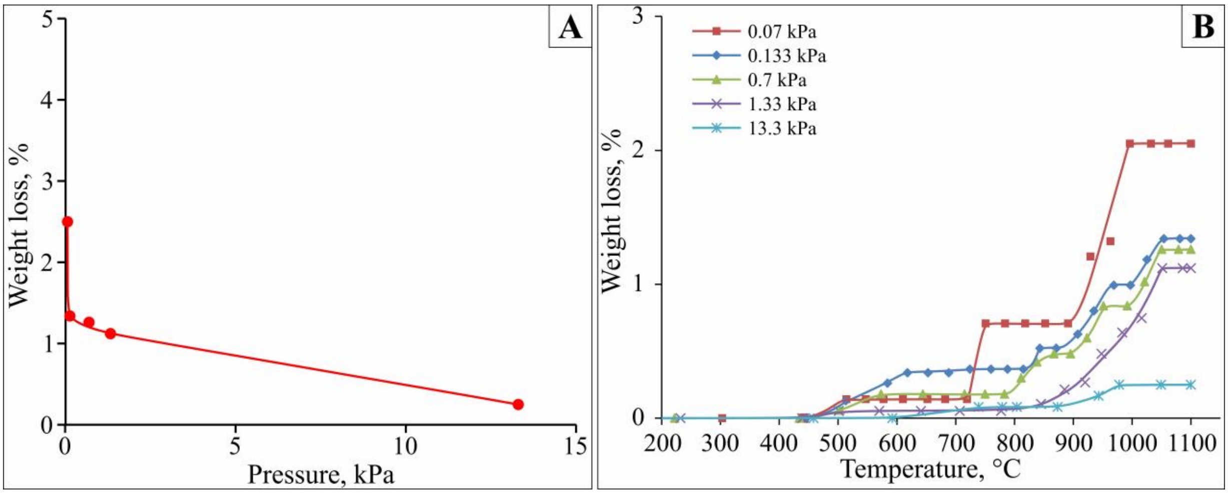

Figure 5 – Dependence of mass loss on pressure (a) and temperature (b)

As can be seen, the data obtained by us are in good agreement with the known values of the temperatures of polymorphic transformations. So, the combination of effects at 185.7, 259, 318, and 470 °C refer to the compound Cu_2Te (or $Cu_{2-x}Te$, where $0 \leq x \leq 0.2$). At the same time, the presence of an endothermic effect at 350 °C is explained by the presence of non-stoichiometric telluride $Cu_{1.75}Te$. The peak on the dDTA curve at 459 °C probably refers to the melting of unreacted elemental tellurium (450 °C). The endothermic effect with maximum development at 507.8 °C probably reflects the decomposition of copper telluride [40]. the polymorphic transformation ε→ζ mentioned by Hansen in [41] is at 834.5 °C.

The residue obtained after thermal analysis is a molten material, although the generally accepted melting point of Cu_2Te is 1125 °C [13]. Therefore, the effect at 948.5°C can be attributed to the melting of copper telluride with subsequent evaporation of tellurium from it. This conclusion is also supported by information [42] about a lower melting temperature (875-1111 °C).

A slight increase in mass loss was observed (Figure 5a) when the pressure was lowered to 0.07 kPa. The curves of copper telluride mass loss (Figure 5b) at continuous temperature increase up to 1100 °C and low pressure (0.07-13.3 kPa) are characterized by two stages. At the same time, the condensation of tellurium in the cold zone of the reactor can also be visually divided into two stages. The first of them refers to process temperatures of about 500 °C and is characterized by a light grayscale (at a pressure of 0.07-0.7 kPa). The second stage occurs in the range of 700-800 °C and is accompanied by a sharp increase in the amount of condensate in the deposition zone and a change of its color to black. At a pressure of 13.3 kPa, condensation of tellurium is noted at higher temperatures. The vacuumization residue is a sintered material with elemental copper on the surface.

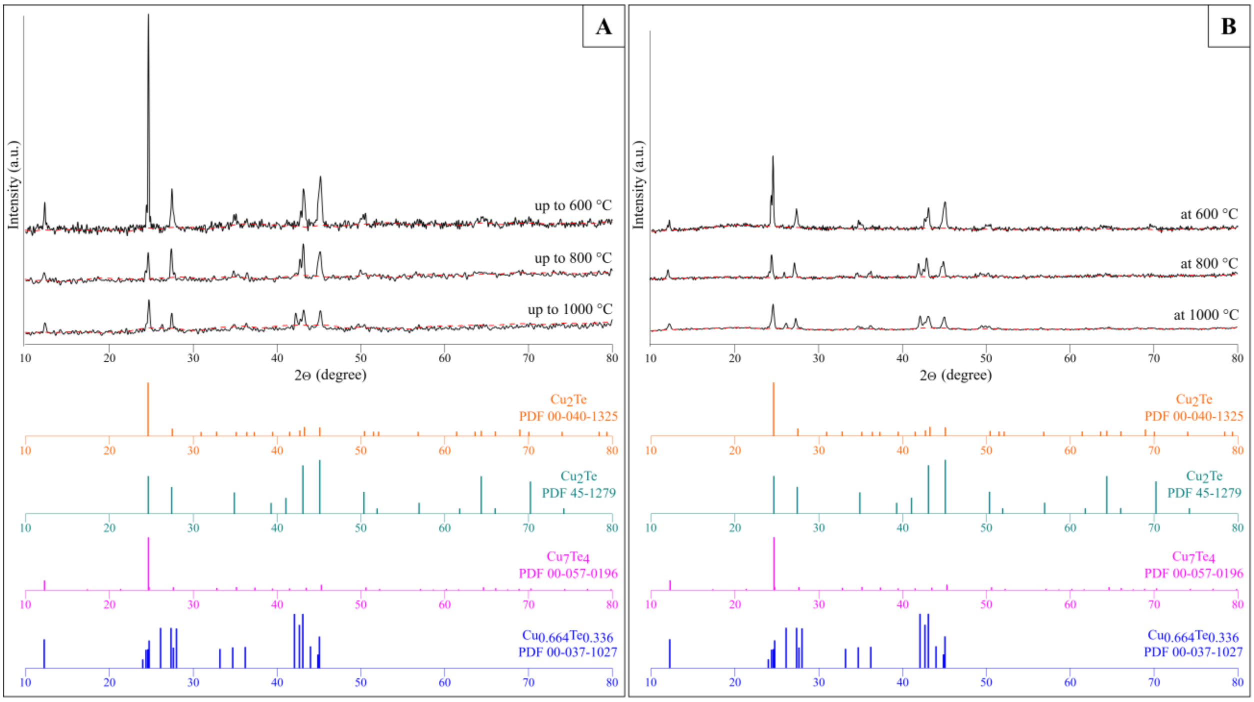

Figure 6 – X-ray radiographs of residues obtained at constant (a) and increasing (b) temperature

Samples intended to analyze possible phase transitions in copper telluride during its heating in vacuum were obtained at a pressure of 0.07 kPa under conditions of constant (600, 800 and 1000 °C) and increasing temperatures (up to 600, 800 and 1000 °C). The X-ray phase analysis results (Figure 6) of the obtained residues showed the absence of formation of new phases relative to the initial composition. At the same time, there are changes in the quantitative ratio of the existing phases in the direction of increase in the amount of $Cu_{0.656}Te_{0.344}$ with increase in the process temperature. It should be noted that the specified phase is predominant with the content up to 86 % in process conditions with heating of samples.

A partial amorphization of the obtained samples, expressed by the presence of an amorphous halo, was also established using X-ray phase analysis. The presence of the latter in the X-ray diffraction patterns is probably related to the partially disordered structure of the material due to polymorphic transitions.

Conclusions

Thus, a laboratory study was performed to investigate the thermal behavior of synthetic copper telluride in an inert atmosphere at pressures of 92 and 0.07 kPa under isothermal and non-isothermal vacuum-thermal conditions.

The results of the thermal analysis showed that the synthesized copper telluride at 185.7, 259, 318, 350, 470, and 834.5 °C undergoes polymorphic transformations established by earlier studies and characteristic for copper tellurides with stoichiometric and non-stoichiometric compositions.

The nonlinear character of the curve of mass loss dependence on temperature was established during the determination of the mechanism of mass loss during the heating of copper telluride in non-isothermal conditions at low pressure. In this case, lowering the pressure in the system insignificantly increases the final value of mass loss of the synthetic sample.

The results of X-ray phase analysis of residues obtained at constant (600, 800, and 1000 °C) and increasing temperatures (up to 600, 800, and 1000 °C) at a pressure of 0.07 kPa showed the absence of formation of new phases relative to the initial composition. Changes in the quantitative ratio of the existing phases towards an increase in the amount of $Cu_{0.656}Te_{0.344}$ were established at the increasing process temperature. Partial amorphization of the obtained samples was also established. It is probably connected with a partially disordered structure of the material due to polymorphic transitions.

The obtained data are theoretical.

Conflicts of interest. The corresponding author declares that there is no conflict of interest.

CRediT author statement. **A. Nitsenko**: Conceptualization, Writing-Original Draft, Methodology, Formal analysis. **X. Linnik**: Writing – review & editing, Investigation. **V. Volodin:** Conceptualization, Methodology. **F. Tuleutay:** Investigation. **N. Bakhytuly:** XRD Investigation.

Acknowledgments. This study was funded by the Science Committee of the Ministry of Science and Higher Education of the Republic of Kazakhstan (Grant AR19576910).

Cite this article as: Nitsenko AV, Linnik XA, Volodin VN, Tuleutay FKh, Bakhytuly N. Pyrolysis of synthetic copper telluride in an inert atmosphere. Kompleksnoe Ispolzovanie Mineralnogo Syra = Complex Use of Mineral Resources. 2025; 335(4):67-77. https://doi.org/10.31643/2025/6445.41

Синтетикалық мыс теллуридінің инертті атмосферадағы пиролизі

Ниценко А.В., Линник К.А., Володин В.Н., Тулеутай Ф.Х., Бахытұлы Н.

Металлургия және кен байыту институты АҚ, Сәтбаев Университеті, Алматы, Қазақстан

Мақала келді: *23 шілде 2024*
Сараптамадан өтті: *16 қыркүйек 2024*
Қабылданды: *26 қыркүйек 2024*

ТҮЙІНДЕМЕ

Жұмыста изотермиялық және изотермиялық емес вакуум-термиялық үрдіс жағдайында инертті атмосферада 92 және 0,07 кПа қысымда синтетикалық мыс теллуридінің жылулық әрекетін зерттеу нәтижелері берілген. Термиялық талдау нәтижелері синтезделген мыс теллуриді 185,7, 259, 318, 350, 470 және 834,5 °С температураларында ерте зерттеулерде анықталғандай стехиометриялық және стехиометриялық емес құрамдағы мыс теллуридіне тән полиморфты өзгерістерге ұшырайтынын көрсетті. Жүйедегі қысымды төмендету синтетикалық үлгінің массалық жоғалуының соңғы мәнін сәл жоғарылататыны анықталды. 0,07 кПа қысымда тұрақты және көтерілетін температурада алынған қалдықтарды рентгендік фазалық талдау нәтижелері бастапқы құрамға қатысты жаңа фазалардың түзілмейтінін көрсетті. Үрдістің температурасының жоғарылауымен бастапқы құрамға қатысты $Cu_{0,656}Te_{0,344}$ мөлшерінің ұлғаюына қарай қолда бар фазалардың сандық қатынасының өзгеруі анықталды.

Түйін сөздер: пиролиз, теллур, мыс, мыс теллуриді, фазалық құрамы, термиялық талдау.

Авторлар туралы ақпарат:

Ниценко Алина Владимировна
Техника ғылымдарының кандидаты, Вакуумдық процестер зертханасының меңгерушісі, Металлургия және кен байыту институты АҚ, Сәтбаев Университеті, Шевченко көшесі, 29/133, 050010, Алматы, Қазақстан. Email: alina.nitsenko@gmail.com; ORCID ID: https://orcid.org/0000-0001-6753-0936

Линник Ксения Александровна
Техника ғылымдарының магистрі, Вакуумдық процестер зертханасының кіші ғылыми қызметкері, Металлургия және кен байыту институты АҚ, Сәтбаев Университеті, Шевченко көшесі, 29/133, 050010, Алматы, Қазақстан. Email: xenija_linnik@mail.ru; ORCID ID: https://orcid.org/0000-0002-0683-1409

Володин Валерий Николаевич
Техника ғылымдарының докторы, профессор, Вакуумдық процестер зертханасының бас ғылыми қызметкері, Металлургия және кен байыту институты АҚ, Сәтбаев Университеті, Шевченко көшесі, 29/133, 050010, Алматы, Қазақстан. Email: volodinv_n@mail.ru; ORCID ID: https://orcid.org/0000-0003-0116-1423

Тулеутай Фархад Ханафияұлы
Техника ғылымдарының магистрі, Вакуумдық процестер зертханасының кіші ғылыми қызметкері, Металлургия және кен байыту институты АҚ, Сәтбаев Университеті, Шевченко көшесі, 29/133, 050010, Алматы, Қазақстан. Email: farkhat_kaldybek@mail.ru; ORCID ID: https://orcid.org/0000-0003-0802-283X

Бахытұлы Наурызбек
Ph.D., Физикалық талдау әдістер зертханасының меңгерушісі, Металлургия және кен байыту институты АҚ, Сәтбаев Университеті, Шевченко көшесі, 29/133, 050010, Алматы, Қазақстан. Email: n.bakhytuly@satbayev.university; ORCID ID: https://orcid.org/0000-0003-3087-0616

Пиролиз синтетического теллурида меди в инертной атмосфере

Ниценко А.В., Линник К.А., Володин В.Н., Тулеутай Ф.Х., Бахытұлы Н.

АО Институт металлургии и обогащения, Satbayev University, Алматы, Казахстан

Поступила: *23 июля 2024*
Рецензирование: *16 сентября 2024*
Принята в печать: *26 сентября 2024*

АННОТАЦИЯ

В работе приведены результаты изучения термического поведения синтетического теллурида меди в инертной атмосфере при давлении 92 и 0,07 кПа в условиях изотермического и неизотермического вакуум-термического процесса. Результаты проведенного термического анализа показали, что синтезированный теллурид меди при температурах 185,7, 259, 318, 350, 470 и 834,5 °С претерпевает полиморфные превращения, установленные ранними исследованиями и характерные для теллуридов меди стехиометрического и нестехиометрического составов. Установлено, что понижение давления в системе незначительно повышает конечное значение потери массы синтетического образца. Результаты рентгенофазового анализа остатков, полученных при постоянной и повышающейся температурах при давлении 0,07 кПа, показали отсутствие образования новых фаз относительно исходного состава. С повышением температуры процесса установлено изменение в количественном соотношении имеющихся фаз в сторону увеличения количества $Cu_{0,656}Te_{0,344}$ относительно исходного состава.

Ключевые слова: пиролиз, теллур, медь, теллурид меди, фазовый состав, термический анализ.

Информация об авторах:

Ниценко Алина Владимировна
Кандидат технических наук, заведующий лабораторией вакуумных процессов АО Институт металлургии и обогащения, Satbayev University, ул. Шевченко 29/133, 0500100, Алматы, Казахстан. Email: alina.nitsenko@gmail.com; ORCID ID: https://orcid.org/0000-0001-6753-0936

Линник Ксения Александровна
Магистр технических наук, младший научный сотрудник лаборатории вакуумных процессов АО Институт металлургии и обогащения, Satbayev University, ул. Шевченко 29/133, 0500100, Алматы, Казахстан. Email: xenija_linnik@mail.ru; ORCID ID: https://orcid.org/0000-0002-0683-1409

Володин Валерий Николаевич
Доктор технических наук, профессор, главный научный сотрудник лаборатории вакуумных процессов АО Институт металлургии и обогащения, Satbayev University, ул. Шевченко 29/133, 0500100, Алматы, Казахстан. Email: volodinv_n@mail.ru; ORCID ID: https://orcid.org/0000-0003-0116-1423

Тулеутай Фархад Ханафияұлы
Магистр технических наук, младший научный сотрудник лаборатории вакуумных процессов АО Институт металлургии и обогащения, Satbayev University, ул. Шевченко 29/133, 0500100, Алматы, Казахстан. Email: farkhat_kaldybek@mail.ru; ORCID ID: https://orcid.org/0000-0003-0802-283X

Бахытұлы Наурызбек
Ph.D., заведующий лабораторией физических методов анализа АО Институт металлургии и обогащения, Satbayev University, ул. Шевченко 29/133, 0500100, Алматы, Казахстан. Email: n.bakhytuly@satbayev.university; ORCID ID: https://orcid.org/0000-0003-3087-0616

References

[1] Gao T, Lv J, Zhou J, Li Y, Li Z. Innovative technology and mechanism for comprehensive recovery of copper, nickel, zinc and iron in electroplating sludge. Separation and Purification Technology. 2024; 336: 126226. https://doi.org/10.1016/j.seppur.2023.126226

[2] Koizhanova A, Kenzhaliyev B, Magomedov D, Erdenova M, Bakrayeva A, Abdyldaev N. Hydrometallurgical studies on the leaching of copper from man-made mineral formations. Kompleksnoe Ispolzovanie Mineralnogo Syra = Complex Use of Mineral Resources. 2024; 330(3):32-42. https://doi.org/10.31643/2024/6445.26

[3] Semushkina L, Tussupbayev N, Turysbekov D, Narbekova S, Kaldybayeva Z. Flotation processing of copper-containing technogenic raw materials using a composite flotation reagent. Kompleksnoe Ispolzovanie Mineralnogo Syra = Complex Use of Mineral Resources. 2023; 324(1):34-42. https://doi.org/10.31643/2023/6445.05

[4] Choudhary S, Dhiman S, Hintersatz C, Matys S, Kutschke S, Tsushima S, Pollmann K, Saravanan V, Jain R. Selective recovery of Cu from copper mold production waste by organic ligands. Journal of Environmental Chemical Engineering. 2024; 12(5): 113398. https://doi.org/10.1016/j.jece.2024.113398

[5] Argyn A, Zoldasbay E, Dosmukhamedov N. Improving the quality of converting products by the joint smelting of high-sulfur copper concentrate with copper-lead matte. Kompleksnoe Ispolzovanie Mineralnogo Syra = Complex Use of Mineral Resources. 2024; 328(1):50-58. https://doi.org/10.31643/2024/6445.06

[6] Chen A, Peng Z, Hwang J-Y, Ma Y, Liu X, Chen X. Recovery of Silver and Gold from Copper Anode Slimes. JOM. 2015; 2:493-502. https://doi.org/10.1007/s11837-014-1114-9

[7] Mahmoudi A, Shakibania S, Mokmeli M, Rashchi F. Tellurium, from copper anode slime to high purity product: A review paper. Metallurgical and Materials Transactions B. 2020; 51:2555-2575. https://doi.org/10.1007/s11663-020-01974-x

[8] Liu G, Wu Yu, Tang A, Pan D, Li B. Recovery of scattered and precious metals from copper anode slime by hydrometallurgy: A review. Hydrometallurgy. 2020; 197:105460. https://doi.org/10.1016/j.hydromet.2020.105460

[9] Mastyugin SA, Naboichenko SS. Processing of copper-electrolyte slimes: Evolution of technology. Russian Journal of Non-Ferrous Metals. 2012; 53:367-374. https://doi.org/10.3103/S1067821212050070

[10] Xing WD, Lee MS. Leaching of gold and silver from anode slime with a mixture of hydrochloric acid and oxidizing agents. Geosystem Engineering. 2017; 20(4):216-223. https://doi.org/10.1080/12269328.2017.1278728

[11] Xiao L, Wang YL, Yu Y, Fu GY, Han PW, Sun ZHI, Ye SF. An environmentally friendly process to selectively recover silver from copper anode slime. Journal of Cleaner Production. 2018.; 187:708-716. https://doi.org/10.1016/j.jclepro.2018.03.203

[12] Ding Y, Zhang S, Liu B, Li B. Integrated process for recycling copper anode slime from electronic waste smelting. Journal of Cleaner Production. 2017; 165:48-56. https://doi.org/10.1016/j.jclepro.2017.07.094

[13] Chizhikov DM, Shchastlivyi VP. Tellurium and Tellurides. Collet's Publishers Ltd.: London, UK. 1970.

[14] Hoffman JE. Recovering selenium and tellurium from copper refinery slimes. JOM. 1989; 41:33-38. https://doi.org/10.1007/BF03220269

[15] Kenzhaliyev B K, Trebukhov S A, Volodin V N, Trebukhov A A, Tuleutay F Kh. Selenium extraction out of metallurgical production middlings. Kompleksnoe Ispolzovanie Mineralnogo Syra = Complex Use of Mineral Resources. 2018; 307(4):56-64. https://doi.org/10.31643/2018/6445.30

[16] Kenzhaliyev BK, Trebukhov SA, Nitsenko AV, Burabayeva NM, Trebukhov AA. Determination of technological parameters of selenium recovery from metallurgical production middlings in a vacuum distillation unit. International Journal of Mechanical and Production Engineering Research and Development. 2019; 9(6):87-98.

[17] Mastyugin SA, Volkova NA, Naboichenko SS, Lastochkina MA. Shlamy elektroliticheskogo rafinirovaniya medi i nikelya [Slime from Electrolytic Refining of Copper and Nickel]. Ural Federal University: Ekaterinburg, Russia. 2013. (in Russ.).

[18] Nitsenko A, Linnik X, Volodin V, Tuleutay F, Burabaeva N, Trebukhov S, Ruzakhunova G. Phase transformations and tellurium recovery from technical copper telluride by oxidative-distillate roasting at 0.67 kPa. Metals. 2022; 12(10):1774. https://doi.org/10.3390/met12101774

[19] Wang S. Tellurium, its resourcefulness and recovery. JOM. 2011; 63:90-93. https://doi.org/10.1007/s11837-011-0146-7

[20] Shibasaki T, Abe K, Takeuchi H. Recovery of tellurium from decopperizing leach solution of copper refinery slimes by a fixed bed reactor. Hydrometallurgy. 1992; 29:399-412. https://doi.org/10.1016/0304-386X(92)90024-T

[21] Nitsenko AV, Burabaeva NM, Tuleytay FK, Seisembaev RS, Linnik XA, Azlan MN. Study of physical and chemical properties of tellurium-containing middlings. Kompleksnoe Ispolzovanie Mineralnogo Syra = Complex Use of Mineral Resources. 2020; 315(4):49-56. https://doi.org/10.31643/2020/6445.36

[22] Xu L, Xiong Y, Song Y, Zhang G, Zhang F, Yang Y, Hua Z, Tian Y, You J, Zhao Z. Recycling of copper telluride from copper anode slime processing: Toward efficient recovery of tellurium and copper. Hydrometallurgy. 2020; 196:105436. https://doi.org/10.1016/j.hydromet.2020.105436

[23] Nitsenko AV, Linnik KA, Tuleutay FH, Burabayeva NM, Seisembayev RC. Fiziko-himicheskaya harakteristika tellursoderzhashchego promprodukta TOO Kazahmys Smelting [Physical and chemical characterization of tellurium-containing industrial product of Kazakhmys Smelting LLP]. Teoriya i tekhnologiya metallurgicheskogo proizvodstva = Theory and technology of metallurgical production. 2021; 3:10-16. (in Russ.).

[24] Xu L, Xiong Y, Zhang G, Zhang F, Yang Y, Hua Z, Tian Y, You J, Zhao Z. An environmental-friendly process for recovery of tellurium and copper from copper telluride. Journal of Cleaner Production. 2020; 272:122723. https://doi.org/10.1016/j.jclepro.2020.122723

[25] Weissburd SE. Fiziko-himicheskie svojstva i osobennosti stroeniya sul'fidnyh rasplavov [Physical and chemical properties and structure peculiarities of sulfide melts]. Metallurgy: Moscow, Russia. 1996. (in Russ.).

[26] Dutchak YaI, Korenchuk NM, Korenchuk SV. Issledovanie davleniya para i termodinamicheskiy analiz splavov sistemy Cu_2S–Cu_2Te [Study of vapor pressure and thermodynamic analysis of alloys of the system Cu_2S–Cu_2Te]. Izvestiya AN SSSR. Neorganicheskie materialy = Proceedings of the Academy of Sciences of the USSR. Inorg. materials. 1975; 11(2):201-203. (in Russ.).

[27] Nitsenko A, Volodin V, Linnik X, Burabaeva N, Tuleutay F. Behavior of copper chalcogenides during vacuum-thermal processing. Metalurgija. 2023; 62(1):125-128. https://hrcak.srce.hr/file/407986

[28] Nitsenko AV, Volodin VN, Linnik XA, Tuleutay FKh, Burabaeva NM. Distillation recovery of tellurium from copper telluride in oxide form. Russian Journal of Non-Ferrous Metals. 2022; 63(3):284-291. https://doi.org/10.3103/S1067821222030105

[29] Lyakishev NP. Diagrammy sostoyaniya dvojnyh metallicheskih sistem: Spravochnik v 3 tomax [State diagrams of double metal systems: Handbook in 3 volumes]. Mashinostroenie: Moscow, Russia. 1997; 2. (in Russ.).

[30] Pashinkin AS, Fedorov VA. Phase equilibria in the Cu–Te System. Inorganic materials. 2003; 39(6):539-554. https://doi.org/10.1023/A:1024003932461

[31] Qiu Y, Ye J, Liu Y, Yang X. Facile rapid synthesis of a nanocrystalline Cu_2Te multi-phase transition material and its thermoelectric performance. RSC Advances. 2017; 36(7):22558-22566. https://doi.org/10.1039/C7RA02145C

[32] He Y, Zhang T, Shi X, Wei S-H, Chen L. High thermoelectric performance in copper telluride. NPG Asia Materials. 2015; e210(7):1-7. https://doi.org/10.1038/am.2015.91

[33] Yagafarova ZA, Bikkulova NN, Nigmatullina GR, Bikkulova LV. Fazovye sootnosheniya v tverdom elektrolite na osnove tellurida medi [Phase relations in the solid electrolyte based on copper telluride]. Fundamental'nye issledovaniya = Fundamental Research. 2016; 11:968-974. (in Russ.).

[34] Gorelik SS, Dubrovina AN, Drozdova GA, Turdaliyev T. Vliyanie izmel'cheniya, pressovaniya i otzhiga na strukturu i svojstva hal'kogenidov medi [Influence of grinding, pressing and annealing on the structure and properties of copper chalcogenides]. Elektronnaya tekhnika. Seriya Materialy = Electron Technique. Materials Series. 1972; 10:73-76. (in Russ.).

[35] Stevels ALN. Phase transitions in nickel and copper selenides and tellurides. Philips Research reports Supplements. 1969; 9:1-124.

[36] Guastavino F, Luquet H, Bougnot J. Etude du diagramme de phase du systeme Cu – Te dans le domaine de la solution solide $Cu_{2-x}Te$ ($0 < x < 0,16$). Materials Research Bulletin. 1973; 8(8):935-942. https://doi.org/10.1016/0025-5408(73)90078-0

[37] Vouroutzis N, Manolikas C. Phase transformations in cuprous telluride. Physica Status Solidi(a). 1989; 111(2):491-497. https://doi.org/10.1002/pssa.2211110213

[38] Tsypin MN, Chipizhenko AA. Osobennosti struktury i svojstv nizzhego tellurida medi [Features of the structure and properties of low copper telluride]. Neorganicheskie materialy = Inorganic Materials. 1974; 10(8):1210-1214. (in Russ.).

[39] Abrikosov NH. Dvojnye i mnogokomponentnye sistemy na osnove medi: Spravochnik [Double and multicomponent systems based on copper: Reference book]. Nauka: Moscow, USSR. 1979. (in Russ.).

[40] Kavirajan S, Harish S, Archana J, Shimomura M, Navaneethan M. Phase transition induced thermoelectric properties of Cu_2Te by melt growth process. Materials Letters. 2021; 298:129957. https://doi.org/10.1016/j.matlet.2021.129957

[41] Huang D, Han R, Wang Y, Ye T. The Cu–Te system: Phase relations determination and thermodynamic assessment. Journal of Alloys and Compounds. 2021; 585(2):157373. https://doi.org/10.1016/j.jallcom.2020.157373

[42] Abrikosov NH, Bankina VF, Poretskaya LV, Skudnova EV, Chizhevskaya SN. Poluprovodnikovye hal'kogenidy i splavy na ih osnove [Semiconducting chalcogenides and alloys based on them]. Nauka: Moscow, USSR. 1975. (in Russ.).

DOI: 10.31643/2025/6445.42
Metallurgy

Development of Software for Hydrometallurgical Calculation of Metal Extraction

[1]Kenzhaliyev B.K., [2]Amangeldy B.S., [2]Mukhanbet A., [2*]Azatbekuly N.,
[1]Koizhanova A., [1]Magomedov D.R.

[1] Institute of Metallurgy and Ore Beneficiation JSC, Satbayev University, Almaty, Kazakhstan
[2] Al-Farabi Kazakh National University, Almaty, Kazakhstan

** Corresponding author email: nurtugang17@gmail.com*

Received: *August 5, 2024*
Peer-reviewed: *August 24, 2024*
Accepted: *September 27, 2024*

ABSTRACT

Hydrometallurgy plays a critical role in the metallurgical industry by providing an efficient method for extracting metals from ores and secondary materials using aqueous solutions. This approach is particularly advantageous for processing low-grade and complex ores, as well as secondary resources that cannot be effectively processed by traditional pyrometallurgical methods. The objective of this study is to develop specialized software to automate and optimize the calculations necessary for metal extraction in hydrometallurgical processes. The software integrates a complete computational framework for automating the various stages of the hydrometallurgical process, including ore composition initialization, total element mass calculations, and the determination of metal concentrations in both metal products (matte) and by-products (slag). The methodology involves the design and implementation of a web-based application using Django for the user interface and MySQL for robust data storage. The computational module, written in Python, automates the mathematical operations required to simulate complex chemical reactions and metal extraction processes. This module supports real-time processing and ensures accurate calculations for each stage of metal extraction, including leaching, extraction, re-extraction, sorption, and electrolysis. The software also features detailed tables and dynamic graphs that allow users to analyze the distribution of valuable metals and assess the influence of key operational parameters on extraction efficiency. The results show that the developed software successfully manages large datasets, enhances the precision of hydrometallurgical calculations, and minimizes the risk of human error. The implementation of the software leads to significant improvements in the economic efficiency of production by optimizing metal recovery rates and reducing operational costs. Additionally, it supports comprehensive process control by providing actionable insights into each stage of extraction, thus improving the quality of the final metal product. Overall, the software represents a significant technological advancement in the field, offering a scalable solution for industries aiming to streamline hydrometallurgical processes.

Keywords: hydrometallurgy, calculation automation, metal extraction, mathematical modeling.

Information about authors:

Kenzhaliyev Bagdaulet Kenzhaliyevich	*Doctor of Technical Sciences, Professor, General Director-Chairman of the Management Board of the Institute of Metallurgy and Ore Beneficiation JSC, Satbayev University, 050010, Almaty, Shevchenko str., 29, Almaty, Kazakhstan. Email: bagdaulet_k@mail.ru; ORCID ID: https://orcid.org/0000-0003-1474-8354*
Amangeldy Bibars Sapargaliuly	*Researcher, Al-Farabi Kazakh National University, 71 al-Farabi Ave., 050040, Almaty, Republic of Kazakhstan. Email: a.s.bibars@gmail.com; ORCID ID: https://orcid.org/0000-0002-4089-6337*
Mukhanbet Aksultan	*Researcher, Al-Farabi Kazakh National University, 71 al-Farabi Ave., 050040, Almaty, Republic of Kazakhstan. Email: mukhanbetaksultan0414@gmail.com; ORCID ID: https://orcid.org/0000-0003-4699-0436*
Azatbekuly Nurtugan	*Junior researcher, Al-Farabi Kazakh National University, 71 al-Farabi Ave., 050040, Almaty, Republic of Kazakhstan. Email: nurtugang17@gmail.com; ORCID ID: https://orcid.org/0009-0007-5843-8995*
Koizhanova Aigul	*Candidate of Technical Sciences, Head of Laboratory Institute of Institute of Metallurgy and Ore Beneficiation JSC, Satbayev University, 050010, Almaty, Shevchenko str., 29, Almaty, Kazakhstan. Email: aigul_koizhan@mail.ru; ORCID ID: https://orcid.org/0000-0001-9358-3193*
Magomedov David Rasimovich	*Research Associate, Master's degree Institute of Metallurgy and Ore Beneficiation JSC, Satbayev University, 050010, Almaty, Shevchenko str., 29, Almaty, Kazakhstan. Email: davidmag16@mail.ru; ORCID ID: https://orcid.org/0000-0001-7216-2349*

Introduction

Hydrometallurgy is a vital field in the metallurgical industry, providing efficient extraction of metals from ores and secondary materials using aqueous solutions. This method plays a key role in the extraction of metals such as copper, gold, and rare earth elements due to its ability to process low-grade and complex ores, as well as secondary resources that cannot be effectively processed using traditional pyrometallurgical methods [[1], [2], [3]]. For example, in studies on the hydrometallurgical treatment of industrial waste from copper production at a copper smelter in Kazakhstan, the process of copper leaching from man-made mineral formations was investigated. Analysis showed that the copper content in the raw material was 0.481%, present in various mineral forms, including sulfates and sulfides [4]. The use of gravity concentration and flotation methods allowed for obtaining concentrates with copper contents of 9.35% and 46%, respectively, and sulfuric acid leaching in a mixing mode enabled copper extraction from the enriched raw material [5].

Research and development trends in hydrometallurgy have evolved significantly over the past several decades. Modern hydrometallurgy has been developing for more than 100 years, with a continuous accumulation of related articles. A bibliometric analysis of articles in "Hydrometallurgy", the most authoritative journal in this field, highlights several key trends from 1975 to 2019 [6]. For instance, in [7] an innovative hydrometallurgical process for selectively recovering base and precious metals from waste-printed circuit boards, showcasing the potential of hydrometallurgy was demonstrated. And as one of the principles of circular hydrometallurgy, which emphasizes designing energy-efficient and resource-efficient flowsheets that consume minimal reagents and produce minimal waste, the implementation of real-time analysis and digital process control is important [8].

Precise calculations in hydrometallurgy are crucial for optimizing the metal extraction process, contributing to reduced production costs, increased product yield, and minimized environmental impact. In industrial production conditions, errors in calculations can lead to significant financial losses and technological problems. Traditional calculation methods, based on manual data entry and basic tools like spreadsheets, are prone to human error and do not provide the necessary accuracy and promptness.

Hydrometallurgical processes include several key stages where accurate metal extraction calculations are important [9]. The first stage involves calculating the extraction of metal from the initial ore, where the solid material transitions into a liquid. This method is used to determine the efficiency of metal leaching from the ore using various agents and leaching conditions [10]. The second stage involves calculating metal extraction from the solution during the extraction and re-extraction processes, where the metal is transferred from the productive solution to the rich electrolyte, which is especially important in copper production. The third stage involves calculating metal extraction in the sorption and desorption processes, where metals are extracted from solutions onto solid sorbents and then desorbed for further use. The fourth stage involves calculating the extraction of the obtained metal on the cathode from the rich solution, which is important in electrolytic processes where metals are deposited on cathodes from rich electrolytes. Finally, the fifth stage includes a combined extraction scheme that covers several stages of the technological process, allowing for a comprehensive assessment of metal extraction efficiency from ore to the final product [11].

One of the central goals of hydrometallurgical process design is to determine what resources are required to produce the desired annual amount of product [12]. Flowsheet simulation is widely used in metallurgical design to provide data for equipment sizing, process strategies, and cost estimates. Simulations are crucial for predicting plant water balance and reagent usage during various study stages [13]. Many other works on the automation and simulation of hydrometallurgical processes have been conducted, mainly aimed at the development, optimization, and practical application of technologies for efficient metal extraction [[14], [15], [16], [17], [18], [19]]. For example, in [14], two processes for a small gold mining enterprise were modeled using PRO/II and Python, allowing for the analysis of the impact of uncertainties on extraction indicators and economic metrics. In [[15], [16]], a modular stationary simulator, PRISMA, was developed for modeling and simulating hydrometallurgical processes using object-oriented programming technology. In [17], the role of simulation software in the design and operation of metallurgical plants, considering mineral processing and hydrometallurgical installations for concentrate and pure metal production, is discussed. The use of JKSimMet software for the size-based design of mineral processing units and METSIM and IDEAS for developing energy and mass balances is highlighted. Modern technologies and software significantly simplify and speed up the calculation process, minimizing human errors and ensuring high accuracy and reproducibility of results. Also, recent research highlights the growing adoption of soft computing techniques, such as artificial neural networks and fuzzy algorithms, which are increasingly used to optimize and control complex, non-linear mineral

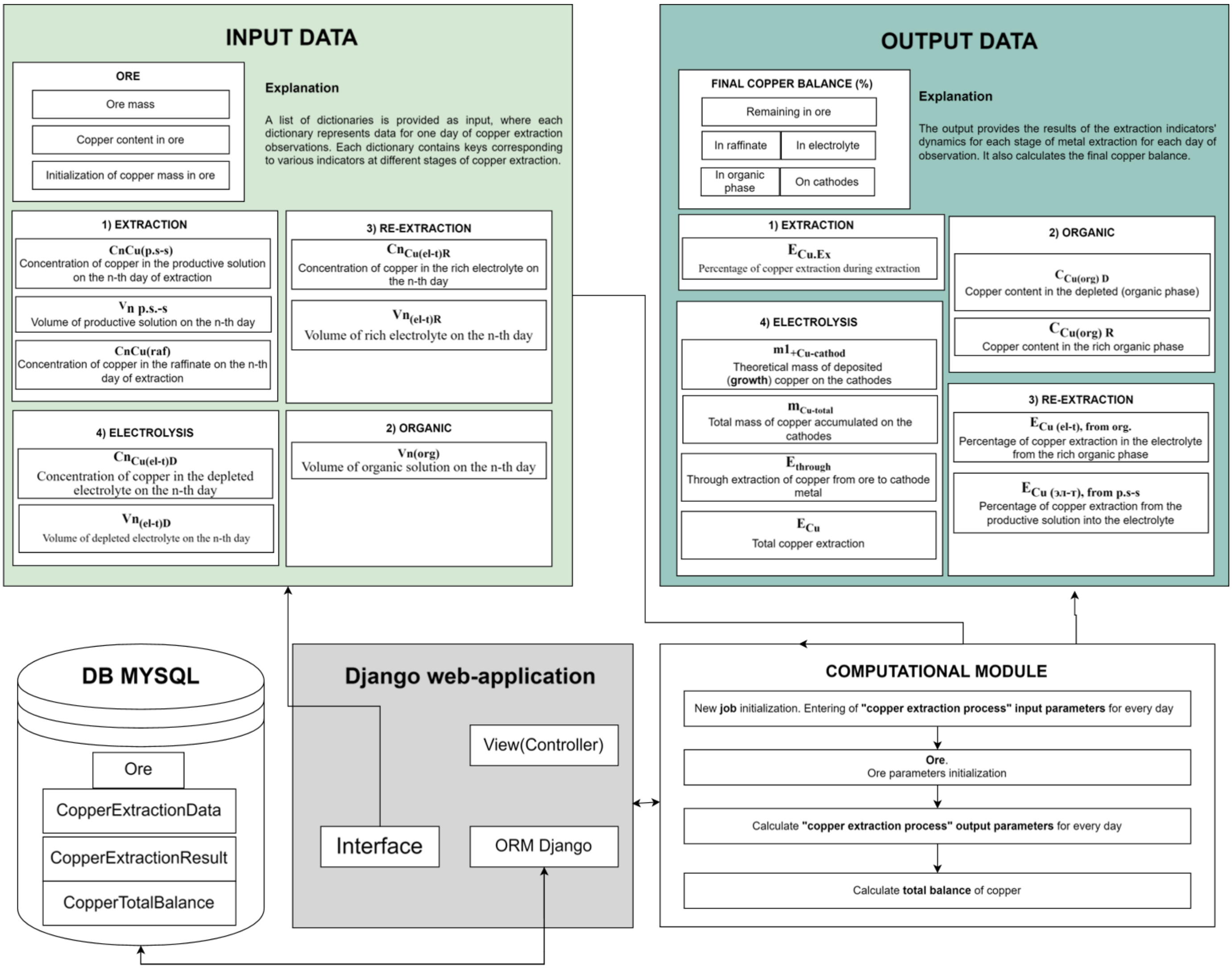

A list of dictionaries is provided as input, where each dictionary represents data for one day of copper extraction observations. Each dictionary contains keys corresponding to various indicators at different stages of copper extraction.

The output provides the results of the extraction indicators' dynamics for each stage of metal extraction for each day of observation. It also calculates the final copper balance.

Figure 1 – General architecture of the system

processing stages, offering advanced alternatives to traditional methods [20].

To address the challenges of automating metal extraction calculations in hydrometallurgical processes, specialized software has been developed. This tool is a web application that automates the calculations of the full combined scheme of the hydrometallurgical metal extraction process, providing accuracy and ease of use.

The use of the developed software offers several advantages. Firstly, it increases the accuracy and reliability of calculations, eliminating human errors and enhancing precision through automation. Secondly, it significantly reduces the time required to perform calculations, allowing for faster production processes. Thirdly, the intuitive interface makes the software accessible to both researchers and production specialists. Thus, the development and implementation of software for automating hydrometallurgical calculations represent a significant step forward in optimizing metal extraction processes.

Experimental part

This experimental part describes the methods and computational processes used to model and calculate hydrometallurgical metal recovery processes. The focus is on the calculations and application of software that automates these processes

1. Architecture

The architecture of our system, shown in Figure 1, is designed to optimize the copper extraction process and includes a MySQL database, a Django web application, and a computational module. Input data is entered through the Django web application and stored in the MySQL database.

The computational module receives the input data, processes it using calculation algorithms, and stores the output data in the database.

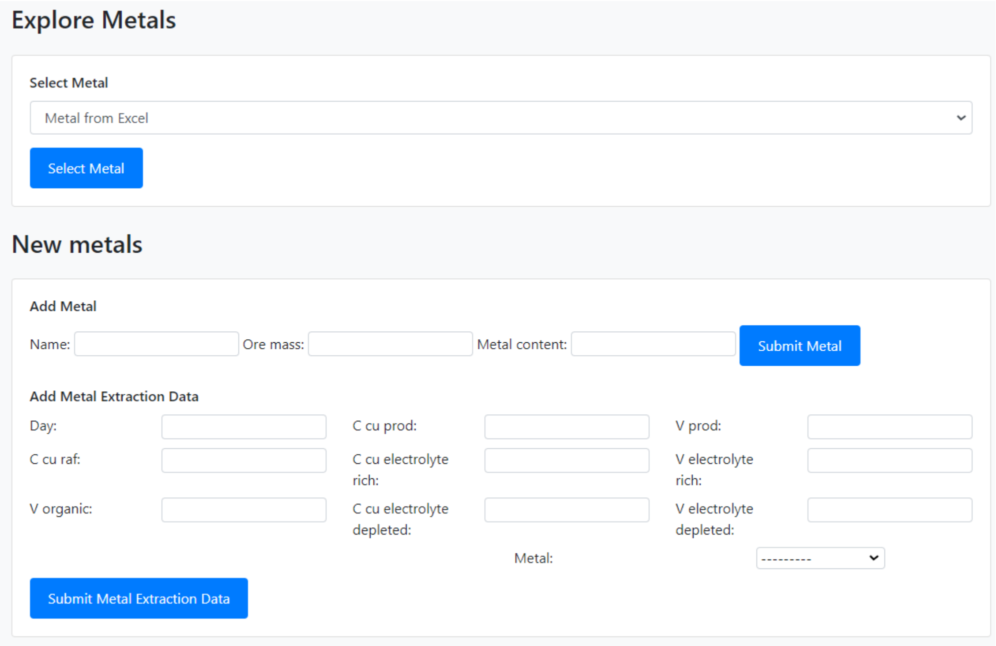

Figure 2 - Explore Metals

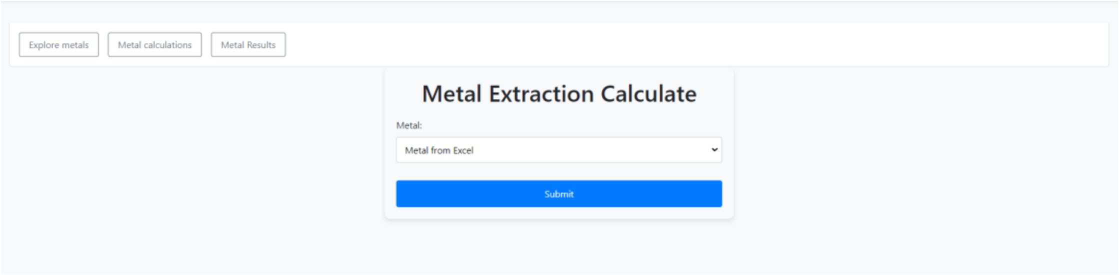

Figure 3 - Metal calculations

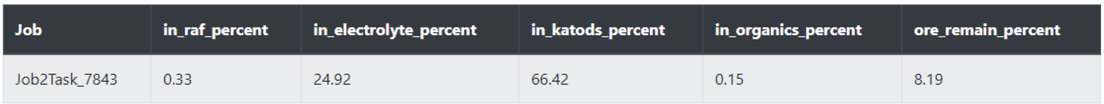

Job	in_raf_percent	in_electrolyte_percent	in_katods_percent	in_organics_percent	ore_remain_percent
Job2Task_7843	0.33	24.92	66.42	0.15	8.19

Figure 4 - Result of calculations (Total copper balance)

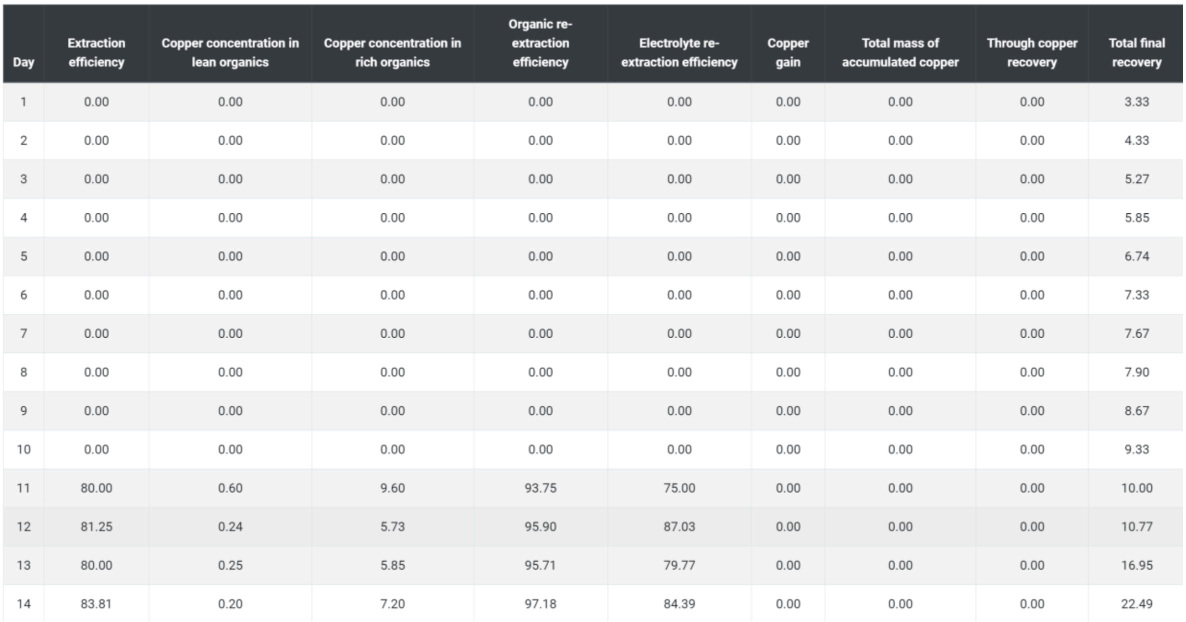

Day	Extraction efficiency	Copper concentration in lean organics	Copper concentration in rich organics	Organic re-extraction efficiency	Electrolyte re-extraction efficiency	Copper gain	Total mass of accumulated copper	Through copper recovery	Total final recovery
1	0.00	0.00	0.00	0.00	0.00	0.00	0.00	0.00	3.33
2	0.00	0.00	0.00	0.00	0.00	0.00	0.00	0.00	4.33
3	0.00	0.00	0.00	0.00	0.00	0.00	0.00	0.00	5.27
4	0.00	0.00	0.00	0.00	0.00	0.00	0.00	0.00	5.85
5	0.00	0.00	0.00	0.00	0.00	0.00	0.00	0.00	6.74
6	0.00	0.00	0.00	0.00	0.00	0.00	0.00	0.00	7.33
7	0.00	0.00	0.00	0.00	0.00	0.00	0.00	0.00	7.67
8	0.00	0.00	0.00	0.00	0.00	0.00	0.00	0.00	7.90
9	0.00	0.00	0.00	0.00	0.00	0.00	0.00	0.00	8.67
10	0.00	0.00	0.00	0.00	0.00	0.00	0.00	0.00	9.33
11	80.00	0.60	9.60	93.75	75.00	0.00	0.00	0.00	10.00
12	81.25	0.24	5.73	95.90	87.03	0.00	0.00	0.00	10.77
13	80.00	0.25	5.85	95.71	79.77	0.00	0.00	0.00	16.95
14	83.81	0.20	7.20	97.18	84.39	0.00	0.00	0.00	22.49

Figure 5 - Table of extraction rate dynamics

The system uses Python and Django for the web application, employing Django's ORM for database interaction and MySQL for data storage. The computational module, also written in Python, ensures reliable and efficient data processing.

2. Data

Various methods are necessary for the successful calculation and analysis of metal extraction in hydrometallurgical processes. Here are the main ones:

1. Calculation of metal extraction from the original ore (solid → liquid):

This method is used to determine the amount of metal that can be extracted from the ore through leaching. The process starts with crushing the ore and immersing it in a solution that dissolves the metal. This method is important for assessing the economic feasibility of mining, as it allows understanding how much metal can be obtained from a specific volume of ore. It is used at various scales, from laboratory tests to industrial processes.

2. Calculation of metal extraction from the solution in the process of extraction/re-extraction (liquid → liquid):

The extraction process involves transferring the metal from the productive solution to the organic phase and then to the electrolyte. This method is used for the purification and concentration of metals, such as copper, before the electrolysis stage. The organic phase absorbs the metal from the aqueous solution, reducing its concentration, and then the metal is transferred to another solution for further processing.

3. Calculation of metal extraction from the solution in the process of sorption (liquid → solid) and desorption (solid → liquid):

Metals from solutions are adsorbed on solid sorbents, such as activated carbon. After the sorbent is saturated with metal, desorption is performed, where the metal is returned to the solution for further processing.

This method is often used for precious metals, such as gold, due to its high efficiency and cost-effectiveness.

4. *Calculation of metal deposition on the cathode from the rich solution:*

At this stage, the metal, which has been concentrated in the electrolyte, is deposited on the cathodes during the electrolysis process. This method allows obtaining pure metal of high purity. The concentration of the metal in the solution must be maintained at a certain level to prevent crystallization and ensure optimal conditions for metal deposition.

5. Combined or complete extraction scheme (through extraction - from ore to cathode metal):

This method involves the sequential application of all the above processes for maximum metal extraction from the ore to the production of finished cathode metal. Using this scheme allows for achieving high efficiency and minimizing metal losses at each stage. The combined approach ensures the integration of various technological processes, leading to the optimization of the entire production cycle, cost reduction, and improvement in the quality of the final product.

In our work, we use the fifth method because it provides the maximum efficiency and completeness of metal extraction from the ore. This allows for minimizing losses and increasing the economic profitability of the process, ensuring full control at each stage of processing.

2.1. Input Data

The system receives a list of dictionaries as input, where each dictionary represents the data of one day's observation of the copper extraction process. Each dictionary contains keys corresponding to various indicators at different stages of copper extraction. The input includes values such as:

For the Ore (Leaching) Stage:

- **Name**
- **Ore mass**
- **Metal content** – Concentration of the desired metal in the ore

- $C_{nCu(p.s-s)}$ – Copper concentration in the productive solution on the n-th day of leaching
- $C_{nCu(raf)}$ – Copper concentration in the raffinate on the n-th day of leaching
- $V_{n(p.s-s)}$ – Volume of productive solution on the n-th day

For the Extraction and Re-Extraction Stages:

- $V_{n(org)}$ – Volume of organic phase on the n-th day
- $C_{nCu(el-t)R}$ – Copper concentration in the rich electrolyte on the n-th day
- $V_{n(el-t)R}$ – Volume of rich electrolyte on the n-th day

For the Electrolysis Stage:

- $C_{nCu(el-t)}D$ – Copper concentration in the depleted electrolyte on the n-th day
- $V_{n(el-t)}D$ – Volume of depleted electrolyte on the n-th day

2.2. Output Data

The output provides the dynamics of indicators for each stage of extraction for each observation day. Additionally, the overall copper balance is calculated (Remaining in the ore, in the raffinate, in the organic phase, in the electrolyte and on the cathodes). With the start of each stage, new indicators for calculation are added (formulas for their calculation also change with the onset of a new stage, as explained in more detail in section 3):

For the Ore (Leaching) Stage:

- $\mathbf{E_{(Cu)}}$ – Total copper extraction

For the Extraction and Re-Extraction Stages:

- $\mathbf{E_{(Cu.Exc)}}$ – Copper extraction percentage during extraction
- $\mathbf{C_{Cu(org)}D}$ – Copper content in the depleted (organic phase)
- $\mathbf{C_{Cu(org)}R}$ – Copper content in the rich (organic phase)
- $\mathbf{E_{Cu(el\text{-}t),\ from\ org}}$ – Copper extraction percentage into the electrolyte from rich organic
- $\mathbf{E_{Cu(el\text{-}t),\ from\ p.s\text{-}s}}$ – Copper extraction percentage from the productive solution into the electrolyte

For the Electrolysis Stage:

- $\mathbf{m_{+Cu\ –\ cathode}}$ – Theoretical mass of copper deposited (growth) on the cathodes
- $\mathbf{m_{Cu\ –\ total}}$ – Total accumulated copper mass on the cathodes
- $\mathbf{E_{through}}$ – Through copper extraction from ore to cathode metal

3. Computational Module

This module connects the input and output data by using the input data to perform mathematical operations and outputs the results of these operations as output data. The module's logic is entirely implemented in Python.

Since the days for the initiation of stages can be chosen independently, for the sake of simplicity, we used pre-selected intervals. This standardizes the process, making it more predictable and manageable. The extraction stage begins on the 12th day, and electrolysis starts on the 19th day. The entire process lasts a total of 30 days.

3.1. Stages and Formulas

As the formulas change with each new stage, it is better to explain them separately and show their changes.

Days 1–10: Leaching

Initially, the mass of the desired metal in the ore is calculated:

$$m_{Cu.init} = (\text{Ore Mass} * \text{Metal Content}) / 100 \qquad (1)$$

Next, using the obtained mass, the total copper extraction (E_{Cu}) is calculated over the next 10 days:

$$E_{Cu} = (C_{Cu} \times V_{p.\ s\text{-}s}) / m_{Cu.init} \times 100\ \% \qquad (2)$$

Days 11–18: Extraction and Re-Extraction

$\mathbf{E1_{Cu\ (el\text{-}t),\ from\ p.s.\text{-}s}}$ (Copper extraction percentage from the productive solution into the electrolyte), $\mathbf{E1_{Cu\ (el\text{-}t),\ from\ org}}$ (Copper extraction percentage into the electrolyte from the rich organic phase), $\mathbf{C_{Cu(org)}D}$ (Copper content in the depleted organic phase), $\mathbf{C_{Cu(org)}R}$ (Copper content in the rich organic phase), $\mathbf{E_{Cu.Exc}}$ (Copper extraction percentage during extraction), and the formula for $\mathbf{E_{Cu}}$ are updated.

$$E_{Cu.Exc} = (C_{nCu(p.s\text{-}s)} - C_{nCu(raf)}) / (C_{nCu(p.s\text{-}s)}) \times 100\% \qquad (3)$$

$$E1_{Cu\ (el\text{-}t),\ from\ p.\ s\text{-}s} = (C1_{Cu(el\text{-}t)} \times V1_{(el\text{-}t)} - C0_{Cu(el\text{-}t)} \times V0_{(el\text{-}t)}) / (C1_{Cu(p.s\text{-}s)} \times V1_{p.s\text{-}s}) \times 100\% \qquad (4)$$

$$E1_{Cu\ (el\text{-}t),\ from\ org.} = (C1_{Cu(el\text{-}t)} \times V1_{(el\text{-}t)} - C0_{Cu(el\text{-}t)} \times V0_{(el\text{-}t)}) / (C1_{Cu\ (org.\ R)} \times V1_{org.}R) \times 100\% \qquad (5)$$

$$C1_{Cu(org)}\ D = ((C1_{Cu(p.s\text{-}s)} \times V1_{p.s\text{-}s} - C1_{Cu\ raf} \times V1_{raf}) - (C1_{Cu(el\text{-}t)} \times V1_{(el\text{-}t)} - C0_{Cu(el\text{-}t)} \times V0_{(el\text{-}t)})) / V1_{org} + C0_{Cu(org)}\ D \qquad (6)$$

$$C1_{Cu(org)}\ R = ((C1_{Cu(p.s\text{-}s)} \times V1_{p.s\text{-}s} - C1_{Cu\ raf} \times V1_{raf}) / V1_{opr} + C0_{Cu(org)}\ D \qquad (7)$$

$$E_{Cu} = (C1_{Cu(p.s\text{-}s)} \times V1_{p.s\text{-}s} - C0_{Cu\ raf} \times V0_{raf} + C0_{Cu(el\text{-}t)} \times V0_{(el\text{-}t)}) / m_{Cu.init} \times 100\% \qquad (8)$$

- 1 - indicators for the current day
- 0 - indicators for the previous day
- R-rich or saturated solution (electrolyte, organic phase)
- D - depleted, poor solution (electrolyte, organic phase)

Days 19–30: Electrolysis

m1+Cu-cathode (Theoretical mass of copper deposited (growth) on the cathodes), mCu - total (Total accumulated copper mass on the cathodes), Eskv. (Through copper extraction from ore to cathode metal). During electrolysis, the formulas for

CCu(org)O, ECu(el-t), from org, ECu(el-t), from p.r-ra, and ECu are updated.

$$m1_{+Cu\text{-}cathode} = (C1_{Cu(el\text{-}t)}R \times V1_{(el\text{-}t)}R - C1_{Cu(el\text{-}t)}D \times V1_{(el\text{-}t)}D) \tag{9}$$

$$m_{n(Cu\text{-}total)} = m_{1+Cu\text{-}cathode} + m_{2+Cu\text{-}cathode} + \ldots + m_{n+Cu\text{-}cathode} \tag{10}$$

$$E_{n(through)} = m_{n(Cu\text{-}total)} / m_{Cu.init} \times 100\ \% \tag{11}$$

$$C1_{Cu(org)}\ D = ((C1_{Cu(p.s\text{-}s)} \times V1_{p.s\text{-}sa} - C1_{Cu\ raf} \times V1_{raf}) - (C1_{Cu(el\text{-}t)} \times V1_{(el\text{-}t)} - C0_{Cu(el\text{-}t)} \times V0_{(el\text{-}t)}) - m0_{+Cu\text{-}cathode}) / V1_{org} + C0_{Cu(org)}D \tag{12}$$

$$E1_{Cu\ (el\text{-}t),\ from\ org.} = (C1_{Cu(el\text{-}t)} \times V1_{(el\text{-}t)} - C0_{Cu(el\text{-}t)} \times V0_{(el\text{-}t)} + m0_{+Cu\text{-}cathode}) / (C1_{Cu\ (org.\ R)} \times V1_{org.R}) \times 100\ \% \tag{13}$$

$$E1_{Cu\ (el\text{-}t),\ from\ p.s\text{-}s} = (C1_{Cu(el\text{-}t)} \times V1_{(el\text{-}t)} - C0_{Cu(el\text{-}t)} \times V0_{(el\text{-}t)} + m0_{+Cu\text{-}cathode}) / (C1_{Cu(p.s\text{-}s)} \times V1_{p.s\text{-}s}) \times 100\ \% \tag{14}$$

$$E_{Cu} = (C1_{Cu(p.s\text{-}s)} \times V1_{p.s\text{-}s} - C0_{Cu\ raf} \times V0_{raf} + C0_{Cu(el\text{-}t)} \times V0_{(el\text{-}t)} + m0_{Cu\text{-}total}) / m_{Cu.init} \times 100\% \tag{15}$$

Result: Copper Balance

The copper balance represents the percentage distribution of copper across various components of the technological process after completing all processing and extraction stages. It shows how much copper remains in each of the following categories:

1. **Residual in the ore:** Copper remaining in the original ore after extraction.
2. **In raffinate:** Copper remaining in the solution used for washing and purification.
3. **In the electrolyte:** Copper is present in the electrolyte after electrolysis.
4. **In the organic phase:** Copper is present in the organic phases (e.g., in extractants).
5. **On the cathodes:** Copper deposited on the cathodes during electrolysis.

This balance helps assess the efficiency of the copper extraction and processing processes and identify losses at various stages of the technological process.

Residual in the ore:

$$Cu_{ore} = 100\% - Cu_{raf} - Cu_{el\text{-}t} - Cu_{org} - Cu_{cathode} \tag{16}$$

Residual in the raffinate:

$$Cu_{raf} = (C_{Cu(raf)} \times V_{(p.s\text{-}s)}) / m_{Cu.init} \times 100\% \tag{17}$$

Residual in the electrolyte:

$$Cu_{el\text{-}t} = (C_{Cu(el\text{-}t)}O \times V_{(el\text{-}t)}O) / m_{Cu.init} \times 100\% \tag{18}$$

Residual in the organic:

$$Cu_{org} = (C_{Cu(org)}O \times V_{(org)}) / m_{Cu.init} \times 100\% \tag{19}$$

Residual on the cathode:

$$Cu_{cathode} = m_{Cu\text{-}total} / m_{Cu.init} \times 100\% \tag{20}$$

Results and Discussion

As a result of the conducted research, a specialized website was created to simplify the process of monitoring parameters during metal extraction.

Main functions of the website:

- Adding input data via the interface
- Calculating the dynamics of output parameters
- Displaying the calculation results in a table

Initially, the user is greeted with the "Explore Metals" page (Figure 2), where they can either select existing data or add their own metal and all input data (section 2.1).

Next, the user should navigate to the "Metal Calculations" page (Figure 3), where they need to confirm the start of the calculation process.

Finally, the user can go to the "Metal Results" section to view the results (Figures 4–5).

As shown in Figure 5, a table displays the daily dynamics of the extraction indicators. This table allows the user to track the progress of the process.

Conclusions

This research and the development of specialized software for hydrometallurgical copper extraction processes have yielded significant technological advancements. By leveraging a Django-based architecture with MySQL as the data storage backbone, the software ensures consistent and accurate data processing, enabling comprehensive monitoring and management of the extraction process. The inclusion of various stages, from leaching to electrolysis, in a single combined extraction method, has proven highly effective for optimizing metal recovery and minimizing operational inefficiencies.

The software's design allows users to input data seamlessly, calculate complex parameter dynamics in real time, and view detailed results through clear tables and graphs. This not only aids in tracking process parameters but also empowers users to perform deep analysis of each stage’s efficiency, making the decision-making process more data-driven and precise. The system, thus, significantly enhances the overall productivity and profitability of the copper extraction process, improving the quality of the final product while reducing both time and costs.

Despite these successes, there is substantial room for future improvements. One promising direction is integrating artificial intelligence and machine learning algorithms into the software. This would enable predictive modeling, allowing the system to forecast outcomes under different conditions and optimize processes accordingly. Such capabilities could enhance the software’s adaptability, especially when dealing with variable ore compositions and changing operational parameters.

Moreover, expanding the software to support multi-metal extraction processes and handle more complex ores will increase its applicability in diverse industrial settings. Future enhancements could also focus on improving the user interface and ensuring the scalability of the system to meet the demands of larger operations. Integration with cloud-based infrastructure for real-time global access and further automating the monitoring of environmental impact during the extraction process would also be valuable additions to the software's roadmap.

Conflict of interest. The corresponding author declares that there is no conflict of interest.

CRediT author statement

B. Kenzhaliyev: Conceptualization, Methodology, Metallurgical Analysis. **B. Amangeldy:** Software Development, Technological Implementation**. N. Azatbekuly:** Practical Testing, Application of Technologies**. A. Mukhanbet:** Process Optimization, Technical Validation. **A. Koizhanova:** Data Analysis, Metallurgical Assessment. **D. Magomedov:** Manuscript Drafting, Reviewing, Metallurgical Interpretation.

Acknowledgements. This research was funded by the Committee of Science of the Ministry of Science and Higher Education of the Republic of Kazakhstan (Grant No. BR21882140)

Cite this article as: Kenzhaliyev BK, Amangeldy BS, Mukhanbet A, Azatbekuly N, Koizhanova A, Magomedov DR. Development of Software for Hydrometallurgical Calculation of Metal Extraction. Kompleksnoe Ispolzovanie Mineralnogo Syra = Complex Use of Mineral Resources. 2025; 335(4):78-88. https://doi.org/10.31643/2025/6445.42

Металл алуға арналған гидрометаллургиялық есептеулер үшін бағдарламаны әзірлеу

[1*] Кенжалиев Б.К., [2]Амангелді Б.С., [2]Мұханбет А., [2]Азатбекұлы Н.,
[1]Қойжанова А., [1]Магомедов Д.Р.

[1] Металлургия және кен байыту институты АҚ, Сәтбаев Университеті, Алматы, Қазақстан
[2] Әл-Фараби атындағы Қазақ Ұлттық Университеті, Алматы, Қазақстан

Мақала келді: *5 тамыз 2024*
Сараптамадан өтті: *24 тамыз 2024*
Қабылданды: *27 қыркүйек 2024*

ТҮЙІНДЕМЕ

Гидрометаллургия металлургия өнеркәсібінде сулы ерітінділерді пайдалана отырып, кендерден және қайталама материалдардан металдарды алудың тиімді әдісін қамтамасыз ету арқылы маңызды рөл атқарады. Бұл тәсіл әсіресе төмен сұрыпты және күрделі кендерді, сондай-ақ дәстүрлі пирометаллургиялық әдістермен тиімді өңдеуге келмейтін қайталама ресурстарды өңдеу үшін тиімді. Бұл зерттеудің мақсаты гидрометаллургиялық процестерде металды алу үшін қажетті есептеулерді автоматтандыру және оңтайландыру үшін арнайы бағдарламалық қамтамасыз етуді жасау болып табылады. Бағдарламалық қамтамасыз ету гидрометаллургиялық процестің әртүрлі кезеңдерін автоматтандыруға арналған толық есептеу жүйесін біріктіреді, оның ішінде руда құрамын инициализациялау, элементтердің жалпы массасын есептеу, металл өнімдеріндегі (штейндегі) және жанама өнімдердегі (шлак) металдардың концентрациясын анықтау. Әдістеме пайдаланушы интерфейсі үшін Django және сенімді деректерді сақтау үшін MySQL арқылы веб-негізделген қолданбаны жобалау мен енгізуді қамтиды. Python тілінде жазылған есептеу модулі күрделі химиялық реакциялар мен металдарды алу процестерін модельдеу үшін қажетті математикалық операцияларды автоматтандырады. Бұл модуль нақты уақыт режимінде өңдеуді қолдайды және сілтілеу, экстракция, қайта экстракция, сорбция және электролизді қоса алғанда, металды алудың әрбір кезеңі үшін дәл есептеулерді қамтамасыз етеді. Бағдарламалық жасақтамада сонымен қатар пайдаланушыларға бағалы металдардың таралуын талдауға және негізгі операциялық параметрлердің өндіру тиімділігіне әсерін бағалауға мүмкіндік беретін егжей-тегжейлі кестелер мен динамикалық графиктер бар. Нәтижелер әзірленген бағдарламалық жасақтама үлкен деректер жиынын сәтті басқаратынын, гидрометаллургиялық есептеулердің дәлдігін арттыратынын және адам қателігінің қаупін барынша азайтатынын көрсетеді. Бағдарламалық қамтамасыз етуді енгізу металл алу көрсеткіштерін оңтайландыру және пайдалану шығындарын азайту арқылы өндірістің экономикалық тиімділігін айтарлықтай жақсартуға әкеледі. Бұған қоса, ол экстракцияның әрбір кезеңіне әсер ететін түсініктер беру арқылы процесті кешенді бақылауды қолдайды, осылайша соңғы металл өнімінің сапасын жақсартады. Тұтастай алғанда, бағдарламалық қамтамасыз ету гидрометаллургиялық процестерді оңтайландыруға бағытталған салалар үшін ауқымды шешім ұсынатын бұл саладағы маңызды технологиялық прогресс болып табылады.

Түйін сөздер: гидрометаллургия, есептеулерді автоматтандыру, металл алу, математикалық модельдеу.

Авторлар туралы ақпарат:

Кенжалиев Бағдаулет Кенжалиевич	*Техникалық ғылымдар докторы, профессор, Металлургия және кен байыту институты АҚ-ның Бас директоры - Басқарма төрағасы, Сәтбаев Университеті, 050010, Шевченко к-сі, 29, Алматы, Қазақстан. Email: bagdaulet_k@mail.ru; ORCID ID: https://orcid.org/0000-0003-1474-8354*
Амангелді Бибарс Сапарғалиұлы	*Зерттеуші, Әл-Фараби атындағы Қазақ Ұлттық Университеті, 050040, әл-Фараби даңғылы, 71, Алматы, Қазақстан. Email: a.s.bibars@gmail.com; ORCID ID: https://orcid.org/0000-0002-4089-6337*
Мұханбет Ақсұлтан	*Зерттеуші, Әл-Фараби атындағы Қазақ Ұлттық Университеті, 050040, әл-Фараби даңғылы, 71, Алматы, Қазақстан. Email: mukhanbetaksultan0414@gmail.com; ORCID ID: https://orcid.org/0000-0003-4699-0436*
Азатбекұлы Нұртуған	*Кіші ғылыми қызметкер, Әл-Фараби атындағы Қазақ Ұлттық Университеті, 050040, әл-Фараби даңғылы, 71, Алматы, Қазақстан. Email: nurtugang17@gmail.com; ORCID ID:https://orcid.org/0009-0007-5843-8995*
Қойжанова Айгүл	*Техникалық ғылымдар кандидаты, зертхана меңгерушісі, Металлургия және кен байыту институты АҚ, Сәтбаев Университеті, 050010, Шевченко к-сі, 29, Алматы, Қазақстан. Email: aigul_koizhan@mail.ru; ORCID ID: https://orcid.org/0000-0001-9358-3193*
Магомедов Давид Расимович	*Ғылыми қызметкер, магистр, Металлургия және кен байыту институты АҚ, Сәтбаев Университеті, 050010, Шевченко к-сі, 29, Алматы, Қазақстан. Email: davidmag16@mail.ru; ORCID ID: https://orcid.org/0000-0001-7216-2349*

Разработка комплексного программного обеспечения для гидрометаллургического расчета извлечения металлов

[1*] Кенжалиев Б.К., [2]Амангелды Б.С., [2]Муханбет А., [2]Азатбекулы Н.,
[1]Койжанова А., [1]Магомедов Д.Р.

[1] АО Институт металлургии и обогащения, Satbayev University, Алматы, Казахстан
[2] Казахский Национальный Университет имени Аль-Фараби, Алматы, Казахстан

Поступила: *5 августа 2024*
Рецензирование: *24 августа 2024*
Принята в печать: *27 сентября 2024*

АННОТАЦИЯ

Гидрометаллургия играет ключевую роль в металлургической промышленности, предоставляя эффективный метод извлечения металлов из руд и вторичных материалов с использованием водных растворов. Этот подход особенно полезен для переработки низкосортных и сложных руд, а также вторичных ресурсов, которые не могут быть эффективно обработаны традиционными пирометаллургическими методами. Целью данного исследования является разработка специализированного программного обеспечения для автоматизации и оптимизации расчетов, необходимых для извлечения металлов в гидрометаллургических процессах. Программное обеспечение включает в себя полную вычислительную структуру для автоматизации различных этапов гидрометаллургического процесса, таких как инициализация состава руд, расчеты общей массы элементов и определение концентраций металлов в продуктах (штейн) и побочных продуктах (шлак). Методология включает разработку и внедрение веб-приложения на базе

Django для интерфейса пользователя и MySQL для надежного хранения данных. Вычислительный модуль, написанный на языке Python, автоматизирует математические операции, необходимые для моделирования сложных химических реакций и процессов извлечения металлов. Этот модуль поддерживает обработку данных в режиме реального времени и обеспечивает точные расчеты на каждом этапе извлечения металлов, включая выщелачивание, экстракцию, реэкстракцию, сорбцию и электролиз. Программное обеспечение также включает подробные таблицы и динамические графики, позволяющие пользователям анализировать распределение ценных металлов и оценивать влияние ключевых операционных параметров на эффективность извлечения. Результаты показывают, что разработанное программное обеспечение успешно справляется с обработкой больших объемов данных, повышает точность гидрометаллургических расчетов и минимизирует риск человеческих ошибок. Внедрение этого ПО приводит к значительному улучшению экономической эффективности производства за счет оптимизации показателей извлечения металлов и снижения эксплуатационных расходов. Кроме того, оно поддерживает комплексное управление процессом, предоставляя практические данные для каждого этапа извлечения, что улучшает качество конечного металлического продукта. В целом, программное обеспечение представляет собой значительное технологическое достижение в данной области, предлагая масштабируемое решение для предприятий, стремящихся оптимизировать гидрометаллургические процессы и повысить эффективность извлечения металлов.

Ключевые слова: гидрометаллургия, автоматизация расчетов, извлечение металлов, математическое моделирование.

	Информация об авторах:
Кенжалиев Багдаулет Кенжалиевич	*Доктор технических наук, профессор, Генеральный директор - Председатель Правления АО Институт металлургии и обогащения, Satbayev University, 050010, Алматы, ул. Шевченко, 29, Алматы, Казахстан. Email: bagdaulet_k@mail.ru; ORCID ID: https://orcid.org/0000-0003-1474-8354*
Амангелды Бибарс Сапаргалиулы	*Исследователь, Казахский Национальный Университет имени Аль-Фараби, 050040, пр. аль-Фараби, 71, Алматы, Казахстан. Email: a.s.bibars@gmail.com; ORCID ID: https://orcid.org/0000-0002-4089-6337*
Муханбет Аксултан	*Исследователь, Казахский Национальный Университет имени Аль-Фараби, 050040, пр. аль-Фараби, 71, Алматы, Казахстан. Email: mukhanbetaksultan0414@gmail.com; ORCID ID: https://orcid.org/0000-0003-4699-0436*
Азатбекулы Нуртуган	*Младший научный сотрудник, Казахский Национальный Университет имени Аль-Фараби, 050040, пр. аль-Фараби, 71, Алматы, Казахстан. Email: nurtugang17@gmail.com; ORCID ID: https://orcid.org/0009-0007-5843-8995*
Койжанова Айгуль	*Кандидат технических наук, заведующая лабораторией, АО Институт металлургии и обогащения, Satbayev University, 050010, Алматы, ул. Шевченко, 29, Алматы, Казахстан. Email: aigul_koizhan@mail.ru; ORCID ID: https://orcid.org/0000-0001-9358-3193*
Магомедов Давид Расимович	*Научный сотрудник, магистр, АО Институт металлургии и обогащения, Satbayev University, 050010, Алматы, ул. Шевченко, 29, Алматы, Казахстан. Email: davidmag16@mail.ru; ORCID ID: https://orcid.org/0000-0001-7216-2349*

References

[1] Anderson C G. Pyrometallurgy. In Reference Module in Materials Science and Materials Engineering. Elsevier. 2016. https://doi.org/10.1016/b978-0-12-803581-8.03609-2

[2] Lakshmanan V I, Halim M A, & Vijayan S. Chemical Processing: Hydrometallurgy. In Innovative Process Development in Metallurgical Industry Springer International Publishing. 2016, 91-108. https://doi.org/10.1007/978-3-319-21599-0_5

[3] Magwaneng R S, Haga K, Batnasan A, Shibayama A, Kosugi M, Kawarabuki R, Mitsuhashi K, & Kawata M. Investigation of Copper and Iron Recovery from Copper Ore by High Pressure Leaching. In International Journal of the Society of Materials Engineering for Resources. The Society of Materials Engineering for Resources of Japan. 2018; 23(1):80-83. https://doi.org/10.5188/ijsmer.23.80

[4] Koizhanova A K, Kenzhaliyev B K, Magomedov D R, Erdenova M B, Bakrayeva A N, & Abdyldaev N N. Hydrometallurgical studies on the leaching of copper from man-made mineral formations. Kompleksnoe Ispolzovanie Mineralnogo Syra = Complex Use of Mineral Resources. 2023; 330(3):32-42. https://doi.org/10.31643/2024/6445.26

[5] Koizhanova A, Bakrayeva A, Yerdenova M, & Magomedov D. Investigation of the efficiency of hydrometallurgical processing of off-balance copper deposits in Kazakhstan. *News of the National Academy of Sciences of the Republic of Kazakhstan. Series Chemistry and Technology.* 2023; *3*(456):117-137. https://doi.org/10.32014/2023.2518-1491.182

[6] Research and development trends of hydrometallurgy: An overview based on Hydrometallurgy literature from 1975 to 2019. Transactions of Nonferrous Metals Society of China. 2020; 30(11):3147-3160. https://www.sciencedirect.com/science/article/abs/pii/S1003632620654504

[7] Željko Kamberović, Milisav Ranitović, Marija Korać, Zoran Andjić ,Nataša Gajić, Jovana Djokić and Sanja Jevtić. Hydrometallurgical Process for Selective Metals Recovery from Waste-Printed Circuit Boards. Metals. 2018; 8(6):441. https://doi.org/10.3390/met8060441

[8] Koen Binnemans, Peter Tom Jones. The Twelve Principles of Circular Hydrometallurgy. Journal of Sustainable Metallurgy. 2023; 9:1–25 https://link.springer.com/article/10.1007/S40831-022-00636-3

[9] Free M L. Hydrometallurgy. In The Minerals, Metals &amp. Materials Series. Springer International Publishing. 2022. https://doi.org/10.1007/978-3-030-88087-3

[10] Chen J Y. Handbook of hydrometallurgy. 2005.

[11] Koizhanova A, Kenzhaliyev B, Magomedov D, Kamalov E, Yerdenova M, Bakrayeva A, & Abdyldayev N. Study of Factors Affecting the Copper Ore Leaching Process. ChemEngineering. 2023; 7(3):54. https://doi.org/10.3390/chemengineering7030054

[12] Giuseppe Granata, Demetri Petrides. Hydrometallurgical Process Design and Economics with SuperPro Designer. https://www.researchgate.net/publication/363475037_Hydrometallurgical_Process_Design_and_Economics_with_SuperPro_Designer

[13] William Hawker, Mike Dry. Simulation software methodologies for hydrometallurgical process evaluation applied to selective acid leaching of mixed hydroxide precipitate. Conference: ALTA 2017 Nickel-Cobalt-Copper. 2017. https://www.researchgate.net/publication/319524523_Simulation_software_methodologies_for_hydrometallurgical_process_evaluation_applied_to_selective_acid_leaching_of_mixed_hydroxide_precipitate

[14] Salas S D, González Y, Cango P, Gómez J C, Koepke R, & Peña-Carpio E. Simulation-Based Analysis of Hydrometallurgical Processes. Case Study: Small-Scale Gold Mining in Ecuador. Minerals. 2021; 11(5):534. MDPI AG. https://doi.org/10.3390/min11050534

[15] Kiranoudis C T, Voros N, Kritikos T D, Maroulis Z B, Marinoskouris D, Papassiopi N, Dimitropoulou O N, Paspaliaris I, & Kontopoulos A. Object-oriented simulation of hydrometallurgical processes: Part I. Requirements and implementation. Metallurgical and Materials Transactions B. 1997; 28:777-784.

[16] Kiranoudis C T, Voros N, Kritikos T D, Maroulis Z B, Marinoskouris D, Papassiopi N, Dimitropoulou O N, Paspaliaris I, & Kontopoulos A. Object-oriented simulation of hydrometallurgical processes: Part II. Application to the bayer process. Metallurgical and Materials Transactions B. 1997; 28:785-793.

[17] Nikkhah Khosrow & Anderson Corby. Role of Simulation Software in Design and Operation of Metallurgical Plants: A Case Study. 1998.

[18] Application of Metalurgical Process Simulation Software SYSCAD in Hydrometallurgy. https://www.semanticscholar.org/paper/Application-of-Metalurgical-Process-Simulation-in-Jing/a0ca3e84eae0eaf26cc48cb5a6688e009fdeee0b

[19] Application of Process Simulation Software METSIM in Metallurgy. https://www.researchgate.net/publication/275406294_Application_of_Process_Simulation_Software_METSIM_in_Metallurgy/fulltext/57aa7f3708ae7a6420bd172e/Application-of-Process-Simulation-Software-METSIM-in-Metallurgy.pdf

[20] Soft Computing Application in Mining, Mineral Processing and Metallurgy with an Approach to Using It in Mineral Waste Disposal. https://www.mdpi.com/2075-163X/13/11/1450

DOI: 10.31643/2025/6445.43
Earth sciences

Technology of production of aluminosilicate refractories for units processing fluorinated waste

[1]Sidorina E.A., [1] Isagulov A.Z. [1*]Rabatuly M., [2] Yang Y.

[1]Abylkas Saginov Karaganda Technical University, Karaganda, Kazakhstan
[2] Northeast Petroleum University, Daqing, China

**Corresponding author email: mukhammedrakhym@mail.ru*

Received: *May 31, 2024*
Peer-reviewed: *June 19, 2024*
Accepted: *October 2, 2024*

Annotation

The aluminium production process through the electrolysis of cryolite-alumina melts involves a series of interconnected, sequential, and parallel technological operations, each defined by a specific level of engineering and technological advancement. The development of the modern aluminum industry is closely tied to the adoption of resource-efficient and environmentally friendly technologies, which focus on recycling secondary materials and industrial waste. Fluorinated carbon-based materials release fluorine into the gas phase at relatively low temperatures when heated, and in thermal units processing fluorinated waste, this fluorine, along with alkali metals, will remain in the gas phase. To enhance the durability of furnace linings against the corrosive atmosphere, refractories with the highest possible density (low porosity) and a high concentration of mullite in the matrix (the finely ground component of the batch) are required. These properties can only be achieved in refractory products produced by the semi-dry pressing method, which ensures high grain packing density and leads to the formation of a ceramic mullite bond after firing.

Keywords: fluorinated carbonaceous materials, crushing, mullite refractories, highly lamellar clay, grinding, mullite-silica products, binding, chamotte, drying, firing.

Information about authors:

Sidorina Yelena Anatolievna	*Master of Technical Sciences, doctoral student of the Department of NTM of Abylkas Saginov Karaganda Technical University, 100027, Republic of Kazakhstan, Karaganda, Nursultan Nazarbayev Ave., 56. E-mail: elena.sidorina.78@mail.ru; ORCID ID: https://orcid.org/0000-0002-4417-8551*
Isagulov Aristotle Zeynullinovich	*Doctor of Technical Sciences, Professor of the Department of NTM, Abylkas Saginov Karaganda Technical University, Nursultan Nazarbayev Ave., 56, 100027, Republic of Kazakhstan, Karaganda. E-mail: aristotel@kstu.kz; ORCID ID: https://orcid.org/0000-0003-2174-9072*
Rabatuly Mukhammedrakhym	*Ph.D., Acting Associate Professor of the Department Development of Mineral Deposits of the Abylkas Saginov Karaganda Technical University, Nursultan Nazarbayev Ave., 56, 100027, Republic of Kazakhstan, Karaganda. E-mail: mukhammedrakhym@mail.ru; ORCID ID: https://orcid.org/0000-0002-7558-128X*
Yang Ying	*Candidate of Technical Sciences, Senior Lecturer Northeastern Petroleum University, Research Institute for the Development of Unconventional Oil and Gas Resources, Daqing, 163318, China. E-mail: yyainngg@126.com; ORCID ID: https://orcid.org/0000-0002-8927-3878*

Introduction

The production of aluminum by electrolysis of cryolite-alumina molten includes several interrelated and sequentially parallel technical processes, each characterized by a certain level of engineering and technology development. Despite the constant progressive development in terms of improving the means and methods of implementing technical processes, several technical problems remain unresolved. The existence of these problems is due to the lack of theoretically and economically informed technical solutions, which are a powerful lever for increasing production efficiency [1].

The development of the aluminum industry at the present stage is associated with developing and implementing resource-saving and environmental technologies for processing secondary resources and technical waste. Implementing technological solutions aimed at reducing material and labor costs in c production and involving illiquid waste and production products in efficient processing will increase competitiveness, economic attractiveness and environmental safety [2].

Since fluorinated carbonaceous materials release fluorine into the gas phase at relatively low temperatures, both fluorine and alkali metals from the same waste will be present in the gas phase within the working area of the fluorinated waste heat treatment plant. To enhance the durability of the furnace lining against the corrosive effects of this atmosphere, it is essential to use refractories with high density (low porosity) and a maximum concentration of mullite in the matrix (the finely ground portion of the material). These characteristics can only be achieved by producing refractories through semi-dry molding, which ensures a high packing density of grains and results in a ceramic-mullite bond after firing [[3], [4]].

For the lining of thermal units that utilize fluorinated carbon waste as fuel or a reducing agent, the use of mullite-silica or mullite refractory pressed and fired products is recommended.

In the production of mullite-silica refractories, two stages are conditionally distinguished: the production of high-alumina chamotte and the production of products. The basis of production is the production of densely baked high-alumina chamotte, which serves as a thinning material and binds when pressing products with high-plastic clay [5].

Production of clay in batches: In the manufacture of mullite-silicon products, finely ground high-plasticity clay is utilized. The characteristics of the raw clay and the degree of grinding directly influence the properties of the final products [[6], [7]].

In the semi-dry production method, where clay is added in limited quantities and needs to be evenly distributed across the surface of the chamotte grains, the maximum particle size is restricted to 0.2-0.5 mm. The process flow for preparing binder clay is illustrated in Fig. 1.1.

After rough crushing to pieces of no more than 50 mm, the clay enters the drying drum for drying, where it is dried in direct flow, i.e. the coolant and clay in the drying drum move in the same direction. In this case, the temperature of the coolant drops sharply at the beginning of the drum due to a large amount of evaporating water from the clay, thereby eliminating the possibility of drying the clay [8].

After rough crushing to pieces of no more than 50 mm, the clay enters the drying drum for drying, where it is dried in direct flow, i.e., the coolant and clay in the drying drum move in the same direction. In this case, the temperature of the coolant drops sharply at the beginning of the drum due to a large amount of evaporating water from the clay and thereby eliminating the possibility of drying the clay.

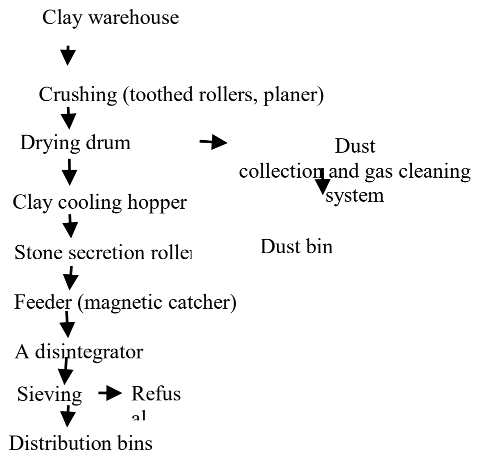

Figure 1.1. - Technological scheme of preparation of binder clay

Flue gases from natural gas combustion, waste heat from kilns, etc. are used as heat carriers. The temperature of the incoming gases into the drying drum is no more than 900 ° C, at the outlet – not less than 100 ° C. The moisture content of clay in the drying process decreases from 15-20 to 7-10%. The residence time of clay in the drying drum is within 20-30 minutes with a drum length of 8-14 m. The capacity of the drying drum is 10-14 t/h. It is not recommended to over-dry the clay, since when grinding such clay is very dusty and may lose its plastic properties.

The grinding of dry clay is carried out in hammer or ball mills [9].

Waste gases containing dust up to 25 microns in size are sent to a dust cleaning system consisting of cyclones, the efficiency of which is not higher than 70-75%. For more efficient purification of gases coming from drying drums, two-stage systems are used, where more highly efficient devices are used in the second stage. Such devices are electrofilters and bag filters, with a degree of dust capture which is at least 98%.

Strict quality standards for mullite-silicon products also extend to the binding clay. The levels of undesirable impurities, such as iron oxides, calcium, magnesium, and others, must be kept to a minimum.

Mullite-silicon products are produced using a multi-chamotte process, with the clay binder comprising 10-20% of the mixture. Different preparation methods for mullite-silicon chamotte are employed depending on the raw materials used.

Utilizing technical alumina or alumina-containing waste (such as slags, spent catalysts, or dust from cleaning processes) allows for the production of all types of mullite-silicon products [10].

The experimental part

The ratio of clay to technical alumina is calculated based on the final product requirements, ensuring that the Al2O3 content in the chamotte is 5-10% higher than in the finished product. This is necessary because the clay used for binding contains a lower Al2O3 content.

Technical alumina, in the form of spherulites, has poor sintering properties, so it is finely ground in vibrating mills along with the dry portion of the binder clay. Steel balls, 10-15 mm in diameter, are used as grinding media. The fineness of the grind is controlled by the residue left on a sieve with 10,000 rel./cm^2, which should not exceed 2% [11].

The mixing of young alumina and clay is carried out in a mixer of the SM-115 type with simultaneous moistening of the mixture to 17-18%. Mixing with waterlogging up to 25-28% is carried out in a two-shaft mixer with subsequent processing and compaction in a vacuum belt press. The resulting blanks with dimensions of 50 × 50 × 50 mm are sent for firing into a rotating furnace

The chamotte is fired at higher temperatures, and the higher the content of A12O3 in the charge. The firing temperature ranges from 1350-1550 ° C. The water absorption of burnt chamotte should be no more than 1-3%. The chamotte coming out of the rotary kiln has the following grain composition, %:

Fraction, mm	>10	10-3	3-0.5	< 0.5
Content, %	30-50	25-30	25-30	5-10

The dust captured by the gas cleaning system contains a lot of technical alumina, so it is fully returned to production at the briquette forming stage [[12], [13]].

Several reactions are possible between the aluminosilicate refractory and the main components of the electrolyte – cryolite and sodium fluoride:

$$18(NaF)_l + 2(Al_2O_32SiO_2)_s + 5(SiO_2)_s = 9(NaAlSiO_4)_l + 3(Na_3AlF_6)_l \quad (1)$$

$$6(NaF)_l + 3(SiO_2)_s + 23(Al_2O_32SiO_2)_s = 3(NaAlSiO_4)_l + 3(Na_3AlF_6)_l \quad (2)$$

$$6(Na_3AlF_6)_l + 23(SiO_2)_l + 23(Al_2O_32SiO_2)_s = 18(NaAlSiO_4)_l + 9(SiF_4)_g \quad (3)$$

The appearance of the refractory samples after operation during one cupola movement is shown in Fig. 1.2. and 1.3.

Figure 1.2 – Samples of refractory after operation in the cupola shaft

Figure 1.3 – Samples of refractory after operation in the furnace of the cupola

The product after use in the shaft (Fig.1.2) carbonized throughout the depth and has molten crusts on the treated surfaces. The shape of the untreated surfaces is mostly preserved, and the crusts from processing are evenly erased. Slag is also visible on the sides, which indicates the penetration of molten components and the vapor phase into the seams between the materials. There is no mechanical destruction of the samples [[14], [15]].

The product after use in the oven (Fig. 1.3) has irregularities, especially on treated surfaces, where molten crusts up to 5 mm thick are visible. Carburization is not observed. The sample is fragmented by internal cracks formed as a result of mechanical action. Melting and compression zones are observed inside the product and at the joints with neighbouring products [[16], [17]].

Discussion of the results

This study observes that the product exhibits a denser structure after operation in the cupola mine than after service in the furnace. This behavior is unusual and suggests the presence of volatile components in the charge melt, which act as stronger sintering agents for aluminosilicate refractories compared to iron oxide and metallic iron, the primary components of the furnace workspace. The uniform influence of the sintering factor on the overall structure of the refractory across the thickness of the lining is noteworthy. For instance, in previous studies [E. A. Sidorina, A. Z. Isagulov, I. D. Kashcheev, K. G. Zemlyanoi, New refractories No. 5 2022 "Development of technology for superdense slag-resistant aluminosilicate refractories" Similar results have also been reported regarding the behavior of aluminosilicate refractories under various operating conditions [[18], [19]]. On the basis of aluminosilicate raw materials of the Republic of Kazakhstan, a technology for producing superdense aluminosilicate refractories with increased slag resistance for thermal processes of utilization of fluorinated carbonaceous waste is proposed. The use of "ceramic" technology, which allows to obtain a structure with a water absorption of less than 1% for both chamotte and refractory products with different Al2O3 content. Further, products after operation in the cupola furnace show a clearly defined melted crust in the working area, formed at the point of contact with molten cast iron. This area, formed as a result of impregnation by molten cast iron and/or slag into the refractory, shows significant modification. In contrast, the transitional and impregnated (slightly modified) zones exhibit structures that differ little from the original refractory, even though the sintering factor in the furnace shaft impacts the structure's density, including the furnace lining. Comparing these findings with other studies on refractory behavior under similar conditions could provide additional insights into the factors influencing the observed structural changes. When selecting a grain composition, an intermittent grain composition is employed, where clay and chamotte are ground together. Grinding high-alumina chamotte presents significant challenges due to its high hardness. Large chamotte pieces are initially crushed in a jaw crusher and then further reduced in size using a ball mill with self-seeding [[20], [21]]. The chamotte stream undergoes repeated magnetic separation to remove metallic iron, ensuring that the content of metallic iron in the coarse fraction does not exceed 0.05%, and in the fine fraction, it does not exceed 0.7%. From the analysis of the literature data, it follows that in order to increase the economic efficiency of metallurgical production, various man-made carbon wastes can be used as fuel and reducing agent instead of significantly more expensive coal and coal coke. The issue of utilization of fluorine and alkali-containing carbonaceous waste from aluminum production is particularly relevant for the Republic of Kazakhstan.

Conclusions

In practice, the following charge compositions are used:

- mullitosilicon products with A12O3 content of 28-45 wt. % contain chamotte fractions 3-1 mm 55-65% and joint grinding of clay and chamotte 35-45%. In the joint grinding, the clay content is 35, and the chamotte is 65%. The total clay content in the charge is ~ 25 %;
- mullite products with A12O3 content > 45 wt. % contain chamotte fractions 3-1 mm 55% and joint grinding of clay and chamotte 45%. In the joint grinding, the clay content is 25, and the chamotte is 75%. The total clay content in the charge is ~ 13%

Mixing is carried out on runners with heavy rollers with strict observance of the order of feeding materials into the mixer. First, a large fraction of chamotte is loaded and a clay slip with a density of 1.30-1.35 g / cm3 is introduced. After 5 minutes of mixing, a finely ground mixture of joint grinding is loaded. The total mixing cycle is 15-20 min. The humidity of the prepared mass is 5-6%.

Pressing of products is carried out on hydraulic presses. To improve the quality of products, the number of presses per minute is reduced to four. The density of the formed raw material, depending on the type of press used, is in the range of 2.70-2.85 g/ cm^3.

Drying of mullite-silica products does not cause difficulties and is carried out in tunnel dryers combined with a tunnel furnace. The final moisture content of the raw material after drying is not more than 2%.

The products are fired in tunnel furnaces with a flat arch of 156 m long and 3.1 m wide. The height from the bottom of the trolley to the arch is 1.1 m . The height of the cage is small, since the firing temperature, depending on the content of Al2O3, ranges from 1350-1550 ° C. The firing duration is 80 h. The low height of the cage is necessary in this case for uniform firing and exclusion of delamination when the coolant moves along the height of the tunnel furnace channel.

Conflict of interest. On behalf of all the authors, the correspondent author declares that there is no conflict of interest.

CRediT author statement: **E. Sidorina**: Conceptualization, Methodology, Software. **A. Isagulov**: Data curation, Writing- Original draft preparation. **M. Rabatuly:** Visualization, Investigation. **Y. Yang**: Software, Validation.

Cite this article as: Sidorina EA, Isagulov AZ, Rabatuly M, Yang Y. Technology of production of aluminosilicate refractories for units processing fluorinated waste. Kompleksnoe Ispolzovanie Mineralnogo Syra = Complex Use of Mineral Resources. 2025; 335(4):89-95. https://doi.org/10.31643/2025/6445.43

Құрамында фторы бар қалдықтарды өңдейтін қондырғылар үшін алюмосиликатты отқа төзімді бұйымдарды өндіру технологиясы

[1*]Сидорина Е.А., [1] Исагулов А.З. [1] Рабатұлы М., [2] Yang Y.

[1] Әбілқас Сағынов атындағы Қарағанды техникалық университеті, Қарағанды, Қазақстан
[2] Солтүстік-Шығыс Мұнай университеті, Дацин, Қытай

Мақала келді: *31 мамыр 2024*
Сараптамадан өтті: *19 маусым 2024*
Қабылданды: *2 қазан 2024*

Түйіндеме

Алюминийді криолит-глиноземді балқымаларды электролиздеу негізінде алу өзара байланысты, бірізді және параллельді технологиялық үдерістер кешенін қамтиды, олардың әрқайсысы инженерлік-технологиялық дамудың белгілі бір жеткен деңгейімен сипатталынады. Қазіргі алюминий өнеркәсібінің эволюциясы қайталама қорларды және техногендік қалдықтарды өңдеуге бағытталған қор үнемдейтін және экологиялық технологияларды әзірлеумен және енгізумен байланысты. Фторлы көміртекті материалдар қыздырылған кезде фторды газ фазасына салыстырмалы түрде төмен температурада шығарады, содан кейін фторлы қалдықтарды өңдейтін жылу қондырғыларының жұмыс кеңістігінде ол газ фазасында болады, сонымен қатар сол қалдықтарда болатын сілтілі металдар. Демек, пеш атмосферасының коррозиялық әсеріне төсемнің беріктігін арттыру үшін матрицадағы ең жоғары тығыздығы (кеуектілігі төмен) және максималды муллит мөлшері (шихтаның ұсақ ұнтақталған бөлігі) бар отқа төзімді заттарды қолдану қажет. Мұндай қасиеттер жиынтығын тек жартылай құрғақ қалыптау әдісімен алынған отқа төзімді өнімдерден алуға болады, бұл дәндердің жоғары тығыздығын қамтамасыз етеді және керамикалық муллит байламы алынғанға дейін күйдіріледі. Муллитті кремний диоксиді немесе қысыммен күйдірілген муллитті отқа төзімді бұйымдар фторкөміртекті қалдықтарды отын немесе тотықсыздандырғыш ретінде пайдаланатын жылу қондырғыларын төсеу үшін қолданылады.

Түйін сөздер: құрамында фтор бар көміртекті материалдар, ұсақтау, муллитті отқа төзімді заттар, жоғары пластиналы саз, ұнтақтау, муллит-кремнийлі бұйымдар, байлам, шамот, кептіру, күйдіру.

	Авторлар туралы ақпарат:
Сидорина Елена Анатольевна	*Техника ғылымдарының магистрі, НТМ кафедрасының докторанты, Әбілқас Сағынов атындағы Қарағанды техникалық университеті, 100027, Нұрсұлтан Назарбаев даңғылы, 56, Қарағанды, Қазақстан. E-mail: elena.sidorina.78@mail.ru; ORCID ID: https://orcid.org/0000-0002-4417-8551*
Исагулов Аристотель Зейнуллинович	*Техника ғылымдарының докторы, НТМ кафедрасының профессоры, Әбілқас Сағынов атындағы Қарағанды техникалық университеті, 100027, Нұрсұлтан Назарбаев даңғылы, 56, Қарағанды, Қазақстан. E-mail: aristotel@kstu.kz; ORCID ID: https://orcid.org/0000-0003-2174-9072*
Рабатұлы Мұхаммедрахым	*Ph.D., Пайдалы қазбалар кенорындарын қазу кафедрасының доцентінің м. а., Әбілқас Сағынов атындағы Қарағанды техникалық университеті, 100027, Нұрсұлтан Назарбаев даңғылы, 56, Қарағанды, Қазақстан. E-mail: mukhammedrakhym@mail.ru; ORCID ID: https://orcid.org/0000-0002-7558-128X*
Yang Ying	*Техника ғылымдарының кандидаты, Солтүстік-Шығыс мұнай университетінің аға оқытушысы, дәстүрлі емес Мұнай және газ ресурстарын дамыту ғылыми-зерттеу институты, Дацин, 163318, Қытай. E-mail: yyainngg@126.com; ORCID ID: https://orcid.org/0000-0002-8927-3878*

Технология производства алюмосиликатных огнеупоров для агрегатов, перерабатывающих фторсодержащие отходы

[1]Сидорина Е.А., [1] Исагулов А.З. [1] Рабатулы М., [2] Yang Y.

[1] Карагандинский технический университет имени Абылкаса Сагинова, Караганда, Казахстан
[2] Северо-Восточный нефтяной университет, Дацин, Китай

Поступила: *31 мая 2024*
Рецензирование: *19 июня 2024*
Принята в печать: *2 октября 2024*

Аннотация

Процесс производства алюминия с использованием электролиза криолит-глинозёмных расплавов включает комплекс взаимосвязанных, последовательных и параллельных технологических этапов, каждый из которых характеризуется определённым уровнем инженерно-технологического развития. Современная алюминиевая промышленность развивается благодаря разработке и внедрению технологий, ориентированных на экономию ресурсов и охрану окружающей среды, что включает переработку вторичных ресурсов и техногенных отходов. При нагревании фторсодержащие углеродные материалы выделяют фтор в газообразной форме уже при относительно низких температурах, что приводит к его присутствию в газовой фазе в тепловых агрегатах, перерабатывающих такие отходы, наряду с щелочными металлами, содержащимися в этих отходах. Для повышения устойчивости футеровки к коррозионными воздействиям печной атмосферы необходимо использовать огнеупоры с максимальной полностью (низкой пористостью) и высоким содержанием муллита в матрице (тонкоизмельчённой части шихты). Достичь такого набора свойств возможно только при производстве огнеупорных изделий полусухим методом формования, который обеспечивает высокую плотность упаковки зёрен и обжиг до получения керамической муллитовой связки. Муллитовые кремнезёмные или мулитовые огнеупорные изделия, обожжённые под давлением, применяются для футеровки тепловых агрегатов, использующих фторуглеродные отходы в качестве топлива или восстановителя.

Ключевые слова: фторсодержащие углеродистые материалы, дробление, муллитовые огнеупоры, высокопластинчатые глина, помол, муллитокремнеземистые изделия, связка, шамот, сушка, обжиг.

Информация об авторах:

Сидорина Елена Анатольевна
Магистр технических наук, докторант кафедры НТМ, Карагандинский технический университет имени Абылкаса Сагинова, 100027, пр. Нурсултан Назарбаев, 56, Караганда, Казахстан. E-mail: elena.sidorina.78@mail.ru; ORCID ID: https://orcid.org/0000-0002-4417-8551

Исагулов Аристотель Зейнуллинович
Доктор технических наук, профессор кафедры НТМ, Карагандинский технический университет имени Абылкаса Сагинова, 100027, пр. Нурсултан Назарбаев, 56, Караганда, Казахстан. E-mail: aristotel@kstu.kz; ORCID ID: https://orcid.org/0000-0003-2174-9072

Рабатулы Мухаммедрахим
Ph.D., и.о. доцента кафедры Разработка месторождений полезных ископаемых, Карагандинский технический университет имени Абылкаса Сагинова, 100027, пр. Нурсултан Назарбаев, 56, Караганда, Казахстан. E-mail: mukhammedrakhym@mail.ru; ORCID ID: https://orcid.org/0000-0002-7558-128X

Yang Ying
Кандидат технических наук, старший преподаватель, Северо-Восточный нефтяной университет, Научно-исследовательский институт разработки нетрадиционных ресурсов нефти и газа, Дацин, 163318, Китай. E-mail: yyainngg@126.com; ORCID ID: https://orcid.org/0000-0002-8927-3878

References

[1] Visloguzova ÉA, Kashcheev ID, Zemlyanoi KG. Analysis of the effect of periclase-carbon refractory quality on converter lining life. Refractories and Industrial Ceramics. 2013; 54(2):83-87. https://doi.org/10.1007/s11148-013-9553-3

[2] Nišić N, Kragović M, Gulicovski J, Gordić M, Stojmenović M. The Incorporation of Waste Sludge into the Production of High-Temperature-Resistant Adhesive Ceramic Materials Applied Sciences (Switzerland). 2023; 13(16). https://doi.org/10.3390/app13169044

[3] Kalytka VA, Korovkin MV, Sh Madi P, Kalacheva SA, Sidorina EA. Universal installation for studying structural defects in electrical and optical fiber materials. Journal of Physics: Conference Series. 2020; 1499(1):012046. https://doi.org/10.1088/1742-6596/1499/1/012046

[4] Kalytka VA, Korovkin MV, Madi PW, ...Kalinin AV, Sidorina EA. Quantum-mechanical model of thermally stimulated depolarization in layered dielectrics at low temperatures Journal of Physics: Conference Series. 2021; 1843(1):012011. https://doi.org/10.1088/1742-6596/1843/1/012011

[5] Aubakirov D, Issagulov A, Kvon S, ...Chsherbakova Y, Arinova S. Modifying Effect of a New Boron-Barium Ferroalloy on the Wear Resistance of Low-Chromium Cast Iron. Metals. 2022; 12(7):1153. https://doi.org/10.3390/met12071153

[6] Issagulov AZ, Kulikov VYU, Kvon SVS, ...Arinova SK, Dostayeva AM. Comparative analysis of graphite inclusions in chrome cast iron structure. Metalurgija. 2021; 60(3-4):285–288.

[7] Ibraev IK, Ibraeva OT. Ispol'zovaniye otkhodov ugleobogashcheniya v metallurgicheskom proizvodstve [The use of coal enrichment waste in metallurgical production] Proceedings of the Congress with international participation and elements of the school of young scientists Fundamental research and applied development of processes for the processing and disposal of technogenic formations. Technogen – 2014. Yekaterinburg. 2-6 June 2014, 359-362. (in Russ).

[8] Patrin RK, Sizyakov VM, Bazhin VYu. Prospects for pyrometallurgical processing of technogenic wastes of aluminum production. Izvestiya vuzov. Non-ferrous metallurgy. 2013; 6:61-63.

[9] Ivankov SI. Troitsky AV. Patented technological solutions for the processing and disposal of large-tonnage wastes of aluminum production. Scientific and technical aspects of environmental protection. 2020; 3:38-102.

[10] Golovnykh N V. Hardening of technological materials and recycling of lining waste for aluminum production electrolyzers. NV Golovnykh. Ecology of industrial production. 2010; 4:47-52.

[11] Ermienko AV. Problemy otkhodov proizvodstva i potrebleniya na Kazakhstanskom elektroliznom zavode (Pavlodar) [Problems of production and consumption waste at the Kazakhstan electrolysis plant (Pavlodar)]. Agrarnyy vestnik Urala=Agrarian Bulletin of the Urals. 2009; 3(57):95-97. (in Russ).

[12] Baranov AN, Nemchinova NV, Anikin VV et al. Pererabotka i utilizatsiya ftoruglerodsoderzhashchikh otkhodov alyuminiyevogo proizvodstva [Recycling and utilization of fluorocarbon-containing wastes of aluminum production. Bulletin of ISTU. 2012; 2(61):63–70. (in Russ).

[13] Terentiev VG, Shkolnikov RM. Aluminum production. Grinberg et al. SPb.: Publishing House of MANEB. 2001, 348.

[14] Kashcheev I D, Zemlyanoy K G. Proizvodstvo ogneuporov [Production of refractories]. St. Petersburg: Doe. 2021, 344. (in Russ).

[15] Allenstein J et al. ed. Pen G, Wutenau H. Ogneupornyye materialy: struktura, svoystva, ispytaniya: spravochnik [Refractory materials: Structure, properties, tests: reference book]. M.: Intermet Engineering. 2010, 392. (in Russ).

[16] Kalytka VA, Bashirov AV, Taranov AV, ...Neshina YG, Sidorina YA. Methods of theoretical researches the properties of electrotechnical materials class of dielectrics with hydrogen bonds. Journal of Computational and Theoretical Nanoscience. 2019; 16(7):2799-2804. https://doi.org/10.1166/jctn.2019.8130

[17] Manzhurin IP, Sidorina EA. Determination of the reduction in the thickness of strip during its shaping in the rolls of a roll-forming machine. Metallurgist. 2013; 56(11-12):941-945. https://doi.org/10.1007/s11015-013-9679-z

[18] Popov RY, Bohdan EO, Dyatlova EM, Komar MV. The application of self-propagating high-temperature synthesis to obtain a protective-strengthening alumina-silica coatings. Proceedings of the National Academy of Sciences of Belarus, Chemical Series. 2019; 55(2). https://doi.org/10.29235/1561-8331-2019-55-2-240-246

[19] Isagulov AZ, Kashcheev ID, Sidorina EA, Zemlyanoy KG. Behavior of the Fireclay Lining of a Coke Gas Cupola Furnace When Melting Cast Iron Using Anode Scrappage in Electrolysis Production. Part 1. Refractories and Industrial Ceramics. 2022; 62(5):492-496. https://doi.org/10.1007/s11148-022-00632-w

[20] Nasrollahi Z, Hashemi M-S, Bameri S, Mohamad Taghvaee V. Neda Nišić, Milan Kragović, Jelena Gulicovski, Milan Žunić,Francesco Basoli/ The Incorporation of Waste Sludge into the Production of High-Temperature-Resistant Adhesive Ceramic Materials/Multidisciplinary Digital Publishing Institute (MDPI)/ Applied Sciences (Switzerland). 2020; 13(16):9044/2023. https://doi.org/10.3390/app13169044

[21] Environmental pollution, economic growth, population, industrialization, and technology in weak and strong sustainability: using STIRPAT modelEnvironment, Development and Sustainability. 2020; 22:1105-1122. https://doi.org/10.1007/s10668-018-0237-5

Complex Use of Mineral Resources. 2025; 335(4):96-109 ISSN-L 2616-6445, ISSN 2224-5243

DOI: 10.31643/2025/6445.44

Earth sciences

Application of the integrated well-surface facility production system for selecting the optimal operating mode of equipment

[1]Moldabayeva G.Zh., [2]Turdiyev M.F., [3]Suleimenova R.T., [4]Buktukov N.S.,
[5] Efendiyev G.M., [3]Kodanova Sh.K., [1]Tuzelbayeva Sh.R.

[1]*Satbayev University, Almaty, Kazakhstan*
[2]*Samarkan State University, Samarkand, Uzbekistan*
[3]*Safi Utebaev Atyrau University of Oil and Gas, Atyrau, Kazakhstan*
[4]*D. Kunaev Institute of Mining, Almaty, Kazakhstan*
[5]*Institute of Oil and Gas of the National Academy of Sciences of Azerbaijan, Baku, Azerbaijan*

* *Corresponding author email: raikhan.suleimenova@aogu.edu.kz*

Received: *September 30, 2024*
Peer reviewed: *October 24, 2024*
Accepted: *October 28, 2024*

ANNOTATION

This work is dedicated to the analysis and development of an integrated production system that combines wells and surface facilities to select the optimal operating mode for equipment. The main focus is on studying data analysis methods, as well as collecting and processing information, which ensures high accuracy in process control and optimal use of technological capabilities. The integration of data from various levels of the production chain, from the well to the surface facilities, opens up new opportunities for optimizing equipment performance and improving resource management quality. Integration of wells and surface facilities – The effective integration of wells and surface facilities is crucial for optimizing production processes, minimizing operational costs, and reducing environmental impact. Integrated management systems allow the automation of many processes, providing continuous monitoring of operating parameters, automatic adjustment of settings, and supplying data for quick decision-making. This includes real-time data collection, analysis, and the use of the obtained information to select optimal operating modes, which helps improve both overall efficiency and safety in production processes. In the modern oil and gas industry, the efficient use of equipment at all stages of hydrocarbon production is of particular importance. Optimizing the operation of wells and surface facilities is a key aspect for increasing economic efficiency and reducing environmental impact. In this regard, the development and application of integrated systems that enable real-time control and adaptation of equipment operating modes has become a relevant and significant task.

Keywords: integrated system, surface facilities, integration of wells and surface facilities, geotechnology, geotechnological methods, well, filtration.

	Information about authors:
Moldabayeva Gulnaz Zhaksylykovna	*Doctor of Technical Sciences, Professor of the Department of Petroleum Engineering, Satbayev University, 050013, Satpayev 22a, Almaty, Kazakhstan. E-mail: moldabayeva@gmail.com; ORCID ID: https://orcid.org/0000-0001- 7331-1633*
Turdiyev Muradim Faizievich	*Candidate of fiz-mat. Sciences, Samarkand State University, Department of "Exact Sciences". E-mail: tmurat-43@mail.ru*
Suleimenova Raikhan Taupikhovna	*Doctor PhD, Associated Press.professor, Safi Utebaev Atyrau University of Oil and Gas, 060027, Baimukhanov, 45A, Atyrau, Kazakhstan. E-mail: raikhan.suleimenova@aogu.edu.kz; ORCID ID: https://orcid.org/0000-0001-7995-5560*
Buktukov Nikolay Sadvakasovich	*Doctor of Technical Sciences, Director of the D. Kunaev Institute of Mining, 050046, Abaya 191, Almaty, Kazakhstan. E-mail: igdkpms@mail.ru; ORCID ID: https://orcid.org/0000-0001-6370-8557*
Efendiev Galib Mammadovich	*Doctor of Technical Sciences, Professor. Institute of Oil and Gas of the National Academy of Sciences of Azerbaijan, Baku, Azerbaijan. Email: galib_2000@yahoo.com; ORCID ID: https://orcid.org/0000-0002-4875-5782*
Kodanova Shynar Kulmaganbetovna	*Candidate of Technical Sciences, Atyrau University of Oil and Gas named after Safi Utebaev, 060027, Baimukhanov, 45A, Atyrau, Kazakhstan. E-mail: S.Kodanova@aogu.edu.kz; ORCID ID: https://orcid.org/0000-0002-1589-4268*
Tuzelbayeva Sholpan Ryskulbekkyzy	*Master of technical sciences, doctoral student, Satbayev University, Almaty, Kazakhstan. Email: s.tuzelbayeva@satbayev.university; ORCID ID: https://orcid.org/0000-0002-1749-6511*

Introduction

Modern technological and economic conditions in the oil and gas industry require increased efficiency and reliability of equipment [[1], [2]]. The contemporary oil and gas sector faces the need to enhance the efficiency and sustainability of its operations. One promising direction is the use of integrated production systems that combine wells and surface facilities [3]. These systems allow for the optimization of equipment operating modes, which contributes to increased productivity and reduced operating costs. This article examines various aspects of the application of such systems and optimization methods, as well as examples of successful implementation and development prospects. Integration of processes at the well-surface facility level not only optimizes operational parameters but also significantly reduces environmental impact, making this study relevant and important for the further development of the industry.

When servicing wells, the operator follows an established route and inspects the condition of surface equipment. The operator records instrument readings, inspects wellhead equipment, and collects fluid samples. As instructed by the supervisor, dynamograms are recorded. The operator participates in well depourification operations [4], transmits information from the sites to the dispatcher, and prepares wells for repair.

A well workover team replaces downhole equipment. More complex repairs, such as formation work, retrieval of stuck equipment, or transitioning to different horizons, are carried out by the well major repair teams.

Automation and Digitalization - Integrated Digital Platforms: Discussion of the role of IT solutions in production management, including real-time monitoring, automatic well control, and predictive equipment maintenance [5].

Robotics and Drone Technologies: The use of automated systems and unmanned aerial vehicles (UAVs) for monitoring, inspection, and even repairs at oilfields.

Computer-Integrated Manufacturing (CIM) is a manufacturing approach where computers control the entire production process. Such integration allows individual processes to share information with each other and initiate actions. Through computer integration, production can become faster and less prone to errors, with the primary benefit being the ability to create automated production processes. CIM typically relies on feedback control processes based on real-time sensor input, also known as flexible design and manufacturing.

A recognized model for a company managing information, responsible for the current level of automation, is the hierarchical model of computer-integrated manufacturing (CIM). According to this model, upper-level systems operate with aggregated data over relatively long periods of time, while lower-level systems work with real-time data streams.

SCADA systems are highly distributed systems used to manage geographically dispersed assets, often spread over thousands of square kilometers, where centralized data collection and control are critical for system operation. They are used in distribution systems such as water supply and wastewater collection systems, oil and gas pipelines, electrical grids, and railway transport systems.

SCADA systems consist of both hardware and software. Typical hardware includes a Master Terminal Unit (MTU) located in a control center, communication equipment (such as radio, telephone lines, cables, or satellites), and one or more geographically distributed field devices consisting of Remote Terminal Units (RTUs) or Programmable Logic Controllers (PLCs), which control actuators and/or monitor sensors.

Research methods

Lower-level models represent elements of data collection (sensors), device control (e.g., controllers, CNC machines), and the automated SCADA system (Supervisory Control and Data Acquisition), interacting with hardware. An overview of integration approaches is shown in Figure 1.

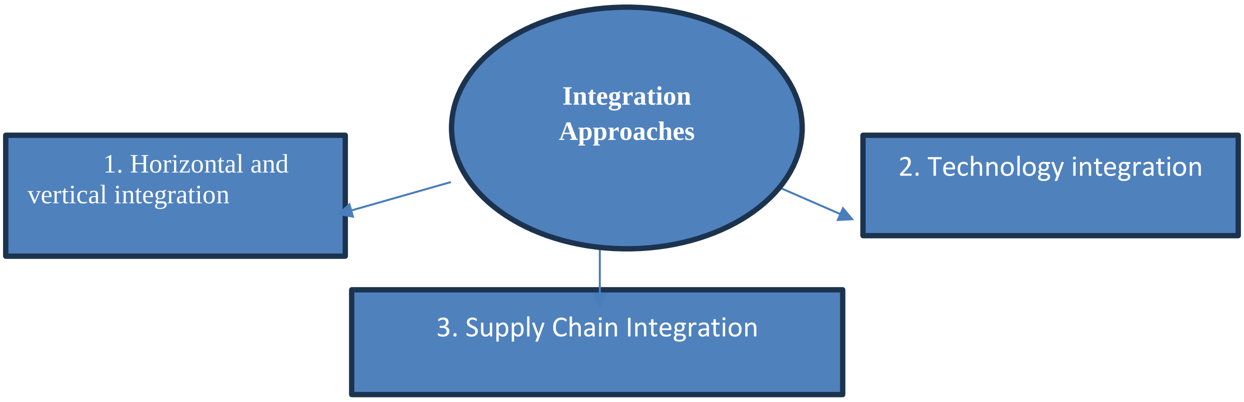

Figure 1 - Overview of Integration Approaches

Providing examples from the practices of large oil and gas companies that have successfully implemented integration approaches. These could be cases from various countries and regions, demonstrating how technological and managerial innovations have helped improve productivity and reduce costs. Summarizing the analysis, highlighting key findings and recommendations for oil and gas companies seeking to enhance their competitiveness and operational efficiency.

The Internet of Things (IoT) is a network of connected devices that collect and exchange data in real-time. In the oil and gas industry, IoT is used to create "smart" wells and surface facilities where all system elements are interconnected and centrally managed [6]. The digitalization of extraction processes enables the creation of digital twins of wells and surface facilities, which assist in simulating and analyzing various operational scenarios. These digital models allow for testing different parameters and conditions without risking real equipment, improving the accuracy and reliability of decisions.

The flow in the water supply pump group is first forecasted using an LSTM network for 24 hours. Then, the water intake pump group's flow is planned for 24 hours, along with the water level in the clean water tank, based on the water supply pump group's flow and engineering expertise. Secondly, nonlinear models of the operating pumps are configured based on historical data. Finally, intelligent joint optimal planning tasks are set, allowing for the minimization of pump consumption and the number of switch-ons, using flow constraints in the intake and supply pump groups, pressure in the main pipe, and water levels in the pump system's clean water tank. The optimal operating schedule for the intake-supply pump groups, setting the pumps' operating configurations at each moment in time, can be obtained using the DP algorithm.

Modern integrated production systems include complex control and monitoring systems that use software and hardware tools to collect, analyze, and visualize data. These systems ensure continuous control over all production stages, from well conditions to the transportation of finished products. Information technologies, such as SCADA (Supervisory Control and Data Acquisition) and DCS (Distributed Control System), play a crucial role in this [7].

One of the main advantages of an integrated system is the ability to enhance hydrocarbon extraction efficiency. By integrating all system components and using modern monitoring and control technologies, operators can optimize extraction processes, reducing losses and increasing productivity. For example, precise control of pumps and valves allows maintaining optimal conditions for oil and gas extraction.

Forecasting the flow in the water supply pump group: Based on historical data analysis, water temperature and pressure in the main clean water pipe are important factors influencing the flow in the water supply pump group. Since the LSTM network can remember and learn long-term data characteristics, a forecasting model is created to predict the water supply pump group's flow using the LSTM network. The forecasted flow in the supply pump group for the next 24 hours is adjusted for the difference between the predicted and actual flow in the supply pump group over the past 24 hours. The output variable is the supply pump group's flow for the next 24 hours.

An LSTM network consists of an input layer, a hidden layer, and an output layer. The LSTM network differs from RNNs by adding a forget gate f_t, input gate i_t, output gate o_t, and memory cell C_t to meet the needs of time series data. These gates can open or close depending on the memory state of the network (the previous network state) [[8], [9], [10]].

Developing an integrated system for optimal equipment operation in the oil and gas industry is a complex project that requires a deep understanding of both technical aspects and management processes. It is crucial to create a system that not only enhances operational efficiency but also takes into account environmental and economic factors. Adaptive control systems enable quick responses to changing extraction conditions and adjustments to equipment operation modes in real time. Such systems use data from sensors to automatically adjust the operating parameters of pumps, valves, and compressors. This allows for maintaining optimal conditions for hydrocarbon extraction and processing, minimizing losses, and increasing productivity.

Production and technological processes have made significant progress. The key is not only to create new equipment components but also to increase the degree of automation in managing production and technological modes at facilities and across utility industries. In this context, it is worth noting that fundamentally new forms of operation have emerged for current and future management systems.

Modern automated control systems can memorize [[11], [12], [13], [14], [15]], compare, and even find optimal modes for controlled processes. They select the best modes based on preprogrammed data, data obtained during the system's operation, as well as process simulations, all of which are implemented with minimal investments. Integrated systems significantly reduce operating costs by more effectively utilizing resources and minimizing equipment downtime. Modern monitoring systems enable quick identification and elimination of malfunctions, reducing repair and maintenance time. Equipment wear is also reduced, extending its service life and decreasing the frequency of replacements. Thanks to optimized operation modes and timely maintenance, the equipment operates longer and more reliably. Integrated systems enable regular equipment condition checks and forecast potential breakdowns, allowing for pre-planned maintenance and the replacement of worn-out components.

Dynamic well modeling involves analyzing well behavior at various production levels, pressure changes, and temperature conditions. Using specialized software suites, such as ECLIPSE and Petrel [[3], [4]], engineers can simulate different well operation scenarios and select the optimal parameters for maximum productivity and extraction stability.

Pipeline flow modeling allows for the evaluation of a system's hydraulic characteristics and the selection of optimal conditions for hydrocarbon transportation. Software packages such as OLGA and PIPESIM are used to conduct hydrodynamic calculations, which help prevent overloads and pressure losses, as well as optimize the operation of pumps and compressors.

The complete system of governing equations that describe the processes in the asynchronous electric drive of centrifugal pumps consists of four groups: electromagnetic equilibrium equations (Kirchhoff's laws) describing the electromagnetic processes in the motor, electromechanical energy conversion equations, equations describing the mechanical load on the motor shaft, and equations representing the output parameters and properties of the energy sources.

The first step was the analytical method, based on the classical definition of the optimal cross-sectional value, which allowed us to determine the qualitative characteristics, laws, and methods to reduce costs in the frequency-controlled electric drive operating under centrifugal load.

The main distinction from known methods is the use of refined mechanical characteristics of the central pump, which we obtained earlier [2].

$$(\omega) = \sqrt[4]{\text{К}_\text{э} \frac{\left(\frac{C_\text{Н} H_\text{С} + \omega^2}{\omega \eta_\text{ЦН}(\omega, H_\text{С})}\right)^2 \omega \quad \begin{matrix}\text{Н} \\ \text{Н}_0\end{matrix}}{\text{К}_0 + \text{К}_\text{СТ} \omega^{\frac{3}{2}}}}$$

Where

k_0 - relative losses in coils, steel and no-load current.

The accuracy of the method is determined by the accuracy of the approximation of the magnetization curve.

Figure 2 shows the dependence of the optimal values of the magnetic flux on the back pressure at the outlet of the pumping unit. The "kink" of curves 2 and 3 indicates a decrease in the operating range of pump wheel speed adjustment with an increase in the value of the static back pressure of the pipeline. The calculation was carried out using the same values of weight loss coefficients [[13], [14], [15], [16]].

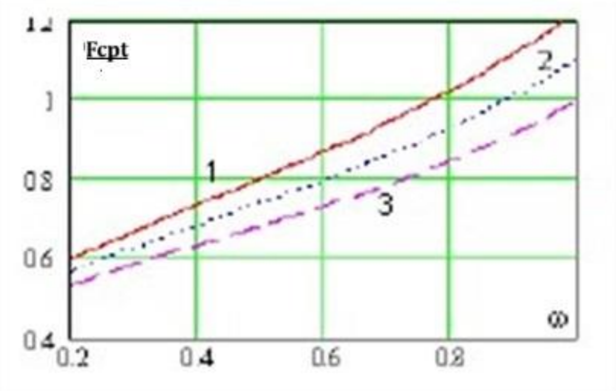

Figure 2 – Fopt Curves(w) for different values of relative pressure losses (w)

When selecting motors and designing the optimal automatic control system (ACS) for the central pump drive, the influence of induction motor (IM) parameters on the variation of optimal magnetic flux across the impeller's speed control range is of particular interest. Specifically, the value of F_{opt} often depends on the distribution of costs based on baseline arterial pressure. Figure 4b shows the results of calculating the optimal magnetic flux value based on inherent cost values common to mass-produced asynchronous motors.

The next phase of research involved the harmonic method, which takes into account the non-sinusoidal distribution of magnetic induction in the machine. In this case, the steel's magnetization curve is approximated by a hyperbolic sine, and the magnetic forces are represented by a series using Bessel functions.

The analytical studies conducted allowed us to establish the main patterns of the frequency-controlled electric drive for a centrifugal pump. The evaluation of real numerical relationships was based on the digital harmonic method of optimal calculation in terms of minimizing costs, accounting for system nonlinearity, precise core geometry, high-frequency control, and other factors. An algorithm was developed to solve this problem.

All processes in the induction motor are described by a system of linear equations of magnetomotive force (MMF) F, electromotive force (EMF) E, and torque M, which are fuzzy functions of the harmonic magnetic induction amplitude along the longitudinal and transverse axes.

Based on the harmonic method, a mathematical model of the "frequency-controlled induction motor – centrifugal pump" system was created, taking into account the technological parameters of the central pump, the geometric parameters of the motor core, and the actual distribution of magnetic induction. The model includes the entire set of electrical parameters, core structural parameters, and, most importantly, accurately considers the nonlinearity of the magnetic circuit.

Numerical studies conducted on the developed model determined the main patterns and methods for reducing motor energy consumption. Optimal laws and frequency control for the central pump drive were calculated for different core options, ensuring minimal motor costs. The obtained IM characteristics confirm the effectiveness of the proposed control algorithms and the high level of energy efficiency.

The created mathematical model can be directly used as an element of the automatic control system for the electric drive according to the "PC-IM" scheme for centrifugal units optimized for energy consumption.

Figure 3 shows the operating characteristics of the system: torque, useful power, consumed power, and power consumption. Using the proposed optimal cost-minimizing frequency control law, the efficiency of the central pump remains high and equal to the nominal value across the entire flow control range.

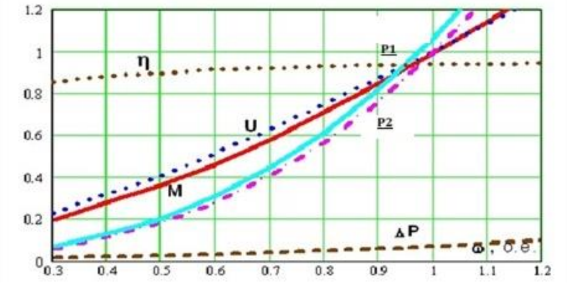

Figure 3 – Operating characteristics of blood pressure in the control range of the central pump with optimal frequency control

The calculation of energy consumption and energy performance of the torque-controlled drive (TCD) has several features compared to other induction motor (IM) control schemes (Figure 4). In the TCD, the rotor speed of the induction motor is adjusted by introducing an additional voltage $\boldsymbol{U_2}$ into the rotor circuit. This voltage can be controlled in terms of magnitude, frequency, and phase.

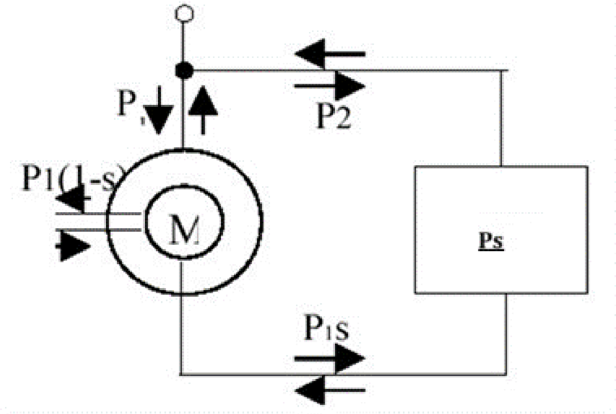

Figure 4 – Two-speed machine

The calculation of the static modes of operation of the DCS is reduced to determining the values of U_2 and δ from a joint solution of the electrical balance and electromechanical balances necessary to ensure the operating mode. Thus, we have obtained a mathematical model of the electric drive of a centrifugal pump according to the scheme of two feeding machines.

The power part of the SCH500 station is made according to a two-transformer circuit with a low-voltage frequency converter of the SM500 series with a voltage of 690 V.

There are many standard sizes for a power of 250 kW and 320 kW. Depending on the output power of the CM500, up to four HTM modules can be installed.

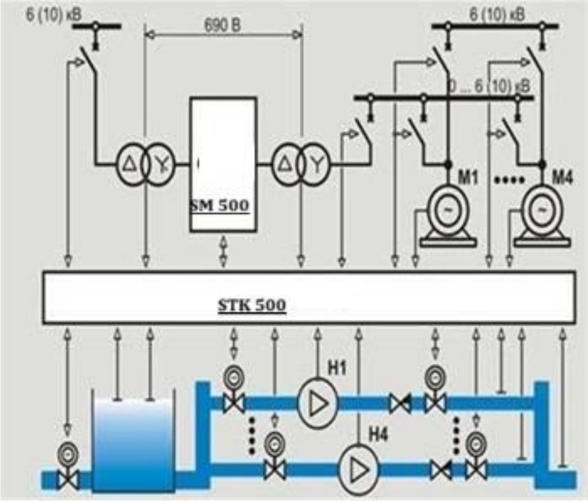

Figure 5 – Description of the station

All HTM modules are identical, with one being the master and the rest as slaves. Synchronization of the parallel operation of the modules is carried out at the "PMO" level. Power transformers can be used in standard configurations, either oil-filled or dry-type.

The KSO cells include switching equipment for group control. Structurally, the CM500 frequency converter (Figure 5) is a set of floor-standing cabinets.

The process controller is based on an industrial computer with a TFT monitor. The controller manages the electrical circuit of the SN500 station and the equipment of the main technological chain of the pumping station.

The power section of the SN500 station is designed using a dual-transformer scheme with a low-voltage frequency converter of the CM500 series, operating at 690V.

There are multiple size options with capacities of 250 kW and 320 kW. Depending on the output power, up to four HTM modules can be installed in the CM500.

All HTM modules are identical, with one being the master and the rest as slaves. Synchronization of the parallel operation of the modules is carried out at the "PMO" level. Power transformers can be used in standard configurations, either oil-filled or dry-type.

The KSO cells include switching equipment for group control. Structurally, the CM500 frequency converter is a set of floor-standing cabinets.

The process controller is based on an industrial computer with a TFT monitor. The controller manages the electrical circuit of the SN500 station and the equipment of the main technological chain of the pumping station.

Information is displayed graphically in three main user windows:

Process window (displaying current information in a technological flowchart);

Control window (setting the operating mode and main control parameters);

Archiving window (access to two main archives: alarm archive and event archive).

Additionally, the controller can expand telemetry functions.

Advantages of using a variable frequency drive (VFD):

Smooth regulation of the motor speed in most cases eliminates the need for additional control equipment, significantly simplifying the technological system, increasing its reliability, and reducing operating costs. A frequency-regulated motor start ensures smooth acceleration without inrush currents or mechanical shocks, reducing stress on the motor and associated transmission mechanisms, thereby increasing their service life. In this case, the power of the drive motors for loaded mechanisms can be reduced according to startup conditions. The built-in microprocessor-based PID controller allows for speed regulation of controlled motors and associated technological processes.

Using feedback from the system to the frequency converter guarantees high-quality speed maintenance of the motor or the controlled process parameter under variable loads and other disturbances.

The frequency converter, paired with an asynchronous motor, can replace DC drive systems.

A frequency converter, supplemented by a programmable microprocessor controller, can be used to create multifunctional drive control systems, including systems with backup mechanical units.

Using a variable-frequency drive (VFD) allows for energy savings by eliminating unnecessary energy consumption. Significant efficiency is achieved by using frequency converters to regulate the operation of pumping units, which were traditionally controlled by throttle mechanisms in pump discharge pipes.

Throttle regulation involves energy losses due to local resistance created by control devices. These losses are eliminated when the pump's performance is controlled by regulating the motor speed. Energy savings from using VFDs in pumps typically amount to 10-30% of the power consumed by pumps under throttle control.

The implementation of variable-frequency drives (VFDs) at water supply and sewage pumping stations allows for optimizing the hydraulic regime of the water distribution network, addressing energy-saving objectives, reducing operating costs, and minimizing pipeline damage by maintaining optimal pressure in the network.

The automation of production processes was carried out in stages. Initially, an automated control system for technological processes was created and put into operation at two sewage pumping stations (SPS). Control over the operation of these stations was provided from the workstation of the dispatcher at the SPS workshop. A central database (CDB) was created on the dispatcher server in the workshop.

Automated operation requires complete monitoring of all parameters and the ability to make correct decisions in any situation. To ensure high equipment reliability, more than a hundred variable indicators characterizing the operation of the equipment, as well as the primary and secondary technological processes, are recorded. At the same time, the number of control actions set by the automated control system reaches twenty types. Almost complete control over the station's operation allowed for the development of control actions for all situations, eliminating the need for manual management from the dispatch room. This provided full protection against unauthorized or accidental access to the automated control system. The high reliability of the specialized controllers ensured monitoring and registration of all parameters characterizing the equipment's operation and the technological process.

Despite the high reliability of the automated control system, the transition to operating the pumping equipment without service personnel was limited by several external factors. The SPS workshop's automated control system was built on its own computer radio network operating at a frequency of 450 MHz. The rapid development of the city, the appearance of new high-rise buildings, and the significant distance between the SPS facilities made it difficult to use the computer radio network at some sites.

Thus, the requirements for the creation of the automated control system at the NDS workshop (Figure 6) expanded, necessitating the use of mobile communication channels and telephone connections (GSM, CDMA modems) due to objective difficulties in data transmission within the computer network.

The PTC PNO allows solving the following tasks (Figure 7):

Continuous monitoring of pumping stations, obtaining key indicators (energy consumption, volume of waste pumped, specific energy consumption);

Obtaining objective and reliable data to justify the selection of pumping equipment during reconstruction;

Processing data on system expenditures and identifying issues in pressure pipelines;

Comparing the operating time of pumping equipment with the standard adjustment interval and optimizing maintenance [[16], [17], [18], [19], [20], [21]].

When creating the control and automation system for KNS, the primary task was to solve the issue of data transmission and to choose the main communication channel between local dispatch centers. Existing power lines were tested. As a result, a data transmission network was created between the local dispatch centers based on existing communication networks, using SHDSL modems.

According to the technological scheme of the NDS, variable indicators characterizing the equipment operation at all stages of the technological process were determined. The selected variables are used for automating the work and/or managing the facilities of the store, taking into account the technological and administrative division. Part of the information received from the communication nodes of local dispatch centers is transmitted to the central dispatch center of the USC for evaluating the technological process, the operation of workshops, their facilities, and the enterprise as a whole. Based on variable indicators, the technical characteristics of local dispatch points and the devices of the central dispatch point have been determined.

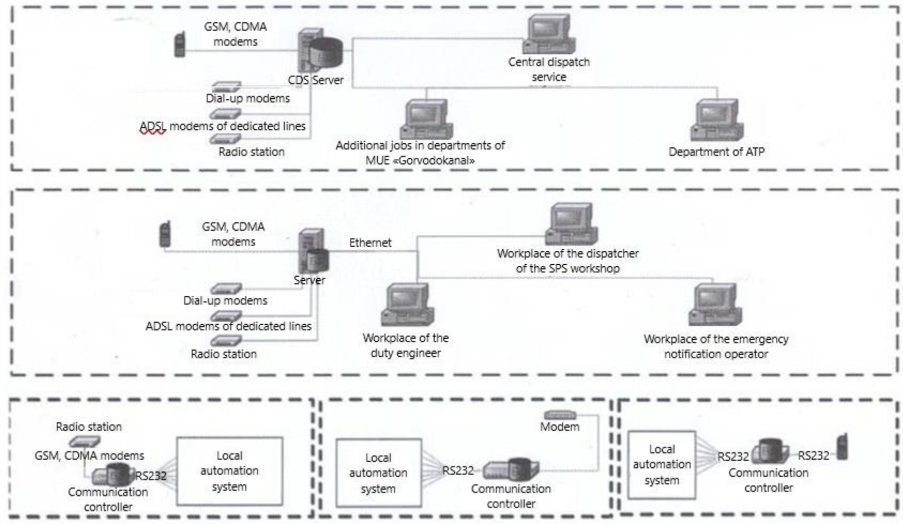

Figure 6 – Block diagram of automation of technological processes in the pumping station workshop

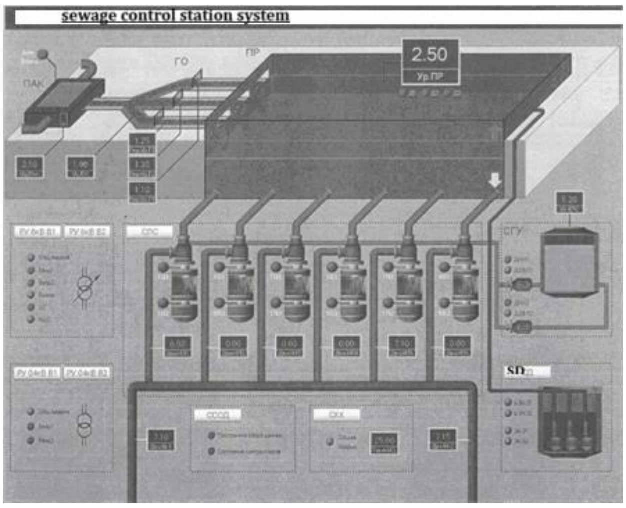

Figure 7 - A fragment of the mnemonic diagram of the dispatching control of a sewage pumping station (6 kV)

The information from the aforementioned facilities is transmitted to SHDSL modems via Wi-Fi wireless data transmission modems (the communication center of the local dispatch point of the corresponding workshop) and then transmitted via special lines to the central dispatch center (CIC) and displayed on the monitor.

The system's performance results showed that:

Low costs for installing special data transmission lines, high noise immunity, reliability, and data transmission speed;

Wireless data transmission networks using Wi-Fi technology are characterized by high mobility of data collection points, reliability, noise immunity, high data reception speed, low installation costs, and short implementation time;

In general, a local computer network has been created for the system, providing information from control measuring instruments and equipment control systems in local control centers for all workshops and in the Central Dispatch Center (CIC).

It is worth noting the possibility of dual use of the technical and software solutions included in the APKS (Automated Process Control System) for related tasks. For example, the technical and software tools of the SPC shop's APCS (Automated Process Control System) are used for analyzing pressure in water supply lines at control points. Information received from the water supply system pressure sensors is sent to the local automation system and transmitted to the central database of the pumping station, from where it is further transmitted to the central dispatch point. Measurement results, after processing, are displayed in the water supply service work centers and in the central control point.

The design solutions adopted are based on the experience of existing automation systems and are aimed at maximizing the coverage of technological process parameters on a unified information platform "Wander-ware," ensuring both the length of parameters and their interconnection in the technological chain and information flows.

Based on the design solutions, in 2009, the automatic filter washing systems of NFS-1 and NFS-5 are planned to be commissioned, and the internal pressure monitoring system expanded to 45 control points in the water supply network.

At present, plans are underway to equip the relevant divisions with new control and measuring equipment to use objective results for the implementation of APCS capabilities, enabling the acquisition of comprehensive characteristics of technological processes in automatic mode. Predicting equipment conditions and performing preventive maintenance are important aspects of optimizing operational modes. The use of predictive analytics and machine learning technologies allows predicting possible failures and planning maintenance in advance. This reduces the likelihood of emergency situations and helps maintain equipment in optimal condition.

Equipment required for automation: The SIMATIC S7-1200 PLC is a new family of Siemens microcontrollers designed for various low-level automation tasks. These controllers are modular and versatile. They can operate in real-time and can be used to create relatively simple local automation blocks or units supporting complex automatic control systems.

This algorithm is designed to control the main and backup pumps operating alternately in the same network. It is used for controlling circulation pumps in heating and hot water supply systems. In combination with a shutoff and control valve, the controller can be connected to a system using water from a tank. In this device modification, two inputs are used: the first can be connected to a switch, closing which initiates the algorithm, and the fourth input is connected to a pressure sensor. This could be a flow sensor that closes the output contact when the required pressure is achieved in the network or modern pressure sensors with a single current output. A pressure relay is used to control the main and backup pumps. A third relay can be connected to an alarm system or a third pump.

The automatic control system ensures even use of the main and backup pumps by alternating their operation. The pump operation time is programmed by the user (the maximum possible pump operation time is 63 days). In case one of the pumps fails, the device switches to the other, triggering an LED alarm indicator. If all pumps fail during operation, the third relay is activated, triggering an alarm or switching on backup pumps (without pressure control in the main line).

In the algorithm based on pressure sensor use, during pump start-up, the pressure sensor readings are not monitored for the user-specified time period (30 seconds by default). Additionally, the controller ignores short-term (2 seconds by default) drops in pressure sensor readings.

System efficiency analysis

Integrated well-surface facility systems and operational mode modeling open up new opportunities for improving the efficiency and reliability of the oil and gas industry. Implementing such technologies requires significant investments and a highly skilled workforce, but the long-term benefits—such as reduced costs and increased productivity—justify these efforts. Modern technologies and approaches to production process management allow for achieving high results and ensuring sustainable development of the industry.

A specific model corresponds to the basic scheme of the Integrated Production Planning (IPP). The main task of particular modifications is to fully declare all temperatures and losses at any given time and in each region of the GIS. Key information for modifications includes the selection of heat exchangers for heating, ventilation, and hot water supply systems; the choice of the standard forecasting interval, up to one calendar month, which is analyzed in full; and brief details about the modeling area, including temperature diagrams of the heat carrier. Depending on the external atmospheric temperature, the heat carrier temperature, and the heat source, the thermosensitive heat carrier at the IPP inlet and the predicted heat recovery vary. The controllers' resources are linked to temperature and temperature changes incorporated into heat theory, which are connected to the changes in natural products. Based on the properties of the control valve, it causes changes in the flow rate within the sleeve element and the valves.

The effect of incoming heat on the temperature Ti(t) can be determined by the gain factor k and a first-order system with a time constant τ. The influence of ambient temperature can be represented as a first-order system with a gain factor and time constant. The water temperature Tu(t), supplied to the heat exchanger loop, is regulated by a PI controller. The PI controller is one of the most versatile controllers. Essentially, it is a proportional controller (P-controller) with an additional integrated component. This integrated component, as the name implies, is added primarily to eliminate the static error inherent to the proportional controller. The integral part acts as an accumulator, accounting for the history of the current input variable to the PI controller (1) (Figures 8-10).

$$W(S) = \frac{1}{30s+1} + \frac{1}{2s+1}) \times \frac{1}{20s+1} \text{"}= \frac{(30s+1)(2s+1)}{(30s+1)(2s+1)(20s+1)} \qquad (1$$

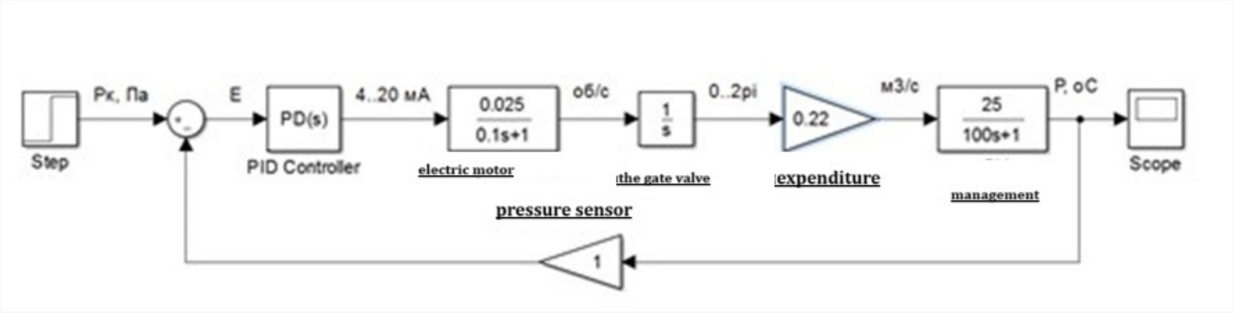

Figure 8 — Mathematical model in the Matlab environment

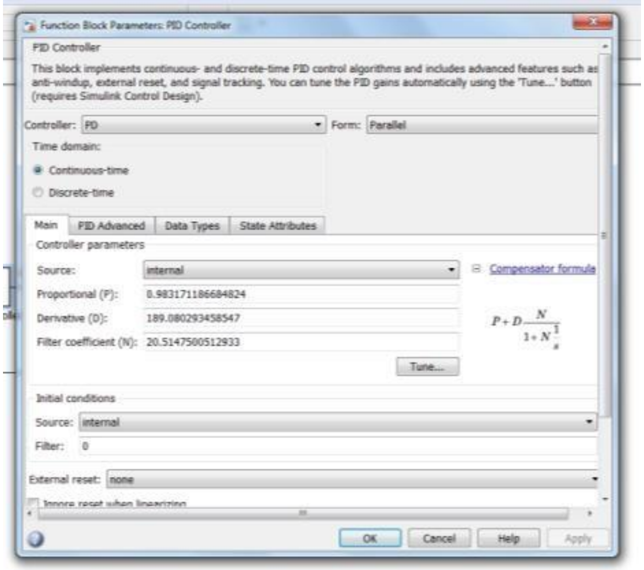

Function Block Parameters: PID Controller

PID Controller

This block implements continuous- and discrete-time PID control algorithms and includes advanced features such as anti-windup, external reset, and signal tracking. You can tune the PID gains automatically using the 'Tune...' button (requires Simulink Control Design).

Controller: PID Form: Parallel

Time domain:

● Continuous-time

○ Discrete-time

Controller parameters

Source: internal

Proportional (P): 0.983171186684824

Derivative (D): 189.080293458547

Filter coefficient (N): 20.5147500512933

$$P+D\frac{N}{1+N\frac{1}{s}}$$

Initial conditions

Source: internal

Filter: 0

External reset: none

☐ Ignore reset when linearizing

Figure 9 – Parameters of the PI controller
The following parameters of the PI controller are set in the Matlab environment

Conclusions

This study emphasizes the critical importance of developing and applying integrated management systems in the oil and gas industry to enhance efficiency and reduce environmental impact. Automation and optimization of processes at all levels of hydrocarbon production, from the well to surface facilities, are key elements for achieving these goals. The implementation of developed algorithms and software, as well as their successful testing and adaptation in real-world conditions, demonstrate the potential for significant improvements in operational efficiency and economic benefits.

The research also revealed that integrating modern technological solutions and analytical methodologies can lead to a deeper understanding and better management of production processes, which will inevitably reduce environmental impact and improve the safety of operations. These findings represent a valuable contribution to the scientific community and provide practical guidelines for application in the industry.

In the future, based on the data obtained and the methods developed, the scope of integrated systems application will be expanded, along with the investigation of their adaptability to different conditions and the specifics of various fields. The prospects for further research include the development of advanced models for adaptation and optimization, which will promote the broader adoption of these technologies in the industry.

The shift toward more sustainable and economically efficient production methods is becoming an integral part of the oil and gas industry's development. The implementation of integrated management systems not only increases overall productivity but also enables companies to comply with stringent international environmental safety standards. This, in turn, enhances the companies' reputation in the global market, boosts their competitiveness, and opens up new investment opportunities and market access.

Focusing on the use of advanced technological solutions and analytical tools makes the industry more adaptive to market changes and better prepared to respond to challenges such as fluctuations in hydrocarbon prices and regulatory changes. This approach not only optimizes current processes but also helps predict future changes in production parameters, ensuring stability and resilience in operations.

Additionally, the development and application of integrated systems create a foundation for continuous learning and skill improvement among employees. The adoption of the latest technologies requires ongoing professional development and training, which leads to an increase in internal expertise and improves the quality of work at all levels. This, in turn, fosters a culture of innovation and a drive for continuous process and performance improvement.

Based on the research conducted, the following recommendations can be formulated for the development of integrated production management systems in the oil and gas industry:

Digitization and data integration: Expand the use of digital technologies for data collection, storage, and analysis. This will improve process understanding at all levels and enable more effective resource management and response to changes in the production environment.

Development of adaptive systems: Design systems that can adapt to changing operating conditions and market demands. Adaptive management systems will help maintain optimal operating parameters under various conditions and reduce the risk of losses due to unforeseen circumstances.

Conflict of interest. The corresponding author declares that there is no conflict of interest.

CRediT author statement: **G. Moldabayeva**: Supervision, Conceptualization, Editing; **M. Turdiyev**: Methodology, Validation; **R. Suleimenova**: Writing draft preparation; **N. Buktukov**: Data curation; **G. Efendiyev**: Visualization, Investigation; **Sh. Tuzelbayeva**: Reviewing, Software.

Acknowledgements. This research was funded by the Committee of Science of the Ministry of Science and Higher Education of the Republic of Kazakhstan (Grant No. AP19674847)

Cite this article as: Moldabayeva GZh, Turdiyev MF, Suleimenova RT, Buktukov NS, Efendiyev GM, Kodanova ShK, Tuzelbayeva ShR. Application of the integrated well-surface facility production system for selecting the optimal operating mode of equipment. Kompleksnoe Ispolzovanie Mineralnogo Syra = Complex Use of Mineral Resources. 2025; 335(4):96-109. https://doi.org/10.31643/2025/6445.44

Жабдықтың оңтайлы жұмыс режимін таңдау үшін ұңғыманы және жер үсті өндірісін басқарудың біріктірілген жүйесін қолдану

[1*]Молдабаева Г.Ж., [2]Турдиев М.Ф., [3]Сулейменова Р.Т., [4]Буктуков Н.С., [5]Эфендиев Г.М., [3]Коданова Ш.К., [1]Түзелбаева Ш.Р.

[1] Satbayev University, Алматы, Қазақстан
[2]Самарқан мемлекеттік университеті, Самаркан, Өзбекстан
[3]Сафи Өтебаев атындағы Атырау Мұнай және газ университеті, Атырау, Қазақстан
[4] Д.Қонав атындағы Тау кен институты, Алматы, Қазақстан
[5] Әзірбайжан Ұлттық Ғылым академиясының Мұнай және газ институты, Баку, Әзірбайжан

Мақала келді: *30 қыркүйек 2024*
Сараптамадан өтті: *24 қазан 2024*
Қабылданды: *28 қазан 2024*

ТҮЙІНДЕМЕ

Бұл жұмыс жабдықтың оңтайлы жұмыс режимін таңдау үшін және жер үсті құрылымдарын біріктіретін интеграцияланған өндірістік жүйені талдау мен әзірлеуге арналған. Негізгі назар деректерді талдау әдістерін зерттеуге, ақпаратты жинау мен өңдеуге бөлінген, бұл процестерді басқарудың жоғары дәлдігін және технологиялық мүмкіндіктерді тиімді пайдалануды қамтамасыз етеді. Ұңғымадан жер үсті нысандарына дейінгі өндіріс тізбегінің әртүрлі деңгейлерінен деректерді біріктіру жабдық жұмысын оңтайландыру үшін және ресурстарды басқару сапасын арттыру үшін жаңа мүмкіндіктер ашады. Ұңғымалық және жер үсті қондырғыларын тиімді біріктіру өндірістік процестерді оңтайландыру және пайдалану шығындары мен қоршаған ортаға әсерді азайту үшін өте маңызды. Интеграцияланған басқару жүйелері көптеген процестерді автоматтандыруға, жұмыс параметрлерін үздіксіз бақылауға, баптауларды автоматты түрде түзетуге және жедел шешім қабылдау үшін деректер ұсынуға мүмкіндік береді. Бұл нақты уақытта деректерді жинауды, талдауды және алынған мәліметтерді пайдалана отырып, оңтайлы жұмыс режимдерін таңдауды қамтиды, бұл өз кезегінде өндірістік процестердің жалпы тиімділігін және қауіпсіздігін арттыруға көмектеседі. Қазіргі заманғы мұнай-газ өнеркәсібінде барлық өндіру кезеңдерінде жабдықты тиімді пайдалану мәселесі ерекше маңызға ие. Ұңғымалар мен жер үсті құрылымдарының пайдалану процестерін оңтайландыру экономикалық тиімділікті арттыру және экологиялық әсерді азайту үшін маңызды аспект болып табылады. Осыған байланысты жабдықтың жұмыс режимдерін нақты уақыт режимінде бақылауға және бейімдеуге мүмкіндік беретін интеграцияланған жүйелерді әзірлеу және қолдану өзекті әрі маңызды міндетке айналуда.

Түйін сөздер: интеграцияланған жүйе, жер үсті жабдықтары, ұңғыма мен жер үсті жабдықтарын интеграциялау, геотехнология, геотехнологиялық әдістер, ұңғыма, сүзу.

Молдабаева Гульназ Жаксылыковна	***Авторлар туралы ақпарат:*** *Техника ғылымдарының докторы, Сәтбаев университетінің Мұнай техникасы кафедрасының профессоры, 050013, Сәтбаев 22а, Алматы, Қазақстан. E-mail: moldabayeva@gmail.com; ORCID ID: https://orcid.org/0000-0001- 7331-1633*
Турдиев Мурадим Файзиевич	*Физика-математика ғылымдарының кандидаты, профессор, Самарқан Мемлекеттік университеті, "Нақты Ғылымдар" Кафедрасы. E-mail: tmurat-43@mail.ru*
Сулейменова Райхан Таупиховна	*PhD Докторы, қауымдастырылған профессор, Сафи Өтебаев атындағы Атырау Мұнай және газ университеті, 060027, Баймуханов, 45а, Атырау, Қазақстан. E-mail: raikhan.suleimenova@aogu.edu.kz; ORCID ID: https://orcid.org/0000-0001-7995-5560*
Буктуков Николай Садвакасович	*Техника ғылымдарының докторы, Д.Қонаев ат. тау-кен институтының директоры, 050046, Абай 191, Алматы, Қазақстан. E-mail: igdkpms@mail.ru; ORCID ID: https://orcid.org/0000-0001-6370-8557*
Эфендиев Галиб Мамедович	*Техника ғылымдарының докторы, профессор, Әзірбайжан Ұлттық ғылым академиясының Мұнай және газ институты, Баку, Әзірбайжан. Email: galib_2000@yahoo.com; ORCID ID: https://orcid.org/0000-0002-4875-5782*
Коданова Шынар Кулмагамбетовна	*Техника ғылымдарының кандидаты, Сафи Өтебаев атындағы Атырау Мұнай және газ университеті, 060027, Баймуханов, 45а, Атырау, Қазақстан. E-mail: S.Kodanova@aogu.edu.kz; ORCID ID: https://orcid.org/0000-0002-1589-4268*
Түзелбаева Шолпан Рысқұлбекқызы	*Техника ғылымдарының магистрі, докторант, Сәтбаев университеті, Алматы, Қазақстан. Email: s.tuzelbayeva@satbayev.university; ORCID ID: https://orcid.org/0000-0002-1749-6511*

Применение интегрированной системы добычи скважина-поверхностное сооружения для подбора оптимального режима работы оборудования

[1]* Молдабаева Г.Ж., [2]Турдиева М.Ф., [3]Сулейменова Р.Т., [4]Буктуков Н.С.,
[5]Эфендиев Г.М., [3]Коданова Ш.К., [1]Түзелбаева Ш.Р.

[1] Satbayev University, Алматы, Казахстан
[2]Самаркандский государственный университет, Самарканд, Узбекистан
[3] Атырауский университет Нефти и газа имени Сафи Утебаева, Атырау, Казахстан
[4]Институт Горного дела им.Д.Кунаева, Алматы, Казахстан
[5]Институт Нефти и газа Национальной академии наук Азербайджана, Баку, Азербайджан

Поступила: *30 сентября 2024*
Рецензирование: *24 октября 2024*
Принята в печать: *28 октября 2024*

АННОТАЦИЯ

Данная работа посвящена анализу и разработке интегрированной системы добычи, объединяющей в себе скважину и поверхностные сооружения, для подбора оптимального режима работы оборудования. Основное внимание уделено исследованию методов анализа данных, сбору и обработке информации, что позволяет обеспечить высокую точность управления процессами и оптимальное использование технологических возможностей. Интеграция данных с различных уровней производственной цепочки, начиная от скважины и заканчивая поверхностными сооружениями, открывает новые возможности для оптимизации работы оборудования и улучшения качества управления ресурсами. Эффективная интеграция скважинных и поверхностных сооружений крайне важна для оптимизации процессов добычи и минимизации операционных затрат и экологического воздействия. Интегрированные системы управления позволяют автоматизировать множество процессов, обеспечивая непрерывный мониторинг параметров работы, автоматическую коррекцию настроек и предоставление данных для принятия оперативных решений. Это включает в себя сбор данных в реальном времени, их анализ и использование полученных сведений для подбора оптимальных режимов работы, что помогает повысить как общую эффективность, так и безопасность производственных процессов. В современной нефтегазовой промышленности особое значение приобретает вопрос эффективного использования оборудования на всех этапах добычи углеводородов. Оптимизация процессов эксплуатации скважин и поверхностных сооружений является ключевым аспектом для повышения экономической эффективности и уменьшения экологического воздействия. В этой связи, разработка и применение интегрированных систем, позволяющих контролировать и адаптировать режимы работы оборудования в реальном времени, становится актуальной и значимой задачей.

Ключевые слова: интегрированная система, поверхностные сооружения, интеграция скважины и поверхностных сооружений, геотехнология, геотехнологические методы, скважина, фильтрация.

Молдабаева Гульназ Жаксылыковна	***Информация об авторах:*** *Доктор технических наук, профессор кафедры Нефтяная инженерия, Satbayev University, 050013, Сатпаева 22а, Алматы, Казахстан. E-mail: moldabayeva@gmail.com; ORCID ID: https://orcid.org/0000-0001- 7331-1633*
Турдиев Мурадим Файзиевич	*Кандидат физико-математических наук, Самаркандский государственный университет, кафедра "Точных наук", Email: tmurat-43@mail.ru*
Сулейменова Райхан Таупиховна	*Доктор PhD, ассоц.профессор, Атырауский университет нефти и газа имени Сафи Утебаева, 060027, Баймуханова, 45А, Атырау, Казахстан. E-mail: raikhan.suleimenova@aogu.edu.kz; ORCID ID: https://orcid.org/0000-0001-7995-5560*

Буктуков Николай Садвакасович	*Доктор технических наук, директор института Горного дела им.Д.Кунаева, 050046, Абая 191, Алматы, Казахстан. E-mail: igdkpms@mail.ru; ORCID ID: https://orcid.org/0000-0001-6370-8557*
Эфендиев Галиб Мамедович	*Доктор технических наук, профессор, институт Нефти и газа Национальной академии наук Азербайджана, Баку, Азербайджан. Email: galib_2000@yahoo.com; ORCID ID: https://orcid.org/0000-0002-4875-5782*
Коданова Шынар Кулмагамбетовна	*Кандидат технических наук, Атырауский университет нефти и газа имени Сафи Утебаева, 060027, ул. Баймуханова, 45А, Атырау, Казахстан. E-mail: S.Kodanova@aogu.edu.kz; ORCID ID: https://orcid.org/0000-0002-1589-4268*
Тузельбаева Шолпан Рыскулбековна	*Магистр технических наук, докторант, Satbayev University, Алматы, Казахстан. Email: s.tuzelbayeva@satbayev.university; ORCID ID: https://orcid.org/0000-0002-1749-6511*

References

[1] Karasevich AM, Kreinin EV. Perspektivy i rezervy energosberejeniya v Rossii [Prospects and Reserves of Energy Saving in Russia]. Gazovaya promyşlennost. 2010; 9:68-71. (in Russ).

[2] Ishkov AG, Khvorov GA, Yumashev MV, Yurov EV, Yesic LK. Sovremennoye sostoyaniye i perspektivnoye razvitiye napravleniy energosberezheniya v transporte gaza [Current state and perspective development of energy saving directions in gas transport]. Gas Industry. 2010; 9:36-39. (in Russ).

[3] Ishkov AG, Yatsenko IA, Pystina NB, Khvorov GA, Yumashev MV, Yurov EV. Metodologiya formirovaniya programm energosberezheniya OAO «Gazprom» v usloviyakh novogo zakonodatel'stva [Methodology for the Formation of Energy Saving Programs of OAO Gazprom in the Conditions of New Legislation]. Gas Industry. 2012; 2:70-75. (in Russ).

[4] Intriligator M. Mathematical methods of optimization and economic theory. M. Intriligator. Per. from English. M.: Progress. 1975, 607.

[5] Kozachenko AN, Nikishin VI, Porshakov BP. Energetika truboprovodnogo transporta gazov [Gas pipeline power engineering]. M.: Oil and gas. 2001, 397. (in Russ).

[6] Karasevich AM, Sukharev MG, Belinsky AV, Tverskoy IV, Samoilov RV. Energoeffektivnyye rezhimy gazotransportnykh sistem i metody ikh obespecheniya [Energy efficient modes of gas transmission systems and methods of their provision]. Gas Industry. 2012; 1:30-34. (in Russ).

[7] Campasti N. Aerodinamika kompressorov [Aerodynamics of compressors]. Translation from English. M.: Mir, 2000, 688. (in Russ).

[8] Kitaev SV, Farukhshina RR. Ekspress-sposob opredeleniya pokazateley energoeffektivnosti gazoperekachivayushchikh agregatov [Express method for determinin the energy efficiency indicators of gas-pumping units]. Transport and storage of petroleum products and hydrocarbon raw materials. 2015; 1:19-22. (in Russ).

[9] Kontseptsiya energosberezheniya i povysheniya energeticheskoy effektivnosti v OAO «Gazprom» na period 2011–2020 godov. Utverzhdena prikazom OAO «Gazprom» ot 08.12.2010 № 364 [Concept of energy saving and energy efficiency improvement in OAO Gazprom for the period 2011- 2020. Approved by Order of OAO Gazprom dated 08.12.2010 No. 364]. (in Russ).

[10] Mikaelyan EA. Modernizasiya gazoturbinnoi ustanovki v selyah energosberejeniya [Modernization of a gas turbine plant for the purpose of energy saving]. Gazovaya promyshlennost. 2010; 10:15-16. (in Russ).

[11] Bulysova LA, Gutnik MN, Vasil’ev VD, et al. GT-16 Gas Turbine Low-Emission Combustor: Results of Tests in a Single-Burner Chamber on the Stagnation Property Test Facility. Power Technol Eng. 2021; 54:695-698. https://doi.org/10.1007/s10749-020-01272-1

[12] Sanaye S, Hosseini S. Off-design performance improvement of twin-shaft gas turbine by variable geometry turbine and compressor besides fuel control. Proceedings of the Institution of Mechanical Engineers, Part A: Journal of Power and Energy. 2020; 234(7):957-980. https://doi.org/10.1177/0957650919887888

[13] Mikhailov SA, Mingazov BG, Varsegov VL, Simkin EL, Osipov BM, Yu BM, Tokmovtsev V. Razrabotka metodiki mnogofaktornogo diagnostirovaniya i prognozirovaniya tekhnicheskogo sostoyaniya GPA-16R Ufa s gazoturbinnym privodom AL-31ST. Razrabotka programmnogo obespecheniya dlya rascheta parametrov tekhnicheskogo sostoyaniya GPA-16R «Ufa» [Technical report on the topic: "Development of a methodology for multifactor diagnostics and forecasting of the technical state of the GPA-16R Ufa with the gas turbine drive AL-31ST. Development of software for calculating the technical condition parameters of GPA-16R Ufa]. 2013, 55. (in Russ).

[14] Mikhailov CA, Mingazov BG, Varsegov VL, Simkin EL, Osipov BM, Tokmovtsev YuV. Razrabotka metodiki mnogofaktornogo diagnostirovaniya i prognozirovaniya tekhnicheskogo sostoyaniya GPA-16R Ufa s gazoturbinnym privodom AL-31ST. Razrabotka programmnogo obespecheniya dlya rascheta parametrov tekhnicheskogo sostoyaniya GPA-16R Ufa [Technical report on the topic: Development of a methodology for multifactor diagnostics and forecasting of the technical state of the GPA-16R Ufa with the gas turbine drive AL-31ST. Development of software for calculating the parameters of the technical state of GPA-16R "Ufa"]. 2014, 215. (in Russ).

[15] Mikhailov DA, Golyanov AI. Komp'yuternyy imitator raboty tsentrobezhnogo nagnetatelya [Computer simulator of a centrifugal blower]. Ufa.: IDPO GOU VPO UGNTU. 2007, 32-44. (in Russ).

[16] Osovsky S. Neyronnyye seti dlya obrabotki informatsii [Neural networks for information processing]. M: Finance and statistics. 2004, 344. (in Russ).

[17] Kenzhaliyev B. Innovative technologies providing enhancement of non-ferrous, precious, rare and rare earth metals extraction. Kompleksnoe Ispolzovanie Mineralnogo Syra = Complex Use of Mineral Resources. 2019; 310(3):64-75. https://doi.org/10.31643/2019/6445.30

[18] Zhapbasbayev U, Ramazanova G, Kenzhaliev B, Sattinova Z, Shakhov S. Experimental and calculated data of the beryllium oxide slurry solidification. Applied Thermal Engineering. 2016; 96:593-599. https://doi.org/10.1016/j.applthermaleng.2015.11.114

[19] Kenzhaliyev B, Surkova T, Berkinbayeva A, Dossymbayeva Z, Yesimova D. & Abdikerim B. On methods of modifying natural minerals. Challenges of Science. 2021; VI:128-133. https://doi.org/10.31643/2021.20

[20] Zhapbasbayev UK, Ramazanova GI, Bossinov DZ, Kenzhaliyev BK. Flow and heat exchange calculation of waxy oil in the industrial pipeline. Case Stud. Thermal Eng. 2021; 26:101007. https://doi.org/10.1016/j.csite.2021.101007

[21] Moldabayeva GZh, Suleimenova RT. Effektivnost' primeneniya fizicheskogo vozdeystviya na produktivnyy plast dlya snizheniya vyazkosti i uvelicheniya nefteotdachi plastov [The effectiveness of the use of physical impact on the reservoir to reduce the viscosity and increase oil recovery]. Kompleksnoe Ispolzovanie Mineralnogo Syra = Complex Use of Mineral Resources. 2021; 1 (316):53-61. (In Russ). https://doi.org/10.31643/2021/6445.07

МАЗМҰНЫ
СОДЕРЖАНИЕ
CONTENTS

ENGINEERING AND TECHNOLOGY

METALLURGY

EARTH SCIENCES

Техникалық редакторлар:
Г.К. Қасымова, Н.М.Айтжанова, Т.И. Қожахметов

Компьютердегі макет:
Г.К. Қасымова

Дизайнер:
Г.К. Қасымова, Н.М.Айтжанова

Металлургия және кен байыту институты
050010, Қазақстан Республикасы, Алматы қаласы, Шевченко к-сі, 29/133

Жариялауға 29.10.2024 жылы қол қойылды

Технические редакторы:
Г.К. Касымова, Н.М. Айтжанова, Т.И. Кожахметов

Верстка на компьютере:
Г.К. Касымова

Дизайнер:
Г.К. Касымова, Н.М.Айтжанова

Институт металлургии и обогащения
050010, г. Алматы, Республика Казахстан. ул. Шевченко, 29/133

Подписано в печать 29.10.2024г.

Technical editors:
G.K. Kassymova, N.M. Aitzhanova, T.I. Kozhakhmetov

The layout on a computer:
G.K. Kassymova

Designer:
G.K. Kassymova, N.M. Aitzhanova

Institute of Metallurgy and Ore Benficiation
050010, Almaty city, the Republic of Kazakhstan. Shevchenko str., 29/133

Signed for publication on 29.10.2024